

CONCRETE STRUCTURES

ANNUAL TECHNICAL JOURNAL



Prof. Tamás Paulay

Recent trends in the seismic design of rc buildings

2

Mátyás Gyurity – Kálmán Mohay – Veronika Székely – László Windisch

Overhaul of Buda access ramps of Erzsébet bridge

9

László Polgár – Dr. József Almási – Balázs Karkiss – Péter Varvasovszky – Dr. Csaba Pethő – Erika Tatai

Design process of the load bearing structures of Asia Center

15

Assoc. Prof. Zoltán Kiss

Reinforced concrete frame structures in Eastern Europe

25

Dr. József Almási – György Erdei – Imre Édes – Lóránt Koncz – Prof. Árpád Orosz

External strengthening of a silo in with polypropylene fibre reinforced shotcrete

34

Assoc. Prof. István Bódi – Prof. Robert N. Bruce, Jr.

Implementation of high performance concrete for prestressed concrete bridge girders

43

Dr. Zsolt Huszár

Vibrations of non-uniform tower constructions

54

Dr. András Draskóczy

Main directions of standardization in shear design

59

Tamás Simon

Sand patch method for evaluation of concrete-to-concrete interaction

67

Salem Georges Nehme

Effect of porosity on the properties of concrete

72

Dr. Adorján Borosnyói – Prof. György L. Balázs

Bond of non-metallic (FRP) reinforcement in concrete

76

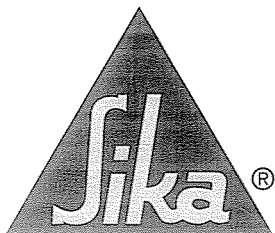
2003

Solutions with Sika Systems

Construction

Construction Chemicals

- **Viscocrete** Concrete Admixtures – High performance Concrete,
- **Sika Waterbars, Sika Swell Profiles** – Watertight Concrete Structures,
- **Sika Repair** Ready to Use Mortars – Concrete repair and protection,
- **Sika CarboDur** – Structural Strengthening,
- **Sikaflex** – Professional joint sealants,
- **Sikagard** coating systems – Long lasting protection for concrete and steel structures,
- **Sikafloor** – Flooring Systems
- **Icosit** – Long lasting corrosion protection for steel structures,
- **Sikaplan** – Roofing Membranes
- Sika shotcrete application systems – **ALIVA** spray equipment,



Sika Hungária Kft. 1117 Budapest, Prielle Kornélia u. 4. • Telefon: (06 1) 371 2020, fax: (06 1) 371 2022 • e-mail: info@hu.sika.com

Solutions with Sika Systems

Editor-in-chief:

Prof. György L. Balázs

Editor:

Prof. Géza Tassi

Editorial board:

János Beluzsár
Assoc. Prof. István Bódi
László Csányi
Dr. Béla Csíki
Assoc. Prof. Attila Erdélyi
Prof. György Farkas
Gyula Kolozsi
Dr. Károly Kovács
Ervin Lakatos
László Mátyássy
László Polgár
Antonia Teleki
Dr. László Tóth
József Vörös
Péter Wellner

English language review by:

Bob Summerfield of
Brit Tech Business Consulting Ltd.

Board of reviewers:

Prof. György Deák
Prof. Endre Dulácska
Dr. József Janzó
Antónia Királyföldi
Dr. Jenő Knébel
Prof. Péter Lenkei
Dr. Miklós Loykó
Dr. Gábor Madaras
Prof. Árpád Orosz
Prof. Kálmán Szalai
Prof. Géza Tassi
Dr. Ernő Tóth
Dr. Herbert Träger

Founded by: Hungarian Group of *fib*
Publisher: Hungarian Group of *fib*
(*fib* = International Federation for
Structural Concrete)

Editorial office:

Budapest University of Technology
and Economics (BUTE)
Department of Construction Materials
and Engineering Geology
Műgyetem rkp. 3., H-1111 Budapest
Phone: +36-1-463 4068
Fax: +36-1-463 3450
WEB <http://www.eat.bme.hu/fib>
Editing of online version:
Ádám Damokos

Technical editing and printing:
RONÓ Bt.

Price: 10 EUR
Printed in 1000 copies

© Hungarian Group of *fib*
ISSN 1419-6441
online ISSN: 1586-0361

Cover photo:
Wellness establishment
Visegrád, Hungary
by Pál Csécssei

CONTENT

- 2 Prof. Tamás Paulay
Recent trends in the seismic design of reinforced concrete buildings
- 9 Mátyás Gyurity – Kálmán Mohay – Veronika Székely – László Windisch
Overhaul of Buda acces ramps and other engineering structures of Erzsébet bridge
- 15 László Polgár – Dr. József Almási – Balázs Karkiss – Péter Varvasovszky – Dr. Csaba Pethő – Erika Tatai
Design process of the load bearing structures of Asia Center
- 25 Assoc. Prof. Zoltán Kiss
Reinforced concrete frame structures in Eastern Europe
- 34 Dr. József Almási – György Erdei – Imre Édes – Lóránt Koncz – Prof. Árpád Orosz
External strengthening of an 8000-ton grain silo in Törökszentmiklós, Hungary with polypropylene fibre reinforced shotcrete
- 43 Assoc. Prof. István Bódi – Prof. Robert N. Bruce, Jr.
Implementation of high performance concrete for prestressed concrete bridge girders
- 54 Dr. Zsolt Huszár
Vibrations of non-uniform tower constructions
- 59 Dr. András Draskóczy
Main directions of standardization in shear design
- 67 Tamás Simon
Sand patch method for evaluation of concrete-to-concrete interaction
- 72 Salem Georges Nehme
Effect of porosity on the properties of concrete
- 76 Dr. Adorján Borosnyói – Prof. György L. Balázs
Bond of non-metallic (FRP) reinforcement in concrete
- 84 *fib* Symposium 2005 Budapest, Hungary

Sponsors:

Foundation for the Technological Progress of the Industry,
Railway Bridges Foundation, ÉMI Kht., HÍDÉPÍTŐ Co.,
MÁV Co., MSC Hungarian SCETAUROUTE Consulting Co.,
Pfleiderer Lábatlani Vasbetonipari Co., Pont-TERV Co., UVATERV Co.,
MÉLYÉPTERV KOMPLEX Engineering Co., Peristyl Ltd., Techno-Wato Ltd., Betonmix
Consulting Ltd., BVM Épelem Ltd., CAEC Ltd.,
Pannon Freyssinet Ltd., STABIL PLAN Ltd., UNION PLAN Ltd.,
BUTE Dept. of Reinforced Concrete Structures,
BUTE Dept. of Construction Materials and Engineering Geology

RECENT TRENDS IN THE SEISMIC DESIGN OF REINFORCED CONCRETE BUILDINGS



Prof. Tamás Paulay

To enable acceptable seismic displacement demands imposed by earthquakes to be estimated, the displacement capacity of a structure needs to be known. This is controlled by selected performance criteria. It is postulated that the assignment of fractions of the required seismic strength to components of the system may be arbitrary. This enables the displacement capacity of a system to be evaluated without the knowledge of its strength. A redefinition of some traditionally used structural properties, such as stiffness, is a prerequisite of applications. The study of a reinforced concrete mixed framewall system illustrates rationale, acceptable extents of approximations and extreme simplicity of application.

Keywords: strain, curvature, displacement, ductility, detailing, strength, stiffness

1. INTRODUCTION

Earthquake shaking imposed on buildings represents perhaps the greatest challenge that a structural designer may need to face. In many countries seismic structural design criteria override all others that relate to reinforced concrete building systems. Limit state design procedures which consider structures subjected to gravity loads, wind forces and environmental effects, address hypothetical failure states. However, in regions of significant seismicity the attainment of displacements close to those of a failure state, is almost a certainty. In this scenario safety relies on a small probability of the occurrence of a major earthquake that could create conditions corresponding to an ultimate limit state during the probable time span for the use of the structure.

In contrast to requirements to be satisfied in regions of no or small seismicity, seismic structural design needs generally to address inelastic dynamic response, significant repeated displacement reversals, inevitable stiffness and possible strength degradations. The detailing of the reinforcement in potential plastic regions of the structure is, therefore, of overriding importance. This review attempts to highlight some findings derived from relevant theoretical and experimental research conducted particularly in New Zealand over the last three decades.

Traditional techniques, adopted in early seismic code provisions, attempted to provide adequate strength, in terms of lateral force resistance, largely based on the dynamic response of elastic systems. It was recognized that for rare seismic events lateral design forces can be significantly reduced if proper allowance is made for hysteretic damping. Some associated damage is, however, inevitable. This presented a major challenge to researchers to identify the sources of large deformation capacities in a composite structure comprising essentially brittle concrete and adequately ductile steel. An astute choice of a kinematically admissible plastic mechanism needs to be made. To ensure that only the suitably chosen mechanism can be mobilized during a large earthquake, a hierarchy in the relative strengths of components is also required. These concepts are embodied in the philosophy of "capacity design" (Park and Paulay, 1975, Paulay and Priestley, 1992).

More recently emphasis in seismic design strategies was placed on satisfying identifiable performance criteria. Instead

of providing only seismic strength, the importance of realistic predictions of displacement capacities of structural systems, associated with specific performance criteria, is being recognized.

To aid simplifications, without which the adoption of new concepts in seismic design cannot be expected, deliberate approximations need to be made. These are considered to be compatible with the inevitable crudeness of the prediction of magnitudes of earthquake-induced displacement demands.

Certain redefinitions of structural properties, for example the relationship between strength and stiffness, may be viewed by some readers as being controversial.

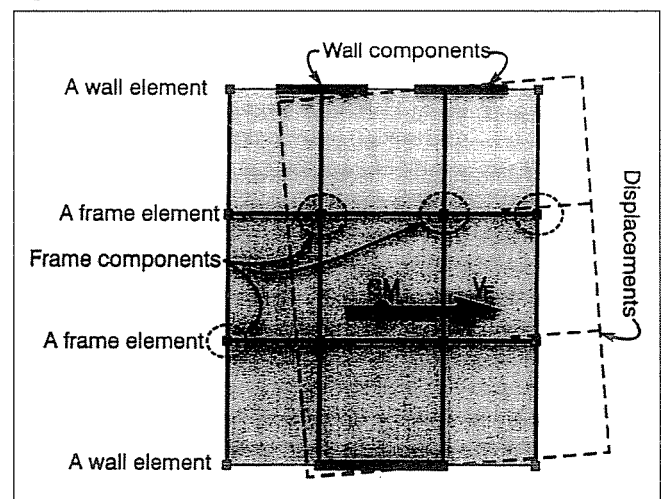
2. A DISPLACEMENT FOCUSED SEISMIC DESIGN APPROACH

2.1 Terminology used

In this study of earthquake-induced displacements of buildings, reference are made to the structural system.

A structural system comprises lateral force-resisting elements, generally arranged in orthogonal directions. Typical elements are bents of ductile frames or interconnected walls

Fig. 1 Nomenclature



in the same plane. Due to torsional effects, elements of the system may be subjected to different displacements.

A lateral force-resisting element may comprise several components. The components will, however, be subjected to identical lateral displacements. Typical components are beams, columns, beam-column subassemblages or individual walls.

Fig. 1 illustrates typical elements and components of an example structural system. In the technical literature the terms component and element are often used to describe the same part of the system. Distinct differentiation between components and elements are made in this study.

2.2 Displacement limitations

Following currently accepted seismic design aims, maximum displacements imposed on reinforced concrete elastoplastic systems are deemed to be controlled by:

- The displacement capacity of critical components of the system corresponding with the adopted, i.e., codified, quality of detailing for construction.
- The magnitude of the storey drift, (the lateral displacement of a level relative to that of an adjacent level) satisfying the specific performance criterion, specially chosen for a building system.
- The more severe limit may then establish the target displacement capacity of the ductile system.

2.3 The tools of displacement estimates

Traditionally the structural design process starts with experience-based estimates of dimensions, particularly component sizes which are likely to satisfy functional requirements of the building. Once this information, based on architectural and engineering perspectives, is available, with the knowledge of the material properties, strength-independent displacement estimates, adequate for purposes of seismic design, can be readily made.

2.3.1 Nominal yield curvature

A fundamental property of a structural component is the nominal yield curvature at its critical section or sections. This will define its response in the elastic and postelastic domain of behaviour when it is subjected to monotonically increasing displacements. In reinforced concrete members, it is more realistic to base curvature estimates on quantifiable section properties, rather than on assumed or recommended (Paulay and

Priestley, 1992) values of flexural rigidity, $E_c I_e$, where E_c is the modulus of elasticity of the concrete and I_e is the second moment of effective sectional area of the cracked component. In seismic design it may be assumed that extensive cracking will occur over the full length of components.

Fig. 2 shows flexural strength-curvature relationships for a typical structural wall section. With some experience the neutral axis depth associated with the development of steel yield strain at the extreme tension fiber can be readily estimated. As stated, for purposes of seismic design, a high degree of precision in the estimation of component properties is not warranted. However, if necessary, this estimate can be subsequently verified once details of the flexural reinforcement provided are known. For a given steel tensile yield strain, Σ_y , and the location of the neutral axis depth, ξD_w , the curvature at the onset of yielding is established as $\phi_y = \Sigma_y / (\xi D_w)$, where D_w is the overall depth of the section. When details of the reinforcement are known, the associated yield moment, M_y , may also be evaluated. The need for this will, however, seldom arise. The designer will primarily address the nominal (ultimate) flexural strength, M_n , at a section, as constructed, when strength requirements for the components are known.

For seismic design purposes the bilinear simulation on the nonlinear moment-curvature relationship, as shown in Fig. 2.b, is convenient and adequate. With linear extrapolation this leads to the definition of the nominal yield curvature

$$\phi_y = (M_n / M_y) \phi_y' = \eta \Sigma_y / D_w \quad (1)$$

where the coefficient $\eta = (M_n / M_y) / \xi$ recognizes the ratio of the nominal to yield strength in flexure and the relative position of the neutral axis. Effects of strain hardening with increasing curvature ductility may also be included. These, however, are not shown here.

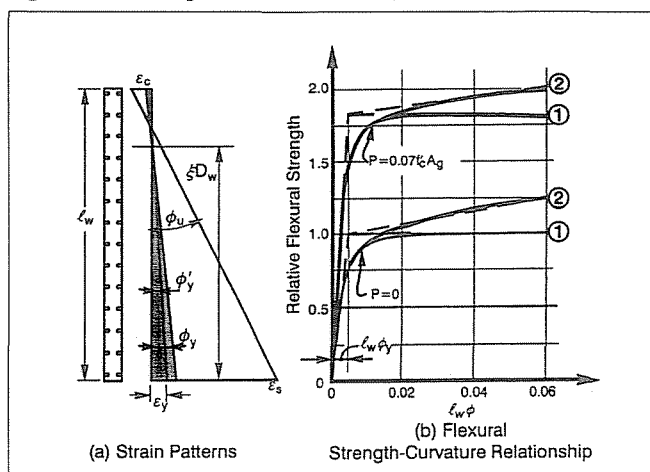
Extensive studies of a variety of sections, conducted at the University of Canterbury, confirmed previous findings (Priestley, Kowalsky, 1998) that for specific types of members, such as walls or beams, the variation of the value of the parameter η is relatively small. For example the amount of reinforcement used at a section hardly affects the nominal yield curvature. Neither do moderate axial compression loads, commonly encountered in structural walls, affect nominal yield curvature to any significance. However, the effect on flexural resistance is very pronounced. Fig. 2.b, where the (cylinder) compression strength of the concrete is denoted as f_c' , illustrates this feature.

A message of this review of the nominal yield curvature is, that it should be considered as a material property. It is insensitive to, and for design purposes essentially independent of, section strength. The definition presented here contradicts with the widely used terminology, whereby $\phi_y = M_y / (E_c I_e)$.

2.3.2 Nominal yield displacement

An approach, similar to that used in defining the nominal yield curvature at a cracked reinforced concrete section, based on bilinear simulation of force-displacement relationship for a component, may be utilized. Fig. 3 shows familiar features of this simulation. The strongly nonlinear response of component i from the onset of cracking till the development of its nominal strength, V_{in} , is of little interest with respect to estimations of displacements in the inelastic range of behaviour. The shaded area in Fig. 3 indicates essentially linear response after the occurrence of repeated displacements not exceeding that associated with the yield strength, V_y , and the yield curvature, ϕ_y' of the component. Hence the nominal yield displace-

Fig. 2 Flexural strength-curvature relationships for a wall section



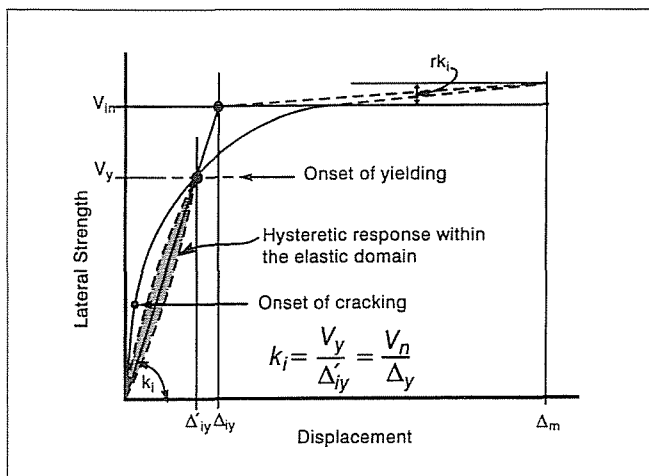


Fig. 3 Bi-linear simulation of force-displacement relationship

ment, D_y , an essential reference value, may be based on the nominal yield curvature, j_y , at the critical section. It is important to note that the nominal yield displacement, D_y , is also strength-independent!

In this study, only conservatively estimated flexural deformations were considered. If refinement appear to be necessary, other sources of distortions, such as due shear and anchorages, may be readily included. Subsequent examples will illustrate applications.

2.3.3 Component stiffness

An important conclusion, drawn from the bilinear simulation of the force-displacement relationship for a component, is the definition of its stiffness, stated in Fig. 3. Contrary to usage in traditional design practice, the stiffness of a reinforced concrete component, with given dimensions and material properties (ϵ_y), is proportional to the strength which the designer will eventually assign to it (Paulay, 2001a).

Fig. 3 clearly shows the range of strengths, i.e., when $V_y < V < V_n$, over which stiffness so defined would significantly underestimate displacements. In terms of ductile structural response this transitional range of behaviour is in general of little interest.

The bilinear simulation shown in Fig. 3 allows the displacement ductility, applicable to component i to be more realistically quantified as

$$\mu_{i,\Delta} = \Delta_m / \Delta_{iy} \quad (2)$$

The displacement ductility, μ_{Δ} , of a system, to be defined subsequently, is an essential parameter of current strength and displacement-based seismic design procedures.

2.4 Freedom in the assignment of strengths

As stated previously, the nominal yield curvature at the critical section of a component with given dimensions, ϕ_{iy} , and hence its nominal yield displacement, Δ_{iy} , may be considered in seismic design to be independent of the nominal strength. Therefore, fractions of the total required nominal strength of a system may be assigned arbitrarily to its components or elements (Paulay, 2000). Implications of this freedom in assigning component or element strengths, are thus:

- Irrespective of the strengths assigned to components, characterized by bilinear force-displacement relation-

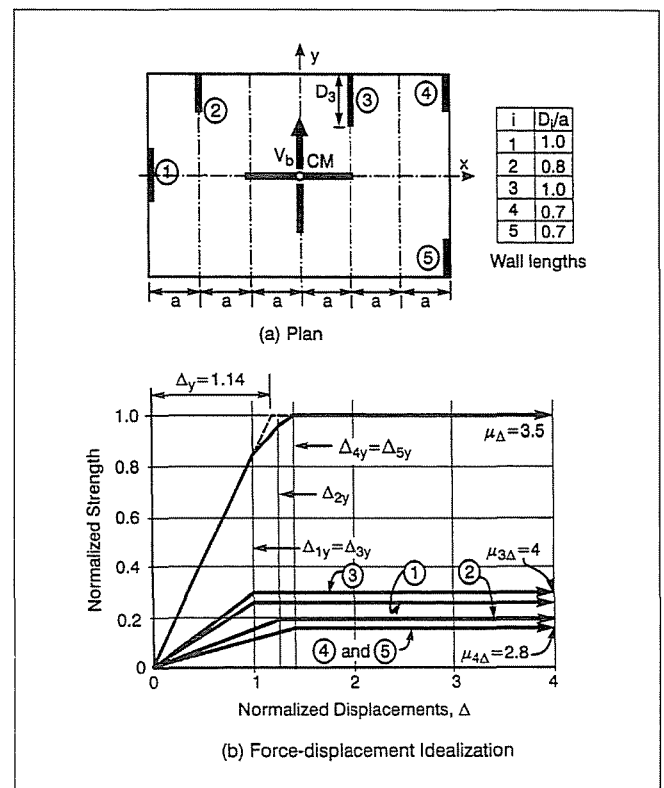


Fig. 4 The model of a wall system

ships, they will commence yielding when the imposed system displacement approaches the relevant nominal yield displacement.

- Simultaneous onset of yielding of components of elements, such as walls, with different overall depths, and hence different aspect ratios, is not possible.
- Lateral force-resisting components of a system with different nominal yield displacements, when subjected to identical translational limit displacements, will be subjected to different displacement ductility demands.
- A structural system, comprising elements with different nominal yield displacements, does not exhibit a distinct yield displacement. Existing definitions of the yield displacement of systems are often ambiguous. Hence a redefinition is required.
- To ensure that all components of a ductile system will perform satisfactorily, the displacement capacity of the system should be restricted to that of its component with the smallest displacement capacity.

Arbitrariness in strength assignment imparts to the astute designer the ability to choose from a number of possible, viable and appealing solutions. To illustrate the relevance of the structural features listed above, a somewhat idealized system, deliberately made simple, is studied here briefly.

Fig. 4.a shows the plan of a structure in which lateral forces in the Y direction are resisted by five rectangular reinforced concrete cantilever walls of identical heights but different length, D_y . Slender components with very small lateral strength, intended for the transmission of gravity loads only, are not shown in Fig. 4.a. A single large wall element is provided to resist seismic forces in the X direction.

Design approaches, based on traditional definitions of component stiffness, would assign nominal wall strengths, i.e., base shear, in proportion to D_y^3 . Under identical element translations this would require the reinforcement ratios in Walls (1) and (3) to be 43% larger than for Walls (4) and (5). However, if nominal strengths are made proportional to say, D_y^2 , all walls would require the same ratio of vertical reinforcement. This

would enable identical arrangement of bars to be used in all walls.

Wall strengths so provided would, however, result in this case in a strength eccentricity of $0.095a$. With some 6% reduction of the strength of Wall (1) and a corresponding increase of Walls (4) and (5), even this relatively small eccentricity would be eliminated. Thereby torsional phenomena, affecting element seismic displacement demands primarily in the postyield domain of response, would be negligible (Paulay, 2001b), and would thus not need to be addressed. It may be shown that the strength-dependent stiffness eccentricity, would also be rather small ($0.21a$, i.e., approximately 4% of the length of the plan).

The bilinear simulation of the translational behaviour of the system and its 5 components is presented in Fig. 4.b. Displacements plotted are normalized in terms of the nominal yield displacement of Walls (1) and (3), taken as unity. The force-displacement modelling of the elements with different strength and stiffness properties, demonstrates that:

- During monotonic displacements of the system the sequence of component yielding, from that of Wall (1) to Wall (5), is independent of wall strength. Nominal yield displacements of the walls are inversely proportional to wall lengths, D_i .
- The superposition of the bilinear response of elements results in a nonlinear response of the system.
- Assuming bilinear simulation also for the system, would be justified. This assumption allows the equivalent nominal yield displacement of the system to be expressed as

$$\Delta_y = \sum V_{in} / \sum (V_{in} / \Delta_{iy}) = \sum V_{in} / \sum k_i \quad (3)$$

In this example $\Delta_y = 1.00 / 0.879 = 1.14$ displacement units. It is to be used as a reference value to enable the displacement ductility capacity of the system to be gauged. It is seen in Fig. 4(b) that at this displacement Walls (1) and (3) would have entered the inelastic domain, while the other walls are still elastic.

- As stated previously, the displacement capacity of the system should be limited to that of its critical elements, i.e., Walls (1) and (3). In this example it is assumed that appropriate detailing of the reinforcement in all walls, allows a wall displacement ductility capacity of $\mu_{id} = 4$ to be relied on. Therefore, the displacement capacity of the system is to be limited to that of Wall (1), $\Delta_u = 4 \times 1 = 4$

units. The displacement ductility capacity of the system, often referred to as global ductility, is thus to be restricted to $\mu_d = 4.0 / 1.14 = 3.5$. Contrary to current codified methods, the global ductility of a system should not be assumed, but made dependent on the displacement capacity of its critical element.

This simple example is presented in support and illustration of the claim (Paulay, 2000) that the displacement capacity of systems can be established before its required strength is determined.

3. AN EXAMPLE FRAME-WALL SYSTEM

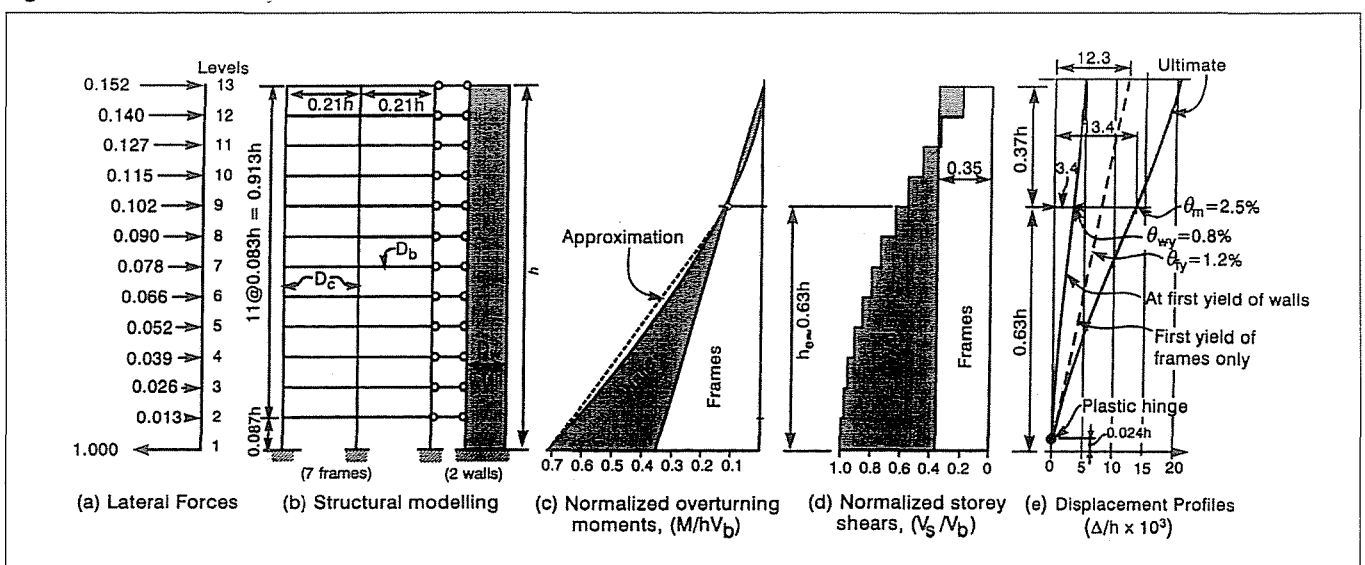
An attractive mode of seismic resistance in medium to high rise buildings may be achieved with the use of interacting cantilever walls and frames, extending over the full height. Before the arrival of the computers, these systems represented one of the most formidable challenges to the analytical skills of structural engineers. With the appreciation of some limitations of the uses of bilinear modelling, generally insignificant in a nonlinear seismic scenario, both required strength and displacement capacity can be readily estimated.

This example intends to demonstrate how, already at the preliminary stage of the design, such simple behaviour-based predictions can be made, even for such a complex structure. The strategy used exemplifies a deterministic design philosophy, whereby the designer simply 'tells the structure' what it should do in the event of a major earthquake.

Displacement compatibility under lateral force is assumed to be assured by infinitely rigid floor diaphragms. The traditional design approach to the distribution of seismic strength to different elements, based on elastic behaviour, was extensively studied (Paulay, Priestley, 1992). However, issues of displacement predictions, relevant to this type of ductile structures, are less familiar.

A prototype structure, shown in Fig. 5.b, will illustrate several postulated, yet unconventional, design concepts. A symmetrical 12 storey reinforced concrete building comprises seven identical frames and two cantilever walls, each with an aspect ratio of $A_{wr} = 7.1$. Dimensions are expressed in terms of the total height, h , of the structure. For modelling purposes the 9 elements are condensed into two elements, one com-

Fig. 5 A ductile frame-wall system



prising 7 frames and the other 2 walls, respectively, as seen in Fig. 5.b. A typical seismic design force pattern is shown in Fig. 5.a. These equivalent static forces lead to moment and shear force patterns presented in Figs. 5.c and d, respectively. Possibilities for the assignment of the lateral forces to the two very different elements, and associated displacement limits, are of prime interest. It is restated that, within rational limits, fractions of the overturning moments, M , and associated storey shear forces, V_s , to be sustained by the chosen ductile mechanism of the system, may be assigned to the wall and frame elements in an arbitrary manner.

The mechanism chosen for this structure comprises plastic hinges at the base of the walls and the columns and at each ends of the beams. Other regions of the components will be provided with sufficient reserve strength to ensure that no inelastic deformations of significance would occur while ultimate target displacements are being developed.

To illustrate the principal steps of displacement estimates, familiar simple expressions, reflecting component behaviour, will be used. Benchmark deformations are independent of strength provided. Displacements will be able to be compared with component dimensions, shown in Fig. 5.b. For design practitioners the latter are more meaningful quantities. The symbols D_b , D_c and D_w define the overall depths of beams, columns and walls, respectively.

3.1 The assignment of relative element strengths

A consideration, encountered in practice, could be a limitation on the transmission of relatively large overturning moments by the walls. These moments may impose excessive demands on the foundations. Significant deformations of the foundation structure could adversely affect displacement limits applicable to the superstructure.

One attractive solution could result in beams, which, at the ultimate limit state, would be subjected to identical seismic strength demands. This implies that beams at all levels, carrying also identical gravity loads, could have the same dimensions and identically detailed reinforcement. Thereby the storey moment capacities, i.e., the product of the lateral displacement-related nominal storey shear forces of the frame element and the storey height, would be made identical. The corresponding shear forces across the upper 9 storeys of the frames, associated with the identical nominal strengths of the beams, would be the same. It is transparent that the major motivation in this search for suitable distribution of component strengths is practicality in construction.

The development of identical nominal storey shear strengths over the full height of the frame element, shown in Fig. 5.d, corresponds to the application of a single lateral force at roof level. In this example it was judged that this single roof level force, shared by 7 frames, could be 35% of the total base shear, i.e., 5% per frame. As Fig. 5.d shows, with this decision, the contributions of the walls and frames to the resistance of storey shear forces, V_s , are determined. Subsequently diaphragm forces, associated with this allocation of strengths, with appropriate magnifications for dynamic effects, to be examined subsequently, will need to be carefully considered.

The corresponding contribution of the frame element to the resistance of overturning moments, M , will thus increase linearly from level 13 to its maximum, $0.35hV_s$, at the base. The remainder of the overturning moments, to be resisted by the

walls, is shown by the shaded area in Fig. 5.c. With this choice the total overturning moment at the base of the system would be resisted by the two condensed elements in close to equal proportions.

3.2 Displacement considerations

3.2.1 Wall deformations

It was established that yield deformations are proportional to the yield strain of the reinforcing steel used. To simplify subsequent expressions and to provide a better feel for relative magnitudes, it is assumed that in this example $\varepsilon_y=0.002$, i.e., the yield strength of the steel is 400 MPa. As Fig. 5(c) shows, with the approximate location of zero wall moment, the effective height of an equivalent cantilever wall may be defined by $h_e=0.63h$. For seismic design purposes the variation of wall moments over this height is assumed to be linear. The nominal yield curvature of the wall base, as stated in Eq. (1), is thus

$$\varphi_{wy} = 1.8 \times 0.002 / (0.14h) = 0.0257/h \quad (4a)$$

where for typical rectangular wall section $\eta = 1.8$. This leads to the nominal yield displacement of the wall at the effective height to be

$$\Delta_{wy} = \varphi_{wy} h_e^2 / 3 = 0.0257 \times 0.63^2 h^2 / 3 = 3.4 \times 10^{-3} h \quad (4b)$$

The slope of the wall at the same height, h_e , is

$$\theta_{wy} = \varphi_{wy} h_e / 2 = 0.0257 \times 0.63 / 2 = 8.1 \times 10^{-3} \text{ rad.} \quad (4c)$$

These are important benchmark values because the deformed shape of the entire structure will be controlled by that of the wall element.

3.2.2 Storey deformations of frames

Nominal interstorey yield deformations of frames in which the yielding of columns is suppressed by appropriate capacity design procedures, referred to in the introduction, originate primarily from the nominal yield curvatures in the potential plastic hinges of beams. Additional elastic deformations will occur due to shear effects in beams, columns and joints, and flexural rotations of columns. Because, compared with nominal yield rotations of beams, the contribution of elastic deformations, listed above, are relatively small, these may be estimated. Details are not given here. It has been shown (Priestley, 1998) that a reasonable estimate, particularly for seismic assessments, of the nominal yield drifts of storeys in frames, is

$$\theta_{fy} = 0.5 \varepsilon_y A_{br} = 6.15 \varepsilon_y = 0.0123 \text{ rad.} \quad (5)$$

where A_{br} is the aspect (span/depth) ratio of the beams, in this example taken as 12.3.

3.2.3 Relationships between ductilities of elements

A comparison of the wall rotation and the nominal yield drift of the frame at level h_e , obtained from Eqs. (4c) and (5), shows that, at the nominal yielding of the wall base, the drift in the critical storey, will be only $\theta_{wy} / \theta_{fy} = 8.1/12.3 = 66\%$ of the nominal yield drift of the frames.

The generally accepted maximum seismic storey drift, associated with the ultimate limit state, is in the order of 2.5%, i.e., 1 in 40. With this limit the associated displacement

ductilities imposed in the walls and the frames may now be compared with their displacement capacities. Using Eq. (4c) the acceptable plastic rotation at the wall base should be limited to

$$\theta_{wp} = 0.025 - 0.0081 = 0.0169 \text{ rad.} \quad (6)$$

The corresponding plastic wall displacement at level h_c will be thus

$$\Delta_{wp} = (h_c - 0.5 \ell_p) \theta_{wp} = 0.97h_c \theta_{wp} = 0.0103h \quad (7)$$

where the length of the equivalent plastic hinge was found (Paulay and Priestley, 1992) to be $\ell_p = 0.0324h$.

Therefore, the displacement ductility demand on the wall should be limited to

$$\mu_{w,d} = (\Delta_{wy} + \Delta_{wp}) / \Delta_{wy} = 0.0137 / 0.0034 \approx 4 \quad (8)$$

This value can be readily achieved with appropriate detailing of the plastic hinge region at the wall base.

The corresponding storey displacement ductility imposed on the frame element in the vicinity of the effective height is

$$\theta_{wmax} / \theta_{ty} = 0.025 / 0.0123 \approx 2 \quad (9)$$

This limited ductility capacity can be very easily achieved.

The deformed shapes of the structure and its elements, associated with these benchmark displacements, are summarized in Fig. 5.e.

3.2.4 Relationships between ductilities of elements and that of the system

This preliminary study of an example frame-wall structural system enables the ductility relationships between elements, i.e., walls and frames, and the total system to be clarified. These relationships are not likely to change substantially as the detailed design progresses. Fig. 6 illustrates the bilinear modelling of force-displacement relationships for the elements and the system.

The relationship between displacement ductilities, with reference to the effective height, h_c , is very similar to that shown for a wall system in Section 2.4 and Fig. 4. Hence the specific values, applicable to the example framewall system, can be presented here.

The stiffness of the elements, based on the definition given in Fig. 3, and the total unit base shear force, are:

$$k_{wall} = V_{w1} / \Delta_{wy} = 0.65 / 0.00340 = 191$$

$$k_{frame} = V_{f1} / \Delta_{fy} = 0.35 / 0.00775 = 45$$

$$\Sigma k_i = \text{the system stiffness} = 236$$

Therefore, from Eq. (3), the equivalent nominal yield displacement of the system, Δ_y , a rather important reference value, is

$$\Delta_y = \Sigma V_{i1} / \Sigma k_i = 1.00 / 236 = 4.24h \times 10^{-3} \quad (10)$$

i.e., approximately 0.67% of the effective height. The corresponding displacement ductilities are, therefore:

$$\text{Walls } \mu_{w,d} = \text{as given by Eq. (8)} \approx 4.0$$

$$\text{Frames } \mu_{f,d} = 0.0137 / (0.63 \times 0.0123) \approx 1.8$$

$$\text{System } \mu_{s,d} = 0.0137 / 0.00424 \approx 3.2$$

It is seen thus that the seismic strength, V_b , of the system, corresponding with the specified acceleration spectrum, should be based on a system (global) displacement ductility capacity of 3.2. This procedure should protect the critical element (the walls) against demands exceeding a displacement ductility of 4. As Fig. 3 implies, it will be appreciated that over the approximate range of displacements, $0.5 < \Delta / \Delta_y < 2.5$, multilinear simulation represents tangents to the continuous nonlinear forcedisplacement response of a system, often used in pushover analysis techniques.

3.2.5 Special features of frame-wall systems

When only cantilever walls provide lateral force resistance, as in Fig. 4, their displacement ductility capacity need to be significantly curtailed when aspect ratios, $A_{wr} = h / D_w$, exceed approximately 5. Wall slopes near roof level, associated for example with a system displacement ductility capacity of 3.2, may become excessive.

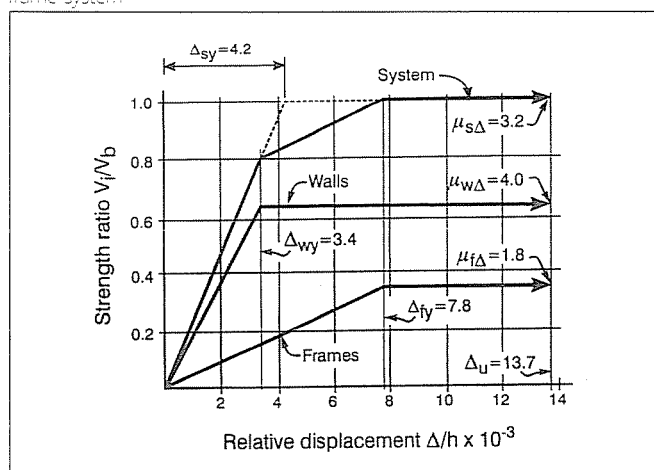
In ductile frames, exceeding approximately 3 storeys, displacement capacities are generally governed by limits on interstorey drift, rather than component deformation capacities. Moreover, during the elastoplastic dynamic response, frame deformations may become sensitive to the effects of higher modes of vibrations.

To a large extent these shortcomings of deformation behaviour of both walls and frames, may be eliminated when such elements are coupled within the building by rigid floor diaphragms (Paulay, 2002).

As stated, system deformations are controlled by those of the walls. The nominal flexural strength of the walls provided at floor levels above the base should be, in accordance with the principles of capacity design, significantly in excess of that indicated in Fig. 5.c. This procedure should ensure that wall sections above the potential plastic region at the base will be subjected, at worst, to very small curvature ductility demands as they are expected to respond in the elastic domain.

When walls, more slender than those shown in Fig. 5.b, are used, for the sake of drift control the approximate location of zero wall moment must be lowered. This can be achieved by assigning a greater share of the base shear, V_b , to the ductile frames. For example an equal sharing by the wall and frame elements of the base shear resistance, would enable the effective height, h_c , to be reduced to approximately $0.38h$. This would enable a rather slender wall, with an aspect ratio of $A_{wr} \approx 12$, to be used without exceeding a drift limit of 2.5%.

Fig. 6 Bi-linear modelling of the force-displacement relationship in a wall-frame system



This issue indicates also how the designer may assign strength to elements to control critical storey drift.

It is emphasised that the restriction of plastic hinge formation only to the base of a wall element will ensure that storey displacement, i.e., drift, imposed on frames will be very similar over the height, h . However, dynamic effects on the elastic portion of the walls should be expected to increase significantly local flexural and shear strength demands recorded in Figs. 5.c and d. To safeguard walls against unexpected ductility demands above the base region, design action, based on lateral static design forces, need to be increased by appropriate dynamic magnification factors (Paulay and Priestley, 1992), details of which are beyond the scope of this presentation.

4. CONCLUDING REMARKS

The presented review attempted to highlight some findings on the seismic design of reinforced concrete buildings derived from relevant theoretical and experimental research conducted particularly in the New Zealand over the last three decades.

- To satisfy the intents of performance-based seismic structural design, the importance of more realistic predictions of target displacement capacities should be recognised. For reinforced concrete structures, addressed here, such displacement limits can be readily and realistically predicted in a rather simple way without the knowledge of the eventual seismic strength required. Therefore, displacement estimates made during the preliminary stages of the design, can immediately expose undesirable features of the contemplated structural system.
- The use of a number of simple principles, often overlooked or ignored in seismic design, was demonstrated. These include: (a) The stiffness of a reinforced concrete component may be considered to depend also on the nominal strength eventually assigned to it. Therefore, element or system stiffness cannot be a priori assumed. (b) The nominal yield curvature of a reinforced concrete section, which represents a characteristic strain pattern, and displacement of a component associated with it, are insensitive to the flexural strength of the section. (c) Because deformation limits applicable to components of a ductile system, exposed to typical seismic moment patterns, are insensitive to component strength, the latter can be arbitrarily assigned to them. This enables the astute designer to distribute the required total seismic strength among components so that more economical and practical solutions, satisfying also stipulated displacement limits, are obtained.
- The estimation of displacement capacities of components of a system enables the critical components to be identified. Hence, instead of assuming global ductility factors for structural systems, their displacement and hence ductility capacity should be made dependent on that of the critical component. Such relationships can be established before strengths are assigned to components.

- The approach, illustrated with the aid of an example wall and a frame-wall structure, can be readily incorporated into existing strength-based seismic design methods. Its major appeal relates, however, to displacement-based seismic design strategies.
- In the seismic design of ductile structures, bilinear modeling of force-displacement relationships for both components and the system may be considered adequate.
- Moment patterns used for the estimation of deformations of elastic elements are based on typical static lateral force patterns. The fact that force patterns encountered during seismic response may be very different, is not considered to invalidate the approach used for the estimates of displacements in systems dominated by the behaviour of reinforced concrete walls.
- No attempt in this presentation was made to estimate displacement demands. It is the designer's responsibility to establish, with the use of a force-based or a displacement-based strategy, the level of seismic strength that will ensure that, for a given seismic scenario, the displacement capacity of the system is not likely to be exceeded.
- The approach presented is design rather than analysis oriented. It is based on very simple principles. It is a useful tool in the hands of a designer, which enables, even for mixed structures considered in this study, efficient, practical and simple solutions to be obtained.

5. REFERENCES

- Park, R., Paulay, T., (1975), "Reinforced Concrete Structures", *John Wiley and Sons, New York*, 769 p.
- Paulay, T., Priestley, M.J.N., (1992), "Seismic Design of Reinforced Concrete and Masonry Buildings", *John Wiley and Sons, New York*, 767p.
- Paulay, T., (2000), "A simple displacement compatibility-based design strategy for reinforced concrete buildings", *Proceedings of the 12 World Conference on Earthquake Engineering*, Paper No. 0062.
- Paulay, T., (2001a), "A redefinition of stiffness of reinforced concrete elements and its implications in seismic design", *Structural Engineering International*, Vol.11, No.1, pp. 3641.
- Paulay, T., (2001b), "Some design principles relevant to torsional phenomena in ductile buildings", *Journal of Earthquake Engineering*, Vol.5, No.3, pp. 273300.
- Paulay, T., (2002), "An estimation of displacement limits for ductile systems", *Earthquake Engineering and Structural Dynamics*, Vol.31, pp. 583599.
- Priestley, M.J.N., Kowalsky, M.J., (1998), "Aspects of drift and ductility capacity of rectangular structural walls", *Bulletin of the New Zealand Society for Earthquake Engineering*, Vol.31, No.2, pp. 7385.
- Priestley, M.J.N., (1988), "Brief comments on elastic flexibility of reinforced concrete frames and significance to seismic design", *Bulletin of the New Zealand Society for Earthquake Engineering*, Vol.31, No.4, pp.246259.
- Tamás PAULAY** (1923) PhD, Drs.h.c., professor emeritus at the University of Canterbury, Christchurch, New Zealand., commenced his studies in 1946 at the Budapest University of Technology and Economics and graduated in 1953 in New Zealand. After 8 years of structural design practice, from 1961 till his retirement in 1989, he was teaching at the University of Canterbury where he also conducted research relevant to the behaviour of reinforced concrete structures subjected to large earthquakes. He is a past president of the International Association for Earthquake Engineering.

OVERHAUL OF BUDA ACCESS RAMPS AND OTHER ENGINEERING STRUCTURES OF ERZSÉBET BRIDGE



Mátyás Gyurity



Kálmán Mohay



Veronika Székely



László Windisch

An overview from the design and construction engineers' standpoint of the project to overhaul the Buda-side access ramps from Erzsébet Bridge and other structures in the immediate vicinity. Since no comparable, comprehensive overhaul had been carried out on Erzsébet Bridge and its surroundings since its opening in 1964 (37 years ago), there was a pressing need for this work, which was carried out in 2001.

Key words: overhaul, closure to traffic, Gerber hinge, bearing replacement, expansion joint replacement, stone surface, abutment, slab bridge, traffic diversion.

1. INTRODUCTION

In 2001, the Buda-side access ramps from Erzsébet Bridge and the local road system were overhauled, an enterprise whose scope took in the entire road system up to the Szirtes Street intersection of Döbrentei Square and Hegyalja Road. As well as the three-branch exit bridge and the adjacent retaining walls, the work involved a comprehensive overhaul of the Buda end of Erzsébet Bridge and its immediate vicinity, including the thermal water drinking hall and pedestrian subway. The system of retaining walls and slab bridge behind the Rác Baths were overhauled, as were the Gellért Hill retaining walls, the Aladár Street retaining wall and the Naphegy Street steps. In connection with the reconstruction work on Attila Road and Szent Gellért Quay that was going on in parallel, all roads and pedestrian pavements in the area were resurfaced.

2. DESIGN

The first comprehensive plan for the Buda-side access ramps from Erzsébet Bridge was produced by Uvater Rt. in 1994–95.

In 1999, under contract to the Transport Department of the Budapest Metropolitan Mayor's Office, Magyar Scetaroute Kft., partly working from the expert opinion of FTV Kemokorr Kft., carried out an engineering survey of the access ramps and an update review of the old plans by Uvater Rt. A new set of working plans was produced incorporating the necessary design modifications.

Fig. 1 The ramp closed to traffic



In spring 2001, the above plans were supplemented with retaining walls and the vicinity of the Buda end of the Erzsébet Bridge, resulting in comprehensive tender and construction plans for the project.

The corrosion inspections were again carried out by FTV Kemokorr Kft., and the road-building and traffic management plans for the area were produced by Közlekedés Kft.

The public procurement tender for general contractor for overhaul of all structures was won by Hídépítő Rt.

The structures involved in the overhaul fell into three main groups:

- the Buda exit bridges and ramps from Erzsébet Bridge,
- the end of Erzsébet Bridge and its vicinity,
- the retaining walls on Hegyalja Road and Aladár Street, and the retaining walls and slab bridge behind the Rác Bath.

2.1 Buda access ramps of Erzsébet bridge

The central part of the work was the overhaul of the access ramps. This is a crucial traffic intersection, and diversions and closures here inevitably have an effect on traffic throughout the city. The earlier proposals envisaged separate overhauls for each of the three bridge ramps. This would have involved somewhat less disturbance to traffic, but would have considerably prolonged the operation. At the end, the overhaul was carried out with all three ramps fully closed to traffic. This enabled the part of the job involving disturbance to traffic to be completed during the summer school holidays, i.e. in a very short time. Overhauling the entire structure at once, and coordinating various phases under a precise timetable, as well as reducing construction time, brought considerable advantages in terms of quality (Fig. 1).

Each access ramp consists of a multi-span reinforced concrete box-girder superstructure standing on 16 hollow reinforced concrete pillars. The structure divides into three parts: the straight section leading from Erzsébet Bridge to Attila Road, and curved ramps towards Hegyalja Road and Rác Bath to the quay, resp. There was a Gerber (compound) hinge providing a break in the continuous structure of the straight branch and the curved branch to Hegyalja Road.

The main findings of the earlier inspection and the pre-overhaul inspection were:



Fig. 2 Dismantled Gerber hinge

- water passing through the gap of the Gerber hinges had caused severe corrosion of the reinforced concrete structure in the vicinity of the hinges,
- the surface water drainage system (gullies and downpipes) had deteriorated,
- the steel roller bearings on the abutment of the Hegyalja Road branch and the neoprene bearings on the other abutments were considerably removed from the position appropriate to the temperature,
- the waterproofing of the expansion joint had failed,
- the waterproofing and the asphalt surfacing had failed throughout the structure,
- the bridge kerbs and railings were damaged.

In addition to this, it had to be anticipated that owing to the failure of the waterproofing, highly corroded structural elements would be found during demolition and would have to be replaced.

The overhaul involved not only correcting the above faults but also eliminating their sources.

2.1.1 Removal of Gerber hinges

The superstructure of the three-branch bridge was divided into three parts by Gerber hinges in two places. After detailed structural calculations, it was determined that the structure had sufficient reserves to permit removal of the Gerber hinges and replacement with a continuous reinforced concrete structure. This would relieve the bridge of two potential sources of faults, and two expansion joint structures.

The plans specified that the concrete needs only be removed in the direct vicinity of the hinge, after relieving the load from the connection and providing temporary support. A flexure-resistant connection would then have been made by internal and external prestressing (i.e. outside and inside the box sec-

Fig. 3 External prestressing rods



tion) after concreting the two structure-ends together. In the event, mainly owing to the undoubted difficulties of implementing the internal prestressing, a design modification was agreed with the contractor and a different approach applied. The essential difference was that the two structure-ends were broken back to a length such that a joint could be made to the existing reinforcing bars, enabling the connection to be made moment resistant (*Fig. 2*).

The exterior prestressing retained from the original plan served only to close working gaps. The structure was prestressed using three 32 mm diameter Dywidag bar on each side. The bars were fixed to the superstructure by anchorages fastened to the lower surface of the deck slab cantilevers and the external surface of the webs by Hilti anchor screws (*Fig. 3*). A condition of tensioning was that the new concrete reach strength of requirements of C30. The prestressing forces were 370 kN and 450 kN. The advantage of external prestressing is that the mechanisms can be easily checked.

2.1.2 Overhaul of the drainage system

The existing drainage involved side-inflow gullies on the ramps leading rainwater through downpipes in the interior of the hollow pillars directly into the drain. The gullies had become blocked, and the concrete around them corroded. The downpipes also failed, and there was water standing in some of the pillars.

Around the gullies, a 1.5 m area around the damaged cantilevered slab had to be demolished and restored after the steel reinforcement had been treated against corrosion.

The new, vertical inflow gullies were made of KO-21 steel according to MSZ 436-74. For aesthetic and cityscape reasons, the system of downpipes in the interior of the pillars was retained, but fully replaced. New cleaning holes were installed at the bases of the pillars where the water drainage pipes are connected, thus rendering the drain system capable of being cleaned.

2.1.3 Bearing replacement and adjustment

The bridge platform on the abutments at Erzsébet Bridge, Rudas Baths and Attila Road rested on neoprene steel plate insert bearings, and these have deteriorated with time. These were removed after relieving the load, and replaced with SHW TYP 1 400×500 mm base area, 69 mm thick steel plate insert bearings. The contractors relieved the strain, as in replacement of the Gerber hinge, by frames and hydraulic hoists of suitable capacity (*figure 4*).

The engineering inspection of the bridge indicated that there was no need to replace the moving bearing on the Hegyalja Road abutment, but it also had to be strain-relieved to perform adjustment.

Fig 4 Hoist frame at the abutment

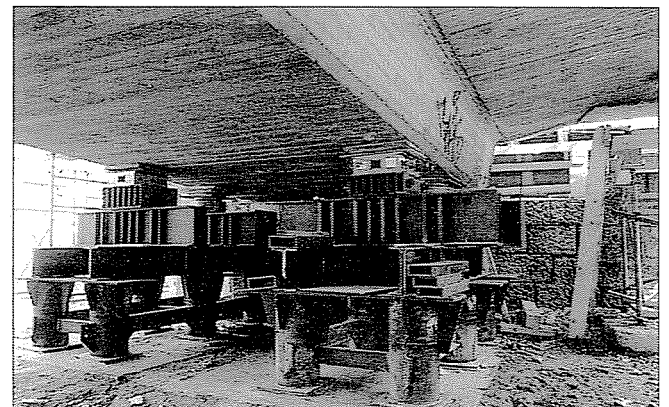




Fig. 5 Renovated bridge deck

2.1.4 Expansion joint structures

The old, degraded expansion joints on the abutments were replaced by new PD 85 dilatation structures. One side of these was concreted into the upper plane of the newly-built backwalls. The new backwalls left an inspection corridor behind the end of the superstructure, enabling the expansion joint structure and the bearings to be inspected and maintained. Steel doors were designed for the end of the corridors for security reasons.

2.1.5 Waterproofing, kerbs, railings, deck assignment, deck surfacing.

The old surfacing, waterproofing, kerbs and railings all had to be removed. Then the surface was prepared and the structural concrete restored with strict adherence to the concrete technology specifications, and special regard to the composite action of old and new structures, shrinkage, etc. Then the full width of the deck slab was treated with sprayed Concretin BA waterproofing.

Formerly, only one traffic lane was available from Erzsébet Bridge towards Hegyalja Road. The design allowed for a wider road surface, enabling two traffic lanes to be laid out (one 3.5 m and the other 4.3 m wide). Instead of the 80 cm wide and 10 cm thick kerbs, the kerbs are now 50 cm wide and the apron wall 20 cm thick. Elsewhere we did not change the former dimensions. The kerb height is 25 cm from the road surface, and the kerb is protected by an L-shaped steel plate. The new kerb concrete grade is C25-24/moderate plastic, f50, watertightness₄ (acc. to the Hungarian Standards), and the reinforcing steel B 50.36. The concrete cover is 3.5 cm. The repaired balustrade is connected to base plates set into the kerb concrete. The kerbs were finished with a cement-based, crack-bridging, salt corrosion-resisting protective coating (Fig. 5).

The road slope varies between 2.0 and 4.5%, mostly in one direction, but the section before the ramp branches separate has a roof profile. The complex cambers required great care during constructing.

The deck surfacing scheme (top downwards) is:

- 35 mm wearing surface (rolled asphalt)
- 60 mm binder course (rolled asphalt)
- 30 mm base course (mastic asphalt)
- 5 mm sprayed waterproofing

A 30 × 50 mm gravel rod longitudinal catch drains were laid into the base course in the deep line of the deck slab (70 cm from the edge of the cantilever), with transverse catch drains at occasional intervals. The material of the catch drains is single-grain (5–10 mm) washed pea gravel conglutinated with synthetic resin, of 15–20% void volume.

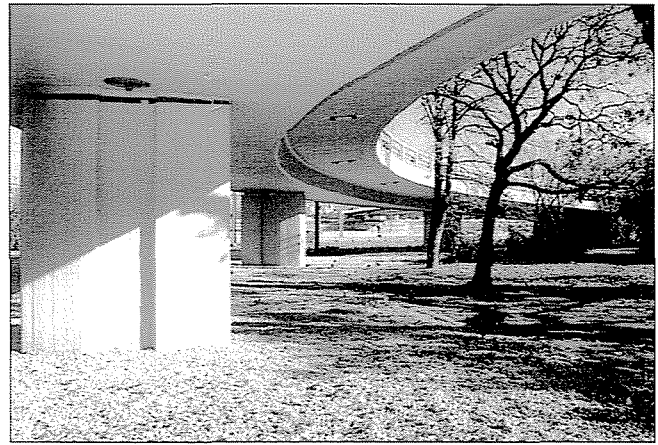


Fig. 6 View from below by day



Fig. 7 View from below by night

2.1.6 Other repairs

New steel doors with security locks were fitted to the inspection openings to the box girders and pillars.

The full concrete surface was covered by a flexible crack-bridging coating, and salt corrosion protection was applied to surfaces exposed to the effects of salting (Fig. 6).

The floodlighting on the lower plane of the cantilever deck section of the superstructure was completely replaced, lending a pleasant aspect to the structure at night (Fig. 7).

The abutments and retaining wall sections were also completely overhauled. The raised reinforced concrete kerbs and balustrades were treated in the same way as on the bridge, and the stone surfaces were renovated and given a protective coating. Mastic waterproofing was applied to the strengthened concrete base under the new double-layer road surface. Ventilation of the backfill was improved by insertion of perforated PVC pipes.

2.2 Buda abutment of Erzsébet bridge and surroundings

Waterproofing was applied to the entire top surface of the bridge abutment block, which contains the anchorage chambers and other technical areas. This extended to the sections under the pavements. New surface layers were applied to the road surface and pavements (Fig. 8).

The pedestrian subway directly behind the abutment was also completely renovated. The stone surfacing layers at the entrances, which were in danger of crumbling, were securely fastened in place, flexible filler being applied in the dilatation gaps, and the transverse drainage channels were renovated.



Fig. 8 Vicinity of the Buda end of Erzsébet Bridge

The thermal water drinking hall, the bridgemaister's office, the transformer house and the pedestrian subway were treated with secondary waterproofing against indirect rainwater. This took the form of waterproofing and suitable road surfacing on the reinforced concrete floor slab under the pavements and roadway.

The limestone finishing of abutments and the north and south retaining walls (which are also the walls of the above areas) directly adjacent to them were fully renovated, as was the entire stone surface of the walls.

2.3 Retaining walls and steps

The smaller retaining wall on Hegyalja Road beside Gellért Hill was judged to be in a critical condition, as was proved by inspections, and so had to be completely demolished. It was replaced by a stone-faced gravity wall. As the continuation of

Fig. 9 New retaining walls beside Gellért Hill

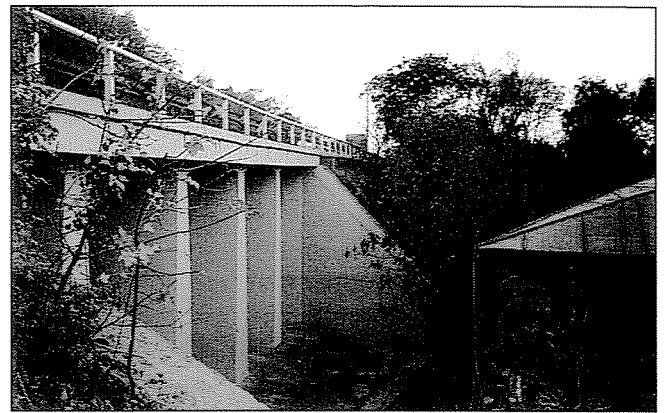
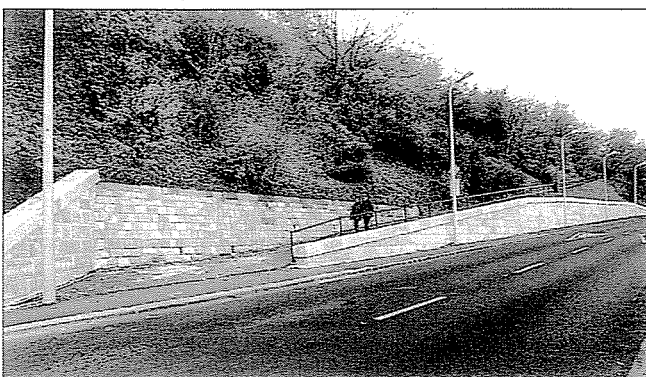


Fig. 10 The 22-m slab bridge

this, and of similar appearance, a retaining wall-like curtain wall was built in front of the hitherto bare rocky section of approximately 15.00 m (*Fig. 9*).

Work on the retaining wall system behind Rác Bath, comprising gravity walls and a 22.00 m long slab bridge consisted of overall surface treatment together with minor surface repairs, grouting and repairs to surface drainage channels and the revetment facing. On the slab bridge, a new raised kerb was constructed and the balustrade repaired (*Fig. 10*). To avoid subsidence of the kind that has occurred in the past, floating slabs were included in the bridge abutments, the deck slab was strengthened with a waterproofed concrete topping, which was then surfaced. A U-shaped drainage system leading out to the surfaced revetment was installed along the Gellért Hill side of the slab bridge and in front of the floating slabs.

The Aladár Street retaining wall was extended about 12.00 m in the eastern direction, eliminating the steps, thus removing an obstruction to pedestrian traffic. The entire stone facing of the existing retaining wall was renovated, new limestone coping stones and balustrades being mounted on the top of the wall.

The dilapidated Naphegy Street steps were completely renovated.

3. CONSTRUCTION, TECHNOLOGY AND TRAFFIC DIVERSION

The management and technical supervision of the overhaul project on Buda approaches to Erzsébet Bridge was carried out by Metróber Kft., and the construction by Hídépítő Rt. and its subcontractors.

The overhaul schedule was specified by contract as follows: *Phase I, involving closure of ramps:*

26 June – 28 August 2001

Phase II, to completion of work involving traffic diversions:

20 September 2001

Phase III, to final completion:

15 November 2001.

The closure of the ramps was preceded by a "zero phase", in which roads were adjusted and corrected as required for the introduction of traffic diversions during the project. This involved kerb adjustments at the Buda end of Erzsébet Bridge and the end of Hegyalja Road, and a new road surface towards Attila Road made by cutting through a green area. When these road works were finished, the access ramps were closed and traffic diverted.

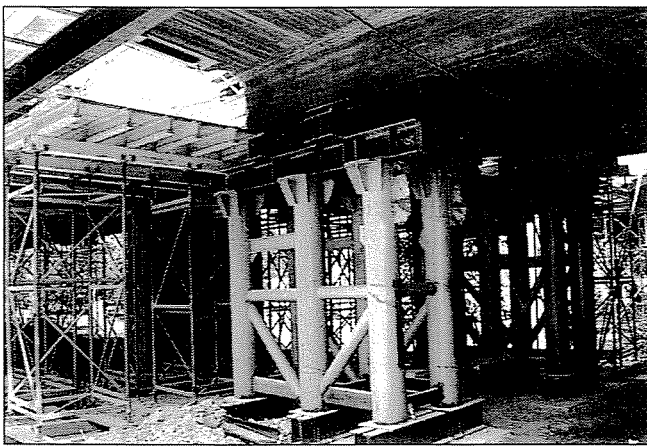


Fig. 11 Heavy scaffolding at a Gerber hinge

In the full diverted state, the Buda direction proceeded beside the access ramps towards Attila Road and Hegyalja Road, and traffic towards Pest proceeded on two lanes in the original direction. At the end of Erzsébet Bridge, two lanes in each direction had to be maintained throughout.

While the ramps were closed, the road surface of Hegyalja Road and the area of the SÁnc Street intersection had to be rebuilt. On this section, traffic flowed alternately on one side or the other, with one lane in each direction.

Phase II required lesser diversions. Kerb adjustments were carried out with local diversions, and major asphaltting at weekends or during less busy periods.

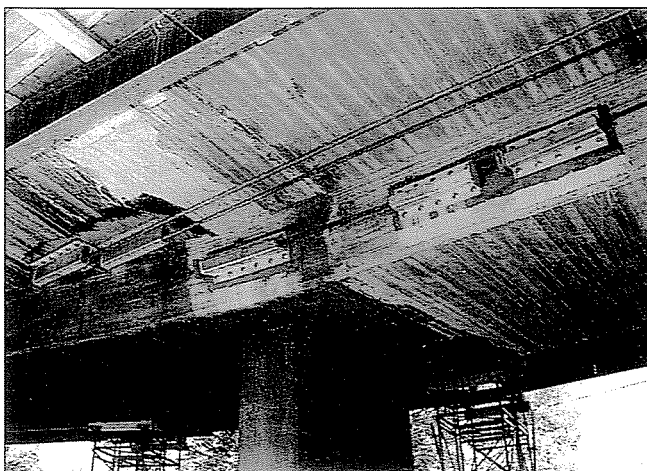
The traffic management and diversion plans for the project were drawn up to meet construction requirements and demands as conditions permitted, and were modified several times as required during the project.

Construction work commenced on 26 June 2001 with handover of the working area.

3.1 Phase I

After the access ramps had been completely closed, building of the reinforced concrete footings for the support frames under the Gerber hinges and beside the bridge abutments commenced, and the steel frame structures installed (*Fig. 11*). When the frames were in place and the superstructure had been supported, demolition of the structure began. Work proceeded concurrently on the two Gerber hinges. The abutments were reconstructed at the same time to allow access to the surfaces for demolition and construction of the kerbs and deck structures.

Fig. 12 After removal of the Gerber hinge



The critical point of the project was the conversion of the Gerber hinges. The demolition had to be executed manually, taking great care to preserve the reinforcing bars intact. Demolition was followed by shuttering, installation of the steel reinforcement and concrete placement (*Fig. 12*).

As the concrete was setting, the mounting holes for the prestressing shoes were drilled, and the steel structures and prestressing bars were mounted in place. Prestressing was carried out when the concrete reached the specified hardness. Hardness was checked by breaking off test pieces and by Schmidt hammer tests.

Demolition of the kerbs and abutments proceeded more quickly, because small machines could be used. Protective scaffolding was installed along the entire 100 m length under the kerbs prior to demolition, and was used as building scaffolding after the demolition, following minor conversion.

Installation of the gullies was followed by waterproofing of the deck slab and construction of the RC kerbs. Demolition and construction of the kerbs and waterproofing took the same time as removal and concreting of the Gerber hinges. After the Dywidag bars had been tensioned, the entire roadway was surfaced at the same time.

The road surface was also overhauled on the retaining wall embankment sections. On the section between the Erzsébet Bridge abutment and the abutment of the straight ramp branch a new reinforced concrete road base was laid. Elsewhere surface levelling was sufficient (*Fig. 13*). Sand asphalt waterproofing was applied to the full surface, followed by the surface layers.

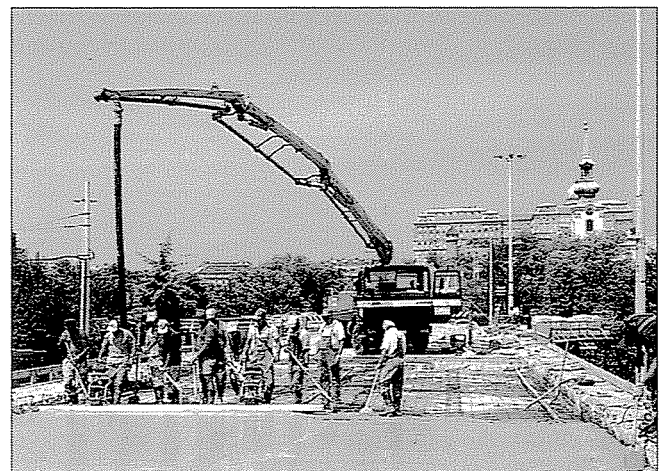
The Hegyalja Road overhaul was performed during phase I, in two traffic diversion stages. In the first stage, the side carrying traffic to Pest was closed and completely overhauled between the end of Erzsébet Bridge and the SÁnc Street intersection. At the same time, the retaining walls beside Gellért Hill were demolished and construction of new retaining walls commenced. The retaining walls could not be completed before the road had been finished, further work having to wait until the other side of the road was finished and at least one traffic lane put into use.

After traffic had been diverted, overhaul of the side of the road going uphill started. The road was resurfaced and the kerbs moved, and at the same time the deck structure and kerbs of the slab bridge above RÁC Baths were rebuilt.

Before completion of the slab bridge work, one traffic lane was returned to its original route, enabling the retaining walls to be completed.

The ramps and Hegyalja Road were fully opened to traffic on 29 August 2001.

Fig. 13 Concreting reinforced roadbed



3.2 Phase II

The second stage involved resurfacing of Attila Road and Döbrentei Square and repair of the pavements.

By 20 September 2001, the Attila Road and Döbrentei Square sections, which had previously served as diversion routes, were finished. The raised kerbs had been rebuilt, the kerb adjustments restored, and after scraping where required, a new asphalt surface was applied to the road.

This phase also included waterproofing and resurfacing of the Buda abutment of Erzsébet Bridge. Two lanes had to be kept open throughout, although narrower than the usual lanes.

3.3 Phase III

The third phase involved finishing work that could be carried out without disturbance to traffic.

This involved complete overhaul of the pedestrian subway under the Erzsébet Bridge abutment, completion of surface treatment on the lower part of the bridge structure, and installation of the floodlighting.

It was in this phase that the areas affected by the project were landscaped.

The technical acceptance procedure was completed on 7 November 2002 (Fig. 14).

Main figures of the reconstruction and overhaul project:

Reconstruction of access ramps:	
Asphalt surface demolition:	730 m ³
Reinforced concrete structure demolition:	340 m ³
Sprayed waterproofing:	3,132 m ²
Mastic waterproofing:	2,906 m ²
Road surfacing:	6,038 m ²
Stone facing renovation:	2,049 m ²
Road building:	
Road surface breaking and scraping:	2,050 m ³
Kerb breaking and construction:	2,200 m
Asphalt surfacing:	19,275 m ²
Pavement surfacing:	4,710 m ²
Retaining wall construction:	261 m ²

Major subcontractors:

Strabag Építő Kft.
Hidtechnika Kft.
FKF Rt.
– traffic management work

Fig. 14 The completed project



4. CONCLUSIONS

As with every renovation and reconstruction, the overhaul of the Erzsébet Bridge Buda access ramps provided many lessons. The most important was that the 37 year-old structure, apart from the faults discussed, was in very good condition. This pays tribute to its designers and builders. However the project also revealed some faults deriving from methods that were customary at the time and have since largely become obsolete, their shortcomings having been taken note of in design practice.

Most faults were the result of salt corrosion, a phenomenon unknown when the bridge was designed.

Another lesson, although one that is nowadays a basic design condition, is that structural parts must be accessible. Many faults can be prevented if it is possible to reach and inspect their source, the threatened part of the structure. It must also be possible to replace a faulty element.

It is important for every designer to become familiar with structures built in the past, to gather observations arising from operation, inspections and overhauls, and to incorporate these in designing new structures.

Finally, a well-coordinated relationship between the designer, the contractor, the supervising engineers and the client is a crucial requirement in a renovation project. Design in such an undertaking does not finish at the drawing board or computer. The condition of structures revealed during demolition have to be jointly assessed, and further progress has to be mutually decided. The goal of achieving the best possible technical result must be harmonised with available finance and the necessarily short time-scale. This can only be achieved with the professional commitment, maximum cooperation and mutual respect of all parties concerned.

5. REFERENCES

- Sávoly, P. (1965): "The New Erzsébet Bridge", *Mélyépítéstudományi Szemle* (Civil Engineering Science Review), 1965/4–5, pp. 147–164 (In Hung.)
Lehoczky, K. (1965) "The traffic implications of the new Erzsébet Bridge" *Mélyépítéstudományi Szemle*, 1965/4–5, pp. 165–170 (In Hung.)
Sávoly, P. and et al. (1965): "Aspects of the design", *Mélyépítéstudományi Szemle*, 1965/4–5, pp. 171–226 (In Hung.)

Mátyás GYURITY (1967) graduated in civil engineering in 1992 from the Zagreb University Faculty of Civil Engineering. He started his career in the Bridge and Structural Design Office of Uvaterv Rt., where he learned the basics of the profession from eminent superiors. He joined MSc Magyar Scetaroute Kft. as a design engineer in 1996, and became chief departmental engineer in 2000. His interests extend to reinforced concrete road bridges and steel railway bridges.

Kálmán MOHAY (1960) graduated in civil engineering in 1985. He started work as a structural design engineer in the Building Engineering Department of VEGYTERV, where he learned the profession from outstanding colleagues. In 1989 he joined the Bridges Office of Uvaterv Rt. Finding sympathy with the high specifications, diversity and variety of the bridge design profession, he has been working on bridges ever since, currently as design engineer with MSc Kft.

Veronika SZÉKELY (1946) graduated as a civil engineer from the Faculty of Building of the Budapest University of Technology in 1970. She started her career in the Building Office of Uvaterv, and continued in the Bridges and Structural Design Office of Uvaterv Rt as project leader and senior design engineer. Since 1999 she has been a senior design engineer with MSc Magyar Scetaroute Kft. Her interest is mainly in reinforced concrete road bridges and in other reinforced concrete and steel structures.

László WINDISCH (1955), project engineer, has been working for the Hidépítő company since 1979. He has worked in various capacities in bridge building and overhaul projects in Budapest and surroundings. He has been a construction project manager since 1996.

DESIGN PROCESS OF THE LOAD BEARING STRUCTURES OF ASIA CENTER



László Poigár



Dr. József Almási



Balázs Karkiss



Péter Varvasovszky



Dr. Csaba Pethő



Erika Tatai

One of the biggest European structures of the turn of the century is being erected in international cooperation in Budapest. The project is a pioneering example of globalisation. Despite all initial difficulties, there is no doubt that this is the way to go. The scale of the project is best described by the floor spaces of the first and the second phase: 120,000 sq metre and 88,000 sq metre, respectively. The characteristic column grid of 8 m × 16 m, the constant and variable load of 20–25 kN/sq metre beyond the own weight of the load-bearing structure and the approved 71 cm overall depth posed a tough task for the structural designers.

Keywords: structural design, Eurocode, pre-fabrication

1. INTRODUCTION

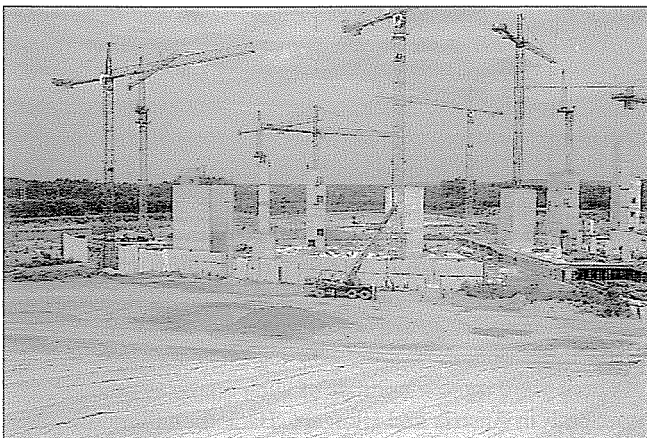
The ASIA Center, located in the 15th District of Budapest will be one of the biggest structures in Central-Europe. Alone the floor space of approximately 210,000 sq metres is indicative of the scale of the building. The Chinese investor, the application of the principles of Feng Shui, the main contractor (Strabag) and the Austrian–Hungarian designer team make the project all the more interesting. Planning started at the end of 1999, the earth- and foundation works commenced in February 2000 (Fig. 1).

The whole structure was completed by the spring/summer of 2003. The reinforced concrete works alone comprise such a serious task that they deserve to be given an account of in *CONCRETE STRUCTURES*. The process of construction could be followed on a daily basis by means of the photographs published at [internet](#).

2. BIRTH OF THE STRUCTURAL CONCEPT, PRELIMINARY STUDIES

The Austrian Lackner & Raml Ltd. searching for a Hungarian structural engineering designer contacted Plan 31 Mérnök Ltd. upon the proposal of Strabag in 1999.

Fig. 1 A bird's eye view of the construction site



The starting conditions of designing the load-bearing structure of the multi-storey building with a characteristic column grid of 8 m × 16 m were as follows:

- The need for floors with the smallest possible structural depth and of an acceptable price. Considering the scale of the building, it was essential that the entire HVA and services system should be installed under the load-bearing structures so that they do not obstruct the design and the execution of the project.
- The need for a structural concept that facilitates the quick execution, possibly using prefabricated reinforced concrete elements.

At the beginning of the design process we could, to some extent, rely on the Árkád department store whose construction was already going on at that time (another main contract of Strabag), but in that case the designers elected to guide the HVA and services pipelines through the floor beams and thereby to employ a larger vertical clearance (the Árkád department store has a column grid of 10 m × 16.5 m and a structural depth of 1.6 m).

In the case of the ASIA Center we had to effect some serious compromise to achieve a structural depth of 71 cm, which, considering the column grid of 8 m × 16 m (1/22.5) is a very good performance.

Another option could have been an entirely monolithic reinforced concrete structure prestressed by sliding cables, which was not advantageous because of the highly complicated floor plans and the dimensions of the structure.

On the other hand, the concept of a fully prefabricated concrete structure had to be rejected too, because the low vertical clearance made it necessary to employ a monolithic concept.

In the case of the *Lurdy Department Store* and the *Interspar Pesterzsébet Hypermarket* we collected some favourable experience with the simultaneous application of very wide, low depth main beams, pre-stressed double-T floor elements and monolithic top concrete. In the case of these structures we could use prefabricated passing columns, stressed and prefabricated beams and floor elements.

In the case of ASIA Center an optimal solution could be achieved by means of a *monolithic column + monolithic beam* (8 m span) + *prefabricated, prestressed concrete T panels* (with a mass limit of 6 tons imposed by the capacity of the tower cranes) + *monolithic top concrete* concept.

Suspending the ends of the T panels could have made the main beams' formwork and reinforcement somewhat less complicated (for suspended beam-ends see Szalay, 1988). After detailed analyses we decided to use the "traditional" method, however: cantilever beams with straight half joint like butts.

After the analysis of the structural concepts and the decision-making process execution planning could commence in February 2001.

April–May 2001 was an especially important period in the structural design of the project. Let us quote from the evaluation written by Mr. Raml at the time:

"As far as the evaluation of the structural concept of the above building is concerned, the most important criteria are as follows:

SOPHISTICATED FLOOR PLANS

The plans supplied by Lengger Architects fulfil the client's needs (Feng Shui spirituality). The arched outlines and the oblique systems of axes result in a structure that is entirely different from other shopping centres. The basic column grid agreed upon with the client is 8 m × 16 m which lends itself for both a monolithic or prefabricated reinforced concrete structure.

BASIC TECHNICAL CONDITIONS

The number of floors planned and the floor heights prevent the use of full-height, prefabricated columns. Theoretically it would be possible to partly prefabricate vertical elements, such as walls, staircases, elevator shafts, columns and combine them with monolithic reinforced concrete.

It would be desirable to build the horizontal structural element, i.e. the floor monolithically. This would enable the construction company to adapt to the floor plans flexibly and to lengthen the prefabricated structural elements floor by floor.

If the floors were constructed entirely from prefabricated floor elements, then a significant number of special elements should be created which would make the lengthening of columns a lot more difficult.

The biggest problem of the construction of the monolithic slab floor is how to limit deflection. This could be achieved by using large expanded column heads sized in proportion to the large grid of 16 m × 8 m. Deflection could further be decreased by incorporating pre-stressed concrete shuttering panels.

FLEXIBILITY OF USE

During the initial period of planning (1 month before the submission deadline of the building permit plans) the final use of a large number of rooms was not clear. Only the deep-level garage and the spaces related to catering seemed to have taken their final shape.

This meant that the structure to be erected had to be suitable for a flexible use and division of floor bays. Internal partition walls had to be connected to the other load-bearing elements of the structure and there had to be an opportunity for subsequent cutting through the floor for services. Experience has shown that in the case of TT floor element the necessity of subsequent cutting in the ribs must also be reckoned with (Fig. 2.).

INCREASED DEMANDS CONCERNING HVA AND SERVICES

Beyond the partly low structural depth a significant amount of pipelines and cable networks must be accommodated.

In the case of a prefabricated floor structure, which could

best be constructed from reinforced or pre-stressed concrete TT floor elements, there would be a need for a high number of rib cuttings. Mainly due to the large penetrations needed for the voluminous ventilation ducts the double-T panels can not be used and maybe some new columns would have to be added to the structure.

If it was possible to construct a monolithic floor; then only the vertical connecting shafts would have to be specified exactly, the horizontal pipelines could be installed without limitations.

CONSTRUCTION TIME

During the preliminary discussions we inquired about the available TT floor element manufacturing capacities of the Hungarian prefabricating plants. Based on the construction experience of a project of a similar size (Lurdy Ház Department Store) 5–6 TT elements per production line seemed feasible. With 3 plants this would mean approximately 15 elements a day. This coincides with our findings in Austria and Germany.

This would mean that for the first construction phase comprising approx. 115,000 sq. metres and requiring 2875 TT panels (40 sq. metre per piece) 190 days would be needed, let alone the manufacturing difficulties of the many different elements.

If three plants were commissioned with the production, another drawback would be that there would be no way to have them compete with each other's price quotations.

If we insisted on prefabrication of vertical structural elements, then we could exploit the capacities of more than one prefabrication plant; in the case of a monolithic slab floor several companies could be invited to increase the speed of construction.

Construction could go on at more than one locations simultaneously without being exposed to the capacity constraints of the manufacturing plants.

COSTS

At the state of the design process in 2002 it was very difficult to estimate the costs considering all aspects referred to above. Below is a simple comparison of the costs of the two different construction systems:

Prefabricated TT panels in the 16 m span direction, prefabricated main beams in the 8 m span direction, approx. 0.425 m slab substitute thickness, approx. HUF 30,000/sq metre.

Monolithic slab with point support, approx. 0.55 m slab substitute thickness (slab+column head), approx. HUF 27,500/sq metre.

With all due reservations regarding such rough estimates it can be declared that there are no obvious differences between the two systems. On the other hand, the installation difficulties of HVA and services are a very important aspect.

PROPOSAL

It is fairly obvious that the most expedient and economical solution would be to combine prefabricated and monolithic elements. The majority of floors could be made of modular floor panels (shuttering panels) or a shuttering system that can be relocated easily. The necessary column lengthenings do not pose serious difficulties. In the case of a monolithic floor slab the floor penetrations and floor edges etc. are not problematic either."

There were quite a number of such analyses made at that time, both in Austria and Hungary. Back then there were sig-

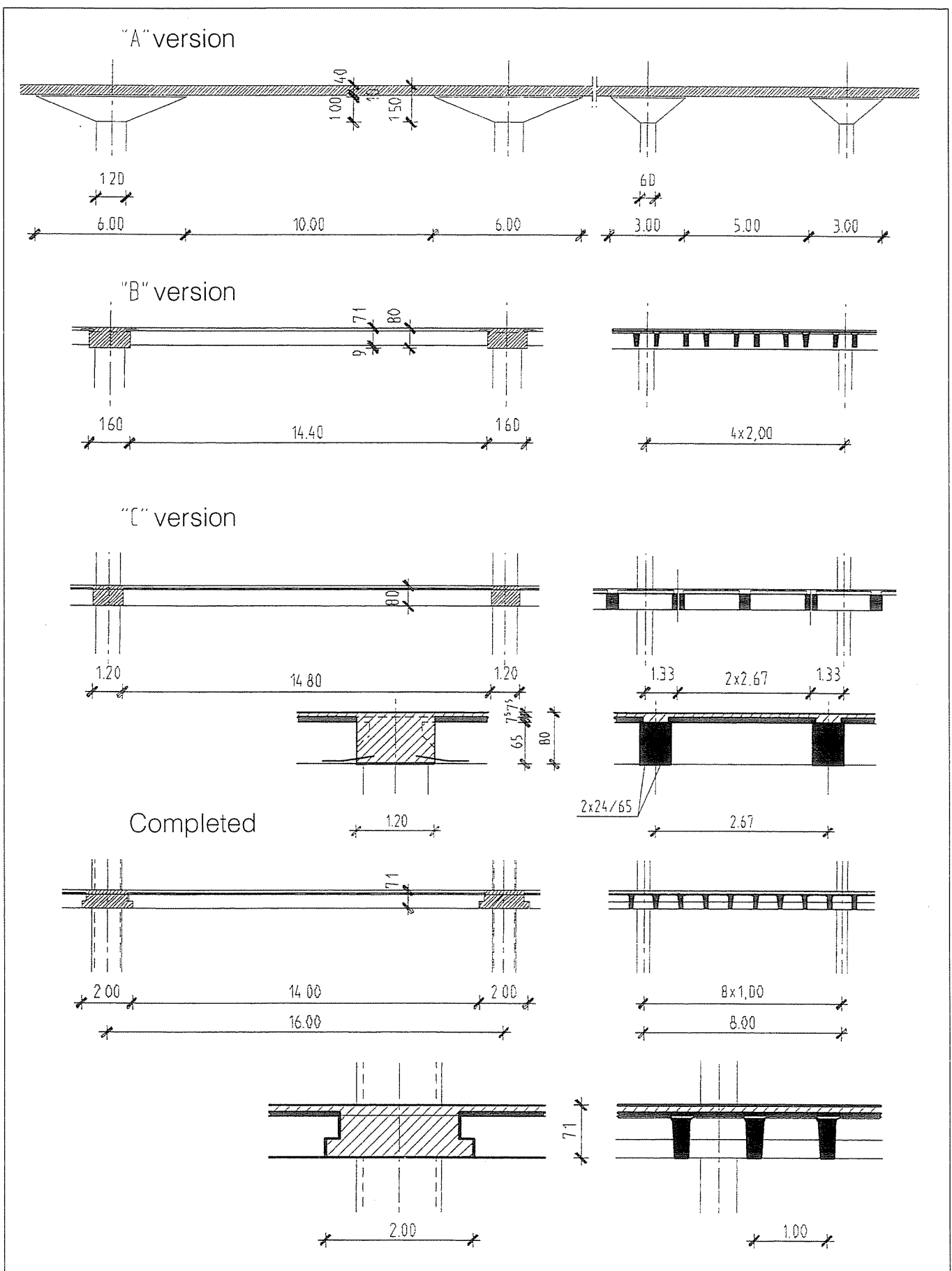


Fig. 2 Various structural elements

nificant differences between the ideas of Lackner & Raml and PLAN 31 Mémnök Ltd. concerning the structural concept of the building. This resulted mainly from the different building traditions and from the different price structures (these issues will be familiar for anyone who has ever worked with foreign

designers). At the time the Austrian partner was evidently reluctant to employ prestressed concrete floor panels. As it turned out during the design meetings this was due to the fact that the specifications of ÖNORM and DIN for prestressed concrete lagged behind modern structural design principles (they were

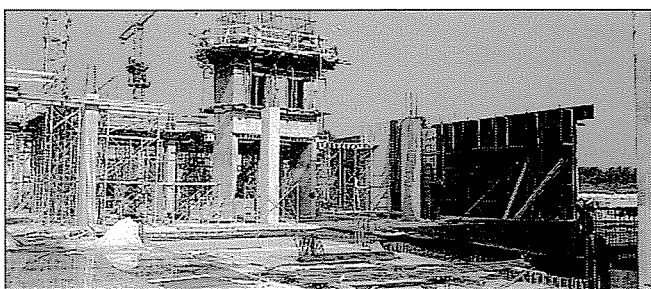


Fig. 3 An elevator shaft constructed with sliding formwork

based on 40-year-old know-how), while our MSZ and especially EC2 are based on crack control. Therefore we have been free in determining the level of prestressing and setting deflection and hogging by varying the ratio between the quantities of the prestressing strands and the normal steel reinforcing bars for at least two decades (and of course we do not determine the concrete cross section on the basis of Magnel's straight line, either).

The use of EC2 – we had agreed upon this at the beginning of the design process, as no international design project could afford not to use it – and the calculations made by the 'abacus' software made it highly convincing that using T and double-T panels is the way to go.

In the meantime, Strabag Ltd. had been working on the construction technology. They decided that the maximum mass of any one element must not exceed 6 tons. In the case of a multi-storey building of such a large ground plan area, the placing of the tower cranes is also a factor of prime importance.

It became reasonable to sub-divide the 8 m span into 8×1 m. Thus, the optimum length of T-elements turned out to be 14 m, which meant the final width of the monolithic beams was 2 m.

Also considering the aspects of HVA the final maximum structural depth was 71 cm (this had to be increased in exceptional cases only, e. g. where the Feng Shui principles required that columns are erected on top of certain beams).

As it was foreseeable, after the basic principles and the structure were finalised, several non-conforming methods had to be employed as well.

The column grid of $8 \text{ m} \times 16 \text{ m}$ was at some places modified to $8 \text{ m} \times 8 \text{ m}$. In the floor bays with a span of 8 m the main contractor required that a floor comprising shuttering panels should be constructed. In these bays there will be 8 cm thick floor elements (shuttering panels) + 22 cm monolith reinforced concrete slabs with a span of 6 m between the 2 m wide beams.

The stiffening cores, the staircases and the elevator shafts formed another set of issues where Hungarian and Austrian ideas diverged. In Hungary it is becoming the standard to build such projects with a sliding formwork (*Fig. 3.*), while in Austria large panel formworks are used for the stiffening cores. Here again, the differences are the result of the diverging cost aspects and work traditions of the two countries.

One big advantage of using sliding formworks is that work-intensive elements are manufactured at the beginning of the construction, and if the flights of stairs are installed at a relatively early stage, then pedestrian traffic is made significantly easier for the rest of the construction time and workers can communicate within the safety of the cores (*Fig. 3.*).

What is a great advantage during construction, however, can make the design process a lot more complicated. The sliding formworks of the cores quickly reach the top floors, so the joints of all floors must be defined at the beginning of the design process. This, considering the complicated character of the building, posed extreme difficulties in the beginning: monolithic beams, T-panels, floor elements had to be connected to each other, internal staircases and stairheads had to

be created. However, all these efforts paid dividends at during the construction phase.

3. DIVISION AND ORGANISATION OF STRUCTURAL DESIGN TASKS

An international design team can only handle the overall design of such a large project involving a foreign client and a foreign main contractor (Strabag International). Lengger Architects (Villach, Austria) coordinate the design of the whole structure. The Hungarian subsidiary of Lengger Architects is Makat Ltd. We are getting used to such design projects without frontiers by now.

Structural design is coordinated by the Austrian Lackner & Raml Ltd. (Villach). Their Hungarian partners are Uvaterv Co (foundation, watertight basin), Caec Statikus Iroda Ltd. (monolithic columns, walls, beams) and Plan 31 Mérnök Ltd. (floors, staircase cores, elevator shafts). Participating Hungarian companies employed further sub-designers.

Coordination between the designing architect and the various participants and the preparation of structural layouts, formwork plans were (and are) the task of Lackner & Raml Architects and involved continuous feedback from their Hungarian partners.

With such large projects, coordination of the teamwork is a huge task in itself. All participants must follow a strict order of positioning, arrangement and documentation.

All statical calculations were made by the participants themselves for their relevant parts of the structure. Dimensioning was based on Eurocode 2, or rather on ENV 1992-1-1 and ENV 1992-1-3, to be precise.

All data supplies were based on reference load values to prevent any errors. It would have been ambiguous to specify calculated values (which is the EC2 equivalent of "critical load" of the MSZ, the Hungarian Standards). For such international design projects the common international language could only be EC2 (and the related EN 206 etc.).

Naturally, all plans were drawn with CAD methods and the Internet played a key role in the flow of information. All plans were delivered on 1 CD ROM and in 3 printed copies in strictly specified (.dwg and .plt) formats. Plans finalised for execution were also published in an extranet for internal use only, so all designers could see on their computers the plans made by other designers. The order of documentation is illustrated by the compulsory "blueprint stamp" to be placed on each and every plan.

The structural design documentation of the "male" and "female" building parts constructed in the first phase (approx. 120,000 sq. metres) consists of some 4000 plan sheets (the design process was completed in December 2001) – this illustrates the absolute importance of a design order.

Below is a summary written by Uvaterv Co. and Caec Ltd. of their respective tasks related to the project.

4. DESIGN TASKS OF UVATERV: FOUNDATION WORKS AND THE WATERTIGHT BASIN

4.1 General description of the foundation

The building is supported by a slab foundation combined with piles. The slab with a thickness of 80 cm (its thickness is

increased at the piles) and the perimeter walls are watertight up to the critical groundwater level. Uvaterv Co. was awarded a contract to design these structures.

4.2 Soil and groundwater

The original site was almost plain, the average ground level was 119–120 m above Baltic Sea. Under the humous surface layer there are very deep fluvial sediments from the Pleistocene and Holocene periods; the sediments are mainly sand soils whose coarseness increases with the depth. Between the granular strata there are lenticular deposits of thin transient and bound strata (silt and muddy rock-flour). The water permeability of the grainy measures varies between $k = 10^{-3} - 10^{-6}$ m/s. The surface of the Miocene substratum varies between 101.1–106.0 m above Baltic Sea. Clay and silt soils have good watertight qualities ($k = 10^{-8} - 10^{-9}$ m/s). The critical groundwater level is 117.0 m above Baltic Sea. The expected construction water level is 114.0–115.0 m above Baltic Sea.

4.3 Dewatering

The architectural and structural design of the building commenced in September 2000 and February 2001, respectively. The construction of the large underground floors below the groundwater level posed serious difficulties. The underground parking floors and the technical rooms required a building pit with an approximate depth of 11.0 m and we had to be prepared for about 4 m groundwater level difference during construction. For the evacuation of water from the building pit we had to choose the most suitable from a number of different methods. Open channel dewatering is mostly used up to a depth of 2–3 metres; to overcome a depth beyond that requires active interventions. In the case of sump dewatering there is no need to build a separate structure but the high quantity of water removed (15,000 cu. metres/day) would have posed unsurmountable difficulties.

The most reliable method for the evacuation of water from the enormous building pit seemed to be a wall encircling the entire construction site, even though this is costly and time consuming. Finally, the building pit was constructed with a pulp wall enclosure connected into the silt–clay stratum. This structure was designed by Taupe Ltd. and is cheaper than a cutoff wall. As it can be partially removed after it is not needed anymore, it does not inhibit the flow of groundwater. A cutoff wall would not have been suitable anyway because of the varied outline of the building and of the ramps leading to the underground parking floors.

28 sumps were installed for the dewatering of the construction site which facilitated a quick reduction of groundwater level. For the removal of the small amounts of water seeping into the building pit a few sumps are operated intermittently.

4.4 Earthwork

Excavation was performed in three main phases; in the first one, soil was removed to 116.0–117.0 m above Baltic Sea level. This is where the pulp wall encircling the construction site starts. Here, a set-off was made and excavation continued down to the piling level. After the piling work was completed, the subgrade level of the foundation slab was prepared. The deepest level of the final earthwork is 111.03 m above Baltic

Sea.

The main contractor (Strabag Co.) required that the sandy gravel bedding layer should be omitted. Even though the subgrade level comprised grainy soils, this was not possible. The coefficient of irregularity of the mainly fine-grained sand found here is low ($U = 2.2 - 2.8$). These soils dodge any concentrated loads (e.g. the wheel load of construction machinery), which means that the earthwork needed for the construction of concrete subbase can not be created. Therefore, the bedding layer could not be omitted for reasons of constructability. A layer of 24 cm sandy gravel ($T_{rr} = 95\%$) was placed under the 6 cm thick blinding concrete layer.

4.5 Piling work

For the foundation of the building SOB piles were manufactured. The load bearing capacity of piles was determined arithmetically and by means of loading tests.

The calculation method employed (Berezantsev) adopts a three-dimensional sliding surface under the tip of the pile; dislocation on this surface is inhibited by the stress region formed around the envelope. The weight of the region acting as a lateral load must be reduced by the friction on the boundary surface of the region. The resulting pile load bearing capacities were used for the preparation of load tests.

During the load tests it posed a problem that the anchoring piles did not have enough reinforcement in them, which meant that the piles could not be loaded up to the breaking point (the anchor steels broke, so this was actually an anchor steel test). The test results were still usable because we defined the load bearing capacity of the piles on the basis of a force belonging to a ~10 mm limit dislocation. The limit load bearing capacity of a 15.0 metre long pile with a diameter of 90 and 60 cm is $F_{H_1} = 2800$ kN and $F_{H_2} = 1800$ kN, respectively.

Piling work was performed by BRK Speciális Mélyépitő Ltd. and HBM Ltd. There were 837 and 335 piles manufactured with diameters of 90 cm and 60 cm, respectively. There is no structure above the loading areas, therefore it was necessary to use anchoring piles here to prevent the levitation of the foundation slab.

4.6 The foundation slab

The spring constant of the piles was calculated from the ultimate load-bearing capacity of the pile and the associated dislocation. The foundation slab was calculated as a slab embedded elastically, with the springs being more rigid at the pile locations. Individual piles and groups of 2–5 piles were used to accommodate the varying pile loads (max. 18,000 kN) of the first phase. According to our calculations the foundation slab could – without the piles and with reinforcement – accommodate column loads of 3500 kN.

The foundation slab was constructed in accordance with the requirements of the Austrian standard. The standard, which refers to the critical part of the building below the groundwater level as the “weisse Wanne” (the white basin), groups the various structures depending on the height of the water column and the dryness requirements. Then it specifies the cracking limits of the individual classes, the sizes of concrete slabs and walls that can be manufactured in one stage, the minimum amount of reinforcement and the joint arrangement should be made.

The base reinforcement of the 80 cm thick foundation slab had a diameter of 20/20 mm. At column loads exceeding 6000

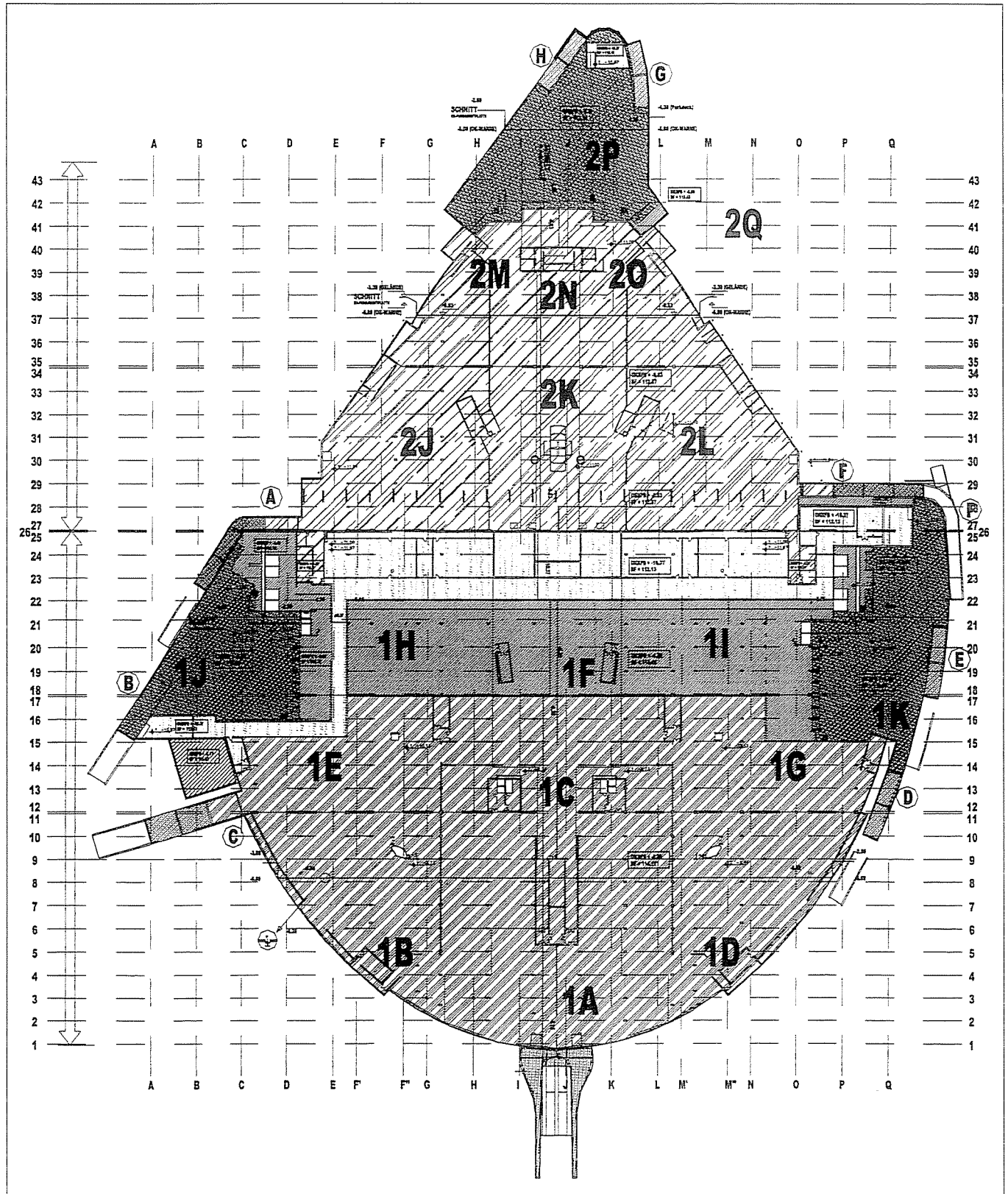
kN, apart from the piles it was necessary to make the foundation slab thicker. The thickness was 1.04 metre and 1.20 metre at the 2- and 3–5-pile groups, respectively, with a splay of 45°. To accommodate the increased bending moment a reinforcement with a diameter of 25/10/20 mm was used, the cracking limit (0.15 mm) could be achieved with a mesh of 10/15/15 mm diameter. For the purpose of punching reinforcement we used hoops with a diameter of 14 mm and 16 mm.

The foundation slab of the building has no expansion joints; it is separated with displacement joints from the loading areas and the ramps only (the slab thickness is a mere 50

cm here). There are two expansion joints in the structure of the underground floors (along axes 11–12 and 17–18). The foundation slabs of the first and the second phase have an expansion joint between them.

At the -2nd underground floor there will be parking spaces, technical and storage rooms. Because of the different functions of the various areas the foundation slab has different levels as required by the architectural concept. The characteristic foundation slab top levels of the first phase are as follows: ground level: 120.00 m above Baltic Sea (-2.50); parking level: 114.14 m above Baltic Sea (-8.36); storage: 116.45

Fig. 4 Ground plan of the building



m above Baltic Sea (-6.05); service tunnel: 112.13 m above Baltic Sea (-10.37); lorry goods distribution: 113.9 m above Baltic Sea (-8.60). Naturally, mechanical shafts were also built.

The concrete technological report specified the maximum size of the largest slab section to be poured in one stage at 24.0 metre × 24.0 metre. The average section size is 16 metre × 24 metre. There were 160 and 87 slab sections poured in the first and the second phase, respectively. Between the individual slab sections watertight joints had to be created, so the construction joints were filled with expansive rubber and the perimeter was sealed with joint band. At the sinkings and the abutment of the slab sections with different levels it was often not easy to place the joint band. Perimeter walls have a thickness of 40–50 cm, the maximum length to be poured at one stage was 8.0 metres.

One of the difficulties related to the construction of large foundation slabs is the prevention of shrinkage cracks. Even though all provisions of the concrete technology were adhered to, in some sections of the foundation slab 0.1–0.2 mm wide cracks formed, which exceeded the maximum allowable limit. The slab sections most affected were poured during the baking hot periods of the summer and the temperature was above the ideal. In the final form of the building some of these cracks will disappear as the slab will bend under the load. At the present stage of the construction it would not be practicable to fill these cracks. Remedying is to be commenced under favourable weather conditions and after the superstructure has reached 50 per cent completion.

Piling and the dimensioning of the foundation slab were not very complicated tasks. The problems mainly resulted from the following factors:

- because of the protracted decision preparation process the planning and construction times were very short
- the large building is difficult to embrace (*Fig. 4*)
- architectural plans were often modified during the preparation of the reinforcement plans
- coordination of the different structural engineering teams
- design was only a few steps ahead of construction
- all plans had to be prepared in .dwg (AutoCad) format.

5. DESIGN TASKS OF CAEC LTD.: MONOLITHIC COLUMNS AND BEAMS

The office joined the execution design process at a comparatively late stage, in March 2001. In May the first columns of section 1D were already manufactured on the basis of our plans and were followed a few days later by the first reinforced concrete walls and beams. This means that there was only little time left strictly for planning and plotting.

As a result of the lengthy preparations we had a mature load bearing structure concept, which meant that Plan 31 Mérnök Ltd. relieved us of the often time-consuming and tiresome task of coordination with the client.

First we calculated the reaction forces communicated by the superstructure to the foundation, so that Uvateriv Co. could calculate the loads the foundation slab would be exposed to.

5.1 Walls and diaphragms

The individual units of the building between expansion joints

had a sufficient number of staircase and elevator shaft cores necessary for the spatial stiffness – this had been the design task of Plan 31 Mérnök Ltd. The monolithic reinforced concrete walls made with panel shuttering were mainly fire impeding walls at the underground floors and external perimeter walls of the superstructure, whose primary architectural function was to divide the space and had no significant role as load carrying structures.

Certain walls, however, played an important role as part of the load bearing structure, of which the building part extending in a cantilevered manner more than 8 metres long above the lorry ramp in section 1G and 1E is an exciting example.

During the design of the walls we were unfortunately often faced with the fact that at this early stage of the construction the formwork plans did not indicate all the necessary penetrations, and what they did indicate was often modified at a later time. As a result, several plans had to be amended subsequently.

5.2 Columns

In order to expedite the execution and design processes we developed a modular reinforcement system for the columns and beams which had the following advantages:

- *From construction-related aspects:* It enabled us to pre-assemble the majority of the reinforcement which only had to be lifted into place upon delivery. Thereby the time consuming task of steel fixing could partly be “outsourced” from the construction site and arranged at outside locations with larger capacities to expedite the works.
- *From design-related aspects:* The results of the dynamic calculation could be evaluated and prepared for design purposes using the load-bearing levels calculated on the basis of the reinforcement modules. Design could be accelerated by the creation of a computerised modular file system. We employed the “block” features of the AutoCad software. This way the designer had to assemble the plans from the modules specified on the basis of the design analysis (statics) and to supplement the modules with the specific features resulting from the actual location of the module in question.

The general column diameter in the underground levels was 116/50 cm, the columns of the upper levels had a circular cross-section and a diameter of 70 cm or 60 cm.

The reinforcement of the columns was designed under consideration of various aspects in a strict system. Such aspects were: easy assembly, good compaction of concrete, minimum amount and economical use of steel and that the reinforcement of the beams should be able to pass above the columns.

We had prepared detailed plans of the reinforcement joints already at an early stage of the design process in order to coordinate the reinforcement systems of the individual supporting structures. When planning the reinforcement system, every bar had its exact location specified to the centimetre. We defined the ultimate optimum location of every longitudinal bar and reduced the number and/or diameter of the reinforcing bars of columns exposed to smaller loads.

5.3 Beams (*Figs. 5, 6 and 7*)

With the exception of certain 14 metre long perimeter beams at the end of the floor sections all beams were made of cast in

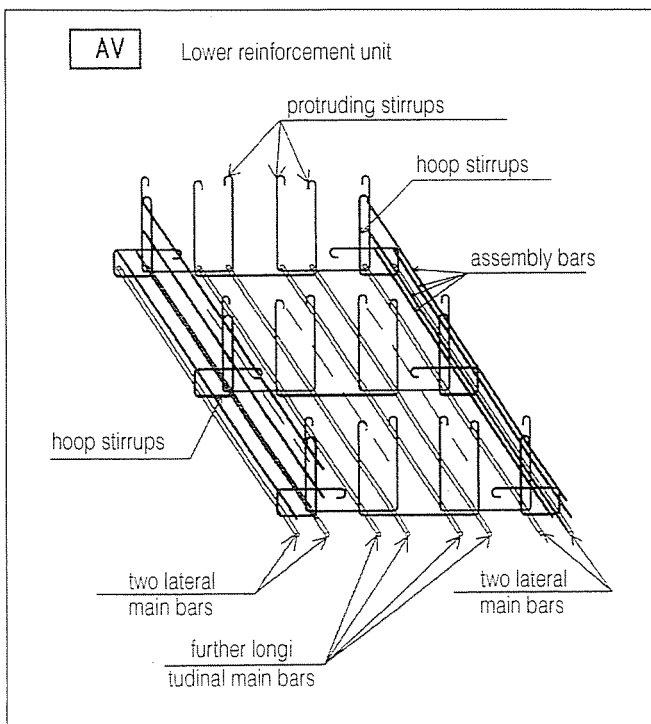


Fig. 5 Scheme of a beam reinforcement assembly

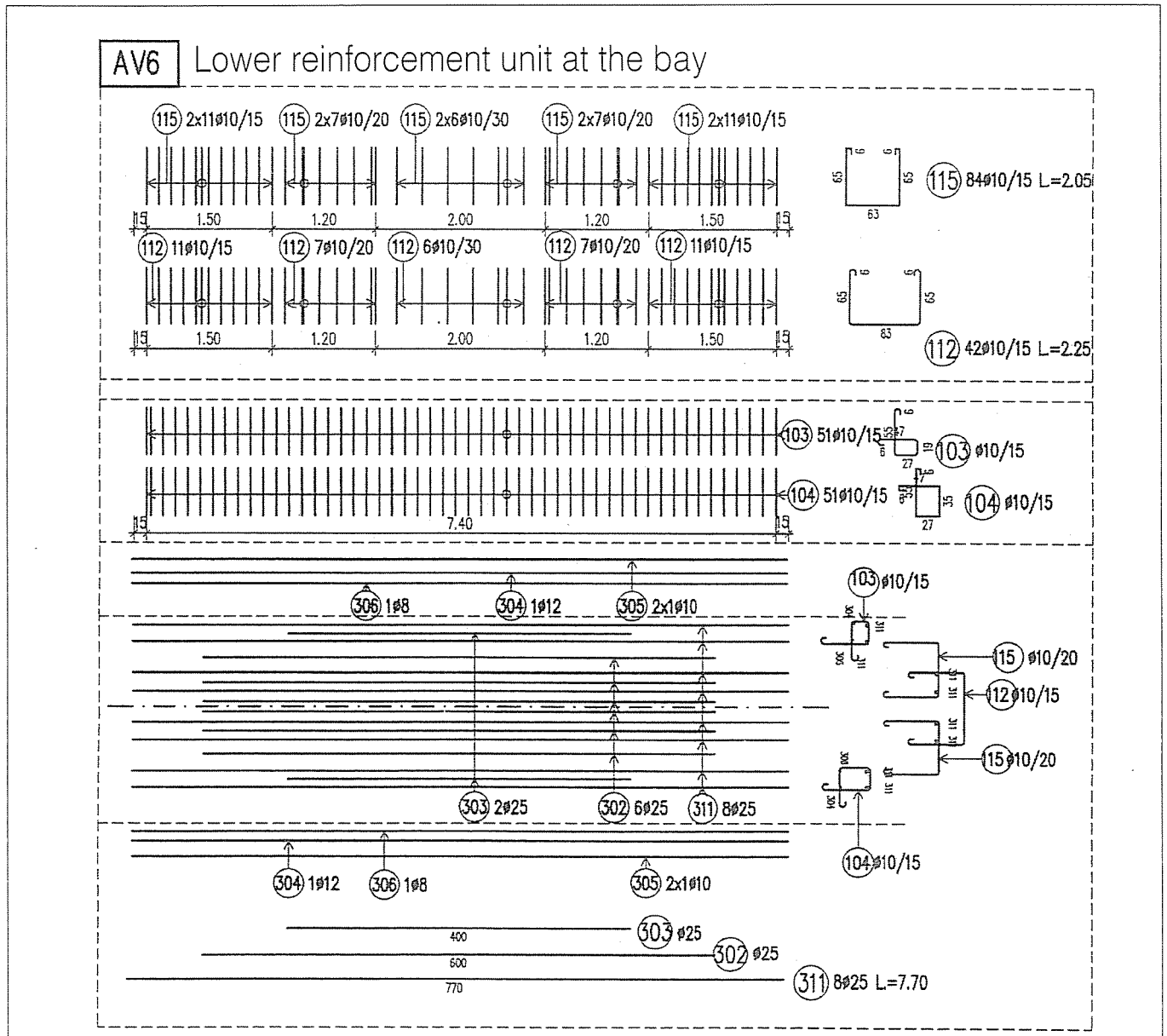
situ concrete. The beams engaged the majority of our design capacities because a large number of often very complicated beams had to be designed. Not even the most common main beams could be considered as conventional with their width of 200 (162) cm and the depth of 71 cm.

One of the interesting features of the load-bearing structure of the building is that – mainly because of the functional differences between the -1st floor and the groundfloor – the loads of walls and columns carrying the loads of more than one levels had to be discharged to columns located at different locations of the floor-plan, which also posed difficulties during the design of beams.

The reinforcement module system was used for the main beams running along the grid axes. The entire reinforcement of the beam was divided into four reinforcement modules between the supports: lower reinforcement module (AV), upper reinforcement module above the support (FV), upper auxiliary reinforcement module (PV) and upper reinforcement module (TV). These reinforcement modules were saved in separate files. The individual modules were supplemented with further modules by changing the number of pieces and the diameters, which resulted in a module library.

The designer after having drawn the formwork of the beam

Fig. 6 The lower reinforcement unit



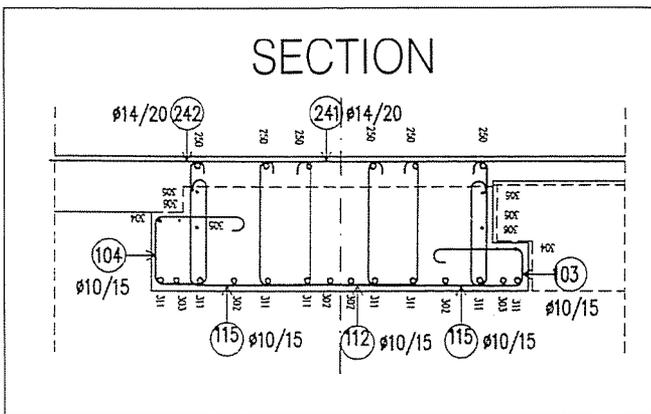


Fig. 7 Beam cross-section within bays

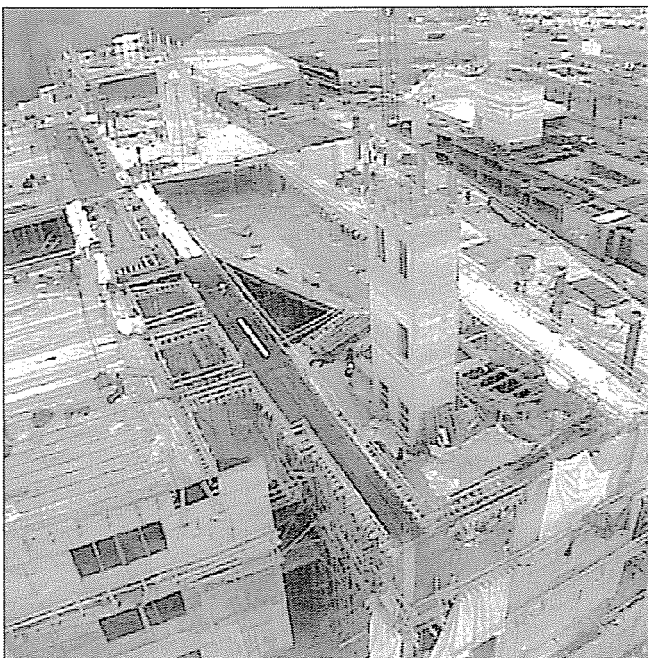
inserted the modules by means of specific handles – the modules recalled the respective cross-sections as well.

Even though the development of the system and the adaptation to a computerised working environment was rather time-consuming, it was worth the effort because our productivity increased significantly. We managed to exploit the biggest advantage of computers: easy duplication and modification.

6. CHRONOLOGY OF ASIA CENTER

- February 2000.** First meeting of Strabag International and Plan 31 Ltd. regarding the ASIA Center Project.
- March 2000.** Contact is made between Lackner & Raml GmbH and Plan 31 Ltd.
- April–May 2000.** Structural variations: Lenger – Lackner & Raml GmbH. – Plan 31. Ltd. One of the most important phases of structural design: the type of structure is decided upon.
- June 2000.** Building permit structural designs (Plan 31 Ltd.)
- July–Dec. 2000.**
 - Invitation of Uvaterv Co. (foundation works, watertight basin)
 - Contract preparation between client

Fig. 8 The “male” section of the building at the end of January 2002



January 2001.

and main contractor (the most time consuming phase of the project)

- Invitation of CAEC Ltd. – the protracted preparation resulted in a significant lack of designer capacity
- The structural design team is complete: Lackner & Raml Ltd., Uvaterv Co., CAEC Ltd., Plan 31. Ltd.

February 2001.

Contracting for the execution design of the supporting structure. First phase: “male” and “female” building part, floorspace of 120,000 sq. metre.

March–Dec. 2001.

Execution design process

May 2001.

Critical phase of execution design process; communication problems emerge. Data supply among individual disciplines mutually delayed.

In the meantime, execution starts in full force

June 2001.

The designers’ team is getting welded together, communication problems are solved (coordination of Internet-based design, of different drawing software and establishment of documentation discipline).

July–Aug. 2001.

Extreme efforts of all participants; summer holidays are abandoned.

September 2001.

Design process back to “normal”. In the meantime it turned out that the decision concerning the structure had been correct: quick execution is feasible, spirits rebounded.

November 2001.

The “male” part is completed (Fig. 8.). Construction of the “female” part is accelerated. Decision is made concerning the 2nd phase (the “Father”); preparation of the design process of the 2nd phase, contracting for the execution design of the 2nd phase (88,000 sq metres).

Jan.–Aug. 2002.

Structural design of the 2nd phase.

June 2003.

ASIA Center opened (projected date).

7. CONCLUSIONS

The design and execution of ASIA Center showed that Hungary already acts as a member of the European Community, at least as far as construction activities are concerned. Eurocode standards are part of our everyday reality, even though they are still not as mature as an EN standard.

8. REFERENCES

Károly SZALAY (1988) *A new type of suspension assembly at the cut-out end of prefabricated reinforced and prestressed reinforced concrete elements (in Hungarian)* (Magyar Építőipar, Issue 9–10, Vol. 98)

THE AUTHORS

László POLGÁR MSc (1943): civil engineer; Technical University of Budapest, Faculty of Civil Engineering; 1966 – Foreman in Hódmezővásárhely, 31. sz. AÉV (State Building Company No. 31.); 1970–71 Structural Designer, IPARTERV; 1971 – Product developing engineer, chief process engineer, head of the Technical Main Depart-

ment, 31. sz. ÁÉV; 1992 – managing director, PLAN 31 Mérnök Ltd., managing technical director, ASA Építőipari Ltd.

Activities: design and construction of prefabricated reinforced concrete structures and industrial floors. Chairman of the Concrete Section of the Hungarian Building Material Association; member of the Hungarian Group of *fib*.

Dr. József ALMÁSI MSc (1940); 1964–1966: Mélyépítő Vállalat (Hungarian State Foundation Engineering Company); 1966–1995: Faculty of Reinforced Structures of the Technical University of Budapest; 1995–to present: managing director of CAEC Ltd.

Activities: execution, education, research, design. A member of the Hungarian Concrete of *fib*.

Balázs KARKISS MSc (1973); static designer of Plan 31 Mérnök Ltd.

Activity: Designer of Óbuda Center, Csaba Center, Metro, Tesco, Praktiker department stores and reinforced concrete structures in Romania and Bulgaria.

Péter VARVASOVSKY MSc (1977); static designer of CAEC Ltd. (MOM Park, Cora Hypermarket Miskolc, Zollner Elektronik Vác manufacturing hall, gate-keeper's lodge and office block, Szeged Sewage Treatment Plant, Trend manufacturing hall).

Dr. Csaba PETHŐ MSc (1948); 1972: static designer of Út- Vasútervező Vállalat (Hungarian State Road and Railroad Design Company); currently the deputy head of the Underground Railway- and Structural Design Office of Uvaterv Co.

Activities: designer of tunnels, underground railways, reinforced concrete structures, underground structures.

Erika TATAI MSc (1973), Technical University of Budapest, Faculty of Civil Engineering; 1997–1999: Geo Terra Geotechnica Iroda. Currently a design engineer of Uvaterv Co.

Activities: designer of reinforced concrete structures and underground parking lots.

REINFORCED CONCRETE FRAME STRUCTURES IN EASTERN EUROPE



Assoc. Prof. Zoltán Kiss

In the last years, a new type of reinforced concrete frame structure has been widely used. When compared to the typically used long-span structures, the main difference consists of the substitution of TT roof panels with large ribbed tucked panels. Such structures are now used across almost the entire Eastern European area with small modifications. One of the main issues regarding use of such structures is their resistance to earthquakes.

Keywords: frame structures, anti-earthquake protection, projecting

1. ANTECEDENTS

The history of development of reinforced concrete frame structures in East Europe have common roots. The period 1948-1960 was defined by monolithic building and precasting in the construction yard which in time developed into industrialized prefabrication. Thus, in the 1970's the "type" structures were developed along with the general tendency of "typization" of the structure. Halls covered with T or TT elements gained more widespread applications when compared to other structural design conceptions.

By the end of the 1980's however, the number of built objects and the demand for other industrial buildings drastically decreased.

Following the political changes, the interest in reinforced concrete structures reached a low ebb and most of the prefabricating factories stopped production. The few which continued to function proved to be hard to sell in the privatization process even at a small price.

The prefabrication industry hardly survived during these years and this was not due to the reinforced concrete industry, which has proved to be one of the main construction materials used throughout the world.

Meanwhile, the imported steel structures (Lindab, Buttler, Astron etc) appeared on the market. Thanks first of all to the intensive marketing activity of the producers, this type of structure was a success. On the other hand, it was made just a too few same activity for the reinforced concrete.

This situation starts to improve after the arrival of the first foreign investors and after the completion of some commercial and industrial buildings. In Hungary development started immediately after the political changes, while in Romania only at the end of 1990's. In the Ukraine this is only now expected to develop over the next few years. This process has a non-uniform character.

This mode of thinking and the efficiency of the foreign investor employed with market economy rules had an effect even on the structures of the halls.

The actual price of the steel structures is higher than reinforced concrete owing first of all to severe fire protection standards. Many fires occurring in Romania or outside the country have proved the efficiency of reinforced concrete structures. In these cases it was sufficient to change some beams, because of the large bending-deflection, but the steel structures were completely damaged. Owing to this aspects, at this time at the tenders for halls, near steel structures appear success-

fully the reinforced concrete structures, and we can say that in the contest between the steel and the concrete, by the construction of the halls, the concrete leads in Hungary and even in Romania too.

2. MODERN FRAME STRUCTURE FOR HALLS

We can define "modern structures" as those structures which appear with the first foreign investors in Romania, and still define the ground floor halls. In Eastern Europe the Metro stores represent the challenge.

The Metro and Macro store-chain, with over 350 commercial outlets across Europe emphasize the consumer's comfort whether the store is in London or in Moscow.

Why is this structure an innovation? Compared to the old structures the roof solution is the major change. The halls built before were covered with heavy elements made of prestressed concrete, ECP or TT type. Modern halls are made with tucked iron panels with large tucks. In most of the western countries, the tucked iron panels, protected against corrosion, had been taken out the market of reinforced concrete covers.

The structures made in this way can be named "light reinforced concrete frameworks", because their own weight of structure is between 160-200 daN/m², while the halls covered by prestressed concrete elements have the weight between 350-450 daN/m².

The advantage of tucked iron panels consists of the fact that the admissible distance between the wedges increases up to 7.5 m, or in cases when the hall has the span up to 7.5 m it might abandon using wedges. The minimum thickness of the tin is 0.88 mm, but in case of larger spans and bigger snow loadings this can reach up to 1.5 mm thick. In snow agglomeration areas two overlapped tucked iron panels may be used. By eliminating the heavy surface elements made of reinforced concrete or prestressed concrete, considerable reduction in the self weight of the structures can be achieved. This reduction at the roof level is a real gain regarding the structure's behavior during seismic movements.

After the eight commercial halls built in Hungary by Metro with a framework of reinforced concrete, the construction program started in Romania in 1996. The first two halls built in Bucharest were of a mixed structure: the roof structure from

steel (for the first time in Metro store history) and the columns from reinforced concrete. This was due to the short time period and the danger of seism. The protection cover for fire applied to the steel elements, together with the overdimensioning because the seismic area in which they were constructed, made the cost of investment double compared to similar examples from other countries.

In the case of the third Metro store – built in Timi^ooara – the investor imposed that the structure to be made completely from reinforced concrete.

The constructors' desire that in the case of the Metro stores to be built in Romania – that the experience accumulated in similar constructions made in Hungary – was obvious. So, the reinforced concrete framework blueprints for the stores in Timi^ooara and Bra^oov were elaborated by PLAN 31 MÉRNÓK Ltd. (Hungary). By the same token, the construction elements were manufactured by ASA ÉPÍTŐIPARI Ltd., a firm whose factory location is Hodmez^ovásárhely. For the hall in Bra^oov many elements were realized in collaboration with the firm Prescon (Bra^oov).

Actually, with the appearance of the PLAN 31 MÉRNÓK Ltd. and ASA ÉPÍTŐIPARI Ltd. the "resurrection" of the prefabricated reinforced concrete industry in Romania was started. The project office PLAN 31 Ro in CLUJ NAPOCA was opened and the prefabrication factory from Turda was bought by ASA ÉPÍTŐIPARI Ltd.

I would like to stress the incontestable contribution of Mr. Polgar László and Mr. Abraham András for the resurrection of the prefabrication industry in Romania.

At the conception stage of the design the bay size was considered for the stores in Bucharest. Instead of the 10x20m spans used in Hungary the 14x21m bay size was chosen. In other respects everything was designed using the existing models from Hungary.

The reinforced concrete framework was executed in 15 weeks and proved to be an efficient solution comparable to a steel structure. There followed the decision to employ the design for subsequent hall structures based upon the structure used in Timi^ooara.

Consequently, the third Metro store from Bucharest and the next eight halls were designed by PLAN 31 Ro, firm from Cluj Napoca, and the building elements were made in the ASA's prefabrication factory from Turda.

Meanwhile, in Bulgaria, Russia and Croatia, Metro stores spread quickly with the investor applying the experience gained in Hungary. The main advantage of these structures is the short

time of execution because for the investor the investment process time and the purchasing cost have major importance. Even if in some countries the wide application of this kind of structures wasn't achieved without obstacles, the advantage mentioned earlier guaranteed certain success. Recognising the behaviour of these structures relative to earthquakes made further positive contributions to the spread of the system through the region.

The latter fact is to acknowledge that Hungary and Ukraine, Romania, Croatia and Bulgaria are active seismic areas.

3. THE EFFECTS OF EARTHQUAKES ON THE NEW FRAMEWORKS

3.1 Seismic conditions

All structural conceptions of an object to be built depends on the proposed location and this why it is vital to have data which respects local expected seismic conditions.

The intensity of an earthquake varies according to the following parameters:

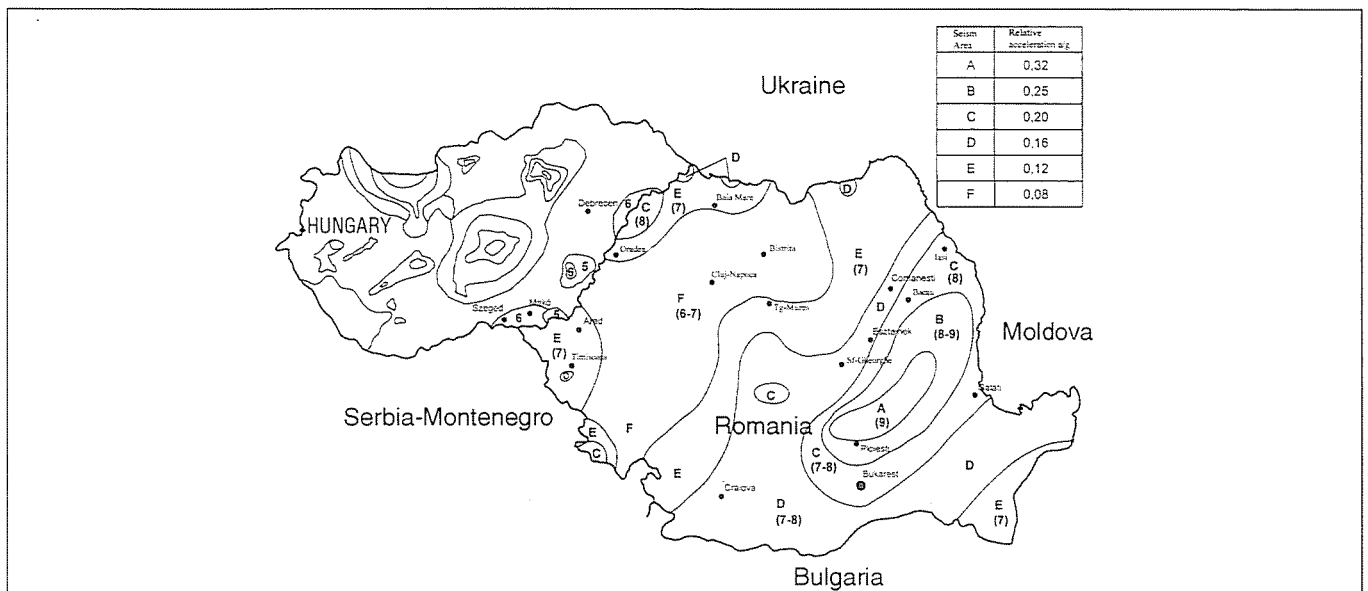
- The hypocenter depth
- The distance from the emplacement to the epicenter
- The earthquake magnitude
- Geological and geographical conditions
- The foundation soil property

There are many epicenters in existence in Romania. The place of the strongest earthquakes measured so far in the country is near the city of Vrancea in the curvature of the Carpathian Mountains. This is the deepest hypocenter in Europe and where strong earthquakes can be expected every 50 years. Seismic areas where surface earthquakes are registered can be found are near Timi^ooara and between Carei and Valea lui Mihai. The moving frequency of these earthquakes is very high, and they appear once in every 100 years.

A structural engineer is interested in the dynamic properties of earthquakes and with which data he/she is able to make verifying calculations.

Usually an earthquake is defined by the measure of seismic intensity and according to the value of seismic acceleration. The seismic map of Romania (Fig. 1) is elaborated and based upon the measured seismic intensity. Accordingly, the strongest earthquakes

Fig. 1 Seismic map



Properties	Area near the epicentre	Area at a distance from epicentre
Soil		
The soil movement		
The movement vertical component		
The seismic speed		

Table 1: Difference between seismic effects

are generated lop-sided oriented on a NE-SW axis. Also observable are the actually recorded seismic areas measured by the standards as noted with the letters from A to F and which depend on the earthquake intensity produced. Additionally, *Fig. 1* records the maximum value of the intensity measured on the Richter scale. Also note that this figure only represents the cities where the structures in question were built. It can also be observed that the most of the halls were built in the areas where the seismic movement is medium or high. Near the border with Hungary are areas with surface earthquakes and in this areas the calculations are made with different values on the two side of the border.

The surface earthquakes properties are:

- direction of propagation
- amplitude
- speed
- acceleration

The places in seismic areas characterized by surface earthquakes are classified depending on the distance to the epicentre:

- at 150 km
- at 25 km
- at 5 km

The different seismic effects which are produced from one distance to another and must be considered.

The difference between the two effects is presented in *Table 1*:

- near the epicentre, the direction of propagation has a higher importance than the stratification of the foundation soil;
- the speed of the movements are very high (3-4 m/sec) in the areas next to the epicentre, and for those far away, it was measured at 0.3-0.5 m/sec;
- the vertical component of the earthquakes is more important than the horizontal one near the epicentre, and their frequency is very different from the horizontal ones.

Further we will present the earthquakes of VI degree (F) because, in case of a well conceived structure executed with attention and with quality materials, this movement do not represent a true danger.

3.2 The questions of the design

It is well known that the seism is a sliding movement with an alternative dynamic effect which produces some plastic areas in the structure. Because they are a complex energetic process

and not static forces, it is very hard to evaluate their effects statically.

A structure's strength to an earthquake depends on the framework's property to develop sufficient potential energy to absorb the kinetic external energy produced by the earthquake. A frame structure, owing to its flexibility through deformation, is able to absorb kinetic energy and survive an earthquake. But is it possible to build any structure which is resistant to a high intensity earthquake without minimal damage being produced?

The statistical data which are available to the design engineers concerning earthquakes is poor and unsure. Therefore, in the design of some structures liable to strong earthquakes the engineer must assume a risk.

The compulsory standards in the structural design do not contain answers to each difficult problem, even if they are under continuous development. For example, the Romanian standard first elaborated in 1977, was resumed in 1990 and at this time it obliges the engineer to use more certain dimensioning. The assumed risk by the engineer does not depend only on themselves or the seismologists, but is also part of the design standards of several countries.

It must determine that the buildings designed by us cannot be considered as perfect because the adopted technical solution and the evaluation of the risk are decisions which are economical in character. Thus, even our structures are not free from financial constraints. On the other hand, we always have to consider that the absolute safety (if we can say that in case of the seism), and an assumed risk which is too high is at the same time inefficient. Thus, we try to establish for each project an optimal risk.

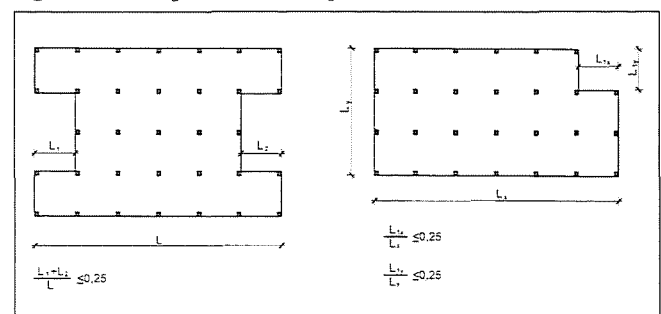
In the case of the strongest earthquakes measured in Romania (1940-1977), the effects of the seismic waves on different structures are visible. The halls prefabricated with reinforced concrete frames had a pretty good behaviour during the seism from 1977, but we have to mention that most of the structures had column distances of 6-9 m and spans of 12-18m.

Ground floor halls designed by us have the bottom of the columns fixed and hinged tops, and this is why the structure's spatial rigidity has a major importance and this applies also to the knots conception, the columns ductility and the stability of the foundation blocks.

a) The rules of the design

Besides the correct dimensioning of the elements, it is recommended always to respect the structural rules, even if they do not look quite complicated in the case of ground floor halls. The shape of the buildings in horizontal and vertical plans are to be regular, to avoid the halls with T or L shapes in the horizontal plan and to avoid torsion of the buildings during an earthquake. If, by architectural design, there is an inevitable concave shape to a hall, the dimensions of the entrances and exits have to be less than a quarter of the total area of the hall (*Fig. 2*). The remedy in the case of a concave shape, both in

Fig. 2 Permitted ground plan arrangement of halls



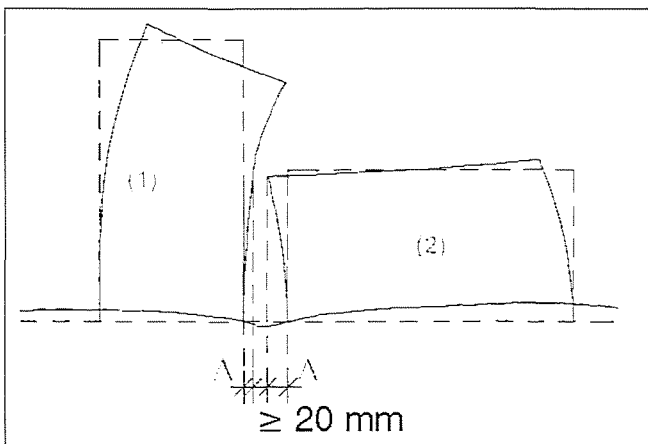


Fig. 3 Definition the seismic joint

the vertical plane and the horizontal, consists in foreseeing seismic joints between the building sections.

The dimensions of the seismic joints and contraction joints are calculated based upon the data derived Fig. 3, with special attention to flexible structures where the movement amplitudes are higher than in the case of rigid frameworks.

$$d \geq \Delta_1 + \Delta_2 + 2 \text{ mm}$$

where:

d – dimension of the seismic joint

Δ_1, Δ_2 , - maximal lateral movements of the buildings at the highest point of the hall. The maximum lateral movement of the ground floor halls is $\Delta_{\max} < H/100$, so we can see that in the case of higher halls the seismic joints become larger by 50–100 mm, especially due to the value of Δ_{\max} which must contain the remaining movement too.

The seismic joint must be conceived in a way to be identical with the contraction joint because they are always realized by columns duality and not with secondary structures.

The maximal dimensions of the seismic joints and contraction joints are the following, depending by the seismic areas:

- 150 mm in E and F areas;
- 120 mm in C and D areas;
- 95 mm in A and B areas

Another important request for the structures placed in the seismic areas is that the self-weight of the structure is to be as light as possible. These new structures fulfill this demand very well. On the other hand, it is very important to understand the special behavior of the structure which depends strongly on the cover rigidity from the washer effect of the tucked panel. However, with regard to this we have less experience of this type of cover, especially when we are concerned with rein-

forced concrete structures. Lately, more and more articles have appeared, proving the efficient washer effect of the tucked panel roof on the halls with steel strength framework.

According to accumulated experience, the greater efficiency of the tucked panel against lateral movement of the compressed areas, of the panels on main beams, when the panels are placed with perpendicular tucks on them, has been proved.

Research carried out in Romania (Dima Mazzolani 1990) and other countries, shows that tucked iron panels fixed on two or four sides to the concrete structure have a washer tendency even better than the wind bracing (Fig. 4). The bearing of the panel fixed on four sides is comparable with the panel fixed only on two sides and the wind bracing together.

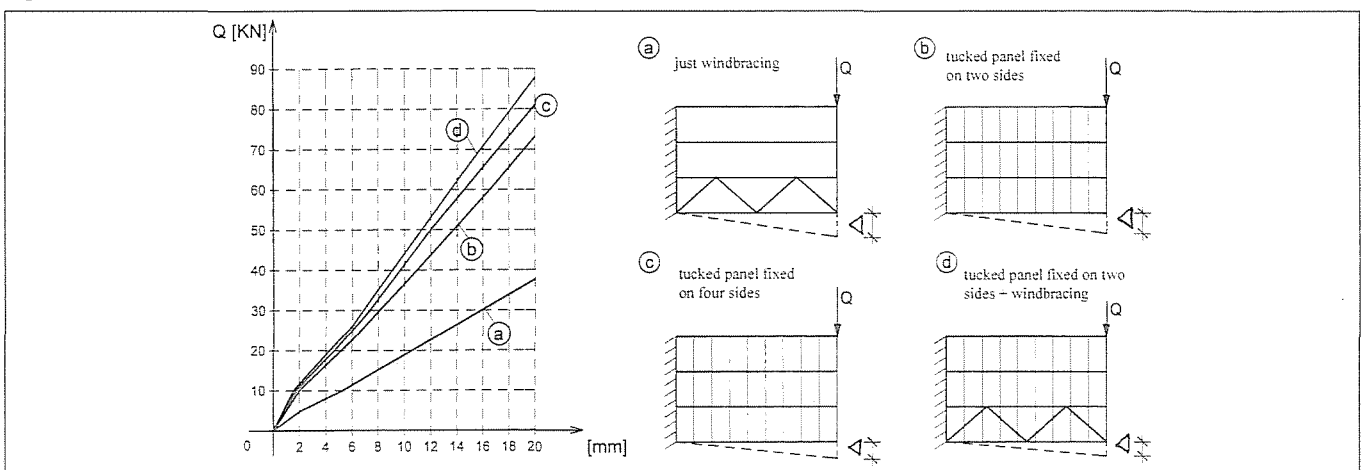
The tucked panel fixed on two sides presumes that the panel is attached with screws in each tuck. The appendage on the two sides is more difficult because the wedges underpin the main beams, so the superior sides of the beams are not in the same plane. This problem could be solved in two ways: using metallic attachment pieces, or with over-concrete of the main beam at the necessary benchmark. This last solution was used at the Metro halls in Bulgaria (Fig. 5). If the spaces between the screws are small enough, the curves “c” and “d” almost superpose. The curves from Fig. 4 were traced with monotone horizontal loadings. For alternatives the technical literature presents very little data. Until there is complete settlement to the problem it is recommended to use horizontal wind bracing under the tucked panels in the plane of the roof to stiffen the structure. We have used this. (Fig. 6)

We choose this solution because if we do not use wind bracing in the B and C zones, we need a tucked panel of 1.25 mm thickness. Using both the wind bracing and the tucked panel, we reduce this thickness to 0.88 mm. In the terms of costs the two solutions have almost identical results, but with the chosen method we reduce the execution speed, the tucked panel being cached only on two sides. According to our conception the horizontal and the lateral washer have effects only against excessive lateral movements.

The existing seismic standards recommend that the structural concept be as simply as possible, with the gravitational loadings to be transferred to the foundation soil through the shortest route possible. It is not recommended that the columns bear on the beams, and in addition that a beam does not bear on another beam. Taking into account this prescription our tender on the ground floor halls is shown in Fig. 7 which accords to the grating and hall placements.

In order to avoid the general twisting of the halls during an earthquake, the arrangement of the reinforcing systems and the distribution of the structure mass must be carefully carried

Fig. 4 Force-deflection curves in case of various roofs



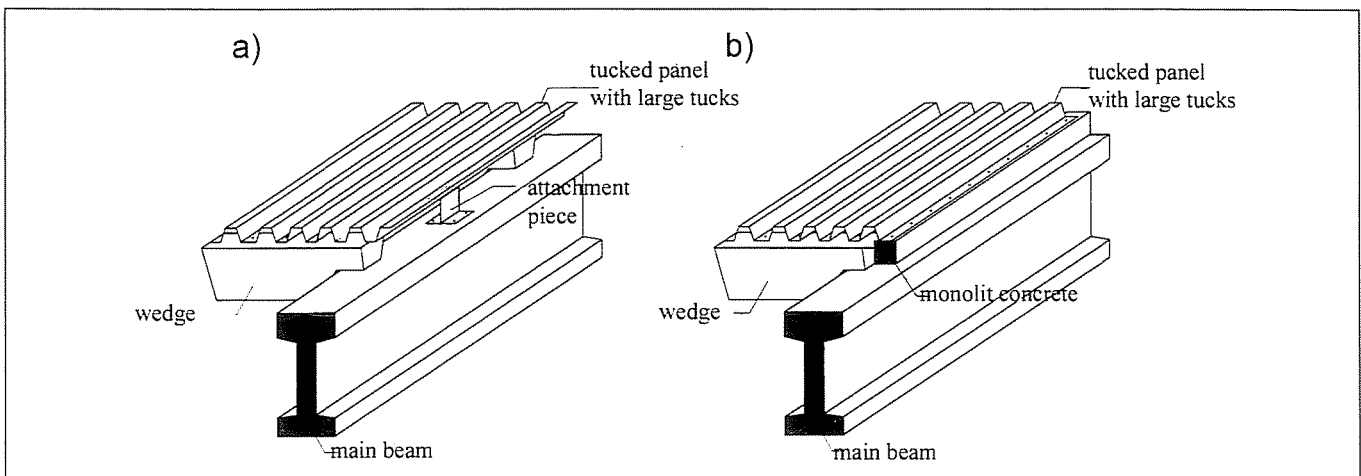


Fig. 5 Tucked panels for metro halls in Bulgaria a) fixed by fasteners b) with counterweight

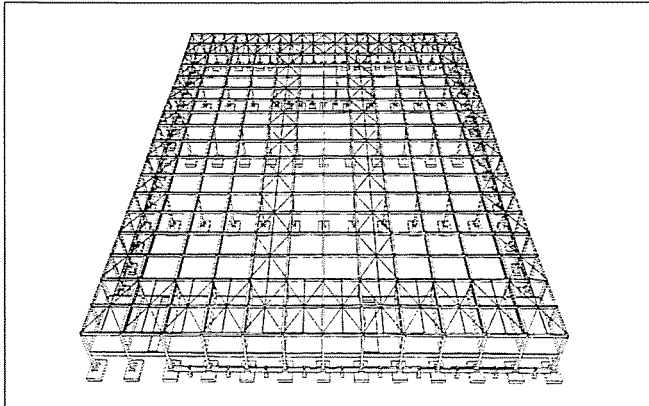
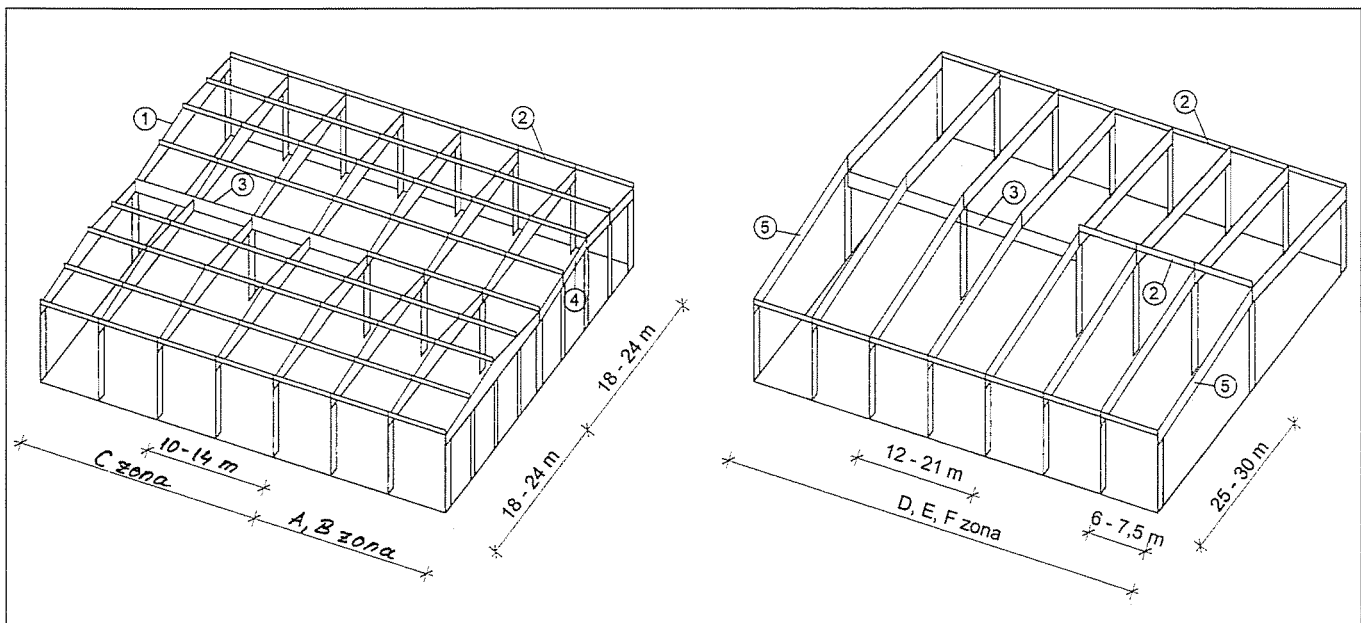


Fig. 6 Horizontal wind bracing under the tucked panels

out. Here we refer to the intermediate floor, which in most cases sends to the marginal columns the loading received, leading to an increased bending moment. So even if on the first sight it seems a strange - that the central columns which take the bulk loading and marginal columns liable to stronger bending moments of the halls - it will have sections with identical dimensions and the reinforcement of the two types of columns is usually identical. On the other hand, we have to be careful with the closure walls and the dividing walls not to work together with the structure, which can result in a negative effect on the movements which brings about hall twisting.

Fig. 7 Arrangement of single storey R.C. frame structure 1-main girder; 2-gantry; 3-longitudinal beam; 4-divided beam; 5-main girder-gantry



3.3 The seismic calculation of structures

When evaluating seismic effects on structures and choosing the design procedures there are two important aspects to consider:

- the structural model chosen must correspond with the static and dynamic properties of the real structure
- the calculation must give results as close as possible to the reality predicted by the pattern movement concerned

Concerning the patterns there are some simplified forms of real structures and the results can not be others than approximations. Most of the automatic calculation programs (Nemetschek Feat 2000, Drain, Grintec Effel 2001, Axis, etc) use the method of the replacement of the seismic effect on the structure with stresses.

In each country, the seismic stress, an inertia force from the acceleration in movement of buildings, is regularized by the standards. The Romanian standard (P-100-92) uses the following relation:

$$S_{M,S} = k_s \cdot k_g \cdot \beta \cdot \Psi \cdot \varepsilon \cdot Q$$

where:

k_s coefficient of the building's importance, depending on the importance classes (1.2 in case of commercial centers, 1.0 for industrial objectives).

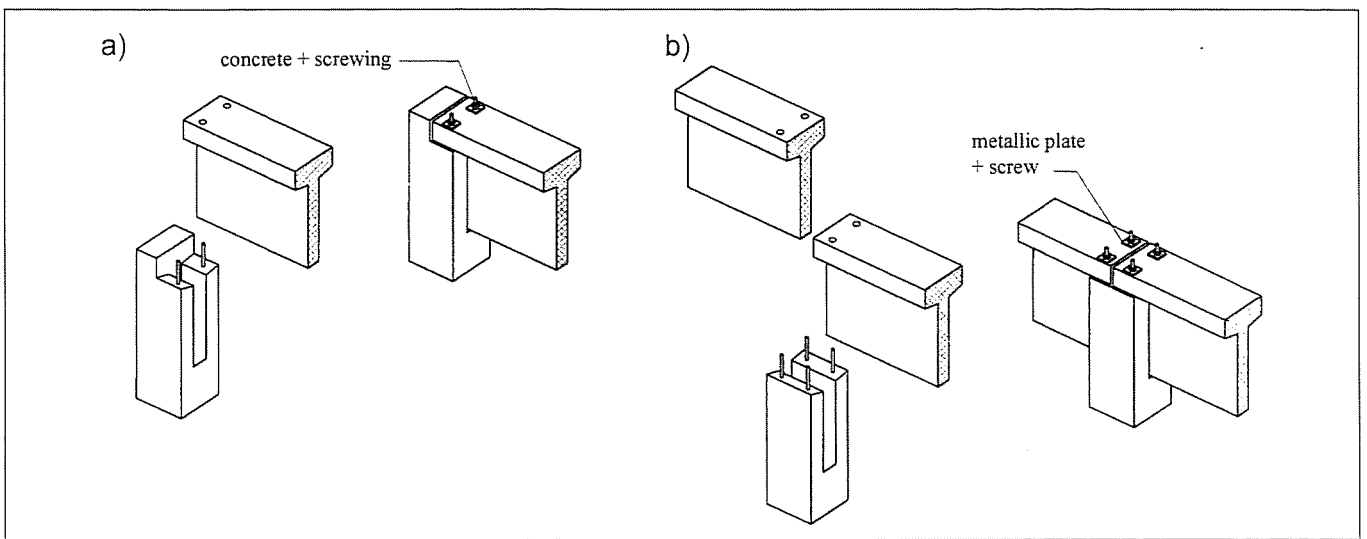


Fig. 8 Knots with pitchforks a) extreme b) intermediate

k_g relative acceleration (Fig. 1)

β dynamic coefficient, depending on the natural period of vibration of the structure (Fig. 11), 2.5 – at the ground floor structures

Ψ coefficient of decreasing seismic effects (0.2 in case of ground floor structures, if the knots between the beams and the columns are articulated)

ε - coefficient of equivalency between the real system and a system with a freedom degree adequate to the own environment

Q – resultant of gravitational loading for the entire structure. The seismic stress must be evaluated for each individual period of vibration, this being a horizontal force applied to the concrete floor.

c) The conception and dimensioning of knots

Technically speaking, the static structure knots define the domain of using carrying structures. In the area of prefabricated reinforced concrete, the most difficult problem consists in making hinged knots. This system is based first on the knots with pitchforks (Fig. 8). The solution was used more and the novelty is that instead of welded joints, an easier and faster procedure concerning the execution is used – using an arbor. In the case of prefabricated reinforced concrete structures a special problem concerns the achievement of a hinged noose. It is recommended to put the beams into the pitchfork created at the top of the columns. The method was used a long time ago – the innovation consists of the fact that the attachments with solder were replaced by an easier and a faster procedure (from the standpoint of execution) - the screw taps procedure. Ending the assembly phase, the holes around the screw taps are matted with expansive mortar. In the case of dangerous seismic areas, the top of the screw taps is fixed with a supplementary washer and a twist. Depending on the section and the span of the beams other types of noose are used (Fig. 9). Due to powerful local tensions, a danger of local degradation occurs in the underpin area at beams with wide spans.

Using epoxy mortars or metallic pieces are overdone solutions, replacing the rubber bands (neoprene). The advantage of these elastic bands appears in the absorption of seismic energy and in the decreased thermal dilatation effects. Thus, the dilatation length of halls can increase or even double, given the well-known 60 m.

Obviously the knots used in Metro halls in Hungary should be reconsidered because the beams shape was given and the

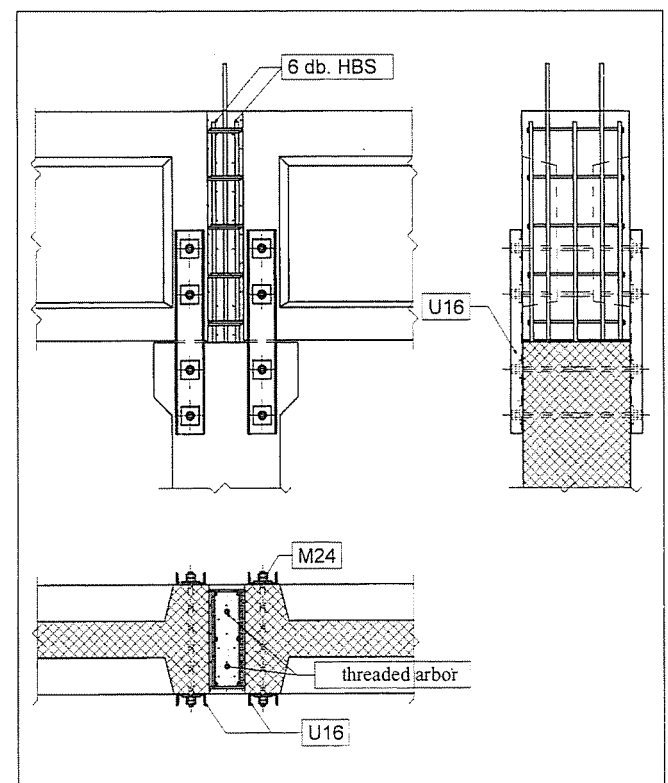
restricted time didn't allow for a new casing. The first knots were conceived with monolith concrete metallic profiles cached with screws. In Fig. 9 we can see the solution with four screws.

Unfortunately, monolith concrete proved to be not the best solution because of the early set-up of the beams. The contraction of the concrete between the prefabricated beams head and the monolith concrete produced crashes. Later, it was adopted only when fixing the beams with metallic pieces.

A new type of main beam was used at the Metro store in Ploiești (seismic area B) and in the next halls, which allowed the use knots with pitchforks (Fig. 10). We attached a lot of these types of knots because the earthquake of 1977 proved it to be a good conception. It is no less important than the fact that owing to this beam we succeeded in reducing by 15% the structure's self-weight.

Obviously, the dimensioning of the metallic elements and of the concrete of a knot should be applied separately for a replacing horizontal force double that of the seismic stress.

Fig. 9 Other knot arrangements



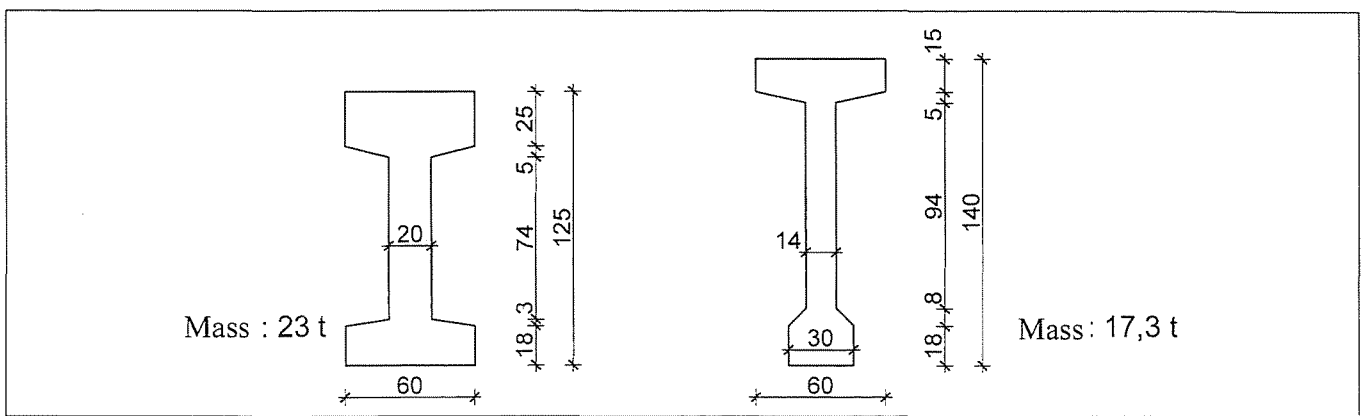


Fig. 10 Main girders at the Metro buildings in Vduntary and Ploesti

d) Reinforcement of the columns

Following more powerful earthquakes there appeared the problem of whether the reinforced concrete itself was of an adequate material strength for the framework to resist the seism.

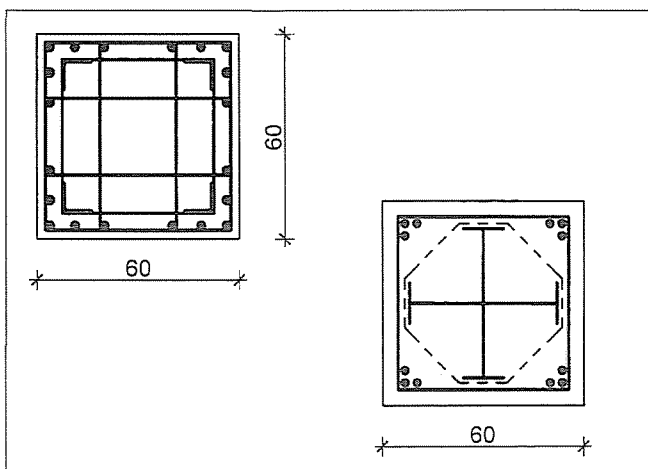
The answer is obvious: weak concrete under reinforced do not correspond to the requirement even in the low seismic areas. Therefore, the minimum strength of the concrete we used for the columns is C30/37. This quality of reinforced concrete is projected to be capable of taking a seismic charge.

The Romanian design engineers usually use columns with large section in powerful seismic areas, but in many cases the sizes of the section are limited. In most cases the concept of the blueprints and interior design limits doesn't allow this size. For example the shelf from commercial halls and the distance between them dictate the transversal dimensions of the columns, so their slenderness will be high close to the allowed limits ($\lambda = l_0 / h = 25 \dots 30$).

To resolve the problem we started with the fact that increasing the static rigidity may have even negative effect to the seismic requirements. We want a flexible structure, ductile and capable of plastic deformation within the allowed maximum displacement limits. In the case of a given section this can be realized only by well conceived reinforcement. The ductility of the columns can be increased by an optimal reinforcement system. In the case of the columns subjected to powerful seism stresses (from the A, B, C areas), we adopt a mixed solution (reinforced concrete columns with rigid metallic profiles). (Fig. 11)

First the ductility of this column is very high. In the case of strong shear forces it is recommended that the longitudinal reinforcement be laid down on more rows from out-in, increasing the capacity of plastic deformation of the column. This column continues to sustain loads even when the con-

Fig. 11 Column with stiff reinforcement



crete stops working. The introduction of rigid reinforcement is sustained in the Romanian standards, which prescribe the reinforcement percent to be 2.5% while in a lot of standards this percent rises up to 6%. The prescription doesn't allow the fragile breaking of the over reinforced sections and its value can be calculated limiting the compressed area of the bending sections. ($x < 0.4 d$).

The maximum reinforcement percent is calculated in the same way in the Romanian standard, and in our opinion its decrease to 2.5% results because of the superposing of reinforcement the percent must be divided by 2. At the ground floor halls this phenomenon is missing, so the upper limit of the percentile we can consider as 6. Unfortunately, this notice does not appear in the Romanian standard.

Obviously where the reinforcement percentage is not higher than 2.5% rigid reinforcement was not used.

The steel used for longitudinal and transversal reinforcement must fulfill the following requests:

- minimum linear extension 12%
- ratio between rupture limit and the corresponding yield point not higher then 1.45
- the yield stress variability not higher than that corresponding to the varying coefficient of 10%

For the reinforced concrete columns the collars must be strong enough. Concerning the transversal reinforcement, the Romanian standard recommends the following:

$$\rho_w > 0.0015 \text{ (0.15\%)} - \text{outside the knots areas}$$

$$\rho_w \geq 0.1 \cdot (0.4 + n) \cdot f_{cd} / f_{ywd} \text{ in the knots area}$$

where:

$$\rho_w = A_{sw} / S_w \cdot b$$

$$n = N / b \cdot h \cdot f_{cd}$$

Not only the longitudinal and transversal reinforcement is great importance but also the anchorage of rigid reinforcements. Avoiding the fragile crashing of the column (through oblique distress in concrete) close to the anchorage will appear straight cracks on its axis.

If the force is lateral, the column will develop a fissure bigger than half of its section. If the direction of the action changes (the force becomes negative), the fissure will appear on the opposite side of the column (Fig. 12).

Joining the two fissures appears a cutting surface next to the fixing. After completing the first action of the lateral force, the column does not return to its initial position and nor do the fissures close completely. This thing is achieved only if the rigid reinforcement has plastic deformation, but now, because of the compressing force.

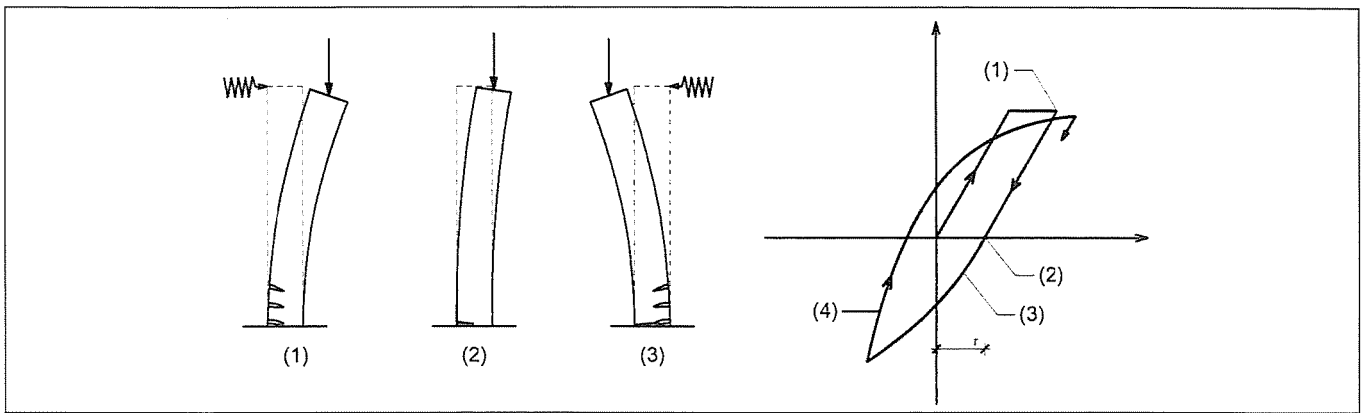


Fig. 12 Cracking of column under alternative eccentric load

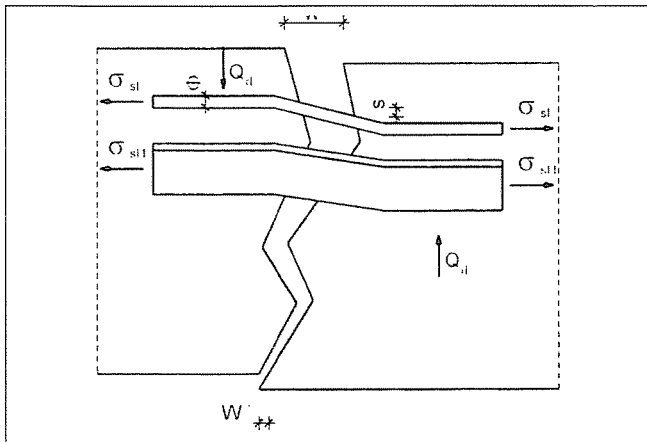


Fig. 13 Dowel effect in open crack

As we know, the extreme cutting forces which appear next to the fissures (normal or oblique) will be taken by the next three interior forces.

- force of friction from the compressed area;
- clenching force between the bars roughness;
- slashing force from the shear resistance of the longitudinal reinforcement and the concrete (Fig.13)

The last force is calculated based on Tassios and Vintzeleov relations from the shear force taken and the bars section. If the longitudinal reinforcement is in a plastic state we can't talk about slashing.

It is considered (but it still needs to be proved by researchers) that the slashing force of the rigid reinforcement is higher whatever the compressed or the stretched side should be.

e) Foundations

At ground floor level for frame structures the design of the correct foundation has an extreme importance. The stability of the columns fixed at the bottom and hinged at the top is ensured by the foundations. This is why their dimensions must be big enough.

Fig. 14 Behaviour of column footing joint under seismic effect

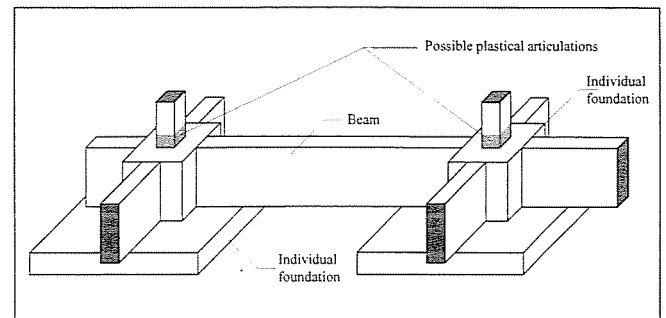
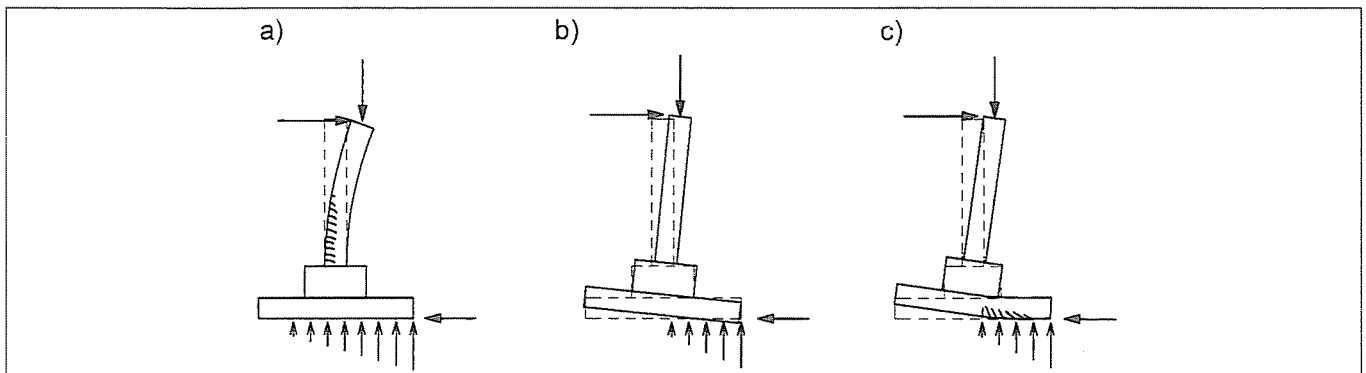


Fig. 15 Connecting of solitaire footings by grid

The foundation system must be simple and uniform between two contraction joints. If it is possible it is better that all the foundation plates are in the same plane.

The role of the bending moment is very important in designing the ground floor hall foundations because of the compressive force from the columns is small.

According to Paulay, at a high earth pressure force the most proper should be the occurrence of the plastic area over the catching of the column in the foundation (Fig.14a). If not the plastic state will appear in the foundation plate (Fig.14b, 14c).

A good method to counterbalance the bending moment seems to be that of attaching the foundation plate to the next foundation with foundation beams. However, this solution is extremely expensive (Fig. 15). In the case of the CORA store in Bucharest, this problem was raised but the tender process proved the cost of making the infrastructure to be 2-3 times higher than the whole hall cost.

Most of the designers - in order to avoid the individual movement of the foundations - use industrial concrete floors. This board loaded correctly with a thickness of at least 20 cm gives an optimal solution to the problem.

The foundation beams become efficient where foundation posts are used because of the weak foundation soil. For plastic

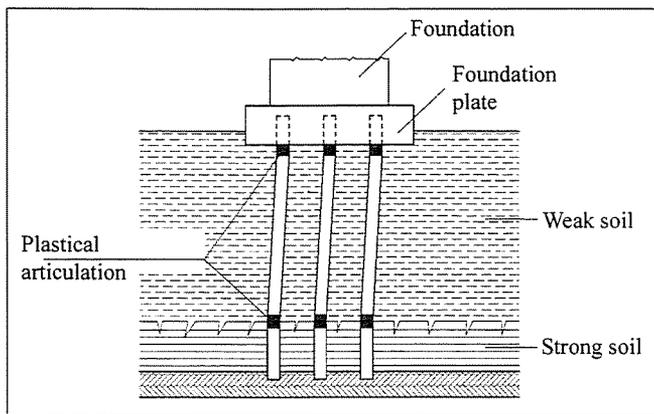


Fig. 16 Place of plastic hinge formation at piles

articulations, the reinforcements of the foundation posts are made with column reinforcement rules (*Fig.16*).

4. WHAT WILL THE FUTURE BRING?

In the future we can expect that the main beneficiary of prefabricated reinforced concrete structures will still remain the commercial objectives. This will be due to the number of the foreign investors and the buying power of the population. The investments do not have limits following the firms Metro, Selgros, Rewe and Billa. These have already established systems within their national commercial objectives other investors are coming: Plaza, Cora, Tesco, Praktiker, etc.

The conception of the structural framework for the halls seems already to be a standard solution and this trend is progressing in the case of industrial halls too.

However there is a general trend to increase spans, so in the case of prestressed beams we have a 36 m span beam. Successful examples are the 24 m span beams of the Selgros stores or the 30 m of the Leoni factories (Arad and Bistrita) (*Fig. 17*).

There is an obvious trend for increasing the spans up to 36 m, which consequently increases the surface of the column. The Renault car factories in Pitesti requested an offer for a hall with the bay of 28x32 m, which means almost 900 m²/

columns. Clearly there is an outstanding question concerning the optimum limit.

The prestressing industry will only be capable of satisfying technical requests when further progress has been completed and which in turn depends on further research. With regard to concrete strength, the use of carbon fibers would be of benefit to increase capacity. Furthermore, concrete with the a carrying capacity by 3 – 4 times bigger that those used anterior may have effects which still unpredictable.

However, we can state that the prefabrication industry in Romania has progressed over the past few years and has achieved performance levels comparable to European standards. For this we can thank firms such as ASA ÉPITÓIPARI Kft. from Turda, even if this process was slow and hard.

On the other hand, globalization and the development of infrastructure and automation have also allowed great progress to be made in structural design.

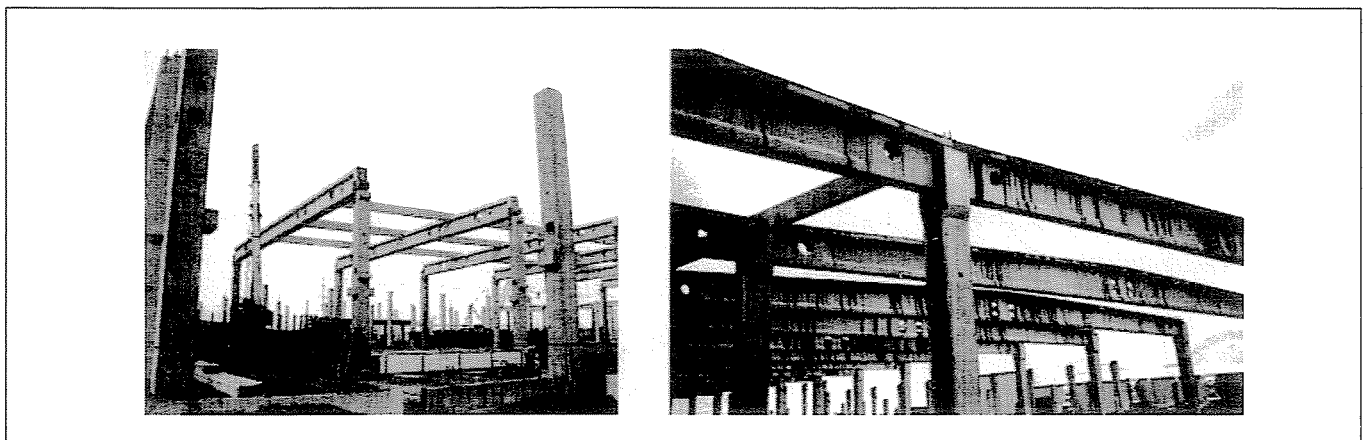
A good example of the cooperation between nations on global planning is the design firm Plan 31 Mérnök Ltd, which has built an international network which includes Hungary, Romania, Bulgaria, and soon Ukraine. This illustrates how the future could look for the entire eastern and central European region.

5. REFERENCES

Csák, B., Hunyadi, F., Vértes, Gy. (1981), "Influence of earthquakes on structures (In Hungarian)", *Műsz. Kiadó* Budapest
 Dima., G., (1999), "The stiffening effect of girdels with corlugated steel plates on floor and wall structures of industrial halls." (In Romanian)
 Mazzolani, F. M. Piluso, V. (1990), "Skin effect in pin jointed steel structures", *Ingenieria sismica*, 3/1990
 Paulay, Th., Bachmann, H., Moser, K. (1990), "Erdbebenbemessung von Stahlbetonhochbauten" *Birkhauser Verlag Basel*
 P – 100 – 92 "Instruction for antiseismic calculation of dweling houses, public, industrial and agricultural constructions." (Romanian design code)

Assoc. Prof. Zoltán Kiss (1950), graduated engineer (1974), doctor of technical science (1977), associated professor at Technical University of Cluj Napoca, Reinforced Concrete Chair, executive director of Plan 31 Ltd. Research interests: prefabricated reinforced concrete structures, industrial concrete planking projection. Member of the Romanian Structure Projecting Organization (AICPS) and the Hungarian Group of *fib*.

Fig. 17 Selgros Pantelimon (24x10 m), Leoni Arad (30x6 m)



EXTERNAL STRENGTHENING OF AN 8000-TON GRAIN SILO IN TÖRÖKSZENTMIKLÓS, HUNGARY, WITH POLYPROPYLENE FIBRE REINFORCED SHOTCRETE



Dr. József Almási



György Erdei



Imre Édes



Lóránt Koncz



Prof. Árpád Orosz

In the external walls of a reinforced concrete grain silo originally completed in 1967, cracks formed and filtering rainwater impeded its operation. The load-bearing capacity of the silo proved insufficient, its steel reinforcement needed corrosion protection and the restoration of its protective cover was deemed necessary. These conditions necessitated thorough repair. After considering various strengthening techniques, an external shell of wire mesh reinforcement and fibre reinforced shotcrete was selected. In order to control crack formation the silo bins were filled with grain during the application of the shotcrete, thus tensile stress in the external shell was basically eliminated. Finally, a protective layer able to bridge surface cracks was applied, which also provided the silo with an aesthetic appearance.

Keywords: reinforced concrete silo, strengthening, restoration, shotcrete, fibre reinforcement, corrosion.

1. INTRODUCTION

The 800-wagon capacity reinforced concrete grain silo in Törökszentmiklós, Hungary, was designed by IPARTERV, and it was put into operation in 1967. See *Figure 1* for the ground plan of the silo block which contains 18 circular bins of 5 m diameter and an adjoining machine room. The thickness of the reinforced concrete walls of the bins and the machine tower is 14 cm and 16 cm, respectively.

The function of the intermediate bins is grain storage. These consist of conical reinforced concrete funnels with centric discharge orifices at the bottom of circular bins. The funnels are supported by a reinforced concrete circular ring beam supported by columns. At the time of construction of the silo block, sliding formwork was applied and there are construction joints between bins 3 and 4 and

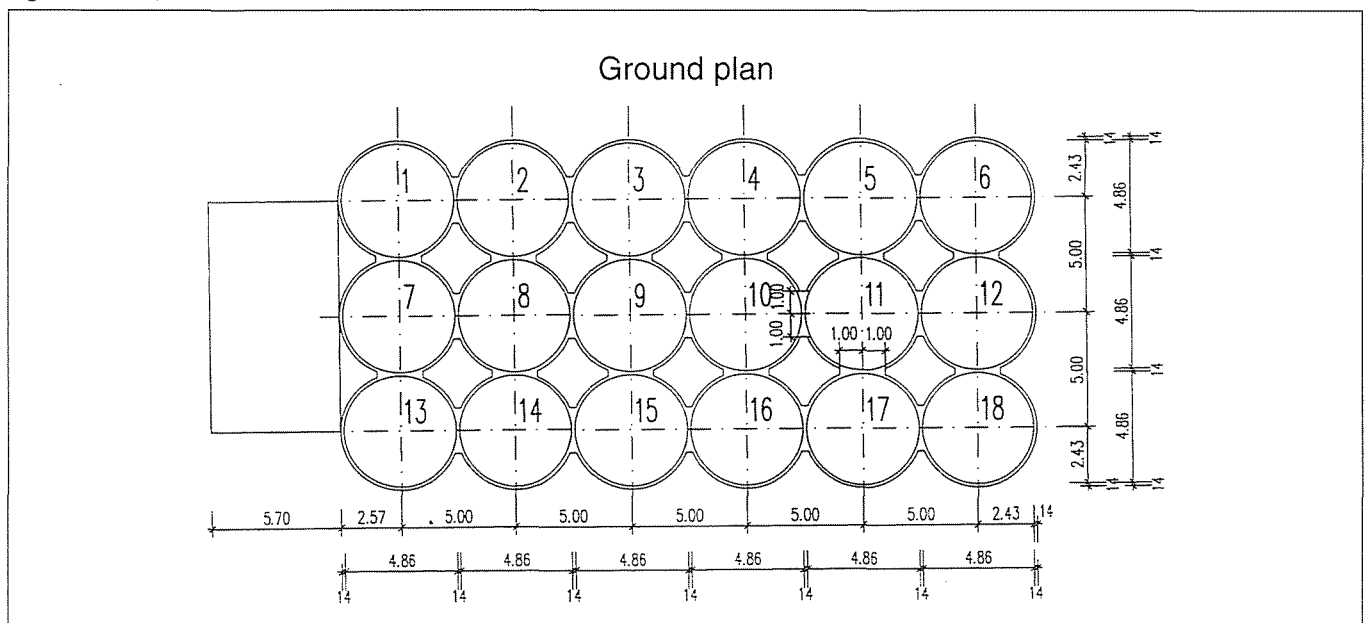
bins 15 and 16 corresponding to the two stages of construction. Since it was presumed at the design stage that hairline cracks would appear in the bin walls a *protective layer* was applied on the external surface. During the lifting process of the sliding formwork local rupture and compaction imperfections were observed at the construction joint, which were mended during construction.

After some years of operation, *vertical cracks formed in the bin walls of the silo*. Cracks of growing intensity in the lower third of the bin walls allowed pelting rain to pass through the wall into the bins.

During the nearly 30 years of service of the silo further defects, *horizontal cracks* and corrosion of the steel reinforcement were observed. This necessitated a thorough examination.

The main findings of the diagnostic examination (Herkó, 1999) of the reinforced concrete bin walls are as follows:

Fig. 1 Ground plan of the silo block (Machine room)



- The steel reinforcement was $2 \times \text{Ø}8/25$ cm according to the plan, which was applied at most locations (but not everywhere) in the construction.
- The concrete cover on reinforcing bars is insufficient (15 mm on the average), which lead to scaling and alligating due to corrosion.
- The protective layer has aged and became brittle, and is thus in need of reconstruction.
- There are great variances in the condition of the different bin walls: some bins are in satisfactory condition while others are rather defective and need urgent repair.
- Concrete strength is generally insufficient (C12 on the average), concrete quality and density is uneven, and there are cavities in the concrete.

2. SELECTING A STRENGTHENING TECHNIQUE

The management of the Alföldi Gabonaipari Rt. (Alföldi Grain Industry Corp.) decided to conduct a competition to find the best method of restoration and strengthening. Competitors proposed the following strengthening techniques:

- Attachment of external and internal *steel bands* on the bins, anchored in the interlocking section of bins.
- Construction of a new, *internal reinforced concrete shell*.
- Construction of an *external shell* of shotcrete.
- Mounting *carbon fibre sheets* on the bin walls.

Techniques a) and b) can be applied to partially strengthen the silo, i.e. after repairing the bins in the worst condition *restoration can be scheduled* according to financial means.

In the case of an *external reinforced concrete shell*, it is difficult to carry out partial strengthening and divide the restoration process into stages. This technique features technological advantages and economic efficiency only if *the whole silo block is restored* at the same time.

Having considered all factors, the operator of the silo selected the strengthening technique that applies an external reinforced concrete shell, and the EKS-Service Ltd. was commissioned to execute the plan (Erdei, 2001). The detailed plan of execution was prepared by CAEC Ltd.

3. THE STRUCTURAL ANALYSIS

3.1 Loads

There are several methods for the calculation of the so-called silo pressure produced by the material stored in grain silos. However, the authors do not wish to introduce them in this paper. In the given case, the procedure proposed by Orosz (1998) was chosen for the following reasons:

- It is based on Janssen's theory, which is most commonly applied.
- It provides pressure values both for the storage and discharge states.
- It provides sets of corresponding values, thus it can be applied not only for vertical but also for skew walls.
- It is easily applicable and conservative, i.e. safe.
- It applies such ideal properties of material, which can be applied in the structural analysis *regardless of the type of corn*. Thus the serviceability of the silo does not depend on the type of corn to be stored in it throughout its life span.

z [m]	z/z ₀	1 - e ^{-z/z₀}	Silo pressure at an arbitrary depth			
			at storage [kN/m ²]		at discharge [kN/m ²]	
			P _v	P _h	P _f	P _h
5	0.99	0.628	28.6	17.2	6.8	28.6
10	1.97	0.861	39.2	23.5	9.4	39.2
15	2.96	0.948	43.2	25.9	10.3	43.2
20	3.95	0.981	44.6	26.8	10.7	44.6
25	4.95	0.992	45.1	27.0	10.8	45.1
27	5.34	0.994	45.2	27.1	10.8	45.2

Table 1 Silo pressures

Physical properties of ideal grain

- Unit weight: $\gamma = 9$ kN/m³
- Coefficient of lateral pressure:
at storage: $k^s = 0.6$
at discharge: $k^d = 1.0$
- Coefficient of wall friction:
at storage: $m^s = 0.4$
at discharge: $m^d = 0.24$

Geometrical data of reinforced concrete bins:

Diameter of the centric surface of the bin wall:

$$D = 5.00 \text{ m}$$

Internal diameter: $D_i = 4.86 \text{ m}$

Wall thickness: $t = 0.14 \text{ m}$

Height of stored grains above the funnel: $H = 27.0 \text{ m}$

The critical depth is the same at storage and at discharge, since,

$$k^s m^s = k^d m^d$$

$$z_0 = D_i / 4km - 4.86 / (4 \times 1 \times 0.24) = 5.6 \text{ m}$$

The *maximum values of silo pressure* produced by the grain stored in a bin of infinite height are as follows:

● At storage

Vertical pressure:

$$p_{v,\max}^s = \gamma z_0 = 45.5 \text{ kN/m}^2.$$

Horizontal pressure:

$$p_{h,\max}^s = \gamma z_0 k^s = 27.3 \text{ kN/m}^2.$$

Friction pressure:

$$p_{f,\max}^s = \gamma z_0 k^s m^s = 10.9 \text{ kN/m}^2.$$

● At discharge

$$p_{v,\max}^d = \gamma z_0 = 45.5 \text{ kN/m}^2,$$

$$p_{h,\max}^d = \gamma z_0 k^d = 45.5 \text{ kN/m}^2,$$

$$p_{f,\max}^d = \gamma z_0 k^d m^d = 10.9 \text{ kN/m}^2.$$

At an arbitrary depth, the silo pressure can be calculated using the Janssen formula:

$$p(z) = p_{\max} (1 - e^{-z/z_0}) \quad (\text{See Table 1.})$$

Note that it is assumed in this calculation method that,

$$p_v^s = p_v^d = p_h^d \quad \text{and} \quad p_f^s = p_f^d.$$

In our case it is sufficient to consider only horizontal pressure. See Fig. 2 for its distribution along the height.

Instead of an exponential pressure distribution, the distri-

bution of the maximum horizontal pressure is given by straight lines drawn from the origin to the critical depth, z_0 , passing through the intersection of a vertical line at $p_{h,max}$ and the tangent of the theoretical curve, according to Orosz's proposal (1998). The theoretical pressure values are lower than these limit lines in all cases so this approximate method proves to be conservative and dependable.

3.2 The state before strengthening

3.2.1 Design forces and ultimate forces

The tensile force in the bin walls, applying the "boiler" formula, is,

$$F_h = n \times R_i \times p_{h,max} = 1.3 \times 2.43 \times 45.5 = 144.0 \text{ kN/m},$$

where, $n = 1.3$ safety factor,
 $R_i = 2.43 \text{ m}$ internal radius of the bin.

The daily and seasonal temperature effect is approximately 10% of the discharge pressure, thus the design ring force is,

$$F_{h,d} = 144.0 + 14.4 = 158.4 \text{ kN/m}.$$

The steel reinforcement according to the original plans:

$2 \times \text{Ø}8/25$; $A_s = 402 \text{ mm}^2/\text{m}$.
 Steel grade: B 60.40, $R_{u,s} = 350 \text{ N/mm}^2$

The ultimate force is,

$$F_{h,b} = 402 \times 350 = 140.5 \text{ kN/m} < 158.4 \text{ kN/m},$$

the deficiency is app. 11%.

In the executed bin walls, the arrangement of reinforcing bars (as found in the explorations) roughly corresponds to the plans. However, due to corrosion, the cross-section of steel bars must be reduced by approximately 10% in the calculation, so the actual ultimate force, assuming steel reinforcement of $A_s \cong 360 \text{ mm}^2/\text{m}$, is,

$$F_{h,ex}^k = 360 \times 350 = 126 \text{ kN/m} < 158.4 \text{ kN/m},$$

and the deficiency is approximately 20%. Such a deficiency of load-bearing capacity necessitates strengthening based on structural analysis.

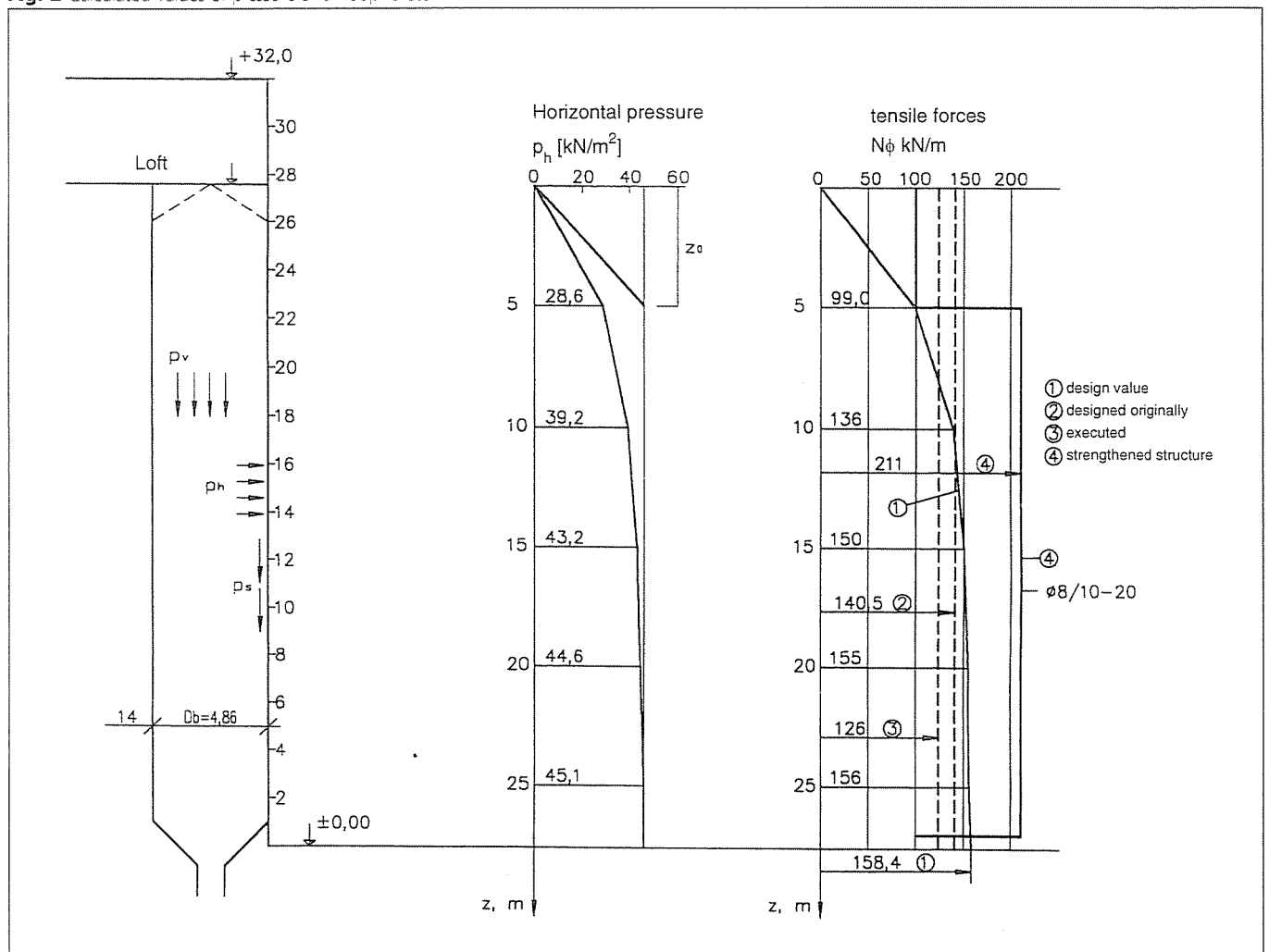
3.2.2 Cracking sensitivity

When carrying out the check of cracking sensitivity a method proposed by Scandinavian researchers was applied, according to which the silo wall is safe if the cracking sensitivity coefficient,

$$k = A_{sh} / D_i \geq 0.24 ,$$

where A_{sh} is the applied horizontal reinforcement [cm^2/m],
 D_i is the internal diameter of the bin wall [m].

Fig. 2 Calculated values of pressure and hoop forces



In our case, substituting the reinforcement *according to plan* gives:

$$k_i = 4.02 / 4.86^2 = 0.17 < 0.24 .$$

substituting the *existing* reinforcement

$$k_i = 3.60 / 4.86^2 = 0.15 < 0.24 .$$

Thus, neither case is safe for cracking sensitivity according to the proposed limit.

The required area of reinforcement based on cracking sensitivity is,

$$A_{s,r} = k \times D_i^2 = 0.24 \times 4.86^2 = 5.66 \text{ cm}^2/\text{m} > 3.60 \text{ cm}^2/\text{m}.$$

Thus, an increase of approx. 60% is necessary.

3.3 THE STATE AFTER STRENGTHENING

Quantity of steel reinforcement

According the structural analysis, when calculating the steel reinforcement needed for strengthening, there are two options:

- taking the existing reinforcement into account and designing supplementary reinforcement, or
- applying the quantity of reinforcement that can take the total tensile force.

In the preliminary examinations it was observed that concrete strength was relatively low and uneven, there were cavities in the concrete at construction joints, the concrete cover was insufficient and there were severe cracks in the bin walls. These facts made it questionable whether overlap splices of the existing steel reinforcement would still be effective. The exploratory examination raised some doubts about the amount of reinforcement actually applied at construction and also about the spacing between reinforcement bars. *Figures 3 and 4* illustrate that these doubts were well grounded. Following high-pressure washing of the surface it was found that splices of insufficient overlapping opened up and the concrete cover peeled. It was also revealed that, at some locations, the distance between reinforcing bars was more than 40 cm instead of the designed 25 cm.

Due to the above-mentioned facts, it was decided to neglect the existing reinforcement and therefore the *total tensile force would be taken by the new, strengthening reinforcement*.

The new reinforcement, according to the design of strengthening, is $\text{Ø}8/10\text{--}20$ welded wire mesh of steel grade B 60.50, which has a cross-sectional area of $A_s = 503 \text{ mm}^2/\text{m}$. The ultimate force is,

$$F_{ult} = 503 \times 420 = 211.0 \text{ kN/m} > F_d = 158.4 \text{ kN/m}.$$

Fig. 3 Opened up overlap joints

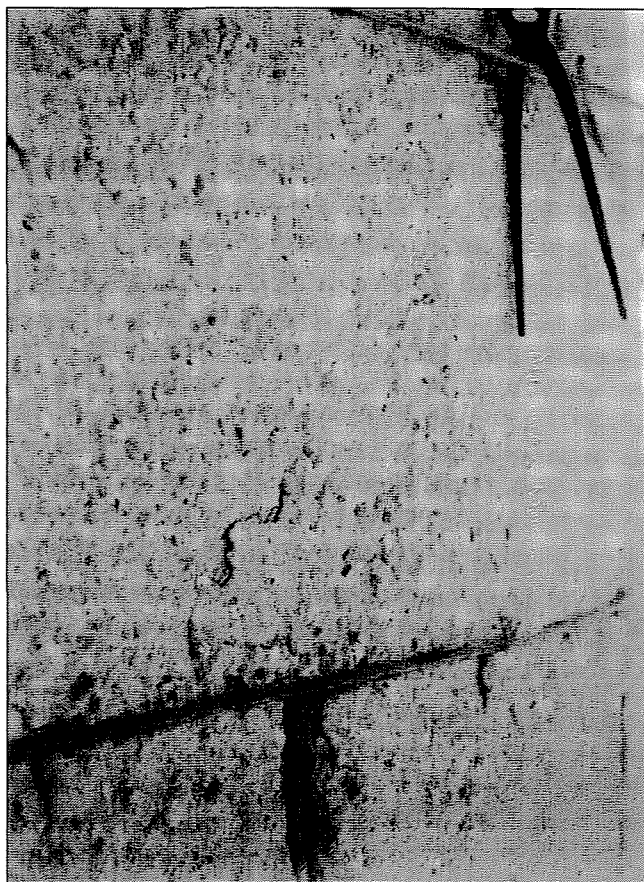


Fig. 4 Spacing of steel reinforcing bars

The cracking sensitivity coefficient is

$$k_i = 5.03 / 4.86^2 = 0.213 < 0.24,$$

which is still less than the proposed lower limit, but it is closer to that.

Anchorage of the welded wire mesh

The dimensions of the welded wire mesh to be placed in the shotcrete shell were chosen in such a way that no vertical splice was necessary, except in the corner bins.

Fig. 5 Reinforcement at the anchorage of the welded wire mesh

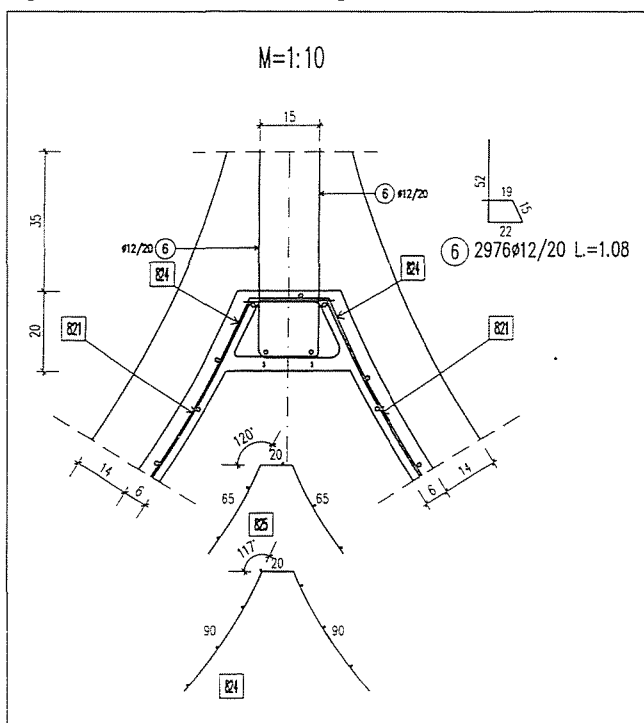




Fig. 6 Anchorage of the welded wire mesh

The anchorage of the welded wire mesh at the junction of the bins is illustrated in Fig. 5. A vertical reinforced rib is formed which is anchored to the junction of the bin walls by tie bars bonded in holes bored into the concrete. *In order to check the efficiency of the anchorage of the tie bars, on-site pull-out tests were performed. The required depth of bored holes and the adhesive strength were determined on the basis of the test results.* This is common to the design of such strengthening structures and it is always necessary to perform such a test since this is the only reliable way to find the anchoring force which depends on the actual concrete strength. See Fig. 6 for structural design details of the anchorage of the welded wire mesh and for the construction joint to be formed.

Filling in the bin during the shotcreting

If the bin is filled in with grain during shotcreting and the discharge pressure and the ring force are produced after hardening of the concrete shell, then no tensile stress will be produced by the silo load in the external shell, and there will be only compressive stress when the silo is empty. This is an effective way of preventing crack formation as well as controlling crack width. However, considering construction safety regulations this procedure can be followed only if there is no danger of splitting and failure of the bin during reconstruction.

Assuming that the actual unit weight of the corn ($g = 8 \text{ kN/m}^3$) acts as a short-time load (for approx. two weeks), the hoop force is,

$$N_g^0 = 0.8 \times p_{h,d} \times R_i / 0.9 = 0.8 \times 45.2 \times 2.43 / 0.9 = 99.5 \text{ kN/m.}$$

Considering the ultimate force based on the existing reinforcement, the safety rate is,

$$n = N_{g,ult}^k / N_g^0 = 126 / 99.5 = 1.25 > 1.0.$$

Therefore the silo bin can be filled in at a low risk.

4. PRINCIPLES AND CHARACTERISTICS OF THE STRENGTHENING TECHNIQUE

The *advantages* of the application of an external reinforced concrete shell are as follows:

- The strengthening needed for static reasons, the reconstruction of the bin walls, corrosion protection of the steel reinforcement and the provision of a silo block with an aesthetic appearance can be achieved in a single technological procedure.
- During the execution of strengthening, the operation is independent and there are basically no restrictions.
- Strengthening of a silo block can be performed in a few months.

Nevertheless, the following factors are to be taken into consideration at the application of the strengthening technique:

- The execution can be started *only in good weather conditions.*
- It is advisable to add PP plastic fibre reinforcement to the concrete in order to prevent the formation of shrinkage cracks in the relatively thin (6-8-cm-thick) shotcrete shell.
- Special care should be taken to cure the concrete properly.
- Care should be taken to protect neighbouring buildings and completed surfaces from drifting dust produced at surface cleaning and concrete projection, taking the prevailing wind direction into account.

The technological steps of the strengthening technique are as follows:

- High-pressure sandblasting of the surface.
- Removal of loose concrete flakes and the application of a corrosion protective coat.
- Mounting and fixing the steel reinforcement, i.e. the welded wire mesh and the tie bars.
- *Filling in the bin with grain prior to concrete projection.* The grain should remain in the bin until the new concrete shell is 14 days old.
- Concrete projection, evening; construction joints.
- Application of a protective layer.

Note that the properties of the original concrete of the bins should be taken into account when specification of the shotcrete grade is drawn up since the composite action of the existing wall and the new shell can be ensured only if their values of longitudinal rigidity are close. It is well known that structures of higher stiffness "take more load", and those of lower stiffness "evade loads". *Thus, in order to facilitate a composite action between existing and new structures, it is very important to ensure that their deformation and stiffness properties are close enough.* In our case, due to the low strength of the existing concrete, it was presumed that the shotcrete shell of far higher stiffness would provide the major proportion of the total load-bearing capacity. Therefore, it was deemed to be advisable *to make the new external shell capable of supporting the total silo load, which was taken into account during the design of its reinforcement.*

5. EXECUTION, TECHNICAL INSPECTION AND QUALITY CONTROL

5.1 Pre-treatment of the concrete surface

For the restoration of bin walls, a scaffolding was assembled which provided access to three bins at the same time.

The success of the whole process of reconstruction and strengthening depends on the pre-treatment of the concrete surface. In order to facilitate a composite action between the existing concrete and the shotcrete, the silo surface should be carefully cleaned, loose and alligating concrete parts should be removed until a concrete layer of sufficient strength (app. C12) is reached.

The existing outer cover, the cement mortar and other materials that impede proper contact (limestone and silicate dust, fine sand, etc.) were removed from the bin walls and the surface of the machine room. For surface cleaning a sandblasting method was applied and mobile sand throwing machines (using sharp silica sand of 0.5-1.25-mm grains) were employed. An environment-friendly electric compressor of 20 m³/min capacity provided 7 m³/min/machine air volume and 7-8-bar pressure required for dry sandblasting.

Manual and mechanical chisels were used to remove loose and low-strength concrete. Chiselling-off was at some locations as deep as 50-70 mm. Since this process was simultaneous with sandblasting the revealed reinforcing bars were also sandblasted. The reduction in cross-sectional of the revealed reinforcement bars was *more than the presumed rate*.

After surface cleaning and chiselling, it was observed that more material was needed for replacement than it was presumed based on preliminary examinations.

See *Figures 3 and 4* for concrete surface defects revealed on the cleaned surface.

5.2 Checking the existing concrete of the bin wall

Although the preliminary expert examinations had not provided detailed data, it was obvious that the concrete strength was relatively low and uneven. As it was unclear whether a bond-tensile strength of 1 N/mm² (which is sufficient for the bond joint of the existing bin wall and the new concrete shell) could be achieved, great care was to be taken to anchor the welded wire mesh in the shell.

A visual inspection of the silo led to the conclusion that the formation of vertical cracks was caused by defective grouting of the supporting bar holes. Due to the severe corrosion of the horizontal reinforcement, which led to peeling concrete cover and alligating and bleeding of more than 10mm width, there was a danger of accident, which in turn made a thorough general examination inevitable.

CAEC Ltd. measured the compressive and bond strength of the existing concrete surface and a report on the rupture strength tests of the steel reinforcement was also prepared.

Concrete strength was examined at 5 locations using non-destructive testing, employing Schmidt hammer. The measured mean concrete strength was 16.0 N/mm², the characteristic concrete strength was 12.0 N/mm².

Bond strength was examined by tearing a 50mm adhesive pad off the surface at 5 locations. The mean bond strength was 1.2 N/mm², the measured minimum strength was 0.52 N/mm².

Based on these examinations it was observed that the bond strength was sufficient but uneven. It was established that the concrete grade was C12 and that the ultimate strength of reinforcing bars, corresponding to their measured ultimate strength, was 300 N/mm².

Following each stage of surface cleaning by sandblasting and mechanical and manual exploration, the resulting surface was thoroughly checked for dust, old cover, impurities and other loose matter.

5.3 Properties of shotcrete

Requirements:

- Concrete grade: C 20 (MSZ 4719 – MSZ 4720)
- Maximum grain size: $D_{max} = 8$ mm
- Continuous grain-size distribution
- Low initial crack-proneness
- Maximum size of air pockets: 5 mm
- Dosage of polypropylene plastic fibre: 1.0 kg/m³
- Special care at concrete curing

Accordingly, the deformation capability of the concrete to be applied should be higher than average and PP plastic fibre reinforced concrete satisfies this requirement. A further advantage of plastic fibre reinforcement is that it prevents formation of shrinkage cracks at an early stage, and it reduces the amount of concrete falling off at shotcreting.

Concrete composition

Shotcrete was made of factory-prepared sacked concrete mixture to ensure an even concrete composition.

The total amount of shotcrete was made of factory-made shotcrete mixture for spray application, to which water was added within the ejector (dry process).

The composition of shotcrete is as follows: (weight)

	kg
Water (water-cement ratio = 0.25)	100 l/m ³
Portland cement CEM I 42.5	400 kg/m ³
Mineral sand (0-8 mm)	1689 kg/m ³
Chemical agent	12 kg/m ³
PP plastic fibre	1 kg/m ³

The strength grade of the 25kg sacked concrete, type Keston MM4 and MM8, is C20. Polypropylene fibre was added in the factory.

Strength control of shotcrete

The manufacturer constantly monitored the flexural-tensile strength and the compressive strength of the shotcrete mixture. Monitoring involved the following strength tests:

Laboratory testing of 4 x 4 x 16 cm³ test specimens (conforming to MSZ EN 196-1: 1996, sections 9.2 and 9.3) resulted in 6.88 N/mm² mean flexural-tensile strength and 45.86 N/mm² mean compressive strength. Both of them are higher than the relevant values in the technical specification.

The strength and evenness of projected shotcrete was checked by *tear-off tests applying adhesive pads*. The measured mean tearing-off tensile strength was 1.28 N/mm², which is sufficient to ensure a *proper composite action* with the protective layer.

CAEC Ltd., which prepared the working design, carried out sampling observations.

Concrete grade

Laboratory tests (conforming to MSZ 4715) of 15 x 15 x 15 cm³ test specimens cast on site resulted in a concrete grade of

C20 according to MSZ 4719, based on the compressive strength of the concrete. The test specimens reached the characteristic strength value (of 25 N/mm² for concrete cubes) corresponding to this concrete grade.

The performed tests proved that;

- the shotcrete is of grade C20,
- its quality is even, and
- concrete surfaces are properly evened.

5.4 Reinforcement fixing

Reinforcing steel

According to the strengthening plan, welded wire mesh was fixed on the surface of the bin walls between levels +2.0 m and +22.8 m, +22.8 m and +27.4 m, +27.4 m and +32.0 m is Ø8/10–20, Ø7/10–20 and Ø4.2/10–20, respectively. The steel grade of the wire mesh is B 60.50, MSZ 339 strength class.

Checking the anchorage of the wire mesh

Fig. 5 illustrates the overlap splices of wire mesh fixed on the external surface of the bins and their anchorage at the interlocking section of bins.

To check the reliability of the anchorage, on-site pull-out tests were performed on tie bars bonded into the bored holes of the wall. The average of measured pull-out forces was 55 kN, which is higher than the 39 kN force specified in the specification. Tie bars of Ø12 mm diameter were bonded using adhesive type AM 1000 quick mix (Techno-Wato) in 350-mm-deep and Ø16 mm diameter holes bored in the bin walls.

Fixing the welded wire meshes

Welded wire mesh fixed with dowels to bin walls are arranged in a 50/50 cm grid. These dowels provide the required stiffness during shotcreting and they also ensure a joint to the relatively weak existing concrete.

In case of the given bin size, *the welded wire mesh*, consisting of Ø8 mm steel bars, *can be bent over the surface*. A wire mesh of larger bar diameter would need pre-bending before fixing, and would also cause fixing difficulties.

After checking the cleanliness of the surface, 35-cm-deep holes were bored in the interlocking section of bin walls, into which the *anchoring reinforcement (tie bars)* would be placed. Doubled anchoring bars were bonded in the holes at 20 cm spacing, along the length of the interlocking section of approximately 22 cm width. Bond quality was checked by pull-out tests at random locations.

Before bonding the tie bars, on-site bent, canal-shaped wire mesh was fixed at the interlocking vertical segments of the bins and they were joined to the wire mesh fixed on the bin walls with 0.90 m and 0.65 m overlaps, alternately. Two steel dowels per m² were applied for mounting and fixing the welded wire mesh, and a minimum distance of 1 cm from the wall surface was kept.

The fixing of the 2.40 x 6.00 m wire mesh needed special care and attention with regard to lifting to the required height along the external side of the scaffolding. Some anchored nodes of the scaffolding had to be released so that the wire mesh could be moved to the bin wall. Moreover, some difficulties occurred fixing the bending hoop Ø8 mesh over the bin surface.

5.5 Shotcreting, construction joints

The surface was pre-moistened before shotcreting to obtain a mat surface ideal for shotcrete.

Concrete projection was done from the top to the bottom of the bins.

Due to the *results of the structural analysis* and cracking sensitivity bin walls were *externally strengthened with a 6 cm-thick reinforced shotcrete shell* between levels +2.00 and +26.70 m. In order to *protect the reinforcement against corrosion* and to prevent the outer concrete layer from peeling off, bin walls between levels +26.70 m and +34.00 m were strengthened with 3 cm-thick shotcrete shells with a wire mesh for crack prevention.

The minimum thickness of the concrete cover in the case of the 6 cm-thick and the 3-cm-thick shells was 20 mm and 15 mm, respectively.

At the horizontal construction joints of the concrete shells, rigid cut-off elements (made of steel profiles, bent over the surface of the bin wall) were applied to reduce the formation of hairline cracks. This ensured that the shotcrete shell and the concrete cover were of sufficient thickness and properly compacted. Vertical construction joints were formed at the vertical anchoring ribs. In the first stage, the strengthening shell was only 6 cm thick at the interlocking section of the bins, after which, at the strengthening of the next silo bin in the second stage, the anchoring rib was completed, which entirely covered the construction joint. The concrete crust was removed from the steel reinforcement before the second stage was started.

After the required thickness was reached, the concrete was levelled, partly to facilitate the application of the protective layer and to ensure a continuous and even layer thickness, and partly to provide the silo with aesthetic appearance.

The shotcreting was arranged in such a way that vertical construction joints were formed only at the interlocking sections of the bins. At horizontal construction joints, bent steel profiles (as mentioned above) fixed to the welded wire mesh, were applied.

The applied construction joints feature the following advantages:

- They ensure that the concrete cover over the wire mesh is 25 mm thick and even.
- The stiffness of the steel profile ensures that concrete projected around will be sufficiently compact.
- After the removal of the steel profile, concrete will be shooting on a compact surface to form a new concrete shell.
- The construction joint is perpendicular to the surface, which prevents such a case that levelling of the new shell results in a thin concrete layer on the existing concrete, which may lead to alligating and peeling off.

According to experience, the formation of hairline cracks (which is otherwise unavoidable) is very rare at such construction joints.

By the application of a bent steel profile on a bin wall, an evenly curved surface was formed and earlier rough areas were covered. This provided the silo with an aesthetic appearance.

5.6 Protective layer

The application of a protective layer is indispensable as it covers unavoidable hairline cracks forming in the shotcrete shell (mainly around construction joints, caused by shrinkage, cracks of the existing bin wall and temperature effects). It prevents rainwater from filtering into cracks and having a damaging effect and it provides the silo block with an aesthetic appearance. The application of a protective layer was also advisable

because shotcrete often has air pockets, thus the new shotcrete shell needs special protection against weather effects.

Requirements for the protective layer, applied in layers, are as follows:

- elasticity, capability of bridging cracks.
- capability of adhering to an *existing* surface.
- resistance to UV radiation.
- vapour permeability.
- light reflective properties (to reduce the heat effect of solar radiation).
- ability of being mended.

The applied material, type KESTON FLEX II, satisfies all the above requirements. Based on tear-off tests applying adhesive pads, the surface bond strength was nearly 1 N/mm², thus almost twice the specified value (0.5 N/mm²) was obtained.

The life span of the protective layer is approximately 10-15 years, so its condition should be examined once in every 10 years.

Both the shotcrete shell and the protective layer were applied on the existing, cracked structure, which may lead to formation of hairline cracks due to static reasons and temperature effects. Therefore, a protective layer was selected that can bridge a crack width of 0.2 mm.

6. CONCLUSIONS

After more than 30 years of service the reinforced concrete silo required urgent reconstruction as its defects impeded functional operation. Thorough expert examinations were carried out to explore the defects. It was observed that the cracked state of the silo needed improvement and strengthening was also necessary for structural reasons. After a careful analysis of various strengthening techniques, the optimal technique was selected: construction of an external reinforced concrete shell was proposed.

There are some reinforced concrete silos abroad, namely in Canada (Collins, 1997) and the former Yugoslavia, which were strengthened with shotcrete shells. However, in these silos, the reinforced shell reached only two thirds of the total height of the silo wall, and no external protective layer was applied. In the case of the Canadian silo, *crack formation* in the concrete shell was observed a few years after strengthening, which stresses the importance of the application of an external protective layer that can bridge cracks.

In Hungary, the first silo that was strengthened with an external shotcrete shell was a 20000-ton silo in Marcali (Orosz – Csató – Tamáska, 1999). In this case, a shell was formed along the total height of the silo with reinforcement up to 2/3 of its height, above which reinforcement was applied only at a few locations. However, the total surface of the silo was covered by a protective layer. This was the first silo which employed plastic fibre reinforced shotcrete and the experience gained was promising. Following the strengthening and after three years of operation (with total utilization of capacity) no cracks or defects were observed in the silo. There was only one location (at a horizontal construction joint) where the paint was peeling off.

Compared to these cases, the following improvements were carried out in the strengthening technique applied at the silo in Törökszentmiklós:

- The total height of the new shell is made of shotcrete with reinforcement.
- The reinforcement applied in the strengthening shell is

capable of taking the total tensile force produced by silo load.

- The horizontal reinforcement (the welded wire mesh) has no splices, except at the corner bins.
- There were only horizontal construction joints in the shotcrete shell on the bin wall.
- Application of steel profiles at construction joints had a favourable effect: hardly any hairline cracks were formed after concrete shooting.

During the reconstruction process the client regularly checked the materials to be applied and their quality certificates, either directly or indirectly, via the technical inspector. Each significant stage of the reconstruction was carefully checked, and each completed stage gained acceptance individually.

Based on regular technical inspection and quality control during the reconstruction process, the concrete grade of shotcrete is C20.

The technical inspector observed that surface cleaning, reinforcement fixing, shotcreting projection and curing, together with the application of the protective layer were carried out properly.

It was repeatedly proved that plastic fibres reduce the crack-proneness of shotcrete which has lately been a well-known fact in case of large concrete surfaces (e.g. pavements, carriageways).

The primary advantages of the strengthening technique applying an external shotcrete shell are as follows:

- Structural strengthening, reconstruction and corrosion protection can be performed in the same technological stage.
- During reconstruction the silo can remain in operation with basically no restrictions.
- The protective layer provides the wall long-term protection and an aesthetic appearance.

In future cases of silo restoration more care should be taken when examining the structural condition, both with regard to determining the actual concrete strength and the exploration of the reinforcement.

The contractor kept to the specified time schedule of reconstruction at each stage, thus the client did not have to face any unexpected difficulties in the operation.

The conclusion can be drawn that:

- the introduced strengthening technique is of high quality and effectiveness and its application needs a short time period, and
- it ensures undisturbed operation of the silo for a long time.

7. REFERENCES

- Collins, M.P., Seabrook, P.T., Kuchma, D., Sacré, P. (1997), "External Repair of Cracked Grain Silos", *Concrete International*, 1997. nov. pp. 22-28.
- Erdei, Gy. (2001), "Ajánlategyűjtés szakvélemény a törökszentmiklósi Alföldi Gabona Rt. 8000 tonnás gabonasilójához" (Expert opinion for deliberation of tenders on the 8000-ton grain silo of the Alföldi Grain Industry Corp. in Törökszentmiklós) in Hungarian, 2001. *Manuscript*.
- Folic, R., Ivanov, D., Desovski, Z. (1995), "Results of Testing and Repair of Cells of 8000 Ton Silo". *Proceedings of the Sixth International Conference on Structural Faults and Repair*, London, Volume 3. pp. 67-74.
- Herkó, D. (1999), "A törökszentmiklósi 8000 tonnás vasbeton gabonasiló szerkezeti felülvizsgálata" (Structural examination of the 8000-ton reinforced concrete grain silo in Törökszentmiklós), in Hungarian, *Expert opinion*, 1999. *Manuscript*.
- Orosz, Á. (1998), "Megjegyzések a silónyomás számításához vasbeton gabonasilók esetében" (Notes on the calculation of silo pressure in case of reinforced concrete grain silos), in Hungarian, *BME Építőmérnöki Kar*

Vasbetonszerkezetek Tanszéke Tudományos Közleményei, 1998, pp. 172-180.

Orosz, Á., Csató, Gy., Tamáska, J. (1999), "A marcali 2000 vagonos gabonasiló megerősítése" (Strengthening of a 20000-ton grain silo in Marcali, Hungary), in Hungarian, *Vasbetonépítés*, volume I., 1999/2, pp. 55-62.

Orosz, Á. (2001), "Vasbeton silók javítási módszerének megválasztása" (Selecting a restoration technique for reinforced concrete silos), in Hungarian, *A BME Építőmérnöki Kar Hidak és Szerkezetek Tanszéke Tudományos Közleményei*, 2001. pp. 145-150.

Dr. ALMÁSI, József (1940) Civil Engineer, MSc. Places of employment: Láng Engine Works (1958), Foundation Engineering Company (1964-66), TUB Department of Reinforced Concrete Structures (1967-95). Managing Director of Cronauer Almási Engineering Consulting (CAEC) Ltd. since 1995. He is a member of the Hungarian Group of *fib* and holder of the László Palotás award (2002).

ERDEI, György (1954) Civil Engineer, MSc, Managing Director. Places of employment: HŐTECHNIKA Construction and Insulation Company (1979-81), SZOLNOKTERV (1981-86), PROFIL Engineering Studio (1987-90), MANOKA (Sevilla EXPO '92) (1991-92), REKONTERV Ltd. (1993-95), Erdei and Co. Ltd. (since 1996).

ÉDES, Imre (1951) Civil Engineer. Places of employment: GELKA (1970-71), Fütőber (1975-76), Alföldi Grain Industry Corp. (since 1976), Head of the Technical Department.

KONCZ, Lóránt (1967) Civil Engineer, MSc, Technical Manager. Places of employment: Adam Hörning GmbH, Mauer & Söhne GmbH, Germany (1992-95), Technical Manager at the EKS-Service Ltd. (since 1995).

Dr. OROSZ, Árpád (1926) Civil Engineer, MSc, retired University Professor. Places of employment: MÁV Bridge Construction Company (1953), Railway Scientific Research Institute (1954-56). Teacher at the Technical University of Budapest since 1956, Head of the Department of Reinforced Concrete Structures (1977-91). Retired in 1995. Specialist fields: design, restoration and strengthening of reinforced concrete structures, basins, silos, etc.

IMPLEMENTATION OF HIGH PERFORMANCE CONCRETE FOR PRESTRESSED CONCRETE BRIDGE GIRDERS



Assoc. Prof. István Bódi – Prof. Robert N. Bruce, Jr.

High performance concrete (HPC) was used in the prestressed concrete piles, pile caps, prestressed concrete girders, approach slabs, bridge deck in several bridges in United States. In the frame of cooperated research (Bruce-Russell, 1998, Russell-Fossier, 2000) the Charenton Canal Bridge (Louisiana) was examined as an excellent exemplar for implementation of high performance concrete in bridge constructions.

The instrumentation program was used to monitor girder curing temperatures, prestressing strand forces, prestress losses, deck strains, and camber. In addition, a concrete materials testing program was conducted to measure compressive strength, modulus of elasticity, modulus of rupture, coefficient of thermal expansion, creep, shrinkage, and permeability. Specific activities also included, data collection, analyses of data, and development of recommendations.

This paper focuses mainly on the results of the research for the precast, prestressed concrete girders. As a result, it is recommended that high performance concrete be used on all future bridge projects where its use is desirable and economical.

Keywords: high performance concrete, prestressed concrete, bridge girder, compressive strain, compressive strength, deflection, temperature, creep

1. INTRODUCTION

Since 1990, the Technical University of Budapest and the Tulane University (New Orleans-Louisiana/USA) are working together on the field of utilization of high strength, high performance concrete in bridge constructions, in frame of joint project of Hungarian –American Joint Research Fund (Bódi-Bruce, 1993-96, Bruce-Bódi, 2002). The research team had also the prestigious support of the Louisiana Department of Transportation and Development.

The Louisiana Department of Transportation and Development (DOTD) has been gradually introducing and evaluating the use of high performance concrete (HPC) in its bridges. Initial applications involved only high-strength concrete. More recently, Louisiana DOTD has been considering the use of HPC for both strength and durability.

In 1992, a 610 mm (24 in) square prestressed concrete pile with a centrally located 305 mm (12 in) diameter circular void and a length of 39.6 m (130 ft) was fabricated. The concrete mix had a cement content of 445 kg/m³ (750 lb/cu yd), a silica fume content of 56 kg/m³ (95 lb/cu yd), and a water-cementitious materials ratio of 0.27. Average concrete compressive strengths at 18 hours and 28 days were 58.3 and 72.1 MPa (8,449 psi and 10,453 psi), respectively. The pile was driven as part of the bridge for State Route 415 over the Missouri Pacific Railroad. The pile was monitored with a pile driving analyzer. Results indicated that driving stresses were within the Federal Highway Administration's (FHWA) driving stress limits and that no pile damage had occurred. The report notes that damage to the pile would have likely resulted if a concrete with a compressive strength of either 34 MPa (5,000 psi) or 41 MPa (6,000 psi) had been used (PCI Plant Certification Committee, 1999).

In 1993, bridges on the Inner Loop Expressway over Ellerbe Road and West 70th Street were constructed in Shreveport using AASHTO Type IV girders. The production concrete used

a cement content of 446 kg/m³ (752 lb/cu yd) and 7 percent silica fume. The specification required minimum concrete compressive strengths of 34 MPa (5,000 psi) at prestress transfer and 59 MPa (8,500 psi) at 28 days. An average concrete compressive strength of 57.9 MPa (8,400 psi) was achieved at 18 hours and an average strength of 77.2 MPa (11,200 psi) at 14 and 28 days.

A 1994 report on research sponsored by the Louisiana Transportation Research Center (LTRC), concluded that the provisions of the *AASHTO Standard Specifications for Highway Bridges* are conservatively applicable for structural members with concrete compressive strengths up to 69 MPa (10,000 psi). The report recommended that Louisiana DOTD considers the implementation of concrete with compressive strengths up to 69 MPa (10,000 psi) in a bridge and that the bridge should be instrumented to measure long-term behavior.

In 1997, the Louisiana DOTD began to design the Charenton Canal Bridge using high performance concrete for both the superstructure and the substructure. High-strength concrete was used in the precast, prestressed concrete piles and girders. High performance cast-in-place concrete was used in the pile caps, approach slabs, bridge deck, barrier slabs, and barrier rails. As part of the project, a research contract was awarded to assist DOTD in the implementation of high performance concrete in the Charenton Canal Bridge. The research program and the results for the bridge girders are the subject of this paper.

2. BRIDGE DESCRIPTION

The Charenton Canal Bridge, shown in Fig. 1, is located in St. Mary Parish on Highway LA 87. The bridge replaced an existing 55-year old reinforced concrete structure. Design of the new bridge was based on the *Louisiana Specifications for Roads and Bridges* using HS 20-44 and HST-18 highway live

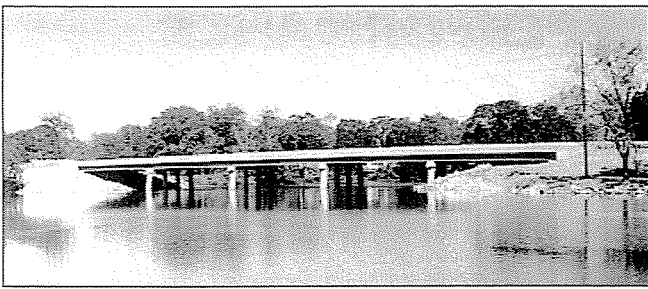


Fig. 1 Charenton Canal Bridge

loading (Louisiana Standards, 1992). The bridge is a 111.3 m (365 ft) long structure consisting of five 22.3 m (73 ft) long spans. A 12.2 m (40 ft) long, 305 mm (12 in) thick approach slab is provided at each end of the structure.

The superstructure of the bridge consists of five prestressed concrete AASHTO Type III girders per span spaced at 3.1 m (10 ft) centers supporting an 203 mm (8 in) thick reinforced concrete deck, as shown in *Fig. 2*. The total width of the bridge deck is 46 ft 14.3 m (10 in). The Type III prestressed concrete girders contain thirty-four 12.7 mm (1/2 in) diameter Grade 270 low-relaxation strands. Eight strands are debonded in pairs for various lengths at each end of the girders. Specified compressive strengths for the prestressed concrete girders were 48 MPa (7,000 psi) at release of the prestressing strands and 69 MPa (10,000 psi) by 56 days. Although the structural design of the girders only required concrete compressive strengths of 41 MPa (6,000 psi) at release of the strands and 62 MPa (9,000 psi) for design, higher strengths were specified to demonstrate that they could be achieved.

The 203 mm (8 in) thick cast-in-place reinforced concrete deck had a specified concrete compressive strength of 29 MPa (4,200 psi) at 28 days and was designed using Louisiana DOTD standard procedures and details. A dead load of 0.575 kN/m² (12 psf) was included to allow for future wearing surfaces. The bridge deck was designed as a continuous span over the girders and satisfied both working stress and load factor requirements. For working stress requirements, the slab was designed as a double-reinforced concrete slab with the main reinforcement perpendicular to the traffic direction. Reinforcement was Grade 60 with 51 mm (2 in) cover to the top reinforcement and 25 mm (1 in) cover to the bottom reinforcement. The transverse deck reinforcement consisted of 19 mm (0.75 in) diameter truss bars and 13 mm (0.5 in) diameter top and bottom straight bars. Longitudinal deck reinforcement consisted of top and bottom 13 mm (0.5 in) diameter bars.

Negative moment continuity over the piers is provided by

longitudinal reinforcement in the deck. No positive moment connection is provided. Diaphragms are provided at each abutment, over each pier, and at midspan.

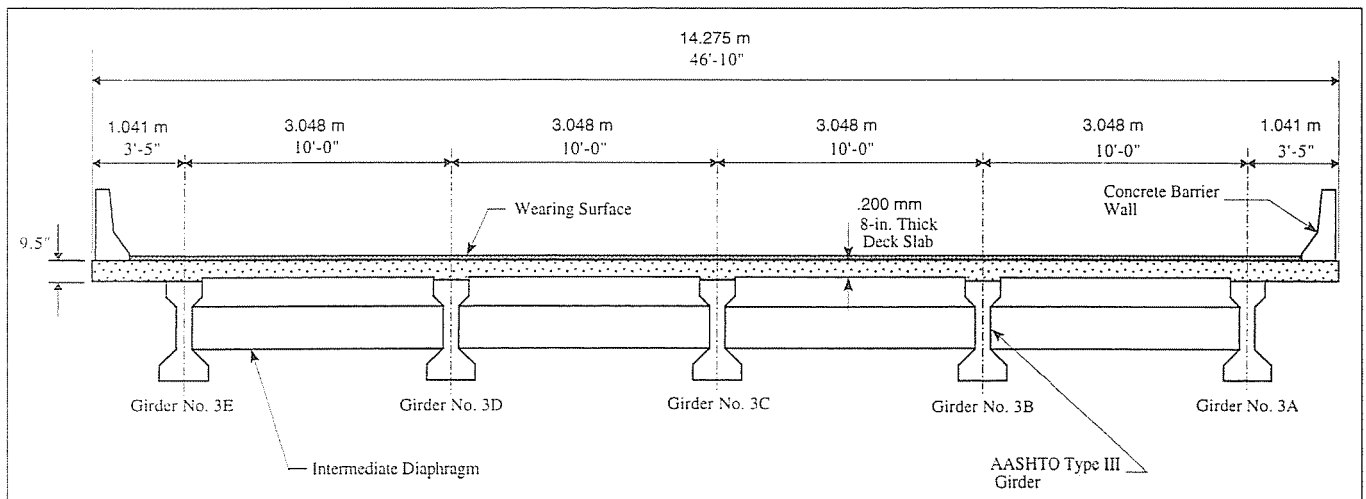
The substructure for the bridge consists of cast-in-place reinforced concrete bents supported on precast, prestressed concrete piles. The specified concrete compressive strength for the bent caps was 29 MPa (4,200 psi). The eight piles at each end bent are 610 mm (24 in) square. A single 350 mm (14 in) square pile supports each end bent wing wall. The four piles at each intermediate bent are 760 mm (30 in) square. Specified concrete compressive strengths for the piles were 28 MPa (4,000 psi) at release and 69 MPa (10,000 psi) no later than 56 days. The use of high-strength concrete in the piles increased their resistance to compressive and tensile driving stresses and allowed the casting and shipping of longer lengths.

Special provisions. The special provisions for the contract included the introduction of three new classes of concrete. The precast concrete used in the prestressed concrete girders and piles was designated Class P (HPC).

The specifications for the Class P (HPC) concrete included the following:

- Compressive strength by 56 days > 69 MPa (10,000 psi)
- Compressive strength at release of prestressing strands for girders > 48 MPa (7,000 psi)
- Compressive strength at release of prestressing strands for piles > 28 MPa (4,000 psi)
- Slump < 255 mm (10 in)
- Permeability at 56 days < 2,000 coulombs
- Optional use of silica fume up to 10 percent by weight of the total combination of cement, fly ash, and silica fume
- Optional use of fly ash with Type I, I (B), II, or III portland cement up to a maximum of 35 percent by weight of the total combination of cement, fly ash, and silica fume
- Maximum temperature rise of 22°C (40°F) per hour if external heat is used
- Maximum concrete temperature of 71°C (160°F)
- Release of prestressing strands before the internal concrete temperature decreases to 11°C (20°F) less than its maximum temperature
- Two recording thermometers showing time-temperature relationship per 61 m (200 ft) of bed
- Two demonstration trial batches of at least 2.3 m³ (3 cu yd)

Fig. 2 Cross section of the Charenton Canal Bridge



Material	Quantities	
	per yd ³	per m ³
Portland Cement T e III	691 lb	410 kg
Fly Ash - Class C	296 lb	176 kg
Fine Aggregate	1,135 lb	673 kg
Course Aggregate - Limestone	1,803 lb	1,070 kg
Water	247 lb	147 kg
Water Reducer, ASTM C494 - T e D	60 oz	2,320 ml
Superplasticizer, ASTM C494 - T e F	150 oz	5,802 ml
Air Entrainment	None	None
Properties		
Water/Cementitious Materials Ratio	0.25	0.25
Slump	7-3/4 in.	197 mm
56-day Compressive Strength on 4x8-in 102x203-mm cylinders	12,057 psi	83.1 MPa
(Chloride Permeability at 56 days)	1,079 coulombs	

Table 1 Approved mix proportions for girder concrete

- Use of match-curing technique with 102x203 mm (4x8 in) cylinders for determination of concrete strengths
- Optional use of non-standard gradations of sand and coarse aggregate if demonstrated in trial mixtures to produce the required concrete properties.

Girder production. The fabricator chose to manufacture the five girders for each span of the bridge in a single line of girders cast at the same time. This resulted in one casting for each span for a total of five castings. The trial placements had indicated that heat curing of the girders was unnecessary as sufficient heat of hydration was generated to allow the release strengths to be developed within an acceptable time period. The approved concrete mix proportions for the girder concrete are shown in *Table 1*. The measured compressive strengths at various ages for the quality control match-cured cylinders prepared and tested by the fabricator are given in *Table 2*. All girders achieved the specified compressive strength of 69 MPa (10,000 psi) by 28 days.

Deck construction. The 200 mm (8 in) thick reinforced concrete deck was cast in two placements. In the first placement, decks of Spans 4 and 5 were cast with a transverse construction joint placed in Span 4 at 1.8 m (6 ft) from the Span 3 end. In the second placement, the 1.8 m (6 ft) length of deck in Span 4 was cast together with the decks of Spans 1 through 3.

The bridge deck concrete was placed in September 1999. For both placements, concrete placement began early in the morning to avoid high temperatures and possible early drying of the concrete surface. Concrete was pumped for both placements. Fogging was started once the surface water sheen started to disappear. Fogging continued for 4-6 hours until the con-

Table 2 Measured compressive strengths for girder concrete
a All tests were made on 102x203 mm (4x8 in) match-cured cylinders
b Measured at 42 days

Span	Units	Release Age (hours)	Strength ^a at Ages of		
			Release	28 days	56 days
1	psi	24	7,618	10,213	11,043
	MPa		52.53	70.42	76.14
2	psi	21.5	7,983	11,504	11,663
	MPa		55.04	79.32	80.42
3	psi	40	7,816	10,600	10,502
	MPa		53.89	73.09	72.41
4	psi	21	7,383	11,545 ^b	10,958
	MPa		50.91	79.60 ^b	75.55
5	psi	23.5	9,852	11,230	12,023
	MPa		67.93	77.43	82.90

Material	Quantities	
	per yd ³	per m ³
Portland Cement T e III	306 lb	182 kg
GGBFS	305 lb	181 kg
Fine Aggregate	1,176 lb	698 kg
Course Aggregate - Limestone	1,900 lb	1,127 kg
Water	238 lb	141 kg
Retarder, ASTM C 494 -T es A and D	36.7 fl oz	1,420 ml
Air Entrainment	4.0 fl oz	155 ml
Properties		
Water/Cementitious Materials Ratio	0.39	0.39
Slump	4 in.	102 mm
28-day Compressive Strength 6x12-in (152x305 mm) cylinders	5,680 psi	39.2 MPa
Chloride Permeability at 56 days	1,019 coulombs	

Table 3 Approved mix proportions for deck concrete

crete was hard enough to walk on. The concrete was then covered with burlap and garden sprinklers placed on the high side of the bridge. This allowed the water to run across the deck and soak the burlap. The burlap was kept wet in this manner for seven days.

The approved concrete mix proportions for the deck concrete are shown in *Table 3*. Average compressive strengths at 28 days for the quality control cylinders were 36.9 MPa (5,349 psi) for Span 38.2 MPa (5,537 psi) for Spans 2 and 3, and 38.6 MPa (5,592 psi) for Spans 4 and 5.

3. OBJECTIVES

Bridge instrumentation. Construction of the Charenton Canal Bridge provided also a unique opportunity to learn about the performance of a bridge built in Louisiana with local materials. Consequently, the precast, prestressed girders and cast-in-place deck were instrumented to determine their performance both during and after construction. Information from this instrumentation program was then used to make recommendations about future design and construction procedures and specifications for bridges built of high performance concrete in Louisiana and in Hungary using the result of the program.

The instrumentation was used to monitor girder curing temperatures, prestressing forces, prestress losses, strains, and deflections. All instrumentation was located in Span 3 of the bridge. The individual girders in Span 3 of the bridge are identified as 3A through 3E, as shown in *Fig. 2*. Details of each type of instrumentation are given in the following sections.

Curing temperatures. Since high-strength concretes contain more cementitious material than used in normal strength concretes, the heat generated during hydration is greater. Since this heat does not escape from the concrete, the temperature of the concrete increases. This, in turn, affects the development of concrete compressive strength and related material properties.

The objectives of the instrumentation program to measure concrete curing temperatures were as follows:

1. Measure the variation with time of concrete temperatures from heat of hydration and curing environment
2. Measure the variation of concrete temperatures in a girder cross section
3. Measure the longitudinal variation of concrete temperatures of a girder
4. Measure the variation of concrete temperatures between girders in the same bed.

The objectives of the measurements were accomplished by installing thermocouples in four girders. In Girder 3A, nine thermocouples were located at three cross sections - midspan, one quarter point, and one end - for a total of 27 thermocouples. In Girders 3B, 3C, and 3D, three thermocouples were located at each midspan for a total of nine thermocouples. In addition to the thermocouples in the concrete, one thermocouple was installed outside the formwork and underneath the protective covering at midspan of each of the four girders and one thermocouple was used to monitor outside air temperature, for a total of five thermocouples. Also, thermocouples were placed in three concrete cylinders that were cured alongside each of the four prestressed concrete girders for a total of 12 thermocouples. The complete program required 53 thermocouples.

Prestressing forces. Measurements were made to determine the change of force in selected prestressing strands from time of tensioning, during curing, and until the strands were detensioned. Six load cells were positioned on strands at the dead end in the prestressing bed.

Prestress losses. Girders 3A through 3D were instrumented to determine prestress losses caused by elastic shortening, creep, and shrinkage. The prestress losses were measured using vibrating wire strain gages. Three gages were placed in each of four girders. The gages were placed at midspan and at the level of the centroid of the strand group. A total of twelve vibrating wire strain gages was installed. Each vibrating wire strain gage was equipped with a sensor to measure temperature at the gage location.

Deflections. Midspan deflections relative to each girder end were measured on Girders 3A through 3D. Immediately after casting and while the concrete was still plastic, steel bolts were embedded in the top surface of each girder at midspan and near both ends to provide permanent fixed reference points for camber measurements. The embedded bolts near each end were positioned above the sole plate. Camber measurements were made using a level to sight elevations at each reference point.

Deck strains. Strains in the concrete deck were measured at three locations using vibrating wire strain gages. All three gages were installed at mid-depth of the deck at midspan. One gage was installed above each center line of Girders 3A and 3B. The third gage was installed midway between Girders 3A and 3B. These gages measured strains in the concrete deck caused by the combined effects of shrinkage and creep of the deck and girders.

Concrete material property tests. A test program to measure compressive strength, modulus of elasticity, tensile strength, coefficient of thermal expansion, creep, shrinkage, and permeability of the concrete was conducted. This test program was in addition to that required by the precast girder producer for quality control.

Concrete compressive strength per AASHTO T 22 and modulus of elasticity per ASTM C 469 were measured on test specimens exposed to two different methods of initial curing. These are designated as match curing and field curing.

Match-cured 102x203 mm (4x8 in) concrete cylinders were produced using the Sure Cure Cylinder Mould System provided by the Federal Highway Administration (FHWA). The cylinders were match cured until release of the prestressing

strands. Then, the specimens were stripped from their moulds and stored in an outdoor environment near the girders until a few days before the age of testing. One specimen representing concrete in each of the four instrumented girders was tested at strand release, 7, 28, and 90 days. One specimen representing concrete in each of three girders was tested at 56 days for compressive strength and modulus of elasticity. The same specimens were used for compressive strength and modulus of elasticity. Tests were conducted by the FHWA.

The field-cured specimens for measurement of compressive strength and modulus of elasticity were 152x305 mm (6x12 in) concrete cylinders cured alongside the prestressed concrete girders under the enclosure that was placed over the girders. This curing procedure represented the current standard Louisiana DOTD curing procedure for Class P concretes. Following release of the prestressing strands, the field-cured cylinders were stripped and stored in an outdoor environment near the girders until a few days before the age of testing. The same cylinders were used for measurement of modulus of elasticity and concrete compressive strength. Five cylinders representing concrete in each of the four instrumented girders were made for the measurement of compressive strength and modulus of elasticity. Tests were conducted by the FHWA.

The modulus of rupture was measured by LTRC on four beam specimens representing concrete from each of the four instrumented girders. These specimens were cured initially alongside the prestressed concrete girders. Following release of the prestressing strands, the beams were stripped and stored in an outdoor environment near the prestressed concrete girders until a few days before the age of testing. Specimens were tested at strand release, 7, and 28 days.

The coefficient of thermal expansion was measured by Construction Technology Laboratories, Inc. (CTL) on one cylinder from each of the four instrumented girders in accordance with CRD C-39. Measurements were made as soon as possible after release of the prestressing strands and at 28 and 90 days. The same four specimens were used for measurements at the different ages.

Creep and shrinkage tests, in accordance with ASTM C 512, were conducted by CTL on cylinders representing concrete used in Girders 3A and 3C. Measurements were made on 152x305 mm (6x12 in) cylinders that were field cured alongside the precast concrete girders. Tests commenced at concrete ages of 2, 28, and 90 days. These specimens were stored in an outdoor environment near the girders until a few days before testing commenced.

Permeability tests in accordance with AASHTO T 277 were conducted by LTRC on samples of concrete cut from 102x203 mm (4x8-in) cylinders representing each of the four instrumented girders. These cylinders were field cured alongside the prestressed concrete girders until a few days before testing at an age of 56 days.

4. DISCUSSION OF RESULTS

Curing temperatures. Concrete curing temperatures were measured to determine the following:

1. Variation of concrete temperatures from heat of hydration and curing environment with time
2. Variation of concrete temperatures in a girder cross section
3. Longitudinal variation of concrete temperatures in a girder
4. Variation of concrete temperatures between girders in the same bed

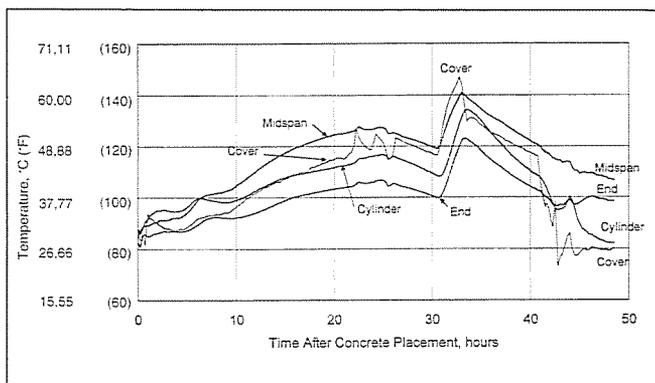


Fig. 3 Concrete temperature versus time for Girder 3A

5. Temperature in cylinders cured according to the state's procedure for conventional strength concrete.

Fig. 3 shows the variation of concrete temperature with time for four different locations as measured in Girder 3A. A concrete age of zero corresponds with first placement of concrete in the girder. The lines marked "Midspan" and "End" each represent the average temperature measured on nine thermocouples at midspan and one end, respectively. The line marked "Cylinder" represents the average temperature of three concrete cylinders cured under the covers. The line marked "Cover" identifies the temperature under the covers measured with a single thermocouple. Concrete temperature at time of placement was 29°C (85°F).

Concrete temperature in the girder increased until an age of about 24 hours. In the trial mixes prior to girder production, the required release strength was achieved by this age. However, for this line of girders, the strength was not sufficient and so it was necessary to undergo a second night of curing before release of the strands. Because the temperature of the concrete started to decrease and the specifications required that the strands be released before the girder temperature dropped 11°C (20°F) from its maximum value, it was necessary to provide additional heat to the girders. This was accomplished by injecting steam under the girder covers. This occurred at 30 1/2 hours after concrete placement. This is clearly depicted in Fig. 3, which shows the beginning of a sharp increase in temperature at about 30 1/2 hours. The injection of steam was stopped after 2 1/4 hours at a time of 32 3/4 hours. In planning the test program, it was anticipated that release strength would be achieved by 24 to 30 hours and that the addition of heat would not be necessary. Since the intent of the research was to investigate the variation of temperatures caused by internal heat of hydration, further discussion will be limited to temperatures that occurred during the first 30 hours.

The variation of temperature with time for the thermocouples placed along the vertical centerline of Girder 3A. Similar temperatures were measured along the vertical centerline at the quarter point of Girder 3A. A different pattern was measured at the end of Girder 3A, as discussed later. The maximum temperature occurred at Thermocouple 3, which was located in the middle of the bottom flange. The next highest temperatures were in the web and top flange. The lowest temperatures occurred at the top and bottom of the sections. These temperatures are consistent with expected results since the temperature increase is generated by the heat of hydration and heat only escapes from the surface of the member. The maximum difference in temperatures measured along the vertical centerline was 9°C (16°F).

Temperatures were measured at the top and bottom flanges

at the centerline and at the quarter point but not at the end of Girder 3A. The temperatures on opposite edges of the same flange were equal but less than the temperature measured in the middle of the same flange. Temperatures in the bottom flange were higher than temperatures in the top flange. The maximum difference between the temperatures measured at the edge and middle of the flanges was 7°C (12°F) and 4°C (7°F) for the bottom and top flanges, respectively.

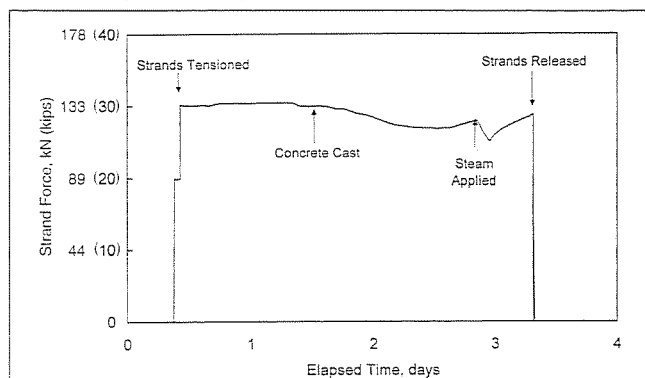
The average temperatures were calculated from the nine thermocouples at each section. The average measured temperatures at midspan and quarter point were very similar. However, the average temperature at the end was as much as 12°C (22°F) cooler. The end cross section selected for the temperature measurements was located at the end of the bed. At this location, the end of the girder is not as effectively enclosed by the covers as at the internal ends of the girders. Consequently, the girder was losing heat through the steel bulkhead at the end of the girder, along the prestressing strands, and through the steel base of the formwork. As an improvement in practice, it is recommended that the covers at the ends of the girders be tightly enclosed around the ends of the girders to retain the heat.

The average temperatures measured in Girders 3A and 3B were identical. Girder 3D had a slightly higher average temperature. In Girder 3C, the average temperature increased at a slower rate than in the other girders from about eight hours after placement. At 20 hours after placement, when Girders 3A, 3B, and 3D were cooling down, the average temperature in Girder 3C was still increasing. The maximum difference in the average temperature between the four girders was 7°C (13°F)

The maximum measured concrete temperature at any location in the four instrumented girders prior to application of the steam was 57°C (134°F) and occurred at the center of gravity of the bottom flange of the girder. The maximum measured temperature in the field-cured cylinders prior to application of the steam was 47°C (117°F). In all situations, the maximum temperatures in the girders were less than the specified maximum value of 71°C (160°F). This was also true after the application of the steam.

Prestressing forces. Although a calibrated hydraulic jack was used to tension the prestressing strands, the jack only provided a measurement of the force before the jack was released. Transfer of force from the hydraulic jack to the strand anchorage and the subsequent changes in strand temperature during the initial curing resulted in a change in the strand force prior to release. To monitor the magnitude of the change in force in the strand at the end of the bed, six load cells were placed on strands at the dead end of the prestressing bed. Fig. 4 shows

Fig. 4 Average prestressing force versus time



the average force in the six strands from the time the strands were first tensioned until they were released, as measured at the dead end of the bed. The average strand force after all strands were tensioned was 134 kN (30.2 kips) or 73 percent of the guaranteed ultimate strength (GUTS). The gradual increase in temperature of the concrete after placement and the rapid increase in concrete temperature when the steam was applied resulted in thermal expansion in the strand and in a decrease in the measured force. At the end of the period during which the steam was applied, the average force had decreased to 112 kN (25.1 kips) or 60 percent of GUTS. Immediately prior to release of the strand, the average force had increased to 128 kN (28.7 kips) or 69 percent of GUTS.

The engineering drawings for the bridge indicated a specified tensile force in the strands of 138 kN (30.98 kips) or 75 percent GUTS. The plant tensioning procedure was to apply an initial load of 8.9 kN (2,000 lb) to each strand and then to extend the strands for a calculated elongation. The calculated elongation takes into account the extension of the strand over the length of the bed for the increase in force from 8.9 to 138 kN (2.0 to 30.98 kips) as well as dead end and live end anchorage seating. The average force measured by the load cells at the dead end of the bed after all strands were tensioned and anchored was 134 kN (30.2 kips). This is well within the 5 percent tolerance indicated in the PCI Manual for Quality Control (PCI Plant Certification, 1999).

Just prior to release, the average force measured by the load cells was 128 kN (28.7 kips). This represents a loss of prestress prior to release of 7 percent of 138 kN (30.98 kips). Part of this loss is caused by relaxation and part by temperature changes with the larger proportion being caused by temperature. It should be noted that the load cells measure the force at the end anchorage. On the assumption that there is no loss caused by friction on the strand through the end abutment, the load cell force is also equal to the force in the strand between the abutment and the end of the nearest beam. This is not necessarily equal to the force in the strand at midspan of each girder if temperature changes have occurred since the strand bonded to the concrete. Prior to bonding between the concrete and the prestressing strand, changes in temperature of the strand causes a change in force in the strand. However, once the strand becomes adequately bonded to the strand, the concrete and the strand expand together so the force in the strand inside the girder no longer equals the force in the strand outside the girder. Since the force in the strand at the end of the bed outside the girder decreases, there is a transfer of force to the girder and so the girder becomes partially prestressed as it expands.

Based on the load cell data, it is not possible to identify when the concrete first bonds to the prestressing steel. However, it probably occurs gradually as the concrete increases in temperature and develops strength. Based on this assumption, the force in the strand during the bonding is probably between the value of 133 kN (30.0 kips) when the concrete was placed and 130 kN (29.2 kips) measured six hours later. This represents an average loss of prestress compared to 0.75 percent GUTS of 4 percent. This includes any losses from relaxation. Consequently, Louisiana DOTD may want to consider including a loss of 4 percent prior to release in calculations of prestress losses for HPC girders. This includes any loss of prestress from relaxation from time of tensioning until the strands are released.

Prestress losses. Three vibrating wire concrete strain gages were installed at the midspan of Girders 3A through 3D to determine prestress losses. The gages were positioned in the

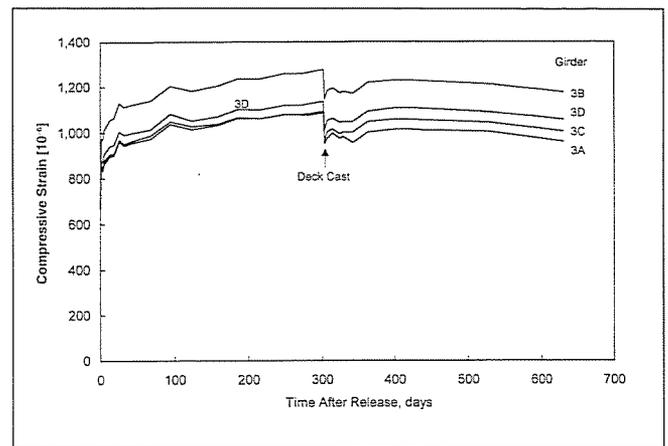


Fig. 5 Concrete compressive strain versus time for girders

bottom flange at the elevation of the center of gravity of the prestressing strands. The measured strains were adjusted to a constant temperature using the temperature measured by a thermistor in the strain gage, the measured coefficient of thermal expansion of the concrete, and the manufacturer's coefficient of thermal expansion of the gage wire.

The average change in strain for each of the four instrumented girders is shown in Fig. 5. A strain of zero was assumed immediately prior to release of the strands. The data show a rapid increase in strain in the first few days after release of the strands followed by a more gradual increase at a decreasing rate. A reduction in the measured strain occurred when the deck of the bridge was cast 302 days after release of the strands.

For comparison with measured data, prestress losses were calculated using the design assumptions and the provisions of the *AASHTO Standard Specifications* (Standard Specifications, 1996). Values are shown in Table 4. The measured values only represent losses caused by elastic shortening, creep, and shrinkage. The measured elastic loss at release is based on the difference in readings taken immediately before and immediately after all strands were released. Releasing strands took approximately 15 minutes. The elastic loss at 631 days is taken as the same value determined at release. The total creep and shrinkage loss is calculated as the difference between the total loss and the elastic loss.

Final losses were calculated using the procedure of the *AASHTO Standard Specifications* for three different sets of assumptions as shown in Table 5. Case 1 corresponds with the values used in the design calculations. Case 2 is based on specified compressive strengths, a haunch thickness as shown on the drawings, a modulus of elasticity of strand as supplied by the manufacturer, and the average span length of the instrumented girders. For both Cases 1 and 2, the stress in the strand after release was assumed to be $0.69 f_s'$, where f_s' = ultimate stress of the prestressing strand. Case 3 is based on meas-

Table 4 Measured and calculated prestress losses

	Measured	Original Design	Standard Specification	
			Specified	Measured
Release				
Elastic	14,336	16,234	15,195	13,194
Relaxation	-	1,600		
Total	-	17,834		
Final^a				
Elastic	14,336	16,234	15,195	13,194
Creep	18,589	25,686	26,328	25,200
Shrinkage		5,750	5,750	5,750
Relaxation	-	1,805	1,877	2,133
Total	32,925	49,475	49,150	46,277

Case	Girder		Deck		Strand Stress after Release	Haunch Thickness	E_s , ksi	Girder Span, ft
	f_{ci} , psi	f'_c , psi	f'_c , psi					
1	6,000	9,000	3,200	0.69f _c	1.0 in.	29,000	71.69	
2	7,000	10,000	4,200	0.69f _c	1.5 in.	28,000	71.57	
3	$E = 5,641$ ksi	$E_c = 6,020$ ksi	$E_c = 4,431$ ksi	As calculated	1.5 in.	28,000	71.57	

Table 5 Assumptions for calculations of prestress losses

ured values of modulus of elasticity of the concretes and a strand stress after release equal to the stress in the strands just after the concrete was cast less the calculated loss from elastic shortening. For purposes of calculating composite section properties, the modulus of elasticity values measured at 90 days were utilized.

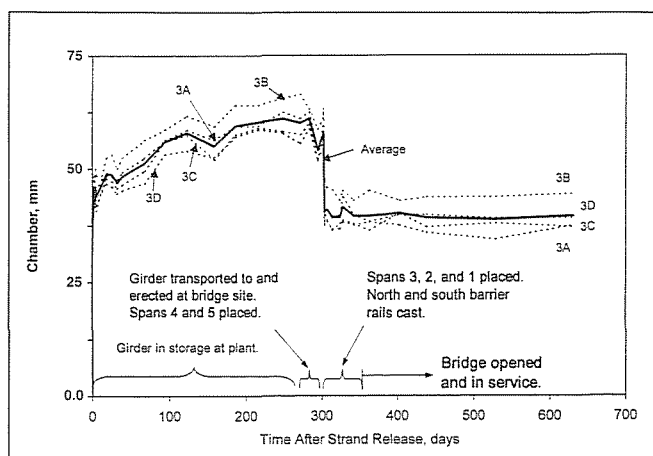
As shown in *Table 4*, use of the measured modulus of elasticity at release gives a reasonable prediction of the elastic losses. Exact agreement may not have been achieved for the following reasons:

1. The measured shortening may include some creep losses.
2. The effective modulus of elasticity of the strand may be different from the manufacturer's value of 193 GPa (28,000 ksi).
3. The modulus of elasticity of the concrete as measured on the match-cured cylinders may be larger than that of the concrete in the girders. The cylinders were stripped after the strands were released and took substantially longer to test than the time it took to release the strands.

For final losses, the measured value of the creep and shrinkage loss is 58 to 60 percent of the calculated values. According to PCI's "Recommendations for Estimating Prestress Losses," 74 percent of the creep and 86 percent of the shrinkage should have taken place by 365 days (PCI Committee, 1975). Measured values are substantially less than the calculated values. Based on these data, it may be concluded that calculations made using the detailed method of the *AASHTO Standard Specifications* will over-estimate creep and shrinkage losses. This is consistent with previous conclusions (Bruce-Russell, Roller, Martin, 1994).

Deflections. Midspan deflections of Girders 4A through 4D were measured relative to their ends. Immediately after casting and while the concrete was still plastic, steel bolts were embedded in the top surface of each girder at midspan and directly above the sole plate at each end. The bolts provided permanent fixed reference points for camber measurements using a surveying level. Prior to casting the bridge deck slab, the reference points in each girder were extended so that they would remain accessible after the concrete deck was placed. Midspan deflections of the individual girders and the average of all four girders are shown in *Fig. 6*.

Fig. 6 Girder midspan deflections versus time



Time after Release, days	Stage	Measured, in.		Calculated, in	
		Range	Average	Design	Actual
0.01	After release	0.89-1.06	1.00	1.41	1.18
0.14	In temporary storage	1.41-1.59	1.47	1.41	1.18
271	Before shipping	2.22-2.66	2.40	2.51	2.07
302	Before deck casting	2.17-2.53	2.30	-	-
303	After deck casting	1.50-1.78	1.61	1.64	1.24
631	Final Reading	1.50-1.78	1.58	0.76-0.87	0.33-0.42

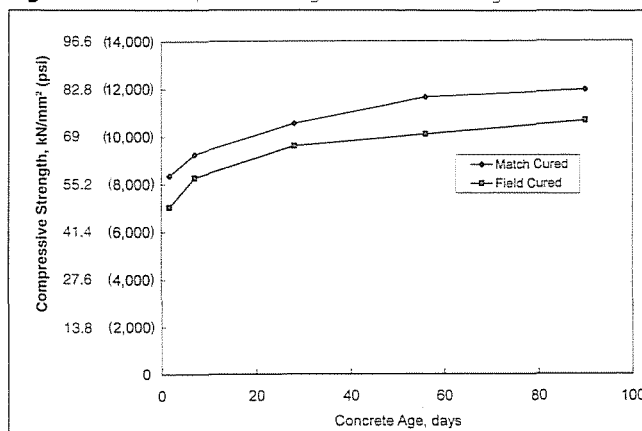
Table 6 Measured and calculated camber

Values of measured camber are compared with values of calculated camber in *Table 6* for various stages of construction. Two sets of assumptions were used for the calculated values. The design values were taken from the CONSPAN program used for the design of an interior girder of the bridge. The actual values are calculated using the measured modulus of elasticity values for the match-cured cylinders tested at release and 90 days and the deck cylinders tested at 90 days. The actual values also include the presence of a 38 mm (1.5 in) thick haunch. Multipliers for long-term deflections were based on the *PCI Design Handbook*, table 4.6.2 for both sets of calculated values (PCI Industry, 1992).

The measured camber at release was less than both calculated values. However, the measured readings were obtained while the girders were still on the casting bed. In this position, friction between the ends of the girders and the casting bed can prevent the full prestressing force from being transferred into the girders. After the girders were lifted from the bed and placed on temporary supports, the measured camber at this time exceeded the calculated values. It is likely, however, that the measured camber includes some deformations from creep and shrinkage as camber increases rapidly following release of the strand. Based on the measured data, the design approach provided a reasonable prediction of camber until after the deck was cast. Based on measured data from the time of deck casting until a concrete age of 631 days, it is unlikely that the final camber will be as low as the 19 to 22 mm (0.76 to 0.87 in) calculated using the design values or 8 to 11 mm (0.33 to 0.42 in) calculated using the actual values. The two calculated final values correspond to the alternate assumptions of simply supported or continuous over two spans after the deck is cast. Very little change in camber occurred after the deck was cast indicating that the long-term multipliers do not provide a reliable means to predict long-term camber.

Concrete material properties. Measurements of compressive strength, modulus of elasticity, modulus of rupture, chloride permeability, coefficient of thermal expansion, creep and shrinkage were made on test specimens representing concrete used in the midspan region of each instrumented girder. Measured concrete properties except creep and shrinkage are given in *Table 7*.

Fig. 7 Concrete compressive strength versus concrete age



Property	Curing	Specimen Size	Girder No.	Concrete Age					
				Release	7 days	28 days	56 days	90 days	
Compressive Strength, <i>psi</i>	Match	4x8-in. cyl.	3A	9,108	8,907	10,619	11,545	12,042	
			3B	8,205	9,849	10,521	11,404	12,424	
			3C	8,514	9,103	11,164	12,189	11,574	
			3D	7,627	9,141	9,958	-	11,761	
			Average	8,364	9,250	10,566	11,643	11,950	
			Field	6x12-in. cyl.	3A	6,472	8,357	9,081	9,583
	3B	6,839	8,588	10,485	10,660	11,601			
	3C	7,785	7,996	9,666	10,283	10,524			
	3D	6,996	8,136	9,205	9,825	10,321			
	Average	7,023	8,269	9,609	10,098	10,668			
	Modulus of Elasticity, <i>ksi</i>	Match	4x8-in. cyl.	3A	5,809	6,056	5,746	6,005	6,012
				3B	5,748	5,537	5,587	5,742	5,773
3C				5,630	6,057	6,215	6,180	6,127	
3D				5,387	5,985	5,660	-	6,168	
Average				5,641	5,909	5,787	5,976	6,020	
Field				6x12-in. cyl.	3A	5,013	5,550	6,052	6,053
3B		5,432	5,524	5,743	5,907	6,230			
3C		5,438	5,997	5,956	5,841	5,784			
3D		5,413	6,381	5,815	6,090	5,595			
Average		5,324	5,938	5,892	5,973	5,974			
Modulus of Rupture, <i>psi</i>		Field	6x6x20-in. beam	3A	779	764	966	-	-
				3B	753	814	916	-	-
	3C			673	808	910	-	-	
	3D			808	929	885	-	-	
	Average			753	829	919	-	-	
	Overall Average			753	829	919	-	-	
Permeability, <i>Cosmoms</i>	Field	4x8-in. cyl.	3A	-	-	-	1,352	-	
			3B	-	-	-	1,272	-	
			3C	-	-	-	1,286	-	
			3D	-	-	-	1,508	-	
			Average	-	-	-	1,355	-	
			Overall Average	-	-	-	1,355	-	
Coefficient of Thermal Expansion, <i>millionths/°F</i>	Field	6x12-in. cyl.	3A	4.68	-	4.55	-	4.03	
			3B	4.75	-	4.37	-	4.67	
			3C	4.73	-	4.72	-	4.23	
			3D	4.90	-	4.43	-	4.37	
			Average	4.77	-	4.47	-	4.33	
			Overall Average	4.52	-	4.52	-	4.33	

Table 7 Concrete material properties - girder concrete

A comparison of average compressive strengths measured on the match-cured cylinders and the field-cured cylinders is shown in Fig. 7. Based on previous research, it was anticipated that the match-cured cylinders would achieve a higher compressive strength at earlier ages than the field-cured cylinders. At later ages, it was anticipated that the reverse would be true. The test results show that the match-cured cylinders had higher compressive strengths at all ages with a difference of average strengths that ranged from 6.60 to 10.7 MPa (957 to 1,545 psi).

The temperatures of the field-cured cylinders were less than the temperatures measured in the bottom flange of the girders and in the match-cured cylinders. Consequently, the field-cured cylinders should have a lower compressive strength at early ages. The lower compressive strengths at release can be seen in Table 7 and Fig. 7. However, the field-cured cylinders continued to have a lower strength even at later ages.

Temperature measurements indicate that the temperature of the field-cured cylinders increased substantially when the steam was injected. It is, therefore, thought that the injection of steam accelerated the early strength gain of the field-cured cylinders. This, in turn, caused the strength gain to be slower at later ages. Since the concrete temperature during hydration influences the development of concrete compressive strength, the match-cured cylinders develop a strength at any age that should more closely represent compressive strength of the concrete in the girder. Consequently, it is recommended that match-cured cylinder be used with high performance concrete girders for determination of compressive strength at all ages.

The values of modulus of elasticity given in Table 7 indicate less difference between match - cured cylinders and field-cured cylinders. The only difference between the average values occurs at release age. For all other ages, the values are essentially identical. In addition, the modulus of elasticity did not increase much after a concrete age of seven days.

A comparison of the modulus of elasticity and compressive

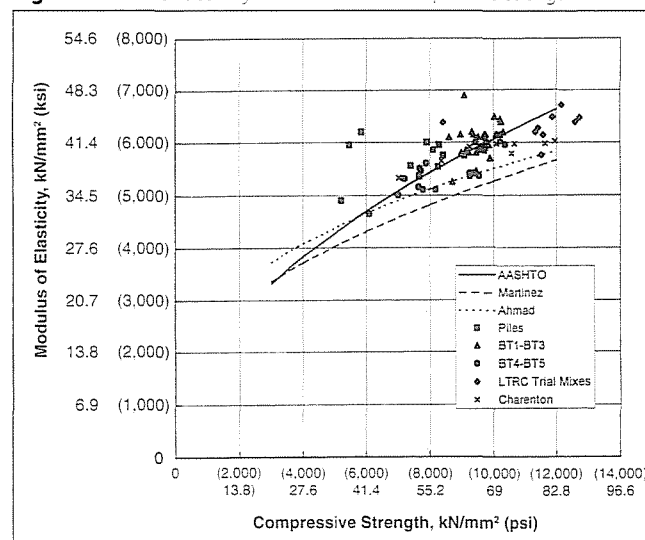
Specimen No.	Concrete Age, <i>days</i>	Compressive Strength, <i>f_c'</i> , <i>psi</i>	Modulus of Rupture, <i>psi</i>	Coefficient k
P1	28	7,400	720	8.37
P1	56	7,660	733	8.38
P2	28	7,900	750	8.43
P2	56	8,290	883	9.70
P3	28	8,410	665	7.25
P3	56	5,250	817	9.00
BT1-2	40	9,570	810	8.28
BT2-2	40	9,900	840	8.44
BT3-2	660	10,180	890	8.82
BTS-1	28	7,680	750	8.56
BTS-2	28	9,250	580	6.03
BTS-3	28	9,550	820	8.39
3A	1.67	6,472	779	9.68
3A	7	8,357	764	8.36
3A	28	9,081	966	10.14
3B	1.67	6,839	753	9.11
3B	7	8,588	814	8.78
3B	28	10,485	916	8.95
3C	1.67	7,785	673	7.63
3C	7	7,996	808	9.04
3C	28	9,666	910	9.25
3D	1.67	6,996	808	9.66
3D	7	8,136	929	10.30
3D	28	9,205	885	9.22

Table 8 Modulus of rupture-girder concrete

strength for the data shown in Table 7 and data obtained on previous LTRC projects is shown in Fig. 8. Also included in Fig. 8 are equations proposed by other investigators and discussed in the Interim Report (Bruce, Russell, Roller, 1998). It is apparent that the most consistent prediction of modulus of elasticity up to a compressive strength of 69 MPa (10,000 psi) is obtained utilizing the AASHTO/ACI equation. Consequently, it is recommended that when values for a specific mix are unknown, Louisiana DOTD continue to use the AASHTO/ACI equation for prediction of modulus of elasticity up to specified compressive strengths of 69 MPa (10,000 psi). For compressive strengths above 69 MPa (10,000 psi), it would be appropriate to use a slightly reduced value unless data for a specific mix are available.

The values of modulus of rupture (*MOR*) obtained from the present study are listed in Table 8 along with values obtained from previous LTRC investigations. The average value of the coefficient from the present study is 9.2 compared to the average value of 8.3 determined from previous studies. For all data, the modulus of rupture had an average value of $8.7\sqrt{f'_c}$ psi ($0.73\sqrt{f'_c}$ MPa). This coefficient is slightly higher

Fig. 8 Modulus of elasticity versus concrete compressive strength



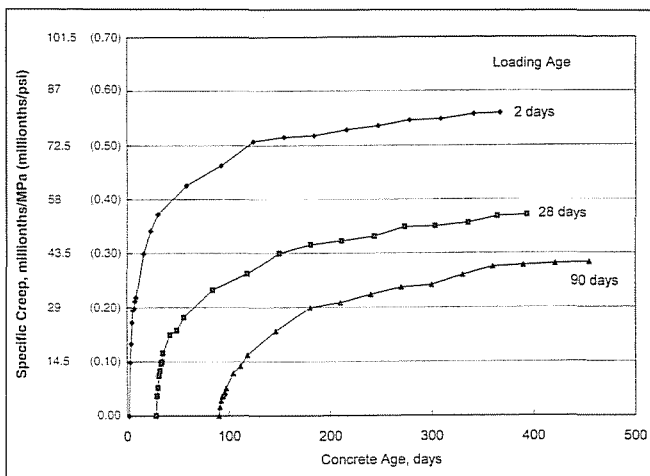


Fig. 9 Specific creep versus concrete age

than the traditional value of $7.5\sqrt{f'_c}$ psi ($0.62\sqrt{f'_c}$ MPa). A higher modulus of rupture can be beneficial in allowing a higher tensile stress at midspan under service load design. However, the values shown in Table 8 only support a small

increase in the allowable tensile stress. In the table $k = \frac{MOR}{\sqrt{f'_c}}$.

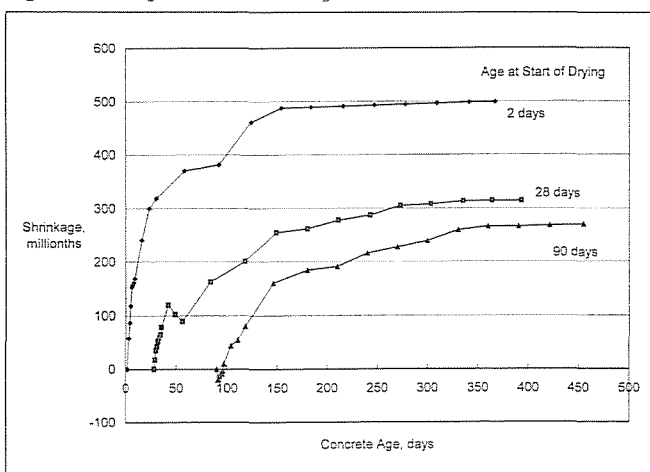
The average chloride permeability determined for concrete used in the girders was 1,355 coulombs at 56 days. This is less than the 2,000 coulombs specified but slightly greater than the values of 1,079 coulombs determined for the approved mix proportions.

Tests to determine the coefficient of thermal expansion of the girder concrete were made at release of the strands, 7 days, and 90 days on field-cured 152x305 mm (6x12 in) diameter cylinders. An overall coefficient of thermal expansion of 4.52 millionths/°F (8.14 millionths/°C) was used to adjust the measured strains for changes in concrete temperatures.

Creep and shrinkage were measured on 152x305 mm (6x12 in) diameter cylinders representing the concrete used in Girders 3A and 3C. Specific creep data for cylinders loaded at 2, 28, and 90 days are shown in Fig 9. These data reflect two phenomena observed with conventional strength concretes the rate of creep decreases with time and the specific creep is less for concrete loaded at later ages.

Shrinkage data for the companion cylinders used in the creep tests are shown in Fig. 10. The specimens were retained on site until shortly before testing began. Consequently, some shrinkage had occurred in the cylinders before measurements began on cylinders identified as 28 days and 90 days. The shrinkage data starting at a concrete age of two days more

Fig. 10 Shrinkage versus concrete age



closely represents the full amount of shrinkage on a 152x305 mm (6x12 in) diameter cylinder exposed to drying at 23 °C (73 °F) and 50 percent relative humidity.

Assessment of the special provisions. The purpose of this section is to discuss the special provisions that were developed for the Charenton Canal Bridge in the light of actual experiences and measured results. Each provision is summarized after the bullet point and followed by a brief discussion.

4.1 Class P(HPC) concrete provisions.

- Compressive strength by 56 days > 69 MPa (10,000 psi)
This provision allowed the contractor to achieve the specified strength no later than 56 days. However, the contractor could not ship the girders until an age of 28 days. Test results showed that the specified design strength was achieved by 28 days on three out of the four instrumented girders as measured using the match-cured cylinders. By 56 days, all three girders for which strengths were measured had compressive strengths in excess of 69 MPa (10,000 psi). Consequently, the fabricator was able to achieve the specified strengths in less than 56 days. However, it is recommended that 56 days be retained to allow the fabricator greater flexibility.
- Compressive strength at release of prestressing strands for girders > 48 MPa (7,000 psi).
For the line of girders cast for Span 3, the fabricator did not achieve the release strength within one day of casting. However, for the other four lines of girders, release strengths greater than 48 MPa (7,000 psi) were achieved at ages ranging from 21 to 24 hours. For one line of girders, a strength of 67.9 MPa (9,852 psi) was achieved at 23 1/2 hours. Consequently, a concrete strength of 48 MPa (7,000 psi) at release of prestressing strands is achievable within 24 hours using local materials.
- Compressive strength at release of prestressing strands for piles > 28 MPa (4,000 psi).
This is a standard provision and was not addressed by the research.
- Slump < 255 mm (10 in).
This provision allowed the fabricator to select the slump. This is different from normal procedures where a slump is specified. The fabricator was required to do trial batches to demonstrate that the concrete would not segregate at the proposed slump. Since the fabricator is in a much better position to select slump for the particular application, it should continue to be used.
- Permeability at 56 days < 2,000 coulombs.
- Test results showed that this permeability was easy to achieve. It is possible that, a lower value could be specified.
- Optional use of silica fume up to 10 percent by weight of the total combination of cement, fly ash, and silica fume.
The fabricator did not use silica fume in the concrete so it was not part of the research. The use of silica fume facilitates the development of early compressive strength.
- Optional use of fly ash with Type I, I(B), II, or III portland cement up to a maximum of 35 percent by weight of the total combination of cement, fly ash, and silica fume.
The fabricator successfully used 30 percent on the project. There does not seem to be any reason to change this provision.

- Maximum temperature rise of 22°C (40°F) per hour if external heat is used.

The fabricator chose not to use external heat for curing. However, some heat was required to prevent the temperature of the girders from dropping more than 11°C (20°F). The temperature rise from heat of hydration was substantially less than 22°C (40°F) per hour. This is a standard provision that should be retained.

- Release of prestressing strands before the internal concrete temperature decreases to 11°C (20°F) less than its maximum temperature.

This provision was included to reduce the likelihood of cracking in the girders prior to release of the strands. It was written on the assumption that the release strength would be achieved at about the same time that the maximum temperature was achieved. When strengths were not achieved and the concrete temperature began to fall, it became necessary to add steam to maintain the temperature. The goal was to prevent the temperature from falling any more and not necessarily to cause a sharp increase in the concrete temperature. However, from a practical standpoint, controlling the application of steam to maintain a constant temperature was difficult. Nevertheless, there needs to be a provision to ensure that the temperature is maintained at or near its peak value if cracking of the girders prior to release is to be avoided.

- Two recording thermometers showing time-temperature relationship per 61 m (200 ft) of bed.

This requirement is twice the number required by the *Louisiana Standard Specifications*. Until additional experience with HPC is attained, this provision should be retained. With the low cost of data acquisition systems, it should not be a major cost to the fabricator.

- Two demonstration trial batches of at least 2.3 m³ (3 cu yd).

For the Louisiana DOTD, the trials provided a demonstration that the concrete would not segregate. For the fabricator, the trials provide a learning curve prior to actual production. For this project, the fabricator was able to identify changes needed to improve concrete production.

- Use of match-curing techniques with 102x203 mm (4x8 in) diameter cylinders for determination of concrete strengths.

Test results have illustrated the differences in concrete temperatures between match-cured and field-cured cylinders and their effect on concrete strength. The use of 102x203 mm (4x8 in) diameter cylinders instead of 152x305 mm (6x12 in) diameter cylinders did not appear to have any disadvantages. Louisiana DOTD should require the use of match-cured cylinders for all projects with specified compressive strengths of 69 MPa (10,000 psi) or greater and allow it as an option for precast, prestressed members with compressive strengths less than 69 MPa (10,000 psi).

- Optional use of non-standard gradations of sand and coarse aggregate if demonstrated in trial mixtures to produce the required concrete properties.

The fabricator used gradations conforming to the *Louisiana Standard Specifications*. The option should continue to be allowed until some experience with its use is obtained. With HPC, there is a trend to consider combined gradings of fine and coarse aggregate rather than separate gradations.

5. CONCLUSIONS

Design and construction of the Charenton Canal Bridge has demonstrated that a bridge using HPC in both substructure and superstructure can be successfully constructed in Louisiana using local materials. In general, the special provisions resulted in the use of appropriate materials and technology for HPC. The only provision that caused some difficulty was the requirement to release strands before the concrete temperature dropped more than 11°C (20°F). This only occurred on one casting out of five.

Specific conclusions from the various aspects of the research are given in the following sections.

5.1 Curing temperatures

Temperature differences measured along the vertical centerline of a girder were as high as 9°C (16°F).

The internal temperature at the center of the bottom flange was as much as 7°C (12°F) hotter than the edges.

The internal temperature at the center of the top flange was as much as 4°C (7°F) hotter than the edges.

The average temperatures measured at the end of a girder were as much as 12°C (22°F) cooler than temperatures measured at a quarter point and midspan.

The average temperatures measured at the midspan of each girder differed by 7°C (13°F).

With the exception of the temperatures measured at the end of one girder, the temperature differences within a girder cross section or between girders are not considered to be excessive. Mass concrete specifications often allow a temperature differential of 20°C (36°F).

Temperatures differences between the match-cured and field-cured cylinders were as much as 17°C (30°F).

5.2 Prestressing forces

The prestressing force in the strand varies from the time the strands are tensioned until they are released. An allowance should be made for the change in force from time of tensioning until release of the strand. Measured strand forces at the end of the bed indicated that a loss of about 4 percent of 0.75 percent of GUTS or 56 MPa (8100 psi) would be appropriate. This loss includes that from relaxation of the strand.

5.3 Prestress losses

Calculations made using the procedures of the *AASHTO Standard Specifications* underestimated prestress losses even when the actual modulus of elasticity was used in the calculation. The underestimate results from the prediction of creep and shrinkage losses.

5.4 Deflections

Calculations of camber made using the PCI multiplier method gave reasonable agreement with measure values prior to deck casting. After deck casting, agreement was not very good.

5.5 Deck strains

Strains measured in the deck were less than 80 millionths after 330 days. A visual inspection of the deck 228 days after casting did not reveal any cracks.

5.6 Concrete material properties

Concrete compressive strengths and modulus of elasticity measured on match-cured cylinders were higher at all ages than corresponding values measured on field-cured cylinders. The AASHTO/ACI equation gave the most consistent prediction of the relationship between modulus of elasticity and concrete compressive strength for strengths up to 69 MPa (10,000 psi). Above 69 MPa (10,000 psi), the equation tended to overestimate the modulus of elasticity.

The measured modulus of rupture had an average value of $8.7\sqrt{f'_c}$ psi ($0.73\sqrt{f'_c}$ MPa). A slightly higher value than $7.5\sqrt{f'_c}$ psi ($0.62\sqrt{f'_c}$ MPa) may be appropriate for design. This would allow an increase in the allowable tensile stress under service load.

Measured rapid chloride permeabilities for the precast, prestressed girder concrete and cast-in-place deck concrete indicated concrete that would be classified as having low chloride ion penetration. Tests on concrete cores taken from the deck and approach slabs indicated a concrete with a very low chloride ion penetration.

6. RECOMMENDATIONS

Based on the DISCUSSION OF RESULTS and CONCLUSIONS, the following recommendations are made for implementation of HPC bridge girders.

1. The special provisions developed for his project should be modified as follows for use on future HPC projects:
 - Reduce the minimum cementitious material content to 362 kg/m³ (611 lb/cu yd).
 - Reduce the maximum water content to 145 kg/m³ (244 lb/cu yd).
- Allow the use of ground granulated blast furnace slag for cast-in-place concrete
2. The use of match-cured cylinders should be considered as an option for precast, prestressed concrete members with specified compressive strengths less than 69 MPa (10,000 psi).
3. In design, consideration should be given to including a prestress loss of 56 MPa (8,100 psi) prior to release of the strands.
4. The long-term multiplier used in the CONSPAN program should not be relied on to give an accurate prediction of long-term camber.
5. When covers are used to contain the heat from the girders, the ends should be closed to minimize heat loss.
6. For design, the AASHTO/ACI equation should be used to calculate modulus of elasticity from concrete compressive strength for strengths up to 69 MPa (10,000 psi). Above 69 MPa (10,000 psi), a slightly reduced value would be appropriate.
7. An increase in the allowable tensile strength under service load design to $0.62\sqrt{f'_c}$ MPa ($7.5\sqrt{f'_c}$ psi) should be considered.

8. Louisiana DOTD should proceed with the implementation of HPC on all bridges where its use is desirable and economical. Specified strengths up to 69 MPa (10,000 psi) and permeabilities less than 2000 coulombs can be specified with the knowledge that they are achievable in practice.

7. REFERENCES

- Aymond, T. W. - Theobald, D., (2000) "High Performance Concrete Extends Life of Charenton Canal Bridge," *PCI Journal*, Vol. 45, No. 4, July-August 2000, pp. 52-62.
- Bódi I., - Bruce, R. N. (1993-1996), "Optimization of the utilization of Extra High Strength Concrete" Research Project of US-Hungarian joint Research Board No.: 417/93.
- Bruce, R. N. - Bódi I. (2002) "Hungarian - American Technology Transfer" Fulbright Challenge and Responses- Proceedings of Conference celebrating the 10th Anniversary of the Hungarian-American Fulbright Commission and the Hungarian Fulbright Association. April 24-25, 2002. Budapest
- Bruce, R. N.- Russell, H. G.- Roller, J. J.- Martin, B. T. (1994), "Feasibility Evaluation of Utilizing High-Strength Concrete in Design and Construction of Highway Bridge Structures," Final Report - Louisiana Transportation Research Center, *Research Report* No. FHWA/LA-94-282, Baton Rouge, LA, 1994, 168 pp.
- Bruce, R. N.- Russell, H. G.- Roller, J. J. (1998) "Implementation of High Performance Concrete in Louisiana Bridges," *Interim Report* - Louisiana Transportation Research Center, Research Report No. 310, Baton Rouge, LA, February 1998, 67 pp.
- Louisiana Standard Specifications for Roads and Bridges, (1992), State of Louisiana, Department of Transportation and Development, Baton Rouge
- PCI Committee on Prestress Losses, (1975) "Recommendations for Estimating Prestress Losses," *PCI Journal*, Vol. 20, No. 4, July-August 1975, pp. 44-75.
- PCI Industry Handbook Committee, (1992) "PCI Design Handbook, Fourth Edition," MNL 120-92, Precast, Prestressed Concrete Institute, Chicago, IL.
- PCI Plant Certification Committee, (1999) "Manual for Quality Control for Plants and Production of Structural Precast Concrete Products," MNL-116-99, Precast, Prestressed Concrete Institute, Chicago, IL.
- Russell, H. G.- Fossier, P. B., (2000). "Design and Construction of the Charenton Canal Bridge, Charenton, Louisiana," Symposium Proceedings, PCI/FHWA/fib International Symposium on High Performance Concrete, Orlando, FL, *Journal of Precast, Prestressed Concrete Institute*, Chicago, IL, pp. 117-127.
- Standard Specifications for Highway Bridges*, sixteenth edition (1996) American Association of State Highway and Transportation Officials, Washington, DC, . 677 pp.

Assoc. Prof. István BÓDI PhD, is working at the Department of Structural Engineering at the Budapest University of Technology and Economics. His main fields of activities are: experimental and analytical investigation of reinforced and prestressed concrete, strengthening of existing concrete and timber structures. Dr. Bódi is a member of the American Concrete Institute (ACI), an associate member of ACI Committee #423 for *Prestressed Concrete*, he is also a member of Swiss Federal Institute of Timber. He has served as a visiting Lecturer at Technical University of Vienna, in 1989 and as a Dr. Korányi Research Scholar at the Ferguson Laboratory of the University of Texas at Austin, in 1989-90. He is also a Board Member of the Hungarian Group of *fib*.

Prof. Robert N. Bruce, Jr. is the Catherine and Henry Boh C hair in Civil Engineering at Tulane University in New Orleans, USA. Dr. Bruce received the Doctor of Philosophy degree in civil engineering from the University of Illinois. He is a Fellow of the American Concrete Institute, a Fellow of the Prestressed Concrete Institute, and one of five United States Delegates to the International Association for Bridge and Structural Engineering. He has served as a Fulbright Research Scholar at the Magnel Laboratory at the University of Ghent, Belgium in 1954; as a Fulbright Lecturer at the Rangoon Institute of Technology in Burma in 1979; and as a Senior Fulbright Fellow at the Technical University of Budapest in Hungary in 2000.

CONVERSIONS

- 1 in = 25.4 mm
1 yd³ = 0.765 m³
1 lb/in² = 1 psi = 0.006895 N/mm²
1 kip/in² = 1 ksi = 6.895 N/mm² = 6.895 MPa
1 lb = 4.448 N
1 kip = 4.448 kN
°C = (°F-32)/1.8

VIBRATIONS OF NON-UNIFORM TOWER CONSTRUCTIONS



Dr. Zsolt Huszár

This paper presents a continuum method for the non-uniform cantilever's dynamic solution in case of undamped free bending vibration. The method for determination of eigenfrequencies and mode shapes is based on the application of Rayleigh's quotient. The eigenfrequencies of the non-uniform cantilever could be obtained by gradual modification of the mode shape of uniform beam. Not only the smallest eigenfrequency as the absolute minimum, but also further ones as local minimum values of Rayleigh's quotient could be received. The continuum method was controlled by a detailed finite element analysis. The results of the two methods have shown a good coincidence. The advantage of the continuum method is that it requires less input data than the finite element analysis.

Keywords: cantilever, non-uniform, Rayleigh's quotient, eigenfrequency

1. INTRODUCTION

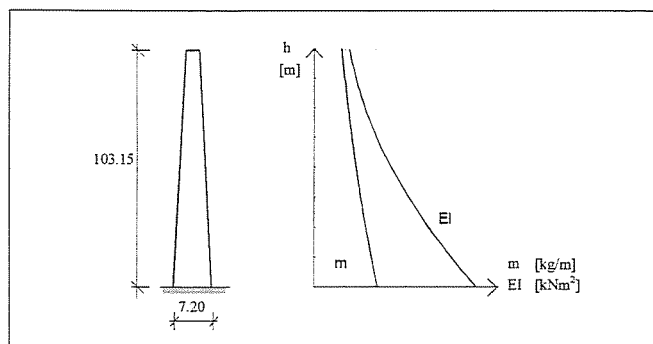
In the practice of structural engineering, there are several constructions, such as chimneys, television towers, and high-rise buildings, which could be modelled by non-uniform cantilevers. For the determination of the eigenfrequencies in the preliminary analysis, simple approximate formulae are very often used. In the detailed calculations finite element models are usually preferred.

For the dynamic solution to such structures with fixed foundations' I have developed a continuum method. Originally the intention of this work was to find the eigenfrequencies and mode shapes of a high ventilating chimney (Fig. 1). From the figure it can be seen that the bending stiffness decreases more quickly upwards than does the specific mass.

2. PRINCIPLE OF THE ANALYTICAL SOLUTION

A continuum method will be presented for the analysis of undamped free bending vibration of non-uniform cantilevers. The method is based on the use of the uniform cantilever's dynamic solution and of the extreme-value property of Rayleigh's quotient. The eigenfrequency of the non-uniform cantilever could be obtained by gradual modification of the mode shape of the uniform beam.

Fig. 1 The specific mass and bending stiffness plotted against height of the investigated chimney



2.1 Dynamic solution to the uniform cantilever

The undamped free bending vibration of uniform beams is described by the next partial homogeneous differential equation (Clough & Penzien, 1975; Vértés, 1985; Pfaffinger, 1989):

$$EI(x) \frac{\partial^4 w}{\partial x^4} + \rho A \frac{\partial^2 w}{\partial t^2} = 0 \quad (1)$$

where, EI = bending stiffness of the beam; A = cross-sectional area; ρ = density of beam material; $w(x, t)$ = function, displacement of beam in z direction; x = variable, length co-ordinate; t = variable, time.

In the case of a cantilever beam the following four boundary conditions should be satisfied: two geometrical conditions (2a) in the fixed bottom section and two static conditions (2b) in the free top section:

$$w(0, t) = 0 \quad (2a)$$

$$w'(0, t) = 0$$

$$M = EIw''(\ell, t) = 0 \quad (2b)$$

$$Q = EIw'''(\ell, t) = 0$$

where M = bending moment in the plane of vibration; Q = shear force in the plane of vibration; ℓ = length of cantilever.

The differential equation (1) can be solved by the separation of the variables. For that purpose the unknown $w(x, t)$ displacement function is considered as the product of two functions, $y(x)$ with the variable of length co-ordinate and $T(t)$ with the variable of time:

$$w(x, t) = y(x)T(t) \quad (3)$$

In this way the partial differential eq. (1) separates into two common differential equations after substitution of (3). The eigenfrequencies and mode shapes could be obtained from eq. (4) containing the length co-ordinate.

$$EIy^{IV} - \omega^2 \rho A y = 0 \quad (4)$$

where ω = circular eigenfrequency of the free bending vibration.

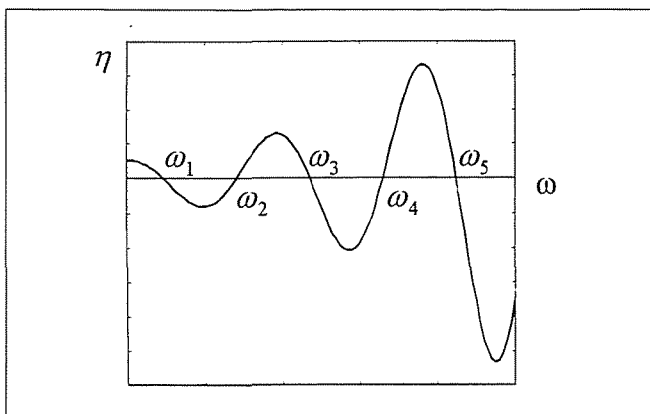


Fig. 2 Function

Looking for the solution in exponential form, the following characteristic equation can be obtained:

$$\alpha^4 - \omega^2 \frac{\rho A}{EI} = 0 \quad (5)$$

The solution of the (5) characteristic equation:

$$\alpha_{1,2} = \pm \lambda_1 \quad \alpha_{3,4} = \pm \lambda_2 i \quad \text{where: } \lambda = \omega^2 \frac{\rho A}{EI}$$

Hence the mode shape of the uniform cantilever (Kollbrunner & Hajdin, 1976; Zalka, 1994):

$$\zeta_0(x) = c_1 e^{\lambda x} + c_2 e^{-\lambda x} + c_3 \sin \lambda x + c_4 \cos \lambda x \quad (6)$$

The ω eigenfrequency, involved in λ argument and the c_i coefficients can be determined from the boundary conditions (2). The four boundary conditions are represented by the following Eqs. in matrix form:

$$[A(\lambda(\omega))] \{c\} = \{0\} \quad (7)$$

where, $[A]$ = 4*4 matrix containing the expressions of the four basic functions of eq. (6) according to the four boundary conditions; $\{c\}$ = vector of 4 elements containing the unknown c_i coefficients.

The eigenfrequencies and the mode shapes could be received as the non-trivial solutions of Eq. (7):

$$\det[A(\omega)] = 0 \quad (8)$$

The ω values, which make the $[A]$ matrix's determinant to zero (8), are the eigenfrequencies of the vibration (Fig. 2).

The zero points of the function $\eta = \det[A(\omega)]$ could be found by iteration (Korn & Korn, 1975).

2.2 Extreme-value property of the Rayleigh quotient for vibrating beams

The Rayleigh quotient referring to fixed vibrating cantilevers could be written as:

$$\omega^2 = \frac{\int_0^l EI[y''(x)]^2 dx}{\int_0^l \rho A[y(x)]^2 dx} \quad (9)$$

Without exact mode shapes, the Rayleigh quotient gives an approximate value for the investigated eigenfrequency,

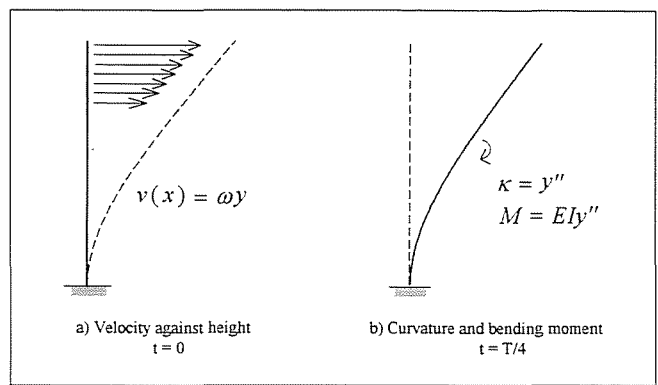


Fig. 3 Mechanical interpretation of the Rayleigh quotient

when substituting an assumed shape of vibration for $y(x)$ into (9). The absolute minimum of the expression (9), the smallest eigenfrequency of the generalised eigenvalue problem (Rózsa, 1974) for vibration is obtained by substituting the true first eigenmode for $y(x)$. Due to orthogonality of mode shapes, further eigenfrequencies represent local minimum values.

To the Rayleigh quotient there could be given a mechanical interpretation considering the free bending vibration of a cantilever. In the following a quarter period of vibration will be examined according to the first mode (Fig. 3).

In $t = 0$, all points of the bar vibrate harmonically in the same phase, crossing the neutral position together (Fig. 3a). The distribution of velocity according to height conforms to the amplitude and in this way also with the shape function y . Expressing the velocity function by ω and y , the total kinetic energy of the bar will be (10). The potential energy is considered zero.

$$E_{kin} = \frac{1}{2} \int_0^l m v^2(x) dx = \frac{1}{2} \int_0^l \rho A (\omega y)^2 dx \quad (10)$$

A quarter period later, in $t = T/4$, the points of the bar take their extreme positions (Fig. 3b). The whole kinetic energy of the bar transforms into potential energy by elastic deformation. The energy accumulated in the bar could be expressed with the $M(x)$ bending moment and the $\kappa(x)$ curvature, where both of them are functions of the y mode shape:

$$E_{pot} = \frac{1}{2} \int_0^l M(x) \kappa(x) dx = \frac{1}{2} \int_0^l EI [y''(x)]^2 dx \quad (11)$$

It is well known that the mechanical energy of an enclosed system is constant. Therefore making (10) and (11) equal with each other, ω^2 can be expressed from this equation. This results in the Rayleigh quotient (9) referring to the vibrating bar:

$$E_{kin} = E_{pot} \Rightarrow \omega^2 = \frac{\int_0^l EI[y''(x)]^2 dx}{\int_0^l \rho A[y(x)]^2 dx}$$

With Rayleigh's method the first eigenfrequency of the uniform cantilever can be easily approximated when supposing the mode shape to be $y(x) = x^3$. Because this third order function does not fulfil the boundary conditions (2b) at the free end of the cantilever, a good approximation could not be expected from quotient (9).

2.3 Dynamic solution to the non-uniform cantilever

In the case of the analysis of non-uniform cantilevers, the effective application of Rayleigh's method requires a well-ap-

proximating $y(x)$ mode shape. That is the aim of the procedure presented below.

The cross-sectional data along the height of the cantilever are expressed with continuous functions:

$$A(x) = A_0 f(x) \quad I(x) = I_0 g(x) \quad (12)$$

where A_0 = area of the fixed bottom section; I_0 = moment of inertia of the same section; $f(x)$ and $g(x)$ = continuous functions to express the variation of cross-sectional data along the height. The functions $f(0)=1$ and $g(0)=1$, both decrease monotonously.

Substituting the above $A(x)$ and $I(x)$ cross-sectional functions into Eq. (4), a differential equation with varying coefficients is obtained for non-uniform cantilevers:

$$EI_0 g(x) y^{IV} - \omega^2 \rho A_0 f(x) y = 0 \quad (13)$$

This equation generally cannot be solved in closed form. Taking functions (12) into consideration, the quotient (9) will be the following:

$$\omega^2 = \frac{EI_0 \int_0^l g(x) [y''(x)]^2 dx}{\rho A_0 \int_0^l f(x) [y(x)]^2 dx} \quad (14)$$

Substituting the mode shape of the uniform beam into (14) will not result in a minimum for ω^2 , because function (6) does not fulfil the differential equation (13) of varying coefficients. An approximation of the mode shape was performed with multiplying two polynoms (Timoshenko, 1928).

The essence of my method is a gradual modification of mode shape (6) to obtain a well-approximating shape function as well as an eigenfrequency for the non-uniform beam. For this purpose the mode shape of the non-uniform beam is taken up as the product of $\zeta_0(x)$ and of a polynomial function of N -th order with $N+1$ coefficients:

$$\begin{aligned} \zeta(x) &= (c_1 e^{\lambda x} + c_2 e^{-\lambda x} + c_3 \sin \lambda x + c_4 \cos \lambda x)(a_0 + a_1 x + a_2 x^2 + \dots) = \\ &= \zeta_0(x) \sum_{n=0}^N a_n x^n = \zeta_0(x) u(x) \end{aligned} \quad (15)$$

The mode shape contains a free parameter, which could be used for normalizing. We can choose one of the coefficients freely (e.g. $a_0 = 1$), so that there remain N free unknown coefficients to set the best approximation of the $\zeta(x)$ mode shape.

Using mode shape (15), the best approximation of the investigated eigenfrequency is available by minimizing the Rayleigh quotient in function of a_1, \dots, a_N coefficients:

$$\omega^2(a_1, \dots, a_N) = \text{minimum!} \quad (16)$$

Condition (16) also implies the best approximation of mode shape (15) in the N dimensional subspace of the $u(x)$ polynomes.

This minimum condition could be expressed by the N partial derivatives of the Rayleigh quotient:

$$\frac{\partial (\omega^2)}{\partial a_i} = \frac{EI_0 \left(\frac{\int_0^l g(x) \{[\zeta_0(x) u(a_i, x)]''\}^2 dx}{\int_0^l f(x) [\zeta_0(x) u(a_i, x)]^2 dx} \right)}{\rho A_0} = 0, \quad a_i \quad (17)$$

The (17) equations with partial derivatives result in a non-linear equation system in a_i coefficients. In practical calculations instead of the direct solution of the non-linear equation system, the Nelder-Mead simplex method was used (Reddy, 1986). This is a heuristic minimum search method and provides an upper bound for ω eigenfrequency. By increasing the order of the modifying polynome, the quotient approximates the real value of the eigenfrequency more and more.

Although $\zeta_0(x)$ fulfils all boundary conditions, however, this is generally not true for the modified function $\zeta(x)$. Following from the differentiation of the (15) product function, the boundary conditions of $x=l$ could be harmed. This can be seen by producing the second and third derivatives of it:

$$\begin{aligned} [\zeta_0(x) u(x)]''_{x=l} &= \zeta_0''(l) u(l) + 2\zeta_0'(l) u'(l) + \zeta_0(l) u''(l) \\ [\zeta_0(x) u(x)]'''_{x=l} &= \zeta_0'''(l) u(l) + 3\zeta_0''(l) u'(l) + 3\zeta_0'(l) u''(l) + \zeta_0(l) u'''(l) \end{aligned} \quad (18)$$

The expressions of bending moment and the shear force contain the (18) derivatives, which should be equal to zero according to (2b). But the last two members of both derivatives generally differ from zero. In this way the modified $\zeta(x)$ function cannot mathematically and exactly fulfil the static boundary conditions (2b). However, in the case of lower eigenfrequencies and adequate a_i coefficients, the function $\zeta(x)$ approximates the true mode shape very closely and provides easy programming. For higher eigenfrequencies the modifying function in (15) does not give good results. By increasing the number of waves in the mode shape function, the unsatisfied (2b) boundary conditions cause larger and larger inaccuracies.

For higher eigenfrequencies a different modifying polynomial function will be applied to satisfy the static boundary condition (2b) too. This requires vanishing the last, still two non-zero members of both derivatives in (18). This results in the following eq. system:

$$\begin{aligned} 2\zeta_0'(l) u'(l) + \zeta_0(l) u''(l) &= 0 \\ 3\zeta_0''(l) u''(l) + \zeta_0(l) u'''(l) &= 0 \end{aligned} \quad (19)$$

The polynome type modifying $u(x)$ function should be taken up in such a way that a power function as multiplier is ordered to each a_i of (16) to satisfy eq. system (19). This power function should contain three members with $b_{1,i}$ and $b_{2,i}$ coefficients, which could be determined from eqs. (19). These partial u_i polynomes are:

$$u_i(x) = a_i (x^i + b_{1,i} x^{i+1} + b_{2,i} x^{i+2})$$

and summing up:

$$u(x) = a_0 + \sum_{i=1}^N u_i(x) \quad (20)$$

where $a_0 = 1$ again.

In this way the static boundary conditions could be fulfilled by the $u_i(x)$ elements of modifying function separately.

The mode shape function of the non-uniform beam with polynome (20), which also gives accurate results in the case of higher frequencies, is:

$$\begin{aligned} \zeta(x) &= (c_1 e^{\lambda x} + c_2 e^{-\lambda x} + c_3 \sin \lambda x + c_4 \cos \lambda x) \left[1 + \sum_{i=1}^N a_i (x^i + b_{1,i} x^{i+1} + b_{2,i} x^{i+2}) \right] = \\ &= \zeta_0(x) u(x) \end{aligned} \quad (21)$$

3. NUMERICAL EXAMPLE

The presented continuum method was applied to the analysis of the non-uniform, reinforced concrete chimney illustrated in Fig. 4. The straight part of the bottom cross-section decreases linearly and is zero at the circular ring section of the top. The wall thickness decreases linearly from 30cm to 20cm as well.

In the vibration analysis uncracked elastic behaviour was supposed, neglecting the axial forces. The eigenfrequencies and mode shapes were determined for bending vibrations about the z-axis. First, substituting uniform cantilevers were calculated. Then the chimney with varying cross-section was analysed using the continuum method. For comparison the calculations of the non-uniform cantilever were also performed with the finite element analysis.

For the continuum method a MATLAB program was prepared, using the Nelder-Mead minimum search and to the finite element calculations ALGOR program was applied.

In the first step using the continuum method for calculating substituting uniform beams, the following eigenfrequencies were obtained (Table 1):

Table 1 contains upper and lower bounds too, being calculated by appropriate coupling of cross-sectional data. To calculate the lower bound, the top section's small moment of inertia was used with the large area as well as the large specific mass of the bottom section. On the contrary, the upper bound can be obtained by coupling the bottom section's large moment of inertia with the top section's small specific mass. The upper and lower bounds represent a wide interval. A good

Fig. 4 The investigated chimney with its bottom and top cross-section

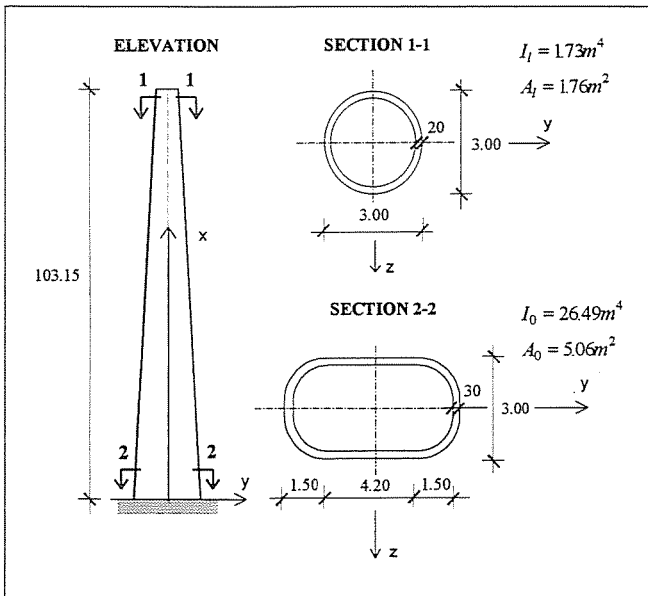


Table 1 Circular eigenfrequencies of different uniform substitution beams, continuum method

	Cross-section	Circular eigenfrequency [Hz]		
		ω_1	ω_2	ω_3
Lower	I_U, A_L	0.671	4.21	11.78
Average	I_{Av}, A_{Av}	2.056	12.88	36.06
Upper	I_L, A_U	4.442	27.81	77.87

Table 2 Circular eigenfrequencies of the non-uniform beam, continuum method

	Circular eigenfrequency [Hz]					
	ω_1	ω_2	ω_3	ω_4	ω_5	ω_{12}
Continuum method	3.110	13.61	33.87	159.5	371.2	674.1

approximation of ω_i would require appropriate substituting cross-sectional data. Unfortunately, in this respect there is no acceptable basis. In this calculation, average cross-sectional data were used on the basis of line integral along the bar. It can be seen from the latter results that these do not give a good approximation.

In the next step eigenfrequencies and mode shapes for the non-uniform beam were determined by the continuum method (Table 2).

From the table one can see not only that the smallest eigenfrequency as the absolute minimum of the Rayleigh coefficient could be obtained, but also larger ω_i frequencies representing a local minimum. This is due to the properties of the mode shape of the uniform beam. The i -th mode shape of it, applied as the starting curve for the minimum search, is more or less orthogonal to the j -th mode shape ($i \neq j$) of the non-uniform beam. Therefore, the Nelder-Mead minimum search also quickly finds the local minimum values. In Table 2, the first three eigenfrequencies were calculated by the simple modifying polynome where $N=5$, according to (15). For calculation of $\omega_6, \omega_9, \omega_{12}$ the modifying function according to (20) was applied with only $N=1$ coefficient, because the advanced polynom already with one free parameter provided a very good approximation.

Finally the continuum method was controlled with the aid of the finite element method (Table 3):

In the first step the bar model was divided into 10 elements, while in the next step a detailed model was used with 103 elements. Similar to the uniform cantilever model, a lower and upper bound was calculated too, coupling the cross-sectional data of the bar elements in the same way as previously. According to expectations, the detailed analysis with 103 elements gave quite narrow intervals for ω_i frequencies. These results are in good coincidence with that of the continuum method.

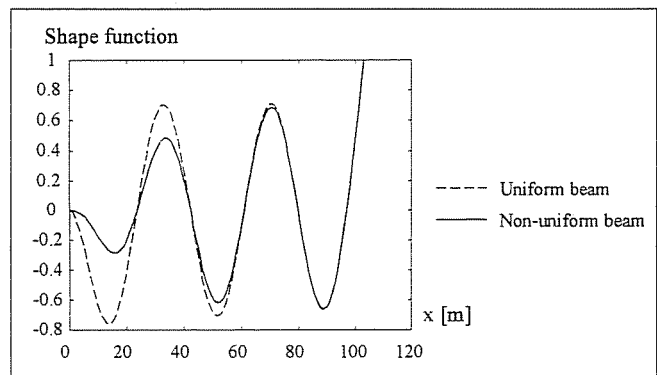
The minimum search finds the coefficients of the modifying polynome. In this way, besides the ω_i eigenfrequencies, the mode shapes could be obtained as well. The mode shapes No. 6 for the uniform and also for the non-uniform cantilevers are presented in a common co-ordinate system (Fig. 5) with normalizing of the top's deflection.

In Fig. 6 the steps of the minimum search for the first eigenfrequency are shown in a three-dimensional co-ordinate

Table 3 Circular eigenfrequencies of the non-uniform beam, finite element method

Element Number	Cross-section	Circular eigenfrequency [Hz]					
		ω_1	ω_2	ω_3	ω_4	ω_5	ω_{12}
10	Lower I_U, A_L	2.803	11.91	28.82	-	-	-
10	Upper I_U, A_U	3.315	14.28	34.81	-	-	-
103	Lower I_U, A_L	3.078	13.49	33.83	154.8	363.3	668.1
103	Upper I_U, A_U	3.130	13.73	34.46	157.8	373.3	680.9

Fig. 5 Mode No. 6, uniform and non-uniform beam



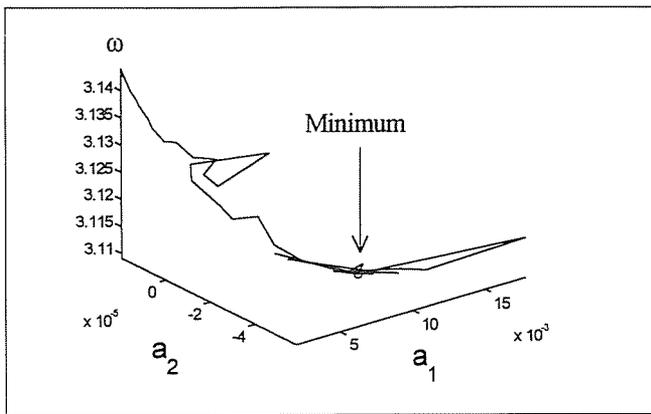


Fig. 6 Steps of minimum search with two a_i coefficients, according to the Nelder-Mead method

system. For the sake of representation in an axonometric system, only two a_i coefficients were used in this calculation.

A spectacular interpretation could be given to the steps of the Nelder-Mead minimum search method if all the members of the series of $\zeta(x)$ approximating functions also as mode shapes are considered. These functions of course cannot be mode shapes of the original non-uniform cantilever because they do not satisfy the differential eq. (1) and the boundary condition (2b). In spite of this, the mode shapes could belong to the investigated structure, when applying additional constraints (e.g. elastic bedding against lateral deflection and curvature of the beam). These extra constraints give additional stiffness to the beam and that is why its eigenfrequencies are larger than that of the investigated structure. In this way the steps of iterations perform a gradual degradation of non-required constraints (similar to the Cross method). This interpretation also shows that the procedure is of upper bound type.

4. CONCLUSIONS

The elaborated continuum method is applicable for dynamic analysis of undamped free bending vibration of structures

modelled by non-uniform cantilevers, as chimneys, television towers, and high-rise buildings.

The essence of the procedure is that the mode shape of the non-uniform cantilever is assumed as the product of the mode shape of the uniform beam and a modifying function. Applying the extreme-value property of the Rayleigh quotient, the eigenfrequencies of the non-uniform cantilever could be obtained by gradual modification of mode shapes. By increasing the order of the modification polynome, the quotient approximates the real value of the eigenfrequency more and more.

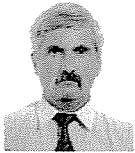
The results provided by this method are as precise as those of a detailed finite element analysis. The advantage of the continuum method is that it requires less input data than the alternative method: the finite element analysis.

5. REFERENCES

- Clough, R. W. & Penzien, J. (1975), "Dynamics of Structures", *New York: Mc Graw-Hill Book Company*
- Kollbrunner, C. F. & Hajdin, N. (1976), "Undamped Vibration of Elastic Thin-walled Beams of Open Deformable Cross-sections". Zürich: *Verlag Leemann*
- Korn, G. A. & Korn, T. M. (1975), "Mathematical Handbook for Engineers" „Matematikai Kézikönyv Műszakiaknak". Budapest: *Műszaki Könyvkiadó*
- Pfaffinger, D. D. (1989), "Tragwerksdynamik". Wien, New York: *Springer Verlag*.
- Reddy, J. N. (1986), "Applied Functional Analysis and Variational Methods in Engineering", *New York: McGraw Hill*
- Timoshenko, S – Lessels (1928), "Festigkeitslehre". *Springer Verlag*
- Rózsa, P. (1974), "Linear Algebra and Applications" „Lineáris algebra és alkalmazásai", *Budapest: Műszaki Könyvkiadó*
- Vértes, Gy. (1985), "Structural Dynamics". Budapest Akadémiai Kiadó
- Zalka, K. (1994), "Dynamic Analysis of Core Supported Buildings", *London: Building Research Establishment*

Dr. Zsolt Huszár (1957) civil engineer, engineer-mathematician, dr. univ., senior research assistant at the Department of Structural Engineering at the Budapest University of Technology and Economics. His main research fields of activities are: structural dynamics, vibration problems of cracked reinforced concrete beams, post-tensioned box-girder bridges, continuum method, stability.

MAIN DIRECTIONS OF STANDARDIZATION IN SHEAR DESIGN



Dr. András Draskóczy

After a short historical review of the developments in shear design, the article summarizes the shear design procedure of reinforced concrete members according to the most important international (FIP 1996 Recommendations, EC 2) and national (DIN 1045-1 2000) standards and recommendations developed in Europe during the last decade. Comparative analysis and proposals are supported by numerical example.

Keywords: shear capacity, variable inclination struts, links

1. INTRODUCTION

When surveying international publications, standards and recommendations of the last decade one can state that there is a constant change in the field of shear design. Beside sketching standard prescriptions held to be the most important from the point of view of effecting Hungarian practice the article treats some essential details of the background research work, analyzing observable tendencies. The author formulates his standpoint through presentation and analysis of a numerical example.

2. DEVELOPMENT OF SHEAR DESIGN

In a simply supported reinforced concrete beam, an arch with tirant is acting (Fig. 1), which has a rise limited by the height of the beam. By the effect of flexural moments produced by a uniformly distributed load, the sections of the arch are exploited approximately at the same rate. The vertical component of the compression force transmitted in the concrete along the arched compression trajectories is on the other hand, due to their small inclination, rather small. Therefore, to equilibrate shear forces it is also necessary to apply shear reinforcement in the direction of the principal tensile stresses or under a small angle to them – suitably in the vertical direction - with increasing intensity towards the support. Ritter and Morsch (1922) introduced the truss model of shear design (Fig. 2). The model consists of a parallel top compression chord, a bottom tension chord and between them of inclined compression

Fig. 1 Principal stress trajectories of simple supported beams and modelling by arch with tie

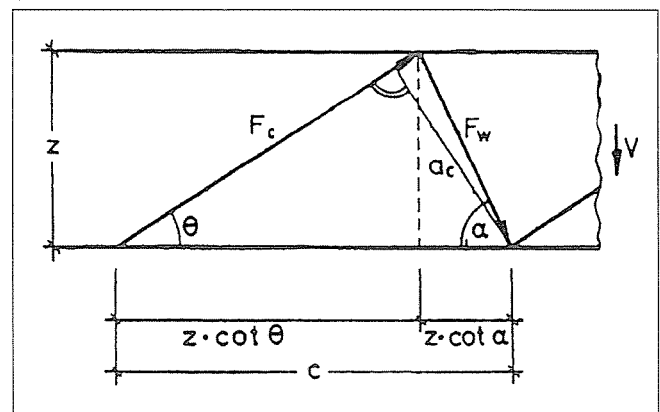
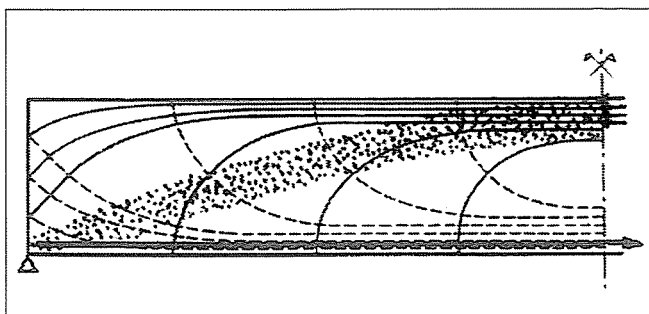
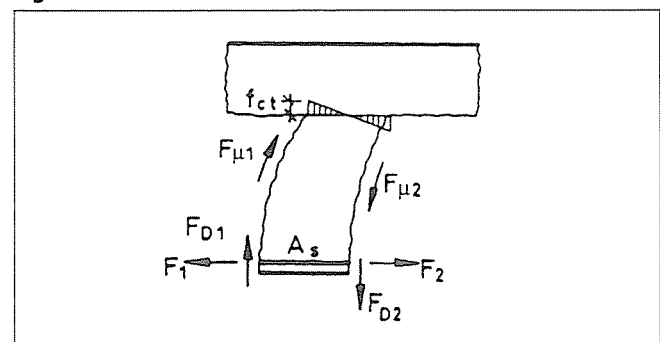


Fig. 2 Truss model by Morsch

struts rising in the direction of the centre of the span. In addition there are tirants acting in the direction of the shear reinforcement and uniformly distributed along the longitudinal axis. This system can function otherwise by relatively small shear forces also, without shear reinforcement. One part of the shear force can be transmitted through friction along the inclined shear cracks. This is adding up to other parts transmitted in the compression zone due to the compression strength of the concrete and at the point of intersection of the crack and the tensile reinforcement by dowel action. The latter model is also called as "teeth model" (Fig. 3). Rupture occurs by breaking of the teeth and turning of the crack direction to horizontal at the foot of the teeth. The shear resistance corresponding to this type of rupture ($V_{Rd,ct}$) is nowadays definitely distinguished from the shear resistance corresponding to the failure of the friction connection in shear cracks of beams designed with shear reinforcement ($V_{Rd,c}$).

Fig. 3 Concrete "teeth model" of beams without shear reinforcement



Coming back to the truss model of Mörsch, it was supposed for a long time that the inclined compression struts are parallel to the shear cracks considered generally under 45° inclination. Elements of shear reinforcement crossing these cracks have to equilibrate by tension the total shear force or the portion of it not resisted by the concrete. The portion resisted by the concrete was mainly attributed to the shear strength of the compression zone (Leonhardt, 1960-ies). Compression failure of the inclined concrete struts indicates the upper limit of the shear resistance, which cannot be overcome by increasing the intensity of the shear reinforcement. Thürlimann et al applied plastic methods at the end of the 1970-ies, considering free choice for the inclination of the compression struts between certain limits (26°–74°). Both of the latter methods were used by the elaboration of the CEB-FIP Model-Code 78. It was on this occasion that the *variable strut method* in a standard appeared first. The inclination angle of the struts (θ) and the permissible compression stress were treated as empirical parameters. The 45° direction was treated distinctly while the portion of the shear capacity attributed to the concrete and determined empirically, could be taken into account only by $\theta = 45^\circ$. This method was called the standard method. A contradictory situation developed: under small shear conditions the standard method proved to be economical considering the quantity of shear reinforcement, because the portion of shear absorbed by the concrete then became dominant. Under greater shear forces, however, the small strut angle (that is the variable strut method) gives more advantageous results because lower angle struts will be intersected by a greater number of elements of the shear reinforcement. The results of the two methods do not compare to each other at $\theta = 45^\circ$. It is therefore hard to understand why these methods were taken as basis of shear design when elaborating ENV 1992-1-1 (EUROCODE 2).

One another development trend was appointed by Kupfer (1964) through his activity during the 1960-ies, who on basis of the principle of the minimum of deformation work developed the truss model by Mörsch. His followers set up conditions for determining the strut inclination.

Gambarova, Kirmair, Mang and Reineck (Reineck, 1990, 1991, 2001) elaborated models for different crack patterns to determine the so-called *crack friction forces* (aggregate interlock) due to relative displacement and rotation of the crack sides. Reineck considered portions of the web between cracks as fields in a plain state of stress instead of uni-axial compression. The idealised inclined compression struts "pass over" the surface of steeper cracks with the help of the crack friction forces. Thus the truss model remains interpretable, and inclination (θ) of the compression "struts" will be determined as a function of the force distribution. Following the proposal of Reineck, this method was also adopted by the 1996 FIP Recommendations.

In Germany – may be as a consequence of some preoccupations that have been developed in the profession due to certain prescriptions of the ENV 1992-1-1 – a new national reinforced concrete standard came into force. The part of DIN 1045-1 (2001) related to shear reflects a standpoint very near to that of the 1996 FIP Recommendations. The most significant difference between the two prescriptions is in the way the crack friction forces are determined, which then influences the strut angle and the necessary quantity of the shear reinforcement too.

The intention of the modification is reflected by the EN 1992-1: 2001, which was not approved yet at the time of publication of the Hungarian original of this article. The new draft seems to break with the standard method ($\theta = 45^\circ$), but

gives only a lower limit ($\theta = 21,8^\circ$) for the variable strut inclination and all other decisions in connection to this problem are entrusted to the designer.

Let us now review the most important relationships concerning shear design of beams of some European regulations valid at present. Construction rules are closely interconnected to the regulations but due to problems of extension they will only be treated when being built into the relationships. Nor will be mentioned such less important differences, for example that in some standards the vertical component of an inclined prestressing tendon force is summed up to the shear resistance force, while in other standards it is subtracted from the design shear force. Rules concerning compression forces acting together with shear will be mentioned, while the relationships concerning the effect of tensile forces – in view of little practical interest – not. The given relationships are valid for both vertical and inclined shear reinforcement, for vertical links $\sin\alpha = 1$ and $\cos\alpha = 0$ can be substituted.

3. REGULATION OF SHEAR DESIGN OF BEAMS

3.1 ENV 1992-1-1 (EUROCODE 2)

3.1.1 Members not requiring shear reinforcement

Design shear resistance of members not requiring shear reinforcement but supplied with minimum shear reinforcement:

$$V_{Rd1} = [\tau_{Rd} k(1,2 + 40\rho_l) + 0,15\sigma_{cp}] b_w d,$$

where $k=1,6-d > 1$ d in m

$$\rho_l = A_{sl}/(b_w d) < 0,02.$$

Capacity of the shear reinforcement and the upper limit of shear resistance corresponding to compression failure of the concrete can be determined depending on the two applicable calculation methods given below.

3.1.2 Members requiring designed shear reinforcement, standard method

By applying the standard method, we adopt a compression strut angle of 45°. The contribution of shear reinforcement to the shear resistance in this case is:

$$V_{wd} = \frac{A_{sw} f_{yw} d}{s} 0,9d(\sin\alpha + \cos\alpha) \quad (1)$$

The shear resistance corresponding to compression failure of the 45° inclined concrete struts is:

$$V_{Rd2} = \frac{1}{2} v f_{cd} b_w \cdot 0,9d(1 + \cot\alpha) \quad (2)$$

where, $v = 0,7 - \frac{f_{ck}}{200} \geq 0,5$ f_{ck} in N/mm²

Design value of the shear resistance:

$$V_{Rd} = \min \left\{ \begin{array}{l} V_{Rd3} = V_{Rd1} + V_{wd} \\ V_{Rd2} \end{array} \right\}$$

Condition of safety:

$$V_{Rd} \geq V_{Sd}$$

3.1.3 Members requiring design shear reinforcement, variable strut method

The shear resistance is:

$$V_{wd} = \frac{A_{sw} f_{ywd}}{s} 0,9d (\cot \theta \sin \alpha + \cos \alpha) \quad (3)$$

By continuous longitudinal reinforcement, the limitation:
 $0,4 \leq \cot \theta \leq 2,5$

should be taken into account, that is θ can be variable between $21,8^\circ$ and $68,2^\circ$. By stapled longitudinal reinforcement the limits are stricter:

The quantity of the shear reinforcement does have an upper limit also:

$$\frac{A_{sw} f_{ywd}}{b_w s} \leq \frac{0,5v f_{cd} \sin \alpha}{1 - \cos \alpha} \quad (4)$$

By vertical links $\sin \alpha = 1$ and $\cos \alpha = 0$ so that (2) and (3) become more simple.

The shear resistance corresponding to the compression failure of the inclined struts in this case is:

$$V_{Rd2} = v b_w 0,9d f_{cd} \frac{\cot \theta + \cot \alpha}{1 + \cot^2 \theta} \quad (5)$$

The value of the design shear resistance force is:

$$V_{Rd} = \min \left\{ \begin{array}{l} V_{Rd3} = V_{wd} \\ V_{Rd2} \end{array} \right\}$$

Condition of safety:

$$V_{Rd} \geq V_{Sd}$$

It is remarkable that by substituting $\theta = 45^\circ$ and $\cot \theta = 1$, (5) results in (2). Similarly by $\theta = 45^\circ$ and $\cot \theta = 1$, (3) results in (1). (1) and (3) can then be used also by the standard method.

3.2 FIP 1996 Recommendations

Equations referring to shear reinforcement concern vertical links because the recommendations do not suggest the use of bent-up bars.

$$V_{Rd} = V_{sw} + V_f$$

$$V_{sw} = \frac{A_{sw} f_{yw}}{s_w} z \cot \beta_{cr}$$

where: $\cot \beta_{cr} = 1,20 - 0,2 \sigma_{xd} / f_{ctm}$,

$$V_f = 0,1 \times (1 - \cot \beta_{cr} / 4) b_w z f_{cwd} \geq 0,$$

$$f_{cwd} = v_2 f_{cd}$$

$$v_2 = 0,8 \text{ if } 0,2z \geq s_w \text{ and } 200 \text{ mm} \geq s_w,$$

$$v_2 = 0,6 \text{ if } 0,2z < s_w < 0,4z,$$

$$v_2 = 0,45 \text{ if } 0,4z < s_w < 0,6z,$$

$$\cot \theta = V_{Rd} / V_{sw}$$

$$V_{Rd,max} = b_w z f_{cwd} \sin \theta \cos \theta.$$

Condition of safety:

$$V_{Rd} \geq V_{Sd}$$

3.3 DIN 1045-1 draft confirmed in December 2000

In case of shear resistance of members without shear reinforcement,

$$V_{Rd,cr} = \left[0,1 \eta_1 \kappa (100 \rho_l f_{ck})^{1/3} - 0,12 \sigma_{cd} \right] b_w d,$$

where $\kappa = 1 + \sqrt{\frac{200}{d}} \leq 2,0$, d in mm

$$\rho_l = \frac{A_{sl}}{b_w d} \leq 0,02,$$

$$\sigma_{cd} = \frac{N_{sd}}{A_c} \text{ in N/mm}^2,$$

$$\eta_1 = 0,40 + 0,60 \frac{\rho}{2200} \text{ for lightweight concrete.}$$

For members designed with shear reinforcement, the strut inclination,

$$\cot \theta \leq \frac{\cot \beta_{cr}}{1 - \frac{V_{Rd,c}}{V_{Sd}}} \leq 3,0,$$

where $\cot \beta_{cr} = 1,2 - 1,4 \frac{\sigma_{cd}}{f_{cd}}$.

Part of the shear force transmitted by friction along the crack is:

$$V_{Rd,c} = \left[2,4 \eta_1 \cdot 0,10 \cdot f_{ck}^{1/3} \left(1 + 1,2 \frac{\sigma_{cd}}{f_{cd}} \right) \right] b_w z.$$

The shear force that can be equilibrated by shear reinforcement is:

$$V_{Rd,sv} = \frac{A_{sw} f_{yd}}{s} z (\cot \theta + \cot \alpha) \sin \alpha.$$

The upper limit of the shear resistance:

$$V_{Rd,max} = b_w z \alpha_c f_{cd} \frac{\cot \theta + \cot \alpha}{1 + \cot^2 \theta},$$

where $\alpha_c = 0,752 \eta_1$.

Conditions of safety for shear: in all sections, where $V_{Sd,w} \geq V_{Rd,cr}$, shear reinforcement should be designed and the following conditions checked.

$$V_{Sd,w} \leq V_{Rd,sv} \text{ and}$$

$$V_{Sd,w} \leq V_{Rd,max}$$

3.4 EN 1992-1:2001, modified draft of EUROCODE 2

Shear resistance of members without shear reinforcement:

$$V_{Rd,cr} = \left[0,12 k (100 \rho_l f_{ck})^{1/3} - 0,15 \sigma_{cd} \right] b_w d,$$

where $k = 1 + \sqrt{\frac{200}{d}} \leq 2,0$, d in mm

$$\rho_l = \frac{A_{sl}}{b_w d} \leq 0,02,$$

$$\sigma_{cp} = \frac{N_{Ed}}{A_c} \text{ in MPa.}$$

In members with shear reinforcement:

$$1,0 \leq \cot \theta \leq 2,5.$$

Strut inclination angle can be freely adopted in the above interval.

The shear force that can be equilibrated by shear reinforcement:

$$V_{Rd,sy} = \frac{A_{sw} f_{ywd}}{s} z (\cot \theta + \cot \alpha) \sin \alpha.$$

The limiting condition concerning the quantity of the shear reinforcement remains valid:

$$\frac{A_{sw} f_{ywd}}{b_w s} \leq \frac{0,5v f_{cd} \sin \alpha}{1 - \cos \alpha}.$$

The upper limit of the shear resistance:

$$V_{Rd,max} = b_w z v f_{cd} \frac{\cot \theta + \cot \alpha}{1 + \cot^2 \theta},$$

$$\text{where, } v = 0,6 - \left(1 - \frac{f_{ck}}{250}\right) \geq 0,5. \quad f_{ck} \text{ in N/mm}^2.$$

When compressive axial force is acting, the upper limit of the shear resistance should be reduced by the factor $1,67 \times (1 - \sigma_{cp,eff} / f_{cd}) < 1$.

Conditions of safety for shear: in all sections where $V_{Ed} \geq V_{Rd,ct}$, shear reinforcement should be designed, and the fulfilment of the conditions below checked i.e.

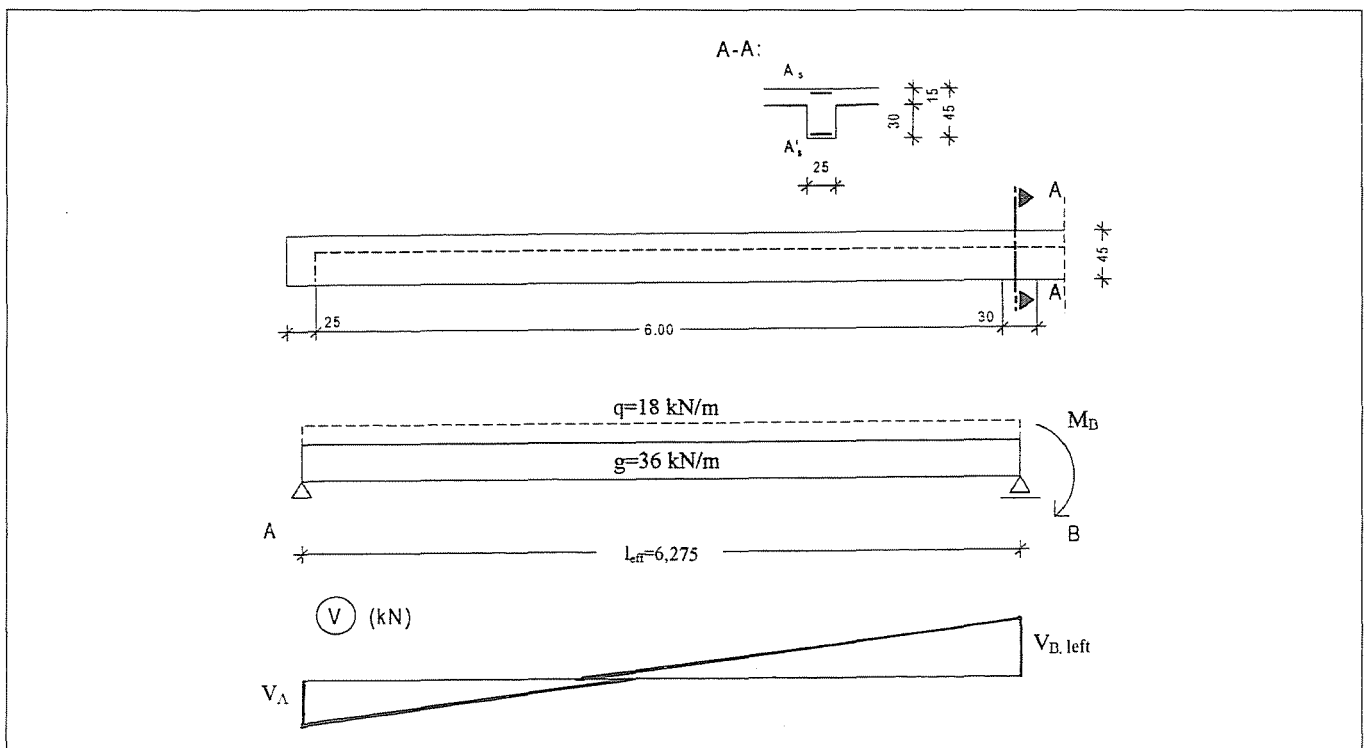
$$V_{Ed} \leq V_{Rd,sy} \quad \text{and} \quad V_{Ed,w} \leq V_{Rd,max}$$

4. NUMERICAL EXAMPLE

Through presentation of the following example we are looking for points of view for the analysis and evaluation of the exposed shear design procedures. The selected problem is a continuous T-beam with three supports and constant cross-section, which is widely used in monolithic construction practice. The portion of the beam requiring shear reinforcement

Concrete grade: C20/25	Concrete cover: 20 mm		
Type of the reinforcement: B500			
Material strengths:	$f_{ck} = 20 \text{ N/mm}^2$	$f_{cd} = 13,3 \text{ N/mm}^2$	$t_{Rd} = 0,26 \text{ N/mm}^2$
	$f_{ywd} = 435 \text{ N/mm}^2$		
Loads:	$g = 6 \times 6 = 36 \text{ kN/m}$		
	$q = 6 \times 3 = 18 \text{ kN/m}$		
Partial safety factors of loads:			
EUROCODE 2, 1996 FIP Recommendations	$\gamma_g = 1,15$	$\gamma_q = 1,5$	$\psi_0 = 0,7$
DIN 1045-1:	$\gamma_g = 1,35$	$\gamma_q = 1,5$	
Internal forces:			
EUROCODE 2, 1996 FIP Recommendations:	$V_{B,left} = 265,12 \text{ kN}$	$M_B = 336,66 \text{ kNm}$	
DIN 1045-1:	$V_{B,left} = 293,03 \text{ kN}$	$M_B = 372,10 \text{ kNm}$	
Longitudinal reinforcement designed for flexure at support B:			
EUROCODE 2, 1996 FIP Recommendations:	$A_s = 7 \text{ } \emptyset 16 + 3 \text{ } \emptyset 20, A'_s = 2 \text{ } \emptyset 16 + 2 \text{ } \emptyset 20$		
DIN 1045-1:	$A_s = 8 \text{ } \emptyset 16 + 3 \text{ } \emptyset 20, A'_s = 3 \text{ } \emptyset 16 + 2 \text{ } \emptyset 20$		

Fig. 4 One span of a reinforced concrete beam with three supports cast integral with the floor slab



	ENV 1992-1-1 Standard method	1996 FIP Recommendations	DIN 1045-1 2000	EN 1992-1:2001 1 st draft
Shear resistance of the concrete section without shear reinforcement kN	$V_{cd}=63.18$	No data	$V_{Rd,ct}=58.86$	$V_{Rd,ct}=70.63$
Upper limit of the shear resistance* kN	$V_{Rd2}=363.59$	$V_{Rd,max}=356.17$ (339.9)	$V_{Rd,max}=408.5$ (363.6)	$V_{Rd,max}=250.75$
$\cot\theta^*$	1	1.27(1.43)	1.60(1.92)	2.5
Shear reinforcement 1. At $V_{Sd,max}$ 2. At midpoint of the designed portion of the beam 3. Minimum links In parenthesis: A_s mm ² /mm	$\emptyset 8/90(1.12)$ $\emptyset 8/150(0.67)$ $\emptyset 8/300(0.34)$	$\emptyset 8/100(1.01)$ $\emptyset 8/150(0.67)$ No data	$\emptyset 8/100(1.01)$ $\emptyset 8/175(0.58)$ $\emptyset 8/250(0.40)$	$\emptyset 8/150(0.67)$ $\emptyset 8/200(0.51)$ $\emptyset 8/300(0.34)$
Total cross-section of the shear reinforcement along the designed portion in % of the value according to ENV 1992-1-1	100%	95%	88%	68%

Table 1 Results of the numerical example

Remark.: * Values given in parenthesis refer to the midpoint of the designed portion of the beam

on one side of the interior support will be investigated. The internal forces caused by uniformly distributed permanent and variable loads are given. As an approximation, we do not consider the effect of partial actuation of the variable load inside the spans; the shear diagram is taken as linear. *No effect producing axial force is acting.* The longitudinal reinforcement is given. In the section above the interior support compression reinforcement was also designed for flexure.

Let us design the shear reinforcement near support B in the first span using vertical links.

The most important results according to the four different standard prescriptions are summarised in (Table 1.)

5. NOTATION

Notations of the same meaning but used in a different way in different references are given, separated by a comma.

5.1 Data concerning cross-sections

A_c	concrete cross-section
A_s, A_{sw}	area of the cross-section of the shear reinforcement
A_{sl}	cross-sectional area of the effective longitudinal tensile reinforcement
b, b_w	web thickness of the beam
d	effective depth
k	factor depending on the depth of the section (in ENV 1992-1-1 and in EN 1992-1:2001 given by different expression!)
s, s_w	spacing of equidistant elements of the shear reinforcement along the axis of the member
z	lever arm of the internal compression and ten-

α	angle between elements of the shear reinforcement and axis of the member
η_l	reduction factor for lightweight concrete
κ	factor depending on the depth of the member
ρ_l	ratio of the tensile reinforcement

5.2 Material characteristics, resistance of the cross-section

f_{cd}	design value of the compression strength of the concrete
f_{ck}	characteristic value of the compression strength of the concrete
f_{cm}	mean value of the tensile strength of the concrete
f_{yw}, f_{ywd}	design value of the yield stress of the shear reinforcement
f_{yd}	design value of the yield stress of the reinforcement
f_{1cd}	design value of the uni-axial compression strength of the concrete
v_2	factor used by the determination of maximum allowable compression stress of the concrete struts
V_{Rd}	design value of the shear resistance of the cross-section
$V_{Rd,c}, V_f$	design value of the shear force transmitted by friction along cracks
$V_{cd}, V_{Rd1}, V_{Rd,ct}$	design value of shear resistance of the cross-section without shear reinforcement
$V_{Rd2}, V_{Rd,max}$	design value of the shear force corresponding to the compression failure of the web, upper

	limit of the shear resistance
V_{Rd3}	design value of the shear resistance of the cross-section designed with shear reinforcement
$V_{wd}, V_{sv}, V_{Rd,sv}$	shear resistance of the cross-section limited by the shear reinforcement
α_c	factor limiting the compression stress in the compression struts
ν	factor depending on the characteristic strength of the concrete
ρ	density in dN/m^3
τ_{Rd}	design value of the shear strength of the concrete

5.3 Effects

N_{Sd}, N_{Ed}	axial force acting in the cross-section with the effect of loads or prestressing force, negative if compression, with the exception of ENV 1992-1-1, where positive means compression
$V_{Sd}, V_{Sd,w}, V_{Ed}$	design value of shear force caused by exterior effects
β_{cr}	angle between crack direction and the axis of the member
σ_{cp}	normal stress caused by axial force, positive for compression
$\sigma_{cd}, \sigma_{sd}, \sigma_{cp,eff}$	design value of normal stress caused by axial force (negative for compression)
θ	angle between concrete struts and the longitudinal axis of the member

6. STATEMENTS

By analysing the exposed shear design methods and results of the numerical example, we can state the followings:

1. *The truss model by Mörsch continues to be generally accepted.*

2. *Shear design is based on the determination of three limit values:*

- Shear resistance of the concrete section without shear reinforcement ($V_{Rd1}, V_{Rd,c}$)
- Shear resistance due to the shear reinforcement ($V_{wd}, V_{Rd,sv}$)
- Upper limit of the shear resistance corresponding to the compression failure of the concrete struts, which can not be increased by shear reinforcement ($V_{Rd,max}$)

There is an understanding within the profession concerning research, that results should be condensed into these three quantities, thus not complicating too much practical design work.

3. Since the emergence of the idea of the *variable strut inclination* (θ) the value of the inclination has become the most essential issue because it influences the above 2nd and 3rd limit rather significantly.

Further statements will be formulated concerning some of the limit values of shear resistance and of the strut angle. For simplicity, investigated regulations will be referred to by abbreviated but unambiguous denominations.

4. *Shear resistance of concrete sections without shear reinforcement* ($V_{Rd1}, V_{Rd,c}$)

Reineck emphasizes that it is important to distinguish this value from the fraction of the shear force transmitted by friction along cracks of beams designed with shear reinforcement. This was really respected when making the new draft of EC 2. As a consequence, the value V_{Rd1} and the so-called standard

method disappeared, according to which this value - V_{Rd1} - can be added to the part of the shear force equilibrated by the shear reinforcement.

Its determination is based upon empirically, taking into consideration in one way or another the following characteristics and effects:

- Cross-sectional dimensions
- Tensile strength of concrete, i.e. its square root (DIN, EC 2 new draft)
- Dimension effect (κ or k factor), which is aimed to take into consideration the additional force transmitted by friction in closer cracks of beams of smaller height. The formula given in EC 2 draft and in DIN is the same.
- Dowel action, which is built into the relationship through the effective tensile steel ratio (as a factor in the DIN, as an additive term in EC 2). The new EC 2 draft corresponds to DIN in this respect, too.
- Effect of compressive axial force by 10 to 15%, of which the shear force that can be equilibrated without shear reinforcement is increasing.

In our numerical example the quantity of shear reinforcement necessary according to the new draft of EC 2 is 20% less than that needed according to the new DIN prescriptions. This can mainly be attributed to the difference of the safety factors of loads.

5. *The shear resistance attributed to the shear reinforcement* ($V_{wd}, V_{Rd,sv}$) is proportional to the tensile force developing in elements of the shear reinforcement at yield, which intersect the sloping line of given inclination drawn between the axis of the tension and compression chord. There is a full consensus in that the shear reinforcement yields at rupture. The fundamental question is the steepness of the inclined straight line, which can be 45° (EC 2 standard method), can be in the direction of cracks (FIP Recommendations) or the strut angle θ (DIN, EC 2 new draft). We'll come back to this question later – which gives an explanation to the differences of the quantity of necessary shear reinforcement between variants of the numerical example.

6. *In connection with the shear resistance limited by the compression failure of the concrete* ($V_{Rd,max}$), three statements will be given. The first is the problem of the permissible compression stress, which is to be reduced because of the irregular surface of the struts, the disturbing action of elements of the shear reinforcement passing through the struts and due to the effect of eventual axial force. FIP Recommendations proposed a separated notation to indicate the value of the reduced compressive stress: f_{cd} , and the extent of reduction – varying between 0.45 and 0.8 – depends on the link intensity along the struts and on their spacing, which appears to be logical. The new DIN gives a relatively large factor: 0.75, based on tests, and allows further reduction for light concrete. The new EC 2 draft insists on its earlier relationship, giving values between 0.5 and 0.6. Our second remark concerns the explicit taking into account of the unfavourable effect of the axial compression force, only in the new draft of EC 2. A reduction factor should be used if the axial force produced by an exterior effect causes a compression stress greater than two thirds of the design compression strength of the concrete. Attention should be called finally to the important role of the strut inclination angle. The magnitude of $V_{Rd,max}$ is proportional to the value of the trigonometric expression given in different forms below:

$$\frac{\cot \theta}{1 + \cot^2 \theta} = \frac{1}{\cot \theta + \tan \theta} = \sin \theta \cos \theta .$$

In Fig. 5 values of the expression are shown as a function

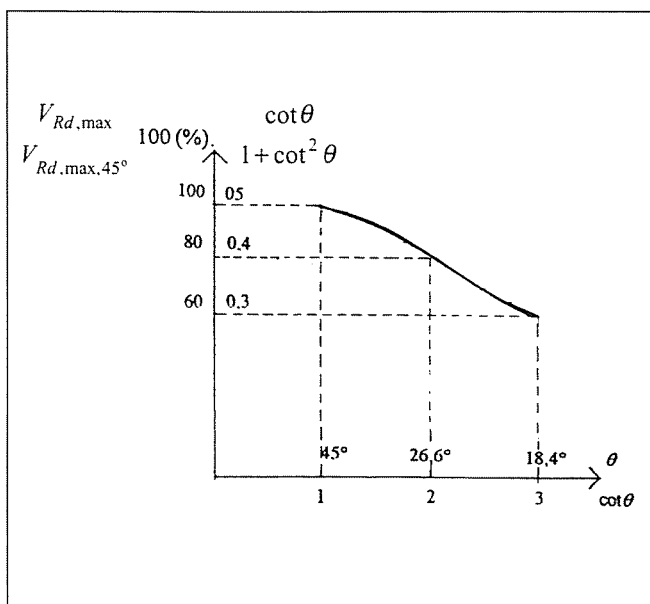


Fig. 5 Specific decrement of $V_{Rd,max}$ as a function of the strut inclination angle

of $\cot \theta$. Along the vertical axis it is also indicated, by what extent the maximum value of $V_{Rd,max}$ at $\theta=45^\circ$, i.e. $\cot \theta=1$ is decreasing while $\cot \theta$ reaches its highest limit ($\cot \theta=3$) given by the DIN, corresponding to a strut inclination angle of $\theta=18.4^\circ$. The extent of the reduction is 40%, and the almost linear function has an inflexion point above the interpretation domain,

7. Inclination angle of the compression struts (θ)

Test results and theoretical investigations have shown that a compression strut direction flatter than the 40 to 45 degrees inclined cracks can also develop, which leads to more economical solutions concerning the shear reinforcement. Referring back to the arch with hidden tirant mentioned in the introduction, by normal span-to-height ratios, an accepted internal lever arm $z=0.9d$ and parabolic arch shape, for a non-prestressed simply supported beam $\cot \theta = 4.2$ ($\theta=13.5^\circ$) would result at the supports. This does not lie very far from the limit set by DIN. The shallow compressed arch and the small inclination compression struts cause on the other hand severe anchorage problems at the external supports.

The quantity of vertical links is inversely proportional to increasing $\cot \theta$. The reduction of the upper limit of shear resistance ($V_{Rd,max}$) is also approximately linearly proportional - but somewhat less intensive - to the increase of $\cot \theta$. While $\cot \theta$ increases from 1 to 3, the shear reinforcement decreases to 1/3, i.e. by 67%, whereas the reduction of $V_{Rd,max}$ is only 40%. As it was referred to earlier and the numerical example also demonstrates: for non-prestressed beams it cannot be expected that by choosing smaller strut inclination angle, the upper limit of shear resistance turns to be definitive and the determination of the condition system $V_{Rd,sy} = V_{Rd,max} = V_{Sd}$

The quantity of vertical links is inversely proportional to increasing $\cot \theta$. The reduction of the upper limit of shear resistance ($V_{Rd,max}$) is also approximately linearly proportional - but somewhat less intensive - to the increase of $\cot \theta$. While $\cot \theta$ increases from 1 to 3, the shear reinforcement decreases to 1/3, i.e. by 67%, whereas the reduction of $V_{Rd,max}$ is only 40%. As it was referred to earlier and the numerical example also demonstrates: for non-prestressed beams it cannot be expected that by choosing smaller strut inclination angle, the upper limit of shear resistance turns to be definitive. This would mean that the determination of the necessary shear reinforcement and of the strut inclination limit should be made on the

basis of the condition system $V_{Rd,sy} = V_{Rd,max} = V_{Sd}$

From among the normative prescriptions investigated in the present article the DIN can be considered unique in that - based on tests and, in the first line, thanks to the theoretical activity of Reineck - it gives proposals for the determination of the strut inclination as a function of the force distribution. The basic value is the crack direction modified by the effect of the compression force, which is then modified - decreased - by the crack friction forces and the design value of the shear force. According to the FIP Recommendations the inclination angle is also determined, but only afterwards, with knowledge of the shear reinforcement intersecting the cracks and of the crack friction forces.

In the case of EC 2 not even the new version gives a starting point for the designer to adopt a strut angle, only the limits are given. We have deliberately chosen the smallest allowable strut angle in the numerical example ($\cot \theta=2.5$), by which the intensity of the shear reinforcement reduces almost to half. This problem deserves more careful investigation. The concrete is safe for compression and construction rules are fulfilled. Due to the flat strut angle elements of the tensile reinforcement should be anchored at greater distance, but this condition is automatically fulfilled for the reinforcement designed for negative moment at interior supports

8. Although design of bent-up bars is allowed by the investigated standard prescriptions, neither of the newly edited technical literature nor the technological practise are supporting that method, the FIP Recommendations are explicitly not proposing the use of bent-up bars. In connection with this the EC 2 stipulates that in case of designing shear reinforcement at least half of the shear force should be absorbed by links. Due to the above reasons no bent-up bars were used in the numerical example. However, I will shortly take the opportunity to expose my personal opinion. By bending up not too great diameter - max. $\varnothing 16$ - bars by interior supports, two anchorage lengths can be economised. The advantageous action of these bars resembles that of suspension cables. Due to these reasons - depending on the results of flexural design, bending up of bars at disposal, by respecting limitations of EC 2 - I consider as a very reasonable solution.

7. PROPOSALS

1. The DIN 1045-1 2000 should be highlighted from among the shear design procedures investigated as the one which is more progressive pointing forward, by giving an expression for the determination of the strut angle. This is depending on the force distribution and so it is variable along the axis of the member which better corresponds to reality.

2. The EN 1992-1:2001 draft is similar to DIN 1045-1 in numerous details, but it does not take a stand on the most important question of the strut angle. So it is applicable for practical design only after amendments.

3. By elaboration of rules concerning the strut angle a distinction should be made between exterior and interior supports because anchorage problems emerging by small strut angles can hardly be solved in a correct way by exterior supports. It would be desirable to investigate this problem by laboratory tests.

4. Although yield of the link legs was proved by Leohardt's shear tests of beams using one point elongation measurement per link, for sake of a deeper detection of the anchorage conditions it would imply multipoint measurement along the perimeter of the links.

8. REFERENCES

- CEB-FIP Model Code for Concrete Structures (1978) *CEB-Bulletin d'Information No. 124/125*, Paris
- EN 1992-1:2001 (1st draft), Eurocode 2: Design of concrete structures. Part 1: General rules and rules for buildings, pp. 103-108.
- FIP Recommendations 1996, "Practical Design of Concrete Structures", pp. 6-5 – 6-11.
- Kollár, L.-Sapkás, Á. (1999) "Design of beams under shear according to EUROCODE and MSZ 15022" „Nyírt gerendák méretezése az EUROCODE és az MSZ15022 szerint”, *Comparatory study*
- Kupfer, H. (1964) Erweiterung der Mörsch'schen Fachwerkanalogie mit Hilfe des Prinzips vom Minimum der Formänderungsarbeit, *CEB-Bull. No. 40*, pp. 44-57.
- Lenkei, P. (2000) "The European structural design codes and the national application documents" „Az európai tartószerkezeti szabványok és nemzeti alkalmazási dokumentumok”, *Vasbetonépítés II. 2.* pp. 35-37.
- Leonhardt, F.-Walter, R. (1964) Schubversuche an Durchlaufträger, *Deutscher Ausschuss für Stahlbeton Heft 163*, Verlag von W. Ernst und Sohn Berlin, 1964.
- Leonhardt, F. (1965) Die verminderte Schubdeckung bei Stahlbetontragwerken, *Der Bauingenieur 40*, H. 1, pp 1-15.
- Litzner, Ü. (1997) Grundlagen der Bemessung nach Eurocode 2 in Beispielen, *Beton-Kalender 1997*, pp. 577-710.
- Mörsch, E. (1922) Der Eisenbetonbau, seine Theorie und Anwendung, 1. Band, 5. Auflage, Verlag von Konrad Wittwer, Stuttgart
- Reineck, K.-H.-Hardjasaputra, H. (1990) "Zum Dehnungszustand bei der Querkraftbemessung profilierter Stahlbeton- und Spannbetonträger", *Bauingenieur Band 65* (1990), pp. 73-82.
- Reineck, K.-H. (1991) "Ein mechanisches Modell für Stahlbetonbauteile ohne Stegbewehrung", *Bauingenieur Band 66*, pp. 157-165
- Reineck, K.-H. (1991) "Ein mechanisches Modell für das Tragverhalten von Stahlbetonbauteilen ohne Stegbewehrung", *Bauingenieur Band 66*, pp. 323-332
- Reineck, K.H. (2001) "Hintergründe zur Querkraftbemessung in DIN 1045-1 für Bauteile aus Konstruktionsbeton mit Querkraftbewehrung", *Bauingenieur Band 76*, April 2001, pp. 168-179.
- Szalai, K.-Kovács, T. (2000) "Changing of load capacity requirements according to MSZ in 20th Century and their comparison to Eurocode" „Az MSZ szerinti teherbírás követelmények változása a XX. században, és azok összehasonlítása az EUROCODE szerintiakkal”, *Vasbetonépítés II. 3.* pp. 76-82.
- Thürlimann, B. (1978) Shear strength of reinforced and prestressed concrete beams, *CEB Bull. no. 126*, pp. 16-38.
- Zilch, K.-Rogge, A. (2001) "Bemessung der Stahlbeton und Spannbeton Bauteile nach DIN 1045-1", *Beton-Kalender 2001*, pp. 205-347.

Dr. Draskóczy András (1947) is senior assistant lecturer at the Budapest University of Technology and Economics, Faculty of Architecture, Department of Strength of Mechanics and Structures, responsible for the practical education of Reinforced Concrete Structures I, lecturer of the subject on the English Speaking Course. He is structural designer and expert of numerous buildings. His earlier field of interest was the non-linear behaviour of reinforced concrete structures. Memberships: Chamber of Hungarian Civil Engineers, Chamber of Hungarian Architects, Scientific Association for Building.

SAND PATCH METHOD FOR EVALUATION OF CONCRETE-TO-CONCRETE INTERACTION



Tamás Simon

During design, manufacturing and construction of prefabricated and in-situ reinforced concrete structures, where the concrete-to-concrete interacting capability is to be calculated, the surface roughness of the receiving concrete is of significance. In the regulations and guidelines the surface roughness of the receiving concrete is not quantified, only described as for example by stating it is very rough, rough, smooth or very smooth. For calculations the surface roughness of the receiving concrete should be measurable and quantified directly or indirectly. This would enable quality control documentation and designer prescriptions with calculable effects. The sand patch method has been used in road construction for a long time to define the surface roughness of pavements. This method is suitable for our purposes. After adoption of the sand patch method, experiments were carried out at the Department of Construction Materials and Engineering Geology of Budapest University of Technology and Economics, to verify the suitability and to determine a precise conformity between the interacting capability and surface roughness of receiving and new concrete layers.

Keywords: concrete-to-concrete interaction, roughness, construction joint

1. MECHANICAL BEHAVIOUR

It is well known that surface roughness provides shear capacity. In practical cases when, for example, prefabricated thin floor planks are used for ceiling construction, the planks are cast with a certain top surface roughness which is the receiving surface and usually has an amount of reinforcement connecting the planks and the in-situ concrete which is cast on site. The top surface of the receiving concrete and the bottom surface of the in-situ concrete form a designed construction joint. The two layers of concrete – when the ceiling is subjected to vertical loads – must work together and the construction joint formed is subjected to shear stresses. Shear forces at the construction joint are cantilevered by three actions; adhesion, dowel action of reinforcement crossing the construction joint and concrete teeth within the receiving concrete surface, if any (Fig. 1). The adhesion and the teeth will act against shear without any relative movement starting between the two concrete layers, while the reinforcement is only working when relative movement develops between the two layers. Any combination of above three actions is possible.

The preparation of a regularly toothed top surface is difficult. The use of excessive reinforcement is expensive, so it is a wish to be able to have a precisely calculable amount of shear resistance in the construction joint due to the adhesion of the two layers. One of the main parameters influencing the interaction between the two layers is the surface roughness of the receiving concrete. At the same time this parameter is de-

finied by verbal descriptions in the regulations which may lead to misunderstandings. For this reason the introduction of a reliable definition and measuring method is required.

2. REGULATORY BACKGROUND (STILL IN FORCE AND PLANNED)

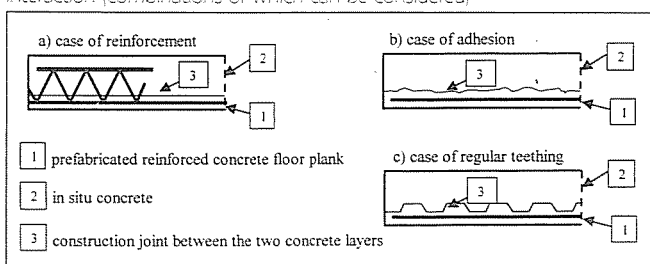
The interacting capability between receiving concrete and new concrete is a very good example of the forced development of regulations by the industry. Over decades many researchers have studied the problem (Balázs, Fogarasi, 1977; Burkhard, 1990; Dulácska, Szederjei, 1972; Gilyén, 2000; Hofbeck, Ibrahim, Mattock, 1969; Orosz, Tassi, Ódor, 1984; Polgár, Stairits, 2001; Pommeret, 1970; Simon, 2002; Szalai, 1967; Walraven, Reinhard, 1981). However, the standards, codes of practices and regulations followed the results of studies only when larger-scale prefabricated reinforced concrete production was started. The intention of the present discussion is also to give representative samples of the regulations of different countries and to give an overview of planned or existing European standards. A complete historical overview is not an intention herein.

The Hungarian Standard (MSZ 15022/4-86) is a very severe regulation in this respect. It allows simultaneous consideration of the effect of concrete teeth, the reinforcement which is crossing the connecting planes and the concrete-concrete friction (in case of normal force) or adhesion only if reinforcement to the minimum extent of 0.1% of the connecting planes is present. Reinforced connection may suffer a maximum shear force, taking into consideration the adhesion only by Eq. (1) to the extent of (MSZ 15022/4-86):

$$V_{Rd1} = A_c \cdot f_{ct,d} \cdot a_f \quad (1)$$

where

Fig. 1 Schematic representation of the cases of concrete-to-concrete interaction (combinations of which can be considered)



Grade of concrete	C10	C12	C16	C20	C25	C30	C35	C40	C45	C50	C55
Ultimate design tensile strength of concrete $f_{ct,d}$ [N/mm ²]	0.7	0.9	1.1	1.4	1.6	1.8	2.0	2.1	2.3	2.5	2.7

Table 1 Values of $f_{ct,d}$ (MSZ 15022/1-86)

A_c is the surface of the concrete taken into consideration, $f_{ct,d}$ is the ultimate tensile strength of the concrete α_f coefficient of the friction, the value of which is:

- in case of slipping layer: 0;
- in case of a surface finish from a formwork: 0.5;
- in case of rough surfaces: 0.8.

The values of $f_{ct,d}$ are given in Table 1.

The Hungarian Standard does not allow simultaneous consideration of shear resistance from friction and adhesion respectively. The limit of shear force due to friction is given by Eq. (2):

$$V_{3d} = N \cdot \alpha_f \quad (2)$$

where N is the perpendicular component of the normal force to the surface. *The roughness of the surfaces are not quantified, the so-called "slipping layer" is not defined.*

British Standard (CP 110:Part 1: 1972) gives maximum values for the allowed horizontal shear stresses for composite beam and slab sections in the function of the grade of the in-situ concrete and of three different Surface Types. In case of Surface Type 1, which is basically an exposed aggregate surface, the regulation allows a shear stress between 0.38 and 0.64 N/mm² in the function of the grade of in-situ concrete. No detailed definition of the surface of the receiving concrete (old concrete) is given; the maximum size of aggregate is not defined. In case of Surface Types 2 and 3 – which is smooth in case of Type 2 and rough in case of Type 3 – reinforcement to the minimum extent of 0.15% of the contact area is prescribed. *The roughness of the surfaces are not quantified and the grade of the in-situ concrete may be higher than the prefabricated one.*

The European Standard prEN 13747-1 (prEN 13747-1:1999) refers to Eurocode 2 (ENV 1992-1-3:1994) which offers Eq. (3) for the evaluation of the design shear resistance per unit length of such connection:

$$\tau'_{Rd} = \kappa_T \cdot \tau'_{Rd} \quad (3)$$

and the standard gives values for τ'_{Rd} in a tabular form (Table 2).

No intermediate values for different surface roughnesses are given. There is no possibility of interpolation between the verbally defined smooth and rough surfaces.

Austrian Standard (ÖNORM B 4700: 2001) gives the formula for the design shear resistance per unit length of the connection for nearly constant loads as follows:

$$\tau'_{Rd} = \kappa_1 \cdot \tau_d + \rho \cdot \kappa_2 \cdot f_{yd} \cdot (\mu \cdot \sin \alpha + \cos \alpha) + \mu \cdot \sigma_N + \rho \cdot \kappa_3 \cdot \sqrt{f_{yd} \cdot f_{cd}} \cdot \sin \alpha \leq \beta \cdot v \cdot f_{cd} \quad (4)$$

Table 2 Values of τ'_{Rd} [N/mm²] (prEN13747-1:1999)

Description of surface	τ'_{Rd}		
	Minimum concrete grade of prefabricated or in-situ concrete		
	≥20/25	≥25/30	≥30/37
Smooth	0.36	0.42	0.47
Rough prefabricated top surface according to 4.3.2 point of 229 W1 9-1:199X*	0.46	0.54	0.61

* Not yet worked out

The first component in Eq. (4), ($\kappa_1 \cdot \tau_d$) gives the load bearing capacity due to adhesion, which is our scope. The other components are responsible for the load bearing capacities due to toothed connection and reinforcement across the connection and normal force acting perpendicularly to the surface of the connection respectively. Our primary interest in this study is the value of κ_1 for which the standard gives 2 in case of a surface which is treated with high pressure water-blasting, and 0 for all other cases (sandblasted, vibrated, smoothed etc.). The value of 2 is also valid for a toothed surface. Austrian Standard (ÖNORM B 4700: 2001) mentions the definition of surface roughness by the sand patch method used in road construction, and gives a minimum value for R as 2,5 mm (R is the depth of the sand in this case). *No intermediate roughness values are given.*

German Standard (DIN 1045:2001-07) deals with the calculation of shear load bearing capacity of the construction joint in its section 10.3.6. DIN 1045:2001-07 gives definitions for the roughness of the surface of the receiving concrete as:

- *very smooth*: the surface which was cast in steel or smooth wooden formwork,
 - *smooth*: only vibrated and no further surface treatment is made, if smoothed or if the concrete is prepared by slipwork or extruder technology,
 - *rough*: if the surface is according to DafStb Heft 525
 - *toothed*: uniform geometric teeth with more than 10 mm in height (described by diagram in the standard, here in Fig. 1)
- Eq. (5) defines the shear resistance per unit length of a construction joint in a non-reinforced case (DIN 1045:2001-07):

$$v_{Rd,ct} = [0.042 \cdot \eta_1 \cdot \beta_{ct} \cdot f_{ck}^{1/3} - \mu \cdot \sigma_{Nd}] \cdot b \quad (5)$$

where:

- η_1 = 1.0 for normal weight concrete; and different values for light weight concrete (given in separate table in another part of the standard),
- β_{ct} = is a roughness factor (here given in Table 3),
- f_{ck} = is the characteristic compressive strength of the prefabricated or in-situ concrete (the smaller is to be considered) in N/mm²,
- μ = the coefficient of friction (here given in table 3),
- σ_{Nd} = value of design normal stress acting on a vertical joint ($\sigma_{Nd} < 0$ as concrete compressive strength)
- $\sigma_{Nd} = \eta_{Ed} / b \geq -0,6 \cdot f_{cd}$ in N/mm²,
- η_{Ed} = the lower value of longitudinal normal force in a vertical joint,
- b = the width of the connecting surfaces.

CEB-FIP Model Code 90 deals with the problem under the title Concrete-to-concrete friction in point 3.9. The difficulty arises from the definition, which states, "The mechanism of shear transfer along a concrete-to-concrete interface which is simultaneously subject to shear and normal compression is called concrete-to-concrete friction." The problem is that, no guidance is given for the case when compressive force is not present perpendicular to the interface. Adhesion of the two concrete layers is neglected. *Smoothness and roughness of the surfaces are not quantified, surfaces are verbally described as smooth or rough.*

Table 3 Values of β_{ct} and μ (DIN 1045: 2001-07)

Case	Joint	
	1	2
	The roughness of the surface is according to the definitions	β_{ct} μ
1	Toothed	2.4 1.0
2	Rough	2.0 ^a 0.7
3	Smooth	1.4 ^a 0.6
4	very smooth	0 0.5

^a If an action to the surfaces is perpendicular and tension, $\beta_{ct} = 0$

Type of surface	κ_T
In-situ (monolithic)	2.5
Rough	1.8
Smooth	1.4
Very smooth	0

Table 4 Values of κ_T [ENV 1992-1-3:1999]

f_{ck}	C12	C16	C20	C25	C30	C35	C40	C45	C50	C55	C60
τ_{Rd}	0.18	0.22	0.26	0.30	0.34	0.37	0.41	0.44	0.48	0.48	0.48

Table 5 Values of τ_{Rd} [N/mm²] [ENV 1992-1-3:1999]

Finally the most recent regulation Eurocode 2 (ENV 1992-1-3:1994) gives the expression for the design value of the shear load bearing capacity of the connection of the composite structure as:

$$\tau'_{Rdj} = \kappa_T \cdot \tau_{Rd} + \mu \cdot \sigma_N + \rho \cdot f_{yd} \cdot (\mu \cdot \sin\alpha + \cos\alpha) \leq 0.5 \cdot v \cdot f_{cd} \quad (6)$$

In Eq. (6) the $\mu \cdot \sigma_N$ and $\rho \cdot f_{yd} \cdot (\mu \cdot \sin\alpha + \cos\alpha)$ components are responsible for the shear load bearing capacity of the connection due to stress from normal force, perpendicular to the surface and the reinforcement across the connection, respectively. This present paper, however, only deals with the effect of the first component ($\kappa_T \cdot \tau_{Rd}$), which is responsible for the design shear load bearing capacity of the connection due to adhesion. In this component the values of κ_T are given in Table 4 and of τ_{Rd} in Table 5.

Smoothness and roughness of the surfaces are not quantified; the surfaces are verbally described as very smooth, smooth or rough.

3. SAND PATCH METHOD

We would not like to compare the slight differences in the sand patch methods used and standardised in different parts of the world. At the same time we give a detailed description of the method given in the Hungarian Standard (UT – 2. – 2.111/77) and highlight the points where most of the regulations differ. We also give the method we used to determine different surface roughness through the SCD number (Simon, 2002). The method described in the standard requires:

- dry, clean, natural sand consisting of particles between 0,06–0,09 mm or 0,09–0,2 mm in size,
- a soft brush,
- a measuring cylinder having volume capacity of 5, 10 and 25 ml ($\pm 0,1$ ml),
- sand smoothener 50–60 mm in diameter, covered with PVC or rubber,
- a ruler, at least 400 mm long,
- denaturated spirit to dry the surface and matches.

In case of on-site measurement, if the surface is moist it must be dried in a circle of 400 to 500 mm in diameter. Surface contamination is to be brushed with the soft brush. A volume of 5, 10 or 25 ml of sand is to be poured onto the surface. (In case of on-site measurement of the sand the measuring cylinder is to be knocked 3 times to the surface and refilled to the mark by sand in order to obtain uniform compaction and horizontal sand surface levelling.) The objective to decide the amount of sand to be used is that, after the sand has been screeded into the voids of the surface using the smoothener, the obtained sand patch should have a diameter of at least 100 and maximum of 300 to 350 mm. Since the formed sand patch is not a regular circle the diameter is to be measured across the four main directions to within ± 5 mm and the mean value

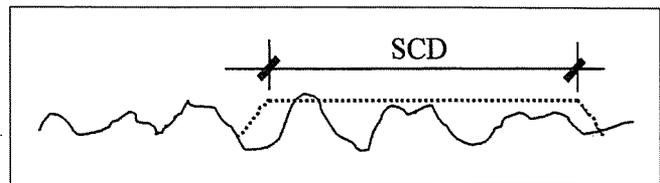


Fig. 2 The truncated sandcone and measurement of SCD number

calculated. The mean diameter is to be used to determine the depth of the sand in mm to two decimal points, using the formula for the calculation of the height of a cylinder knowing the volume and the diameter of the top (or bottom) circular plane.

The main difference in the method regulated in different parts of the world is in the fineness definition of the sand and the volume of the sand to be used. These differences however are not significant.

The method we applied is based on the above-described and varies mainly in the following three points:

- *The first* difference is in the grading of the sand, which is less important in our case since the surfaces to be described are much rougher than in the case of road surfaces. It was also considered, in case of on-site measurements under windy conditions, that the sand particles are blown away more easily if they are small. For these reasons we applied sand of 0/1 mm fraction without further grading (That is sand passing the 1 mm sieve in 100%).
- *The second* difference was in the determination of the volume of the sand used. We found that a uniform volume of the sand could be measured more precisely by mass measurement, since the knocking three times to the surface may give up to more than 5 ml differences in volume. Another point is that we needed more volume of sand due to the rougher surfaces to be measured. For these reasons we batch 100 g of sand which proved to be about 65 ml.
- *The third* difference was in that we measured only the diameter of the top plane of the sand cone in four main directions, calculated the average, and gave the result in mm to two decimal points. We named the average diameter to SCD (Sand Circle Diameter) number. The SCD number was used for further reference, and not the depth of the sand. The reasons were two-fold. When the sand is screeded into a rough surface we observed that the sand body so formed was not a cylinder, but a truncated cone as shown on Fig. 2. The other reason is that the biggest mistake possible to be made is when the diameter of the circle is measured. When calculating depth, this diameter is raised to the power of two, so the measuring error would also be squared, and the error would become more significant. We intended to eliminate the effect of imprecise measurement as much as possible.

4. RELATIONSHIP BETWEEN THE SCD NUMBER AND CONCRETE–TO – CONCRETE INTERACTION

We have verified the applicability of the adopted sand patch method (Simon, 2002). We prepared altogether $3 \cdot 3 \cdot 4 = 9 \cdot 4 = 36$ test specimens (in order to take average values, three of each), with three different surfaces for further research of the shear load bearing capacity of the construction joints of concrete,

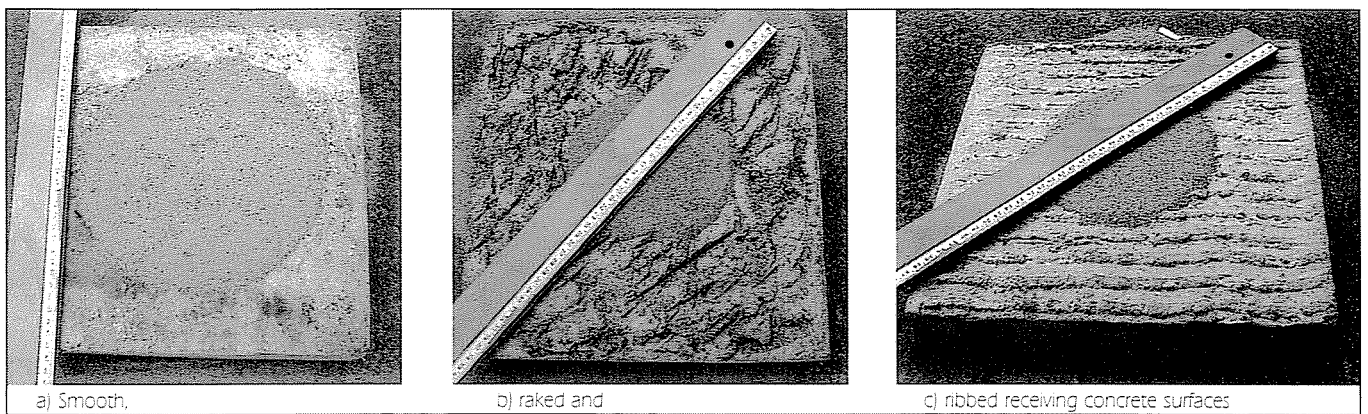


Fig. 3 Types of surfaces in presented tests

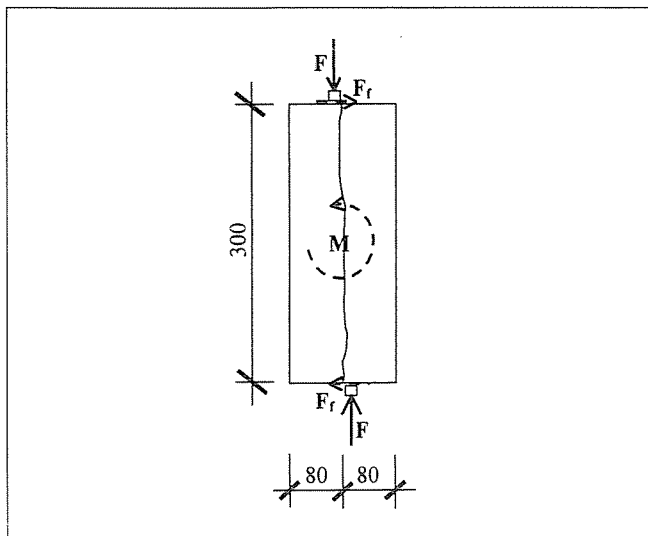


Fig. 4 Side view of the test arrangement (the moment (M) induced by the possible non-coincidence of the shear forces is cantilevered by the frictional forces (F_r) between the concrete-steel, force-transferring surfaces of the loading device)

having four different characteristic strengths. The three different surfaces were: smooth (vibrated, semi plastic concrete with no further surface treatment), raked (randomly roughened) and ribbed (with perpendicular ribs to the load). To be able to visualise the surfaces corresponding to the SCD values we represent them in Fig. 3.

Test specimens were of 300x300x80 mm in size. The designed concrete grades were C12/15; C16/20; C25/30 and C40/50. After 28 days of curing (7 days under water then in laboratory ambient conditions) a new layer of concrete of about 80 mm was poured on the surface of the same designed grade of concrete as the first layer. Following a time period of a further 28 days while the second layer was cured as the first, the prepared specimen construction joints were subjected to a direct shear force under such a test arrangement which ensured that mainly direct shear stress would develop on the concrete-to-concrete bonding surface (Fig. 4).

In Table 6 we summarise the most important concrete properties measured during the preparation of the test samples.

As we can see in Table 6 the mean compressive strength of the concretes we obtained were a little higher than could be expected. During the evaluation had to take into consideration the compressive strength with the lower value out of the two tested layers.

In the following diagrams (Figs. 5-9) we present the tendency of the concrete-to-concrete bond capability in the terms of the SCD number and on the last diagram we present it in one. We would like to draw attention to the fact that these results apply only to clean, uncontaminated surfaces. The ef-

Sign of sample	Designed grade	Mean compressive strength on cubes of 150 mm sides [N/mm ²]	Tested surface	mean SCD value [mm]	Mean shear strength of the construction joints [N/mm]
S1/1-3, old	C40/50		smooth	212.08	0.212
S1/4-6, old	C40/50	45.89	raked	125.67	1.464
S1/7-9, old	C40/50		ribbed	144.58	1.118
S1/2 nd layer	C40/50	48.15			
S2/1-3, old	C25/30		smooth	249.58	0.088
S2/4-6, old	C25/30	44.57	raked	128.33	0.395
S2/7-9, old	C25/30		ribbed	133.00	0.597
S2/2 nd layer	C25/30	43.18			
S3/1-3, old	C16/20		smooth	261.67	0.184
S3/4-6, old	C16/20	42.29	raked	117.50	0.603
S3/7-9, old	C16/20		ribbed	141.25	0.749
S3/2 nd layer	C16/20	36.19			
S4/1-3, old	C12/15		smooth	235.83	0.164
S4/4-6, old	C12/15	30.48	raked	127.50	0.378
S4/7-9, old	C12/15		ribbed	145.83	0.455
S4/2 nd layer	C12/15	29.00			

Table 6 The most important concrete properties measured during the tests. In the first column in the sign "old" against the samples means the first layer of concrete

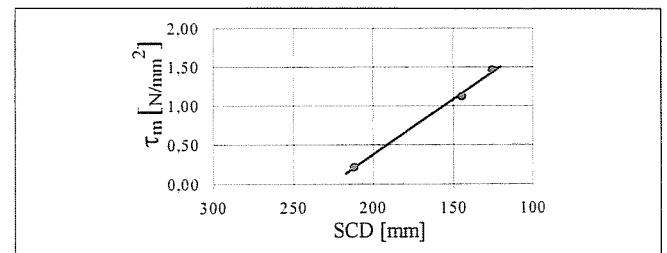


Fig. 5 Mean shear strength of joint against SCD number in case of 45.89 N/mm² mean concrete compressive strength

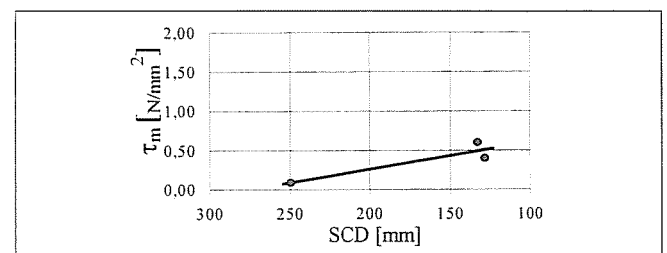
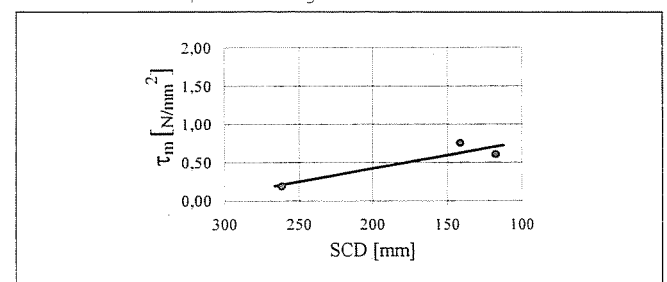


Fig. 6 Shear strength of joint against SCD number in case of 43.18 N/mm² mean concrete compressive strength

Fig. 7 Shear strength of joint against SCD number in case of 36.19 N/mm² mean concrete compressive strength



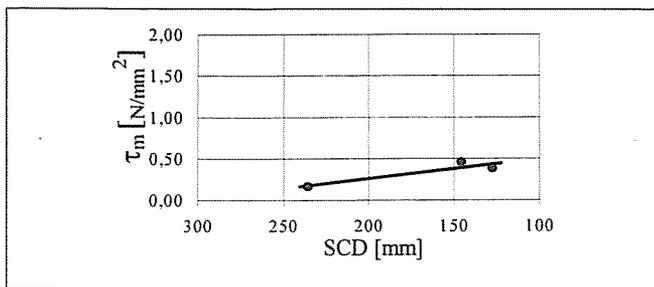


Fig. 8 Shear strength of joint against SCD number in case of 29.00 N/mm² mean concrete compressive strength

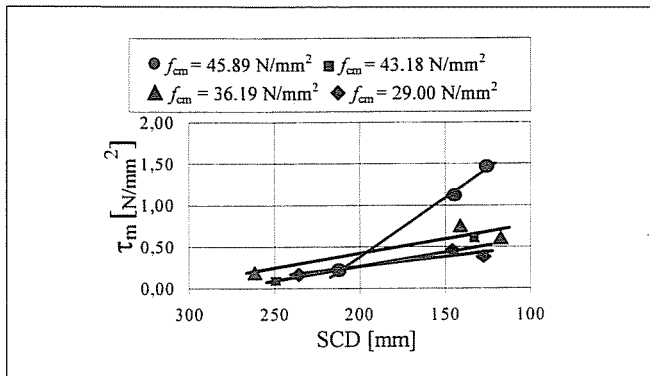


Fig. 9 Shear strength of joints against SCD numbers in case of concretes having mean compressive strength between the values of 45.89 and 29 N/mm²

fect of any coating or contamination on the surface of the receiving concrete must be separately investigated.

In Fig. 9, where the performance of concretes with the four different compressive strength can be best compared, it is significant that concrete with a designed grade of C40/45 follows the change of surface roughness more rapidly. This may draw the attention to more precise evaluation of surface roughness especially in case of high performance concretes.

5. CONCLUSIONS

Due to uncertainties in the existing regulations, and the need for more precise quality control in the determination of surface roughness of an existing concrete structural element, the sand patch method was adopted to quantify the property of the surface of the receiving concrete.

We have studied the main samples of the existing regulations and found that surface roughness determination is nowadays mainly based only on visual observations.

We have adopted and described the sand patch surface roughness measuring method used earlier mainly in road construction and showed its applicability for evaluating the relationship between concrete-to-concrete interacting capability by adhesion and the introduced SCD (Sand Circle Diameter) number.

We offer graphical correlations between the SCD number and shear strength of construction joints for concretes having different mean compressive strength.

Based on Fig. 8 we draw the attention to the observation that in case of concretes having a higher designed grades than

C25/30 the shear load bearing capacity of the construction joint follows a steeper slope in confluence with the surface roughness, which is significant especially in case of high performance concretes.

6. REFERENCES

- Balázs, G., Fogarasi, G. (1977), "Reinforced concrete connections", *Műszaki Könyvkiadó, Budapest*. 1977 pp. 158-169., and 296-298. (in Hungarian)
- Burkhard, M. (1990), "Bemessungshilfen für Verbundplatten mit Gittertragern", *Beton und Stahlbetonbau* 85, H. 1, pp. 11-14.
- CEB-FIP (1993), "CEB-FIP MODEL CODE 1990" *Thomas Telford Services Ltd, London*. pp 113-115.
- CP 110:Part 1: 1972 "British Standard Code of Practice for The structural use of concrete Part 1. Design, materials and workmanship" *British Standard Institution, 2 Park Street London 1980*, points 5.2.5.3 p. 82. and point 5.4.3.4 pp. 87-88.
- DIN 1045-1:2001-07, "Tragwerke aus Beton, Stahlbeton und Spannbeton" *Deutsches Institut für Normung*, pp. 80-82.
- Dulácska, E., Dné Szederjei, I. (1972), "Shear loadbearing capacity of pre-fabricated and in situ concrete connection plane", *Mélyépítéstudományi Szemle* XXII. évf. 8. szám, pp. 375-377. (in Hungarian)
- ENV 1992-1-3:1994, "Eurocode 2: design of concrete structures. Part 1-3: General rules. Precast concrete elements and structures." *European Committee for Standardisation*, pp. 32-36.
- Gilyén, J. (2002), "Design questions of structures made by secondary concreting". *BETON* X. évf. 9. szám, pp. 13-15. (in Hungarian)
- Hofbeck, J. A., Ibrahim, I. O., Mattock, A. H. (1969), "Shear Transfer in Reinforced Concrete", *ACI Journal* Nr. 2. pp. 119-128.
- MSZ 15022/4-1986, "Design of reinforced concrete load bearing building structures – Prefabricated concrete, reinforced concrete and stressed concrete structures", *Magyar Szabványügyi Hivatal*, point 3.1.2, p 4, and in the appendix point F1, pp. 7-8. (in Hungarian)
- Orosz, A., Tassi, G., Ódor, P. (1984), "The results of laboratory examination for ultimate loadbearing capacity of PR prestressed floor planks", *BME Vasbetonszerkezetek Tanszék Report (in Hungarian)*
- ÖNORM B 4700:2001-07, "Stahlbetontragwerke: Eurocode-nahe Berechnung, Bemessung und konstruktive Durchbildung", *Österreichisches Normungsinstitut*, pp. 40-42.
- Polgár, L., Stairits, F. (2001) "PROFIPANEL" *VASBETONÉPÍTÉS* Vol. III. Nr. 3., pp. 75-83. (in Hungarian)
- Pommeret, M. (1970), "Les joints verticaux résistants aux efforts tangents entre grands panneaux préfabriques coplanaires". *Annales de l'Institut Technique du Batiment et des Travaux Publics*. No. 270. pp. 92-93.
- PrEN 13747-1:1999, "Fertigteileplatten mit Ortbetonergänzung" *European Committee for Standardisation*, pp. 29-31.
- UT - 2. - 2.111/77 "Manual for the measurement of pavement roughness by hand tools Clause 3", *Magyar Szabványügyi Hivatal* Ütépítési ágazati szabvány, p 3. (in Hungarian)
- Simon, T. (2002), "Definition of surface roughness for evaluation of concrete-to-concrete bond" *Proceedings Int. Symp. on "Bond in concrete"* Nov. 2002, Budapest (edited by: Balázs, L. G., Bartos, M. J. P., Cairns, J., Borosnyói, A.) pp. 395-403.
- Szalai, J. (1967), "Stress state of co-working concrete and reinforced concrete structures taking into consideration shrinkage and long term deformation" (in Hungarian). *Tankönyvkiadó, Budapest*. (Mérnöki Továbbképző Int. anyag 4588 szám)
- Walraven, J. C., Reinhard, H. W. (1981), "Theory and experiments on the mechanical behaviour of cracks in plain and reinforced concrete subjected to shear loading", *HERON, Concrete Mechanics*, part A. Vol. 26. Nr.:1A

Tamás SIMON (1956), Civil engineer. Between 1983 and 1990 consultant for VIZITERV Consulting Engineering Company for Water Engineering. For two years between 1990 and 92 developing engineer of "kas" Insulation-technics Developing and Constructing Incorporated Company. Since 1992 senior lecturer of Budapest University of Technology and Economics, Department of Construction Materials and Engineering Geology. Main fields of interest: concrete and reinforced concrete structures, concrete technology, quality control. Member of the Hungarian Chamber of Engineers, the Hungarian group of fib and fib TG. 6.2 "Connections".

EFFECT OF POROSITY ON THE PROPERTIES OF CONCRETE



Salem Georges Nehme

Increasing attention is directed to the durability of concrete structures. Porosity, dispersion and volume of pores effect not only durability of concrete but also its strength. The distribution of pores influences the deterioration of concrete while the starting points of the cracks are the pores in the concrete matrix. The effects of cement content and water-cement ratio on the porosity of concrete were studied.

In this paper we will summarise the most important theories regarding the porosity of concrete to show that concrete with identical strength may possess different durability characteristics.

The experimental study was directed to check the relationship between strength and porosity. Water content and grading of aggregate were constant, however, cement content and amount of superplasticiser were varied.

Keywords: porosity, water/cement ratio, durability, water tightness, freeze-thaw resistance.

1. INTRODUCTION

When cement is mixed with water, the chemical reactions of hydration slowly begin to produce new materials (concrete, mortar). Concrete is a random composite material with the fine and coarse aggregate acting as the inclusions and the cement paste acting as the matrix.

The properties of the aggregate are measurable and usually remain constant in time, while the properties of the cement paste depend on the original water/cement ratio, type and quantity of admixtures, hydration time, degree of hydration, and to some extent on the initial particle size distribution.

In the interface transition zone between the cement paste and the aggregates the cement paste microstructure may play a critical role in determining the bulk concrete properties. It is known that bond between cement paste and aggregate surface have higher capillary porosity and larger pores than in the bulk cement paste matrix (Maso, 1980).

The porosity of the interface transition zone and cement paste is the most important coefficient which has an influence on the strength of the concrete. Pore content of 1 V% causes 4-5% loss of strength (Woods, 1968), thus production of concrete higher than 6 V% is impractical.

The presence of capillary pores and air voids influence concrete permeability to a large extent. The ingress of aggressive agents into the pore structure is responsible for various durability problems in concrete structures (aquitardity, corrosivity and freeze-thaw resistance).

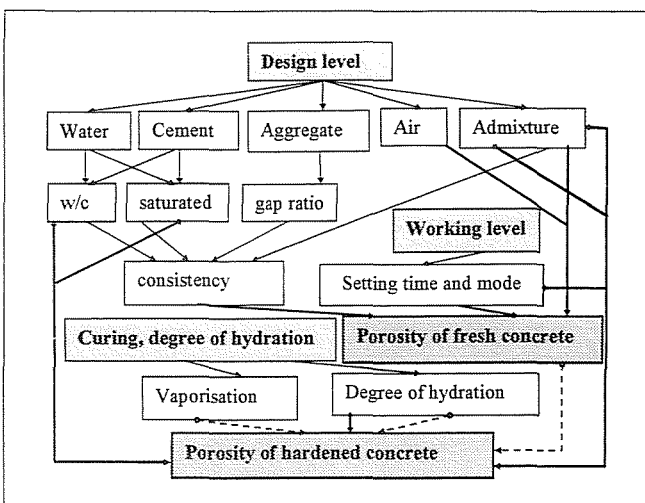
The durability of concrete depends on the type, size and distribution of pores in the concrete. Further factors are the absorption and the connection of the pores and the cracks in the concrete.

The visualisation of the pore content can happen in three levels (Fig. 1). The three levels being design level, working level and post-hydration level.

Chemical reactions proceed at the most favourable rate when the environmental temperature is moderate (about 15°C). On the other hand the degree of hydration affects the pore content and micro-cracking. During hydration capillary pores are developed in those parts of the concrete which are not filled by the excess volume generated during hydration (Neville, 1995).

To minimise and control the porosity of concrete the paste-saturation and the water/cement ratio of concrete have to be optimised. The over-saturated and unsaturated concretes have higher porosities compared to those of paste-saturated concrete. In the first case the difference is caused by the capillary porosity while in the second case it is caused by the quantity of the air pores (Balázs, Erdélyi, Kovács, 1990).

In this paper, the most important theories about the porosity of concrete are summarized in order to show that with the same strength of concrete durability can be varied.



2. POROSITY OF CEMENT PASTE

Calculation with regard to the porosity of fresh-paste is easier. Similarly to the porosity of concrete it should be calculated by subtracting the aggregate:

Initial porosity of hydrated cement:

$$P_0 = 1 - \frac{\rho_c + m_w}{V_{Tc}} = 1 - \frac{\rho_c}{1+x} \cdot \rho_{fc} \quad (1)$$

where:

ρ_{fcp} : body density of the fresh paste,

x : water/cement ratio,

ρ_c : density of concrete,

ρ_w : density of water.

Taking the degree of hydration into consideration, the porosity of hydrated cement can be written as:

$$P = 1 - \frac{(1 + 1.06 \cdot \alpha) \cdot \frac{1}{\rho_c} \cdot \rho_{fck}}{1 + x} \quad (2)$$

According to Halamickova (Halamickova, 1993):

$$P = 1 - \frac{1 + 1.31 \cdot \alpha}{1 + \rho_c \cdot x} \quad (3)$$

where:

α : degree of hydration,

1.31 volume of excess cement.

If shrinkage is not zero:

$$P = 1 - \frac{(1 + 1.06 \cdot \alpha) \cdot \frac{1}{\rho_c} \cdot \rho_{ck}}{1,36} \quad (4)$$

3. DEGREE OF POROSITY OF CONCRETE

The porosity of fresh concrete depends on the following factors:

- 1) saturation of concrete,
- 2) compression or the air content of the packed fresh concrete (air-bubbles),
- 3) quality of aggregate (porosity of aggregate, shape and surface roughness of aggregate),
- 4) air-pore content imported by aggregate artificially (air-pore generator).

The porosity of the hardened concrete depends in addition to the above listed factors on the following:

- 5) water/cement ratio (high water content),
- 6) degree of hydration (age of concrete),
- 7) shrinkage of concrete.

4. EXPERIMENTAL PROGRAMME

To study the porosity of concrete and its influence on durability and concrete strength, it was decided to consider many factors (water-cement ratio, degree of saturation in concrete, degree of hydration, type and content of cement, content of cement paste and initial porosity).

In this research we decided to prepare three series of 10 mixes using two different types of Portland cements (I. CEM I 32,5 SR, II. CEM I 42,5), three different types of superplasticiser (Melment L 10, Rheobuild 888, Glenium 51 self-compaction effect), different water-cement ratios and identical quantity of water.

4.1 Mix proportions

Mix proportions are summarised in *Table 1*. For all concrete mixes, the aggregates were weighed in room-dry conditions and the water contents were constant. For each mix the fol-

Mixture No.	w/c m%	sp/c m%	Quantities, kg/m ³			
			Cement	Water	Aggregate	Superplasticiser
SMII-1	0,4	1,7%	370	148	1925	6,3
SMII-2	0,42	1,0%	350	147	1952	3,5
SMI-3	0,50	1,2%	300	150	1947	3,6
SMI-4	0,58	0,6%	255	148	1983	1,5
SMI-5	0,577	0,6%	260	150	1981	1,56
SMI-6	0,639	0,8%	230	147	2015	1,84
SGI-7	0,46	0,6%	320	147	1981	1,9
SGI-8	0,4	0,6%	370	148	1936	2,2
SRI-9	0,46	1,0%	320	147	1981	3,2
SRI-10	0,4	1,0%	370	147	1936	3,7

w/c: water-cement ratio; sp/c: superplasticiser-cement ratio in mass %

Table 1 Proportions of concrete mixtures

Mixture No.	Consistence by flow test, mm	Unit mass, kg/m ³	Cement paste content, litre	Air-content %
SMII-1	400	2418,0	273	1,8
SMII-2	375	2368,7	263	2,7
SMI-3	395	2392,5	248	1,6
SMI-4	350	2362,5	232	3,1
SMI-5	365	2365,0	232	3,0
SMI-6	380	2360,0	222	3,0
SGI-7	390	2397,5	252	1,5
SGI-8	415	2410,0	270	1,0
SRI-9	380	2365,0	253	3,0
SRI-10	350	2323,0	270	4,4

Table 2 Properties of fresh concrete

lowing fresh concrete properties were measured: air-void, body density and consistence by flow test.

4.2 Properties of fresh concrete

The properties of the freshly mixed concrete (consistence by flow test, unit weight and air content by pressure method) are given in *Table 2*. In this table we show the effect of consistence on the air-void of fresh concrete.

5. RESULTS AND DISCUSSIONS

5.1 Properties of concrete (in 28 days)

The Properties of hard concrete at 28 days (unit mass, strength and porosity) are given in *Table 3* and *Table 4*.

The calculated values of porosity are shown in *Table 3* using the following formula (5):

$$P = 1 - \frac{y + (1 + 1.06 \cdot \alpha) \cdot \frac{1}{\rho_c} \cdot \rho_b}{1 + x + y} \quad (5)$$

where:

P : calculated porosity,

y : aggregate/cement ratio,

ρ_a : density of aggregate,

ρ_b : body density of concrete.

For the presented tests the calculated porosity of concrete by Eq. (5) was determined with $\alpha = 1$.

The measured value of porosity was determined by the following formula:

$$P_1 = 1 - \frac{\rho_b}{\rho} \quad (6)$$

where:

P_1 : porosity of concrete,

ρ_b : body density of concrete,

ρ : density of concrete.

In Eq. (6) we take into consideration the porosity of aggregate as well.

The apparent concrete porosity is calculated using the following formula:

$$P_L = n\% \times \frac{\rho_b}{\rho_w} \quad (7)$$

where:

P_L : apparent porosity of concrete,

$n\%$: humidity of concrete,

ρ_b : body density of concrete,

ρ_w : density of water.

Mixture No.	Wet mass, kg/m ³	Dry mass, kg/m ³	Strength, N/mm ²	Apparent porosity, %	Measured porosity %	Calculated porosity
SMII-1	2420	2396	58,9	2,4	5,30	4,60
SMII-2	2393	2303	45,9	9,0	10,76	8,90
SMI-3	2367	2270	39,6	9,7	11,9	11,1
SMI-4	2353	2249	30,5	10,4	14,16	13,50
SMI-5	2331	2220	29,7	11,1	14,43	14,18
SMI-6	2317	2172	21,4	14,5	17,12	16,80
SGL-7	2422	2391	55,2	3,1	5,49	6,20
SGL-8	2426	2391	52,8	3,5	6,60	4,90
SRI-9	2373	2311	46,4	6,2	10,08	9,40
SRI-10	2401	2345	48,5	5,6	9,46	6,70

Table 3 Properties of hard concrete at 28 days

Mixture No.	Watertight (2 bars), Mm	Decrease of compressive strength due to freeze-thaw 50 cycles, %
SMII-1	4,0	4,15
SMII-2	7,0	7,91
SMI-3	7,5	8,12
SMI-4	8,0	8,83
SMI-5	11,0	10,59
SMI-6	18,0	13,11
SGL-7	4,0	4,22
SGL-8	4,5	4,85
SRI-9	6,0	6,76
SRI-10	5,0	5,95

Table 4 Properties of hard concrete at 28 days

Fig. 2 indicates the decrease in strength and body density as a function of porosity. 1 V% increase in porosity led to 4% strength reduction if porosity is smaller than 12%; if porosity is greater than 12% this 1 V% increase led to 15% strength reduction.

Fig. 3 indicates the decrease in compressive strength due to freeze-thaw cycles and water penetration as a function of porosity. 1 V% increase in porosity led to 1% decrease of compressive strength if porosity is smaller than 6% and 1 mm greater water penetration. If porosity is greater than 6% decrease of compressive strength is 0,7 %.

Fig. 4 indicates the difference between porosity and calculated porosity caused by the degree of hydration. If concrete porosity is smaller than 11% the concrete strength is greater than 45 N/mm².

A decrease of porosity of between 11% and 6% caused an increase of strength from 45 to 52 N/mm². The reason is the movement of the limit from a saturated to an over saturated concrete condition, while the water content remained constant.

6. CONCLUSIONS

High performance concrete has a particularly dense structure of hydrated cement paste with a discontinuous capillary pore system. If porosity is smaller than 6% the concrete possesses a high resistance to external attacks.

A decrease of porosity of between 11% and 6% caused an increase of strength from 45 to 52 N/mm². The reason is the movement of the limit from a saturated to an over saturated concrete condition, while the water content remained constant.

Design considerations and recommendations to minimise

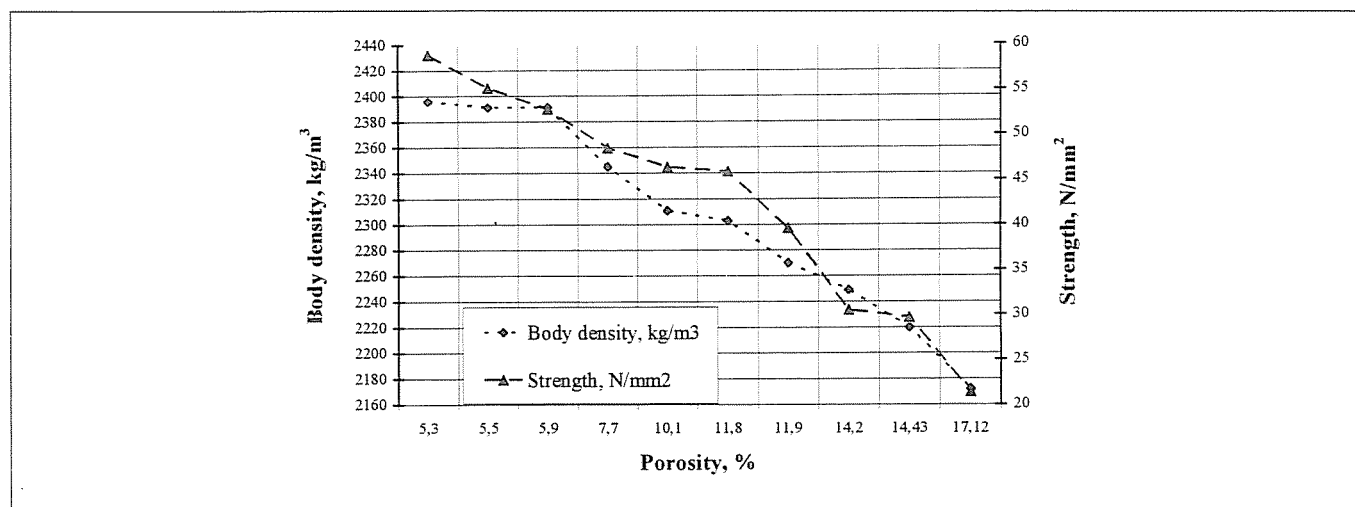


Fig. 2 Relationship between porosity, strength and body density

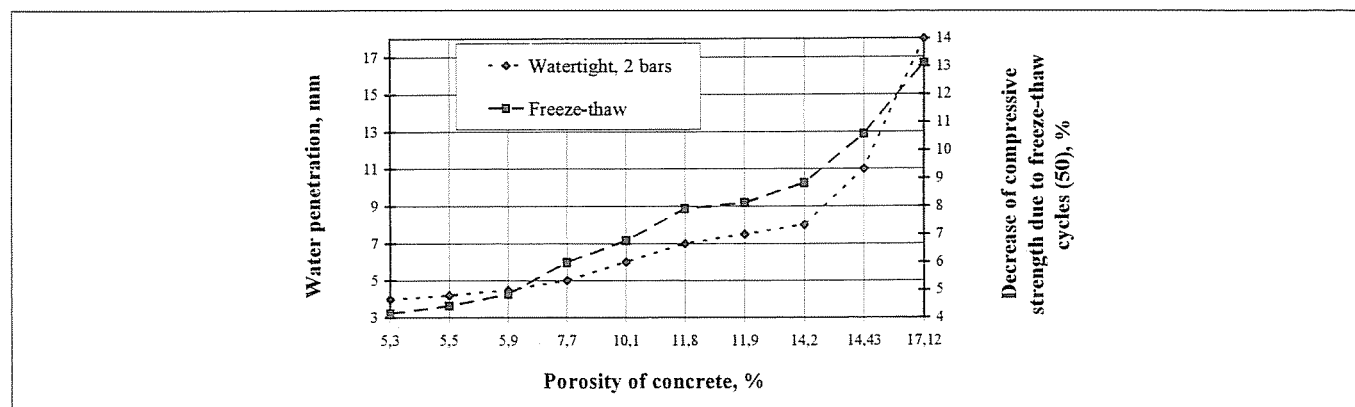


Fig. 3 Relationship between porosity, freeze-thaw and water-tightness

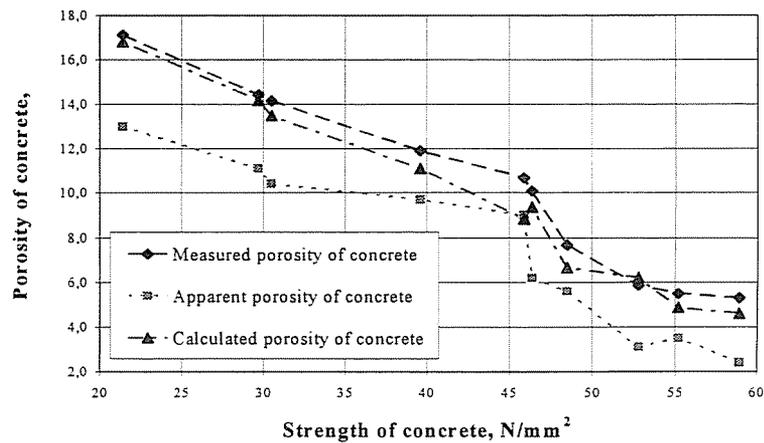


Fig. 4 Relationship between strength of concrete and different porosity

the pore content are the following: concrete should be saturated, water/cement ratio should be low as possible, and air-void content of fresh concrete should be low.

7. ACKNOWLEDGEMENTS

Author gratefully acknowledges the financial support of the Hungarian Research Found (OTKA Grant Nr. T032 525).

8. REFERENCES

Maso, J. C. (1980), "The bond between aggregates and hydrated cement paste," *Proceedings 7th International Congress on the Chemistry of Cement I*, VII-1/3 (Paris).

Woods, H. (1968), "Durability of Concrete Construction", *Amer. Conc. Inst. (ACI) Monograph No. 4.*, Detroit, USA

Neville, A.M., (1995), "Properties of Concrete", *Lomgman Ltd.* Fourth Edition, p. 31.

Balázs, Gy., Erdélyi, A., Kovács, K. (1990); Effect of freeze and deicing salts by durability of concrete. *Building Materials XLII.* volume Nr. 2 (in Hungarian)

Halamickova, P. (1993), "The Influence of Sand Content on the Microstructure Development and Transport Properties of Mortars", *MSc Thesis*, University of Toronto.

Salem G. Nehme (1963) MSc. civil engineer (1992); specialization on concrete structures (1996); research fellow at the Budapest University of Technology at the Department of Construction Materials and Engineering Geology. Main fields of interest are concrete technology, testing of materials, quality control of construction materials. Member of Hungarian Group of *fib*.

BOND OF NON-METALLIC (FRP) REINFORCEMENT IN CONCRETE



Dr. Adorján Borosnyói – Prof. György L. Balázs

Bond of embedded reinforcement is essential both for ultimate limit state (ULS) and serviceability limit state (SLS) of reinforced concrete structures. Corrosion of steel reinforcement induced the development of non-metallic reinforcement that are entirely resistant to electrolytic corrosion. Non-metallic reinforcement are made of Fibre Reinforced Polymers (FRP). Mechanical and bond properties of FRP reinforcement can be different from that of conventional steel reinforcement. Due to various constituent materials, manufacturing processes and surface treatments of non-metallic reinforcement, both bond performance and failure of bond can take place in different ways than in the case of conventional reinforcement. This paper provides a detailed survey of the bond characteristics of FRP reinforcement under static, long-term and cyclic loading as well as under elevated temperatures.

Keywords: Fibre Reinforced Polymer (FRP), carbon fibre, aramid fibre, glass fibre, resin matrix, sand coated surface, bond, durability

1. INTRODUCTION

In the last decades, deterioration of concrete structures due to corrosion of steel reinforcement indicated the importance of design durability for reinforced or prestressed concrete structures. For this purpose, there are several publications available dealing with causes and repair of corrosion of concrete structures (Balázs, Tóth, 1997; 1998; Balázs *et al.*, 1999; CEB, 1989). Four parameters are needed simultaneously for the corrosion of embedded steel: 1) a material to corrode (i.e. steel); 2) oxygen and 3) water (these two components can penetrate into the capillary pores of concrete); 4) alkalinity of concrete has to drop below pH 9 (Balázs, Tóth, 1997; 1998). Low alkalinity results in dissolution of the passive layer which disappears from the surface of the reinforcement.

Non-metallic (FRP) reinforcement provides a promising alternative to steel reinforcement which can avoid rebar corrosion in concrete structures because of the lack of ferrous material available to corrode in the reinforced concrete members.

Non-metallic (FRP) reinforcement, being made of Fibre Reinforced Polymers, have mechanical properties and surface characteristics which can be considerably different from that of the conventional steel reinforcement, leading to several open questions.

The tensile strength and Young's modulus of FRP reinforcement depends mainly on the type of fibres, the volumetric ratio of fibres (usually more than 60 percent), the angle between the fibres and the longitudinal axis of reinforcement, the shape of the cross section of the reinforcement and the type of the

resin matrix. Tensile properties of FRP reinforcing bars are in the range of 700 to 3500 N/mm² in terms of tensile strengths, 38000 to 300000 N/mm² in terms of Young's moduli and 0.8 to 4.0 % in terms of failure strains (Clarke, 1993; Rostásy, 1996; Balázs, Borosnyói, 2000a).

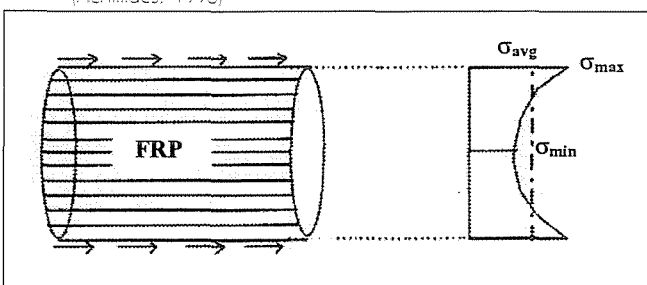
Tensile strength is also influenced by the diameter of the reinforcement (similar effects do not exist in the case of conventional steel reinforcement). Due to shear lag effect fibres located near the centre of the bar cross section are not subjected to as much stress as those fibres that are near the outer surface of the bar (Fig. 1, Achillides, 1998). This phenomenon results in reduced strength and reduced efficiency of larger diameter bars (Calado *et al.*, 1996).

The most important characteristic of non-metallic reinforcement is its linear elastic behaviour up to failure without any plasticity and considerable release of elastic energy. Fig. 2 indicates stress – strain responses of FRP reinforcement in comparison to a conventional steel prestressing tendon (Leadline® and Carbon-Stress® are CFRP bars, FiBRA® is AFRP bar and CBAR® is GFRP bar) (Balázs, Borosnyói, 2000b).

2. SIGNIFICANCE OF BOND IN CONCRETE

Bond between concrete and reinforcement has principal significance on structural behaviour of reinforced concrete which is independent of the type of the reinforcement or the application of prestressing (Balázs, 1991). Without the presence of bond (or a special anchoring device) the constituent elements of the composite material (i.e. concrete and reinforcement) would not be able to carry loads together. Bond performance has an effect on the flexural, shear and torsion load bearing capacity of reinforced concrete members and particularly on serviceability behaviour (Bartos, 1982; CEB, 1992; fib, 2000; Balázs *et al.*, 2002). Tension stiffening and crack widths can be evaluated directly from an analysis based on bond and force transfer. In addition, development lengths, splice lengths and transfer lengths of reinforcing and prestressing bars could not be determined without bond analysis (Balázs, 1993). Bond action can also influence the ductility of a structural member

Fig. 1 Distribution of the longitudinal stresses in a FRP member (Achillides, 1998)



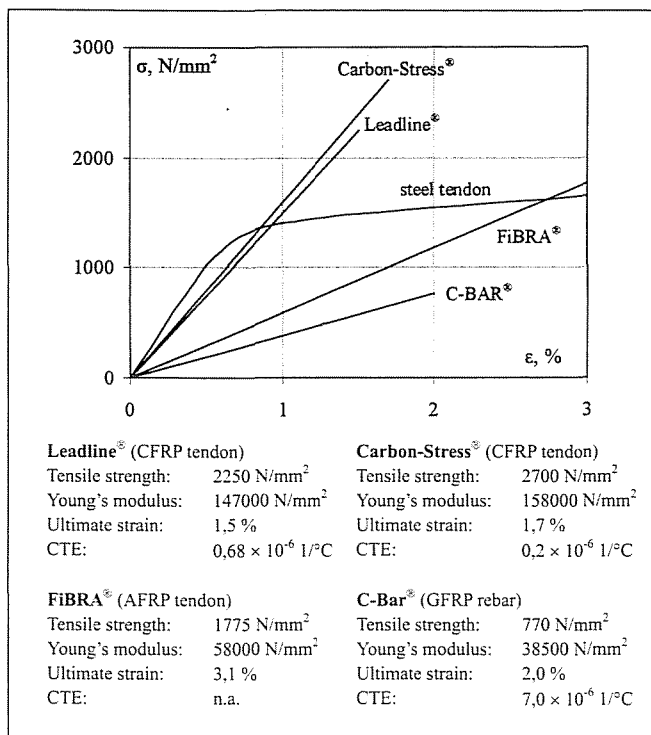


Fig. 2 Stress vs. strain relationships of FRP reinforcement in comparison to that of a steel tendon (Balázs, Borosnyói, 2000b)

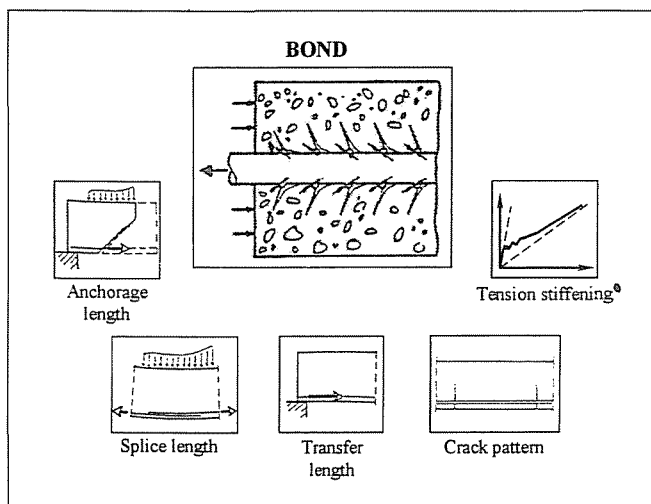


Fig. 3 Bond and structural behaviour (Balázs, 1991)

(Lees, Burgoyne, 1999). Fig. 3 summarises the most important phenomena that are attributed to bond action.

Elastic theory of reinforced concrete cross sections supposes that perfect bond takes place on the reinforcement to concrete interface, without any slippage (relative displacements) between the two constituents. In this way, the balance of inner forces can be calculated simply by the application of the elastic theory of composite cross sections. The assumption of perfect bond is a rather conservative simplification. In the reality, the bond behaviour on the reinforcement to concrete interface is a function of the accumulated slip between the two constituents.

3. BOND IN GENERAL

Bond stresses are the result of the change of forces between reinforcement and concrete. Slip is generated due to the different deformation capacities of the concrete and that of the reinforcement. By definition, slip is the absolute difference (in mm) between those concrete and reinforcement sections

that were in coincidence before loading. Slip is the integral of the difference between the accumulated strains of reinforcement and concrete over ℓ_b bond length.

$$s = u_s(x) - u_c(x) = \int_0^{\ell_b} \varepsilon_s(x) dx - \int_0^{\ell_b} \varepsilon_c(x) dx$$

Bond stress can be calculated as the change of the internal force of steel or concrete related to the interface surface:

$$\tau_b(s) = \frac{\Delta F(s)}{\varnothing \pi \ell_b}$$

The bond strength (τ_{bu}) is the maximum value of the bond stresses. Fig 4 gives a schematic representation of bond stress vs. slip (τ_b -s) responses of deformed and smooth steel reinforcing bars.

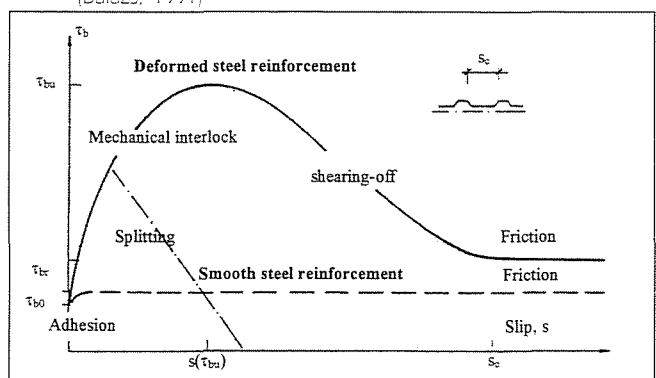
Under relatively small loads bond stresses are represented mainly by *adhesion* and slip is zero. Adhesion results from several actions: shrinkage of concrete during setting, chemical bond between concrete and reinforcement and Van der Waals type molecular forces are the most important reasons of adhesion. Adhesion represents less than 20 percent of bond stresses.

Slip starts to accumulate under loads higher than the adhesion resistance. Slip does not mean that the load bearing capacity of the system is reached. *Mechanical interlock* forces are formed around the reinforcement ribs due to the accumulated slips. Bond force is increased by the longitudinal component of the mechanical interlock forces. On the other hand, the perpendicular component of the mechanical interlock forces induces hoop tensile stresses around the reinforcing bar. Hoop tensile stresses induce micro-cracking in the surrounding concrete. The number of micro-cracks as well as their length and width increases with the increase of loads. Concrete is in a multi-axial stress state in the vicinity of a reinforcing bar according to the confining effect of concrete. Stresses in the concrete can reach much higher values than the uni-axial strength of the concrete. Deformed reinforcing bars can develop considerably higher bond stresses than smooth bars due to the mechanical interlock.

Further increase in the load results in shearing-off of the concrete lugs between reinforcement ribs. Bond force is provided by only *friction*. However, bond resistance is not equal to zero (residual bond strength), but the slips can be increased without limit. Bond action is represented in Fig. 4.

- concrete lugs failure in shear around the reinforcement (*pull-out failure*),
- the case of insufficient concrete cover wherein the micro-cracks can spread to the concrete surface resulting in complete disintegration of the structure (*splitting failure*).

Fig. 4 Typical bond stress vs. slip (τ_b -s) responses of steel reinforcing bars (Balázs, 1991)



It can be concluded that in case of steel reinforced concrete the failure of bond is attributed to the failure of *concrete* locally.

Bond strength of smooth reinforcing bars can be already reached at 0.01 mm slip. In case of deformed reinforcing bars the bond strength is generally reached at more than 1.0 mm slip (Balázs, 1991).

The most important influencing parameter of bond behaviour is the *surface configuration* of the reinforcement (deformation). Rehm (1961) defined a suitable parameter for the measurement of the surface deformation of deformed reinforcing bars, called relative rib area (α_{sb}):

$$\alpha_{sb} = \frac{A_{rb}}{\varnothing \pi s_b}$$

where: A_{rb} area of the front surfaces of ribs of reinforcement
 s_b spacing between ribs of reinforcement
 \varnothing nominal diameter of reinforcement.

The higher the relative rib area, the higher the bond strength is. However, the risk of splitting is also higher. Favourable values of the relative rib area are: $0.05 < \alpha_{sb} < 0.08$.

4. SURFACE CONFIGURATION OF NON-METALLIC (FRP) REINFORCEMENT

Pultrusion is the usual manufacturing process for non-metallic reinforcement. The steps involved in manufacturing with the pultrusion process are the followings: (1) development of parallel orientation of the fibres supplied in rolls, (2) resin bath, (3) hardening of resin in autoclave under specified pressure and temperature, (4) surface treatments, (5) cutting.

Surface treatment of the raw product is essential for adequate bond to concrete. The easiest way to increase bond is to apply a sand coating on the surface of the bar. Sand coating can contain fine sand or aluminium-oxide particles in high strength resin. According to experiments, best result can be achieved by the use of para-polyphenylene-sulphide (PPS) resin (Tepfers, 1998). Another possibility to increase bond capacity can be the application of ribs on the surface. These can be spiral windings of fibre bundles fixed by resin under pressure or special ceramic ribs of a shape similar to that of conventional reinforcement. Ribs and indentations can improve mechanical interlocking between the reinforcement and the concrete, increasing bond strength. Adequate bond between post-

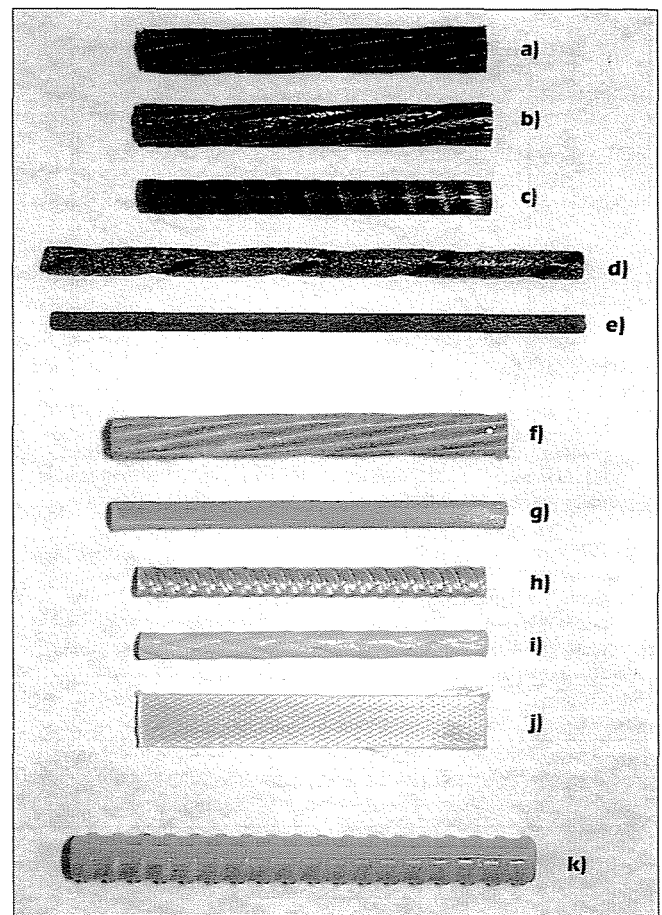


Fig. 5 Surface configuration of FRP reinforcing bars (Balázs, Borosnyői, 2000a)

- a) 7-wire CFRP strand (CFCC®)
- b) 7-wire CFRP strand (NACC®)
- c) indented CFRP tendon (Leadline®)
- d) sand coated, spirally wound CFRP tendon (Carbopree®)
- e) sand coated CFRP tendon (Carbon-Stress®)
- f) 7-wire AFRP strand (Arapree®)
- g) sand coated AFRP tendon (Arapree®)
- h) deformed AFRP tendon (Technora®)
- i) braided AFRP tendon (FIBRA®)
- j) rectangular cross section AFRP tendon (Arapree®)
- k) deformed GFRP bar (C-Bar®)

installed surface treatment and inner layers of FRP rods has significant importance. Failure due to pull-off or shear-off of outer layers has to be avoided. Application of surface deformations on FRP reinforcement can be combined with sand coating as well. A further possibility for prestressing tendons can be the shape of multi-wire strands similar to conventional steel prestressing strands or braided tendons not used for conventional steel tendons. Surface configurations of steel and non-metallic reinforcement are given in Table 1 and Fig. 5.

Table 1 Surface configuration of steel and FRP reinforcement

steel reinforcement	non-metallic reinforcement
<i>non-prestressed</i> - smooth - deformed <i>mesh</i> <i>prestressed</i> - smooth wire - indented wire - strand - deformed rod - threaded bar	<i>prestressed and non-prestressed</i> (with or without sand coating) - smooth - deformed - indented - with periodic ribs - spiral-patterned (with fibre yarn winding) - with concavo-convex resin surface - strand - braided tendon <i>mesh</i> (2D or 3D) <i>rope without resin matrix</i> <i>textile type reinforcement</i>

5. BOND OF NON-METALLIC (FRP) REINFORCEMENT

Bond action of non-metallic (FRP) reinforcement can be different from that of conventional steel reinforcement. Material characteristics, manufacturing processes and surface treatments can influence both bond action and bond failure.

The most important difference can be considered with respect to bond failure. In case of steel reinforced concrete the failure of bond is always attributed to the local failure of *concrete*. In case of FRP reinforced concrete the failure of bond can be influenced by the reinforcement itself; failure can take place in the post-installed surface treatment layers (ribs, sand coating, etc.).

Due to the special surface treatments, the adhesion bond action of FRP reinforcement is usually higher than that of the conventional steel reinforcement. Bond strength of FRP reinforcement is usually more than 80 percent of the bond strength of conventional steel reinforcement. Bond behaviour is physically the same both for FRP and steel reinforced concrete (adhesion, mechanical interlock, friction).

5.1 Bond of smooth FRP reinforcement

Smooth FRP rebars do not have any considerable surface deformations, only a resin, powder or sand coating. Bond action is attributed to only two components: the *adhesion* at zero slip and the *friction* as slip is developed. Mechanical interlock is negligible.

According to Cosenza, Manfredi and Realfonzo (1996), the *bond strength* of smooth FRP rebars is not dependent on the strength of concrete. Bond strength of these rebars is influenced only by the resin of the FRP material (surface roughness, transverse elastic- and shear moduli and Poisson's ratio).

Bond action of smooth rebars without any sand coating is provided mainly by friction. Adhesion results only by weak physical-chemical bond on the surface. Friction resistance is influenced by the mechanical properties of the FRP bar in the transverse direction. Laboratory tests indicated that (due to the limited bond strength) bond action is not able to cause micro-cracks in the surrounding concrete as bond stresses are limited ($\sim 0.2 \text{ N/mm}^2$). Failure of the resin rich outer layers of the FRP bars occurs before any occurrence of micro-cracks in the concrete. This importance of the surface layer was also demonstrated by tests on specially treated FRP bars whenever the resin rich outer layers were removed. Bond strength was found to increase, demonstrating good bond properties of the fibres themselves. However, the fibres still need mechanical protection. As the bond strength of smooth rebars without any sand coating is limited ($\tau_{bu} = 1.19 \text{ N/mm}^2$, Cosenza, Manfredi, Realfonzo, 1996), the application of such reinforcement without anchoring devices is not recommended.

The simplest way to increase the bond strength of smooth FRP rebars is to apply sand coating to the surface. Adhesion bond action is increased considerably and bond strength can be as high as that of the conventional deformed steel reinforcement ($\tau_{bu} = 12.05 \text{ N/mm}^2$, Cosenza, Manfredi, Realfonzo, 1996). On the other hand, bond failure is found to be more brittle with the sudden bond failure of sand coating.

Fig. 6 Bond stress vs. slip (τ_b -s) responses of smooth FRP reinforcement (Cosenza, Manfredi, Realfonzo, 1996)

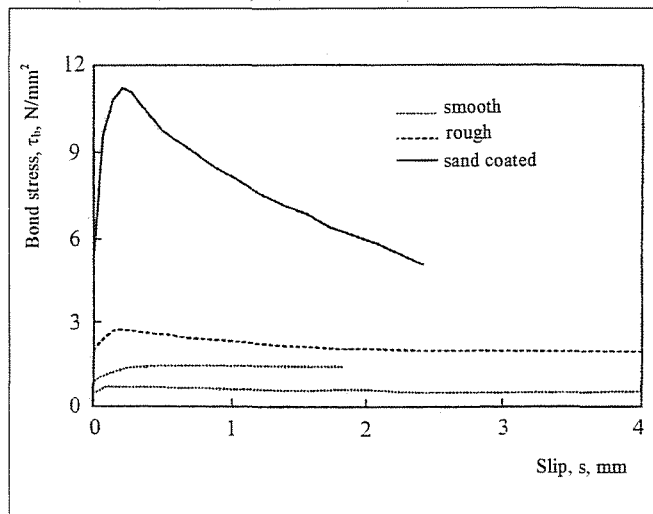


Fig. 6 indicates typical bond stress vs. strain (τ_b -s) responses of smooth FRP reinforcing bars (Cosenza, Manfredi, Realfonzo, 1996).

5.2 Bond of deformed FRP reinforcement

Experimental studies demonstrated that bond action of deformed FRP (ribbed, spirally wounded, indented, etc.) reinforcement resulted mainly from mechanical interlock (similarly to the conventional deformed steel reinforcement). Influence of adhesion and friction has less significance. *Bond strength* of deformed FRP reinforcement is usually similar or higher than that of the conventional deformed steel reinforcement. Bond strength of deformed FRP reinforcement is usually reached at *higher slip* values due to higher deformation capacity of the surface layers. Micro-cracks are formed in the surrounding concrete in pull-out, similarly to the bond behaviour of conventional deformed steel reinforcement. However, in case of favourable deformation capacity of the ribs of the reinforcement (e.g. C-Bar®) less micro-cracks can be witnessed in the concrete (Tepfers, Karlsson, 1997).

Bond failure of deformed FRP reinforcement is influenced by both the concrete strength and the properties of the reinforcement. In pull-out failure, the surface layers can be peeled off, ribs of the reinforcement can fail in shear or ribs can be torn off. Scanning electron microscope (SEM) studies demonstrated that any failure in the surface layers of deformed FRP reinforcement occurs only if the compressive strength of the concrete is higher than 20 to 30 N/mm^2 . At lower concrete compressive strengths ($\approx 15 \text{ N/mm}^2$), shear failure of concrete lugs can be observed with much less bond strength. (Achillides *et al.*, 1997). The residual friction resistance of deformed FRP rebars is much higher than that of the smooth FRP rebars, as the ribs usually do not disintegrate completely from the bar and their failure takes place at different load levels (Cosenza, Manfredi, Realfonzo, 1996).

Some deformed FRP reinforcement is available which can provide even higher bond stresses than conventional steel reinforcement. This behaviour can increase the risk of splitting at prestressed beam ends whenever the concrete cover is inadequate. Experimental studies demonstrated that deformed FRP reinforcement (having the same relative rib area as conventional deformed steel reinforcement) can provide bond stresses as high as that which can be experienced with deformed steel (Tepfers, 1998).

It was also experimentally demonstrated (Al-Zahrani *et al.*, 1996), that the type of bond failure can be changed by a change in rib geometry. Change in rib height and spacing can change the failure mode from rib failure to concrete lugs failure. In this way the optimal rib geometry can be found for a given concrete strength (rib failure and concrete failure at the same time).

When the gluing efficiency of a spiral-patterned (with fibre yarn winding) surface treatment is inadequate, the bond strength of the rebar is found to be small (around $\tau_{bu} = 4.5 \text{ N/mm}^2$), and the peeling behaviour is similar to that of the smooth rebars (adhesion and friction, but no mechanical interlock). Bond strength of spiral-patterned FRP reinforcement with adequate gluing can be as high as $\tau_{bu} = 11.61 \text{ N/mm}^2$ (Cosenza, Manfredi, Realfonzo, 1996). Bond strength of an indented FRP reinforcement can be as high as $\tau_{bu} = 10.2 \text{ N/mm}^2$ (Cosenza, Manfredi, Realfonzo, 1996). Bond strength of deformed and sand coated

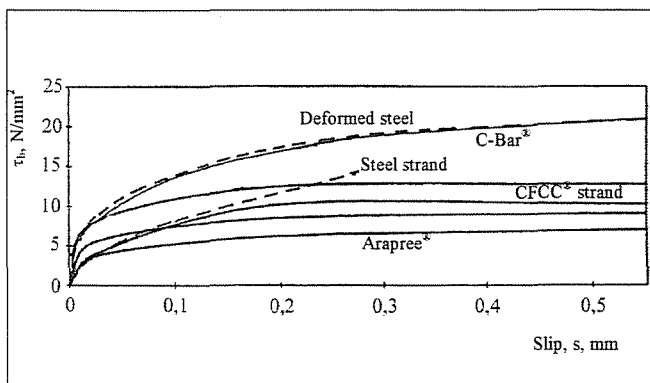


Fig. 7 Bond stress vs. slip (τ_b -s) responses of deformed FRP reinforcement (Tepfers, Karlsson, 1997)

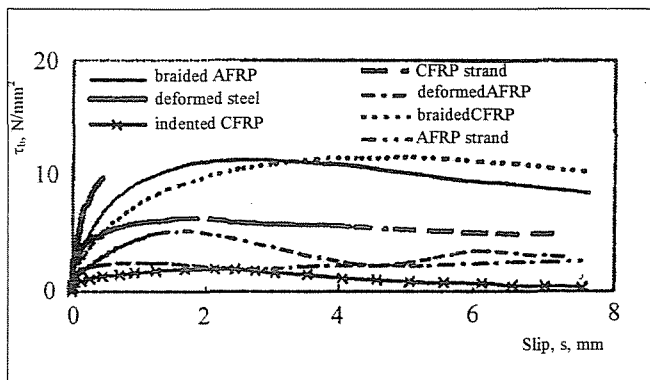


Fig. 8 Bond stress vs. slip (τ_b -s) responses of deformed FRP reinforcement (Wang, Goto, Joh, 1997)

FRP reinforcement can reach $\tau_{bu} = 17.78 \text{ N/mm}^2$ (Cosenza, Manfredi, Realfonzo, 1996).

Another group of the deformed FRP reinforcement covers the braided or stranded prestressing tendons. Their application possibilities are the same as for conventional steel prestressing tendons. Surface configuration can be similar to (FRP strand made of 7 FRP wires), or different from (braided rope-like FRP tendons) the conventional steel prestressing tendons. Their bond strengths were found to be in the range of $\tau_{bu} = 1.6$ to 7.3 N/mm^2 , resulting mainly from friction. In pull-out failure, limited concrete failure is observed with considerable surface abrasion of the FRP tendons (Cosenza, Manfredi, Realfonzo, 1996). Japanese experiments demonstrated a power function between the bond strength of 7-wire CFRP strands and the concrete strength, with an exponent of 0.5 to 0.67 (similar to that of conventional steel strands) (Tepfers, 1998).

It was found experimentally that (keeping the surface configuration unchanged) the higher is the Young's modulus of the applied fibre, the higher the bond strength. The reason for this could be the higher rigidity of the ribs due to the higher Young's modulus, resulting in a less pronounced decrease in mechanical interlock under higher load levels (Wang, Goto, Joh, 1997).

C-Bar[®] is a special GFRP reinforcement for non-prestressed applications developed by Marshall Industries Composites, Inc. The resin matrix is an alkaline resistant vinyl-ester (modified by urethane). Surface configuration is provided by ceramic ribs glued with PPS to the exterior. Bond strength is $\tau_{bu} = 17 \text{ N/mm}^2$ (for 12 mm diameter) and $\tau_{bu} = 18 \text{ N/mm}^2$ (for 15 mm diameter). Residual bond strength is found to be around 55 percent of the bond strength (Tepfers, 1998). According to Swedish experiments, the bond stress vs. slip (τ_b -s) responses of C-Bar[®] GFRP reinforcing bars were found to be similar to the bond stress vs. slip (τ_b -s) responses of conventional deformed steel bars (Fig. 7). Rib failure can be observed on the surface

of the reinforcement if the compressive strength of the concrete is higher than 30 N/mm^2 .

Further bond stress vs. slip (τ_b -s) responses of FRP reinforcing bars can be studied in comparison to steel rebars in Fig. 8 (Wang, Goto, Joh, 1997).

6. SPECIAL FIELDS

6.1 Bond behaviour under long-term and cyclic loads

The influence of long-term and cyclic loads on steel reinforced concrete can be observed twofold:

- bond stiffness (initial tangent of the bond stress vs. slip (τ_b -s) response) is decreased (e.g. CEB-FIP Model Code 1990, Clause 3.1.2., Fig. 3.1.3., p. 86.),
- slip is increased (e.g. Rehm, Eligehausen, 1979).

Fatigue of bond process under cyclic loads can be divided into three phases (Balázs, 1991). In the first phase slip increases with a decreasing rate. In the second phase slip increases with a constant rate, up to the slip value reached at bond strength in a monotonic pull-out test (see $s(\tau_{bu})$ at Fig. 4). In the third phase slip increases with an increasing rate, up to pull-out failure.

The following general statements can be summarised based on the experimental results of bond of FRP reinforcement under long-term loads (Hattori *et al*, 1995; 1997; Tepfers, 1998; Wang, Joh, Goto, 1999):

- Creep of bond (slip increase under long-term loads) is considerably influenced by the surface configuration of the FRP reinforcement (similar to the slip under monotonic loading). The influence of the Young's modulus of the FRP reinforcement was found to be insignificant.
- Creep of bond increases if the load is increased: slip increase is found to double by doubling the pulling force. Slip increase tendency is not influenced.
- Similarly to conventional steel reinforcement the creep of bond is considerable under even low load levels (e.g. 50 percent of the bond strength achieved by monotonic loading).
- Slip increase of AFRP reinforcement in the bond creep process is attributed mainly to the creep of the aramid fibres themselves. Creep of glass and carbon fibres is negligible.
- Slip increase due to bond creep in time: more than 50 percent of the increase can be observed in the first 24 hours of loading and 65 to 85 percent of the increase in the first 100 hours of loading.
- Monotonic testing up to failure after long-term loading indicates no change in the bond strength in case of GFRP and CFRP reinforcement. In case of AFRP reinforcement a decrease of 10 to 15 percent can be observed.

Fig. 9 indicates the increasing tendencies of slip under long-term loading of FRP reinforcing bars.

Slip is increased by cyclic loading as well. However, available information is limited on the bond fatigue of FRP reinforcement under cyclic loads. The field needs concentrated research in the future because slip increase can result in increasing surface damage to the FRP reinforcement under cyclic loads. In this way the damage accumulation can be considerably different than that of the conventional steel reinforcement with no surface damage.

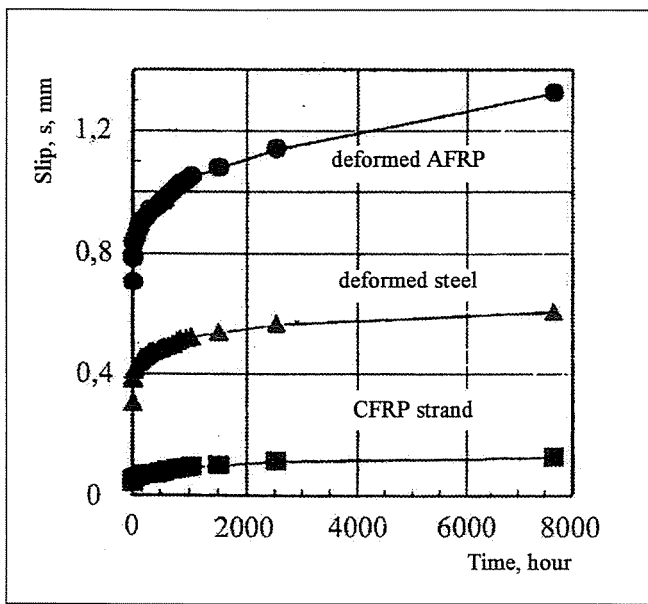


Fig. 9 Slip increase due to long-term loading (Hatton et al., 1995)

6.2 Influence of alkaline environment and elevated temperatures on the bond of FRP reinforcement

Development of non-metallic (FRP) reinforcement followed the identification of risks appertaining to electrolytic corrosion of conventional steel reinforcement. FRP reinforcement is completely able to avoid corrosion problems. On the other hand, particular environmental conditions can have an influence on the durability of bond of FRP reinforcement (Balázs-Borosnyói, 2001; Sumida et al., 2001; Uomoto, 2001).

Resin matrices of FRPs are able to adsorb water and solutions. In aramid fibres water adsorption has an influence on the hydrogen bond in the molecules, resulting a reversible 10 percent loss of the strength. After drying the strength loss is recovered. A similar phenomenon can be found in cases of polymer chains of resins. Polyester and epoxy resin is resistant to water adsorption (Palotás, Balázs, 1980). Glass- and carbon fibres are not able to adsorb water. In the pore water of concrete, several soluble aggressive ions (e.g. chloride) can reach the FRP reinforcement. Strength, bond capacity or durability can be influenced if any physical or chemical reaction takes place at the interface.

Glass fibres were usually made of E-glass, which is not alkaline resistant. E-glass is not able to resist the high alkalinity of concrete (pH 12 to 13.5) without any surface protection. In a high alkalinity environment the damage of Alkaline Resistant (AR) glass fibres can be also observed (Tannous, Saadatmanesh, 1999).

Strong acids and alkalis can be harmful to the secondary molecular bonds of the aramid polymer chain. Degradation (decrease in the degree of polymerisation) and strength loss can be observed. AFRP reinforcing bars can be considered alkaline resistant for the service life of concrete structures.

Carbon fibres are found to be entirely resistant to any acidic or alkaline environment (Sumida et al, 2001; Tokyo Rope, 1993; Uomoto, 2001).

Fig. 10 indicates bond stress vs. slip (τ_b -s) response of a GFRP bar after a several hours of contact with a saturated $\text{Ca}(\text{OH})_2$ solution of 60°C (pH 12.3) (Al-Dulaijan, 1996). Loss in bond stiffness and bond strength can be clearly observed.

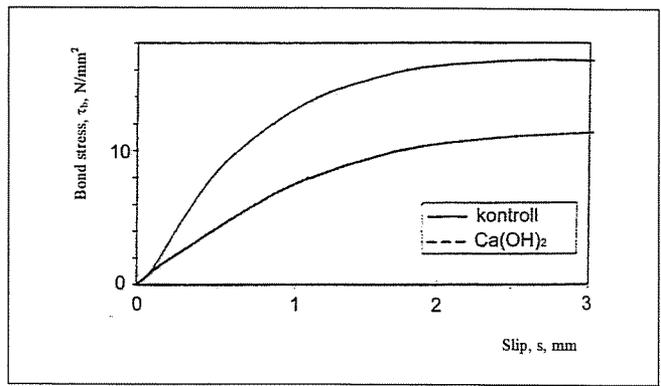


Fig. 10 Influence of alkaline environment on the bond strength of a GFRP bar (Al-Dulaijan, 1996)

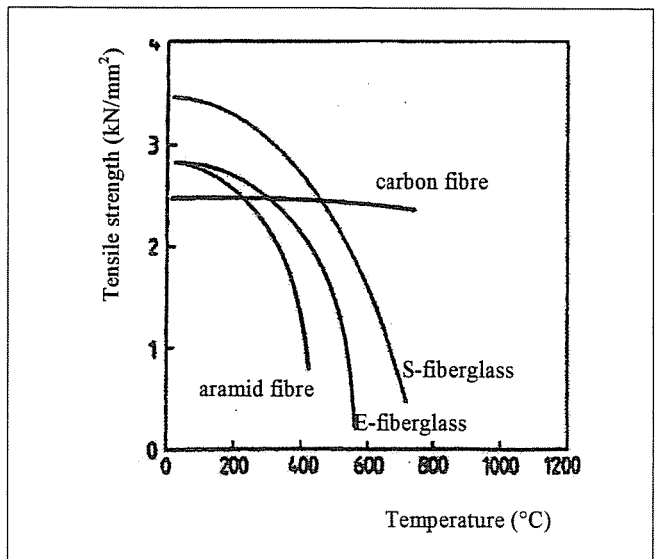


Fig. 11 Heat resistance of fibres (Rostásy, 1996)

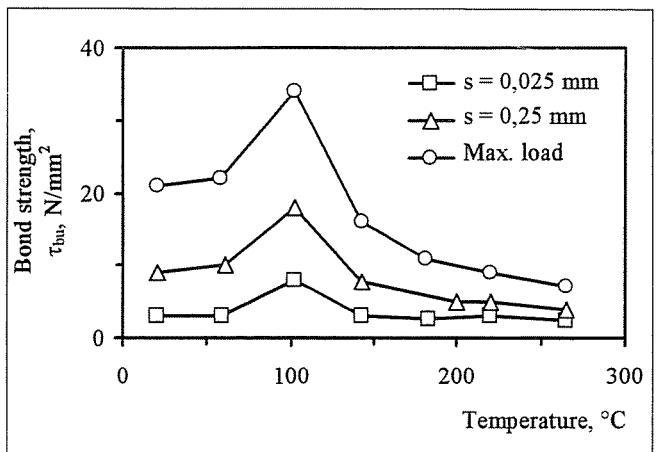


Fig. 12 Influence of elevated temperature on the bond strength of a CFRP bar (after Sumida et al, 2001)

Resistance of FRP reinforcement against elevated temperatures is also a significant issue. Resin matrices usually deteriorate at 150 to 200°C. The heat resistance of FRPs is primarily dependent on the heat resistance of the resin (Sumida et al, 2001). Heat resistance of fibres is usually more favourable than that of the resins. Aramid and glass fibres suffer severe deterioration under 200 to 500°C. Carbon fibres show no deterioration up to 1000°C (Fig. 11, Rostásy, 1996). Surface configuration also has a significant influence on the heat resistance of FRP reinforcement. According to experimental results, the resin matrix of strands, braided tendons or spirally wound reinforcement can deteriorate more easily than that of simple round rebars (Tanao et al, 1997). Decrease in the bond strength of FRP reinforce-

ment can be observed even under 100°C, as the material degradation begins when the glass transition temperature ($T_g = 65$ to 130°C) of the resin is reached. Fire protection of FRP reinforcement can be achieved by higher concrete cover.

Fig. 12 indicates bond strength of a CFRP bar in the function of increasing temperature (Sumida *et al*, 2001). Due to increased temperature the bond strength seems to slightly increase in the beginning and decrease considerably after reaching a peak value. The reasons for this are the following: due to the different coefficients of thermal expansion (CTE) of FRP and that of concrete (Balázs, Borosnyói, 2001), radial compressive stresses are induced in the surrounding concrete under temperature increase. The effect of radial compressive stresses is similar to the confining effect of concrete. The bond strength is increasing. Radial compressive stresses induce hoop tensile stresses at the same time, resulting in the risk of splitting in case of insufficient concrete cover (Lublóy *et al*, 2001). Deterioration of the resin matrix starts when the glass transition temperature (T_g) is reached. As the deterioration starts at the surface, the bond strength is very sensitive to it. Further temperature increase results in a further drop in the bond strength due to further deterioration of the resin matrix. Above 200°C (whenever the resin matrix is completely deteriorated) the bond strength is almost zero (Fig. 12).

7. CONCLUSIONS

The use of non-metallic (FRP) reinforcement provides a promising alternative which avoids corrosion in reinforced concrete. By applying non-metallic (FRP) reinforcement there is no ferrous material to corrode in reinforced concrete.

Non-metallic (FRP) reinforcement is made of Fibre Reinforced Polymers. Their mechanical properties and surface characteristics can be considerably different from those of the conventional steel reinforcement which leads to several open questions. Bond action of non-metallic (FRP) reinforcement can be different from that of conventional steel reinforcement. Material characteristics, manufacturing processes and surface treatments can influence both bond action and bond failure.

Bond action of smooth FRP rebars is attributed to only two components: the adhesion at zero slip and the friction as slip is developed. Mechanical interlock is negligible. The simplest way to increase the bond strength of smooth FRP rebars is to apply sand coating to the surface. Adhesion bond action is increased considerably and bond strength can be as high as that of the conventional deformed steel reinforcement. Bond strength of deformed FRP reinforcement is usually similar to or higher than that of the conventional deformed steel reinforcement. Bond strength of deformed FRP reinforcement is usually reached at higher slips due to higher deformation capacity of the surface layers. Bond failure of deformed FRP reinforcement is influenced by both the concrete strength and the properties of the reinforcement. In pull-out failure, the surface layers can be peeled off, ribs of the reinforcement can fail in shear or ribs can be torn off.

Slip increase due to long-term or cyclic loads can result in considerable surface damage to the FRP reinforcement under cyclic loads. In this way the damage accumulation can be different to that of the conventional steel reinforcement with no surface damage.

Further research is needed on the bond behaviour of non-metallic (FRP) reinforcement under harsh environmental conditions (presence of aggressive ions, wet-dry cycles, freeze-thaw cycles, thermal cycles, elevated temperature, etc.).

8. ACKNOWLEDGEMENTS

Authors gratefully acknowledge the financial support of the Hungarian Research Fund (OTKA Grant Nr. T032 525).

9. REFERENCES

- Achillides, Z. *et al* (1997) "Bond behaviour of FRP bars to concrete", *Proceedings of the Third International Symposium (FRPRCS-3)*, Vol. 2., Sapporo 1997., Japan Concrete Institute. pp. 341-348.
- Achillides, Z. (1998) "Bond behaviour of FRP bars in concrete", *PhD Thesis*, Centre for Cement and Concrete, Univ. of Sheffield, 1998 – *fib* (2000) "Bond of Reinforcement in Concrete", *State-of-Art Report* prepared by Task *fib* Group Bond Models, August 2000
- Al-Dulajjan, S. U. *et al* (1996) "Bond evaluation of environmentally conditioned GFRP/concrete systems", *Proceedings of the 2nd Int. Conference on Advanced Composite Materials in Bridges and Structures (ACMBS-II)*, 1996, pp. 845-852.
- Al-Zahrani, M. M. *et al* (1996) "Bond of FRP to Concrete in Reinforcement Rods with Axisymmetric Deformations" *Proceedings of the 2nd Int. Conference on Advanced Composite Materials in Bridges and Structures (ACMBS-II)*, 1996, pp. 853-860.
- Balázs, G. L. (1991) "Force transfer in concrete", *PhD Thesis* (in Hungarian)
- Balázs, G. L. (1993) "Cracking Analysis Based on Slip and Bond Stresses", *ACI Materials Journal*, July-August 1993, pp. 340-348.
- Balázs, G. L. – Bartos, P. J. M. – Cairns, J. – Borosnyói, A. (Eds.) (2002) "Bond in Concrete – from research to standards", *Proceedings of the 3rd International Symposium*, University Press, BUTE, Budapest, 2002.
- Balázs, G. L. – Borosnyói, A. (2000a) "Non-metallic (FRP) reinforcements in bridge engineering", *Vasbetonépítés*, 2000/1, pp. 45-52. (in Hungarian)
- Balázs, G. L. – Borosnyói A. (2000b) "Corrosion resistant reinforcements for concrete structures", TARTÓK 2000 – VI. Magyar Tartószerkezeti Konferencia, *Proceedings*, Budapest, 2000, May 25-26., pp. 321-333. (in Hungarian)
- Balázs, G. L. – Borosnyói, A. (2001) "Long term behavior of FRP", *Proceedings of the International Workshop Composites in Construction: A Reality*, Capri, Italy, ASCE – CI, pp. 84-91.
- Balázs, G. – Tóth, E. (1997) (1998) "Diagnostics of concrete structures I – II.", *University Press, BUTE* (in Hungarian)
- Balázs, G. – Balázs, G. L. – Farkas G. – Kovács K. (1999) "Protection, rehabilitation and strengthening of concrete structures", *Műegyetemi Kiadó* (in Hungarian)
- Bartos, P. J. M. (Ed.) (1982) "Bond in Concrete", *Proceedings*, International Symposium, Applied Science Publishers Ltd., London, 1982.
- Calado, L. - Castiglioni, C.A.- Agatino, M.R. (1996) "Experimental and Numerical Evaluation of Bond Stress of Concrete Beams Reinforced by GFRP Bars", *Research report*.
- CEB (1989) "Durable Concrete Structures", *CEB Design Guide*, Second edition, 1989
- CEB (1992) "Bond in Concrete – from research to practice", *Proceedings*, International Symposium, Riga, Latvia, 1992.
- CEB-FIP (1993) "CEB-FIP Model Code 1990 – Design Code", Comité Euro-International du Béton, Thomas Telford, London, 1993 (CEB Bulletin d'Information No. 213/214.)
- Clarke, J. L. (1993) "Alternative Materials for the Reinforcement and Prestressing of Concrete", Chapman & Hall, London, 1993
- Cosenza, E. - Manfredi, G. - Realfonzo, R. (1996) "Bond of FRP Rebars to Concrete: Experimental Behaviour and Analytical Models", *Studi e Ricerche*, Vol.17, 1996, pp. 253-282.
- fib* (2000) "Bond of Reinforcement in Concrete", *State-of-Art Report* prepared by *fib* Task Group Bond Models, August 2000.
- Hattori, A. *et al* (1995) "A study on bond creep behaviour of FRP rebars embedded in concrete", *Proceedings of the Second International RILEM Symposium (FRPRCS-2)*, Ghent 1995., L. Taerwe, Editor, E & FN Spon, London, pp. 172-179.
- Hattori, a. – Kawasaki, K. – Miyagawa, T. – Fujii, M. (1997) "Bond behaviours of carbon fiber strand and aramid fiber deformed bar", *Proceedings of the Third International Symposium (FRPRCS-3)*, Vol. 2., Sapporo 1997., Japan Concrete Institute. pp. 349-356.
- Lees, J.M. - Burgoyne, C.J. (1999) "Experimental Study of Influence of Bond on Flexural Behaviour of Concrete Beams Pretensioned with Aramid Fiber Reinforced Plastics", *ACI Structural Journal*, V. 96, No. 3, May-June 1999, pp. 377-385.
- Lublóy, É. – Borosnyói, A. – Bánki, T. – Balázs, G. L. (2002) "Bond of CFRP Reinforcing Bars Under Elevated Temperature", *3rd International Symposium on Bond in Concrete – From Research to Standards*, 20-22 November 2002, Budapest, pp. 684-691.
- Palotás, L.- Balázs, G. (1980) "Engineering materials 3. Concrete-mortar-ceramics-polymers", *Akadémiai Kiadó*. (in Hungarian)

- Rehm, G. (1961) "Über die Grundlagen des Verbundes zwischen Stahl und Beton", *Deutscher Ausschuss für Stahlbeton*, H. 138, 1961
- Rehm, G. – Eligehausen, R. (1979) "Bond of Ribbed Bars Under High-Cycle Repeated Loads", *ACI Journal*, 1979, pp. 297-309.
- Rostásy, F. (1996) "State-of-the-Art Report on FRP Materials", *FIP Report*, Draft, 1996. Unpublished.
- Sumida, A. – Fujisaki, T. – Watanabe, K. – Kato, T. (2001) "Heat resistance of continuous fiber reinforced plastic rods", *Proceedings of the Fifth International Symposium (FRPRCS-5)*, Thomas Telford, London, 2001, pp. 557-565.
- Tanao, H. – Masuda, Y. – Sakashita, M. – Oono, Y. – Nonomura, K. – Satake, K. (1997) "Tensile Properties at High Temperatures of Continuous Fiber Bars and Deflections of Continuous Fiber Reinforced Concrete Beams Under High-Temperature Loading", *Proceedings 3rd Int. Symp. FRPRCS-3*, JCI, 1997, Vol. 2., pp. 43-50.
- Tannous, F. E. – Saadatmanesh, H. (1999), "Durability of AR Glass Fiber Reinforced Plastic Bars", *ASCE Journal of Composites for Construction*, Vol. 3, No. 1, February 1999, pp. 12-19.
- Tepfers, R. (1998) (Ed.) "Bond Models". *State-of-the-Art-Report*. Draft. Chapter 8. Bond of non-metallic reinforcement. Version 6, June 23, 1998. CEB, TG 2/5
- Tepfers, R. - Karlsson, M. (1997) "Pull-out and tensile reinforcement splice tests using FRP C-bars™", *Proceedings of the Third International Symposium (FRPRCS-3)*, Vol. 2., Sapporo 1997., Japan Concrete Institute. pp. 357-364.
- Tokyo Rope Mfg. Co., Ltd. (1993) "Technical Data on CFCC™", Tokyo, October 1993.
- Uomoto, T. (2001) "Durability considerations for FRP reinforcements", *Proceedings of the Fifth International Symposium (FRPRCS-5)*, Thomas Telford, London, 2001, pp. 17-32.
- Wang, Z. – Goto, Y. – Joh, O. (1997) "Bond Characteristics of FRP Rods and effect on Long Term Deflection of Concrete Beams", *Proceedings of the Third International Symposium (FRPRCS-3)*, Vol. 2., Sapporo 1997., Japan Concrete Institute. pp. 389-396.
- Wang, Z. – Joh, O. – Goto, Y. (1999) "Bond creep behaviour of FRP rods and their bond strength after sustained loading", *Transactions of the Japan Concrete Institute*, Vol. 21, JCI, pp. 221-226.

Dr. Borosnyói Adorján (1974) MSc (CEng), PhD, senior lecturer at the Budapest University of Technology and Economics. His main fields of interest: serviceability and durability of reinforced concrete and prestressed concrete structures, application possibilities of non-metallic (FRP) reinforcement in reinforced or prestressed concrete, bond in concrete, strengthening with advanced composites. In his PhD thesis he deals with serviceability of CFRP prestressed concrete members. Member of *fib* TG 4.1 "Serviceability Models" and the Hungarian Group of *fib*.

Prof. Balázs L. György (1958) PhD, Dr. habil, professor in structural engineering, head of department of Construction Materials and Engineering Geology at the Budapest University of Technology and Economics. His main fields of activities are: experimental and analytical investigations as well as modelling reinforced and prestressed concrete, fibre reinforced concrete (FRC), fibre reinforced polymers (FRP), high performance concrete (HPC), bond and cracking in concrete and durability. He is convener of *fib* Task Groups on "Serviceability Models" and "*fib* seminars". In addition to he is a member of several *fib*, ACI, and RILEM Task Groups or Commissions. He is president of the Hungarian Group of *fib*. Member of the *fib* Presidium.

fib Symposium 2005

KEEP CONCRETE ATTRACTIVE

22-25 May 2005, Budapest, Hungary

This is the major Symposium in 2005 for those who intended to believe in the future of structural concrete. Technical sessions, task group and commission meetings will serve the forum of presentations and discussions for engineers as well as architects.

Concrete is an excellent structural material especially owing to its variety in properties, wide range of applicability and reasonable price. The past 150 years taught us how to deal with this material and how to develop it for the increasing requirements.

Significance of concrete seems to be increased even if new types of steel, aluminium, timber and glass products appear. Concrete was and is, however, attractive in many ways. Just remember to its constituent materials available from many local sources, unlimited forms, constructability, economy and aesthetics. We should only keep the significance of concrete by reaching its favourable performance.

Principal aim of the Symposium is to show the potential of concrete as a structural material in order to find optimal properties and applications.

Symposium Topics:

Topic 1 Attractiveness of concrete structures

Architectural appearance. Exposed concrete. Economic and historical aspects. Beauty of concrete structures.

Topic 2 Innovative materials and technologies for concrete structures

Tailored properties of concrete. High performance concrete, fibre reinforced concrete, self-compacting concrete, lightweight concrete, green concrete. Metallic and non-metallic reinforcements. Production and construction techniques.

Topic 3 Modelling of structural concrete

Design and modelling aspects. Modelling of cracking, damage and displacements. Performance based design. Performance criteria.

Topic 4 Sustainable concrete structures

Resource oriented design. Environmentally compatible materials. Structural service life aspects. Retrofitting of concrete structures. Monitoring, maintenance and strengthening techniques.

Topic 5 Prefabrication

Prefabrication and erection techniques. Application of self-compacting concrete in prefabrication. Construction joints.

Topic 6 Fire design of concrete structures

Material and structural behaviour in fire. Fire safety design. Case studies.

Important dates:

30 September 2004 Submission of Abstracts

Min. 150 and max. 300 words abstracts are to be submitted by e-mail including name(s), address(es), phone, fax and e-mail numbers(s) of author(s) together with the suggested Symposium Topic where the abstract belongs to. First author will be considered as corresponding author if not requested otherwise.

30 October 2004 Confirmation of acceptance of Abstracts

31 January 2005 Submission of manuscripts

Symposium Secretariat:

“Keep Concrete Attractive” Symposium Secretariat

Hungarian Group of *fib*

c/o Budapest University of Technology and Economics

Dept. of Construction Materials and Engineering Geology

H-1111 Budapest, Műgyetem rkp. 3.

Tel/Fax: +36-1-463 4068 / 3450

e-mail: fibSympBudapest@eik.bme.hu

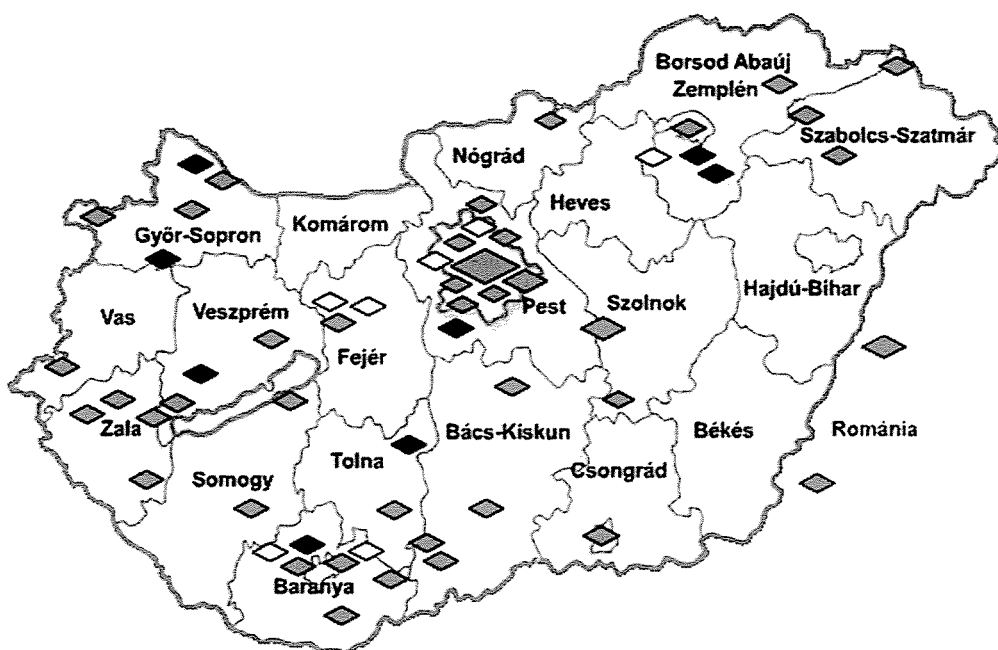
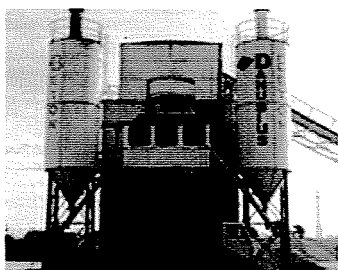
Symposium website: www.eat.bme.hu/fibSymp2005



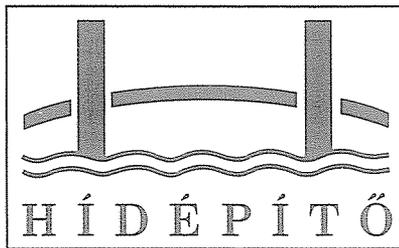
DANUBIUSBETON

The determining firms of Hungary's concrete market

Our main businesses: Production, transport and pumping of concrete
Mining of sand, grave and stone
Production of paving stone
Transport of cement



H 1095 Budapest, Hajóállomás utca 1
tel.: 06 1 215-0874, fax: 06 1 215-6317
www.danubiusbeton.com, www.readymix.hu



ÉPÍTŐIPARI
MESTERDÍJ 1996



HÍDÉPÍTŐ RÉSZVÉNYTÁRSASÁG

H-1138 Budapest, Karikás Frigyes u. 20. Mailing address: H-1371 Budapest 5 P. O. B.: 458
Phone: +36 1 465 2200 Fax: +36 1 465 2222

Extension of the South-Pest Wastewater Treatment Plant



duction of the so-called incremental launching method. In the period from year 1989 up to now yet 22 bridges were constructed by this method, mainly on the base of the designs prepared by the Company's own Technical Department.

Among them distinguishes itself the viaduct made of stressed reinforced concrete in length of 1400 m on the Hungarian-Slovenian railway

In the recent two years a great number of important professional recognitions were awarded the high level activity in the fields of bridge construction and bridge designing.

- High standard Prize of Building Industry for designing and constructing a bridge in length of twice 187 m on the section accessing Budapest of the motorway M5 (2000).

- Innovation Grand Prix for designing and constructing in record-time (one year) viaducts in length of 1400 m and 200 m on the Hungarian-Slovenian railway line at Nagyrákos (2001).

- Prize of Concrete Architecture for designing the viaducts at Nagyrákos (2001).

The State-owned Hidépitő Company, the professional forerunner of Hidépitő Részvénytársaság was established in year 1949 by nationalising and merging private firms with long professional past. Among the professional predecessors has to be mentioned, the distinguished Zsigmondy Rt., that participated, inter alia, in the construction of the Ferenc József (Francis Joseph) bridge which started in year 1894.

The initial purpose of establishing Hidépitő Company was to reconstruct the bridges over the rivers Danube and Tisza, destroyed during the Second World War, and this was almost completely achieved.

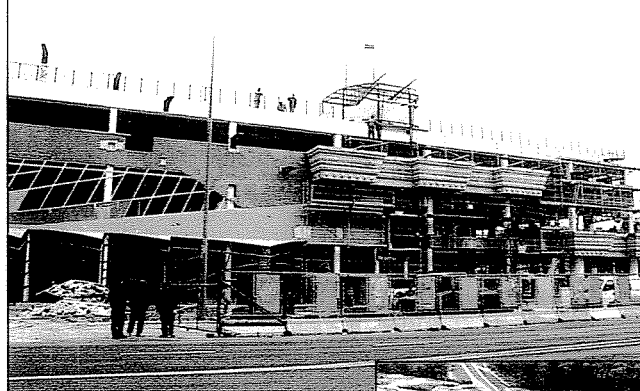
The next important epoch of the "Hidépitők (Bridge Builders)" was to introduce and to make general the new construction technologies.

Even among these can be judged to outstanding the bridge construction by balanced cantilever method, the experts having participated in it were awarded the State Prize. By this technology were constructed five bridges in the region of rivers Körösök and this was applied at the flyover of Marx square (today Nyugati square) in Budapest, still the most up-to-date two-level crossing in the capital requiring the minimum maintenance works.

The next big step was the introduction of the so-called cast-in-situ cantilever bridge construction method. This technology was applied for four bridges constructed over great streams, among them can be found the bridge with largest span (120 m) in Hungary made of stressed reinforced concrete, the road bridge over river Tisza at Szolnok.

An important result of the technologic development in the bridge construction was the intro-

The Market Hall "Lehel" in progress of construction



duction of the so-called incremental launching method, near the Slovenian State Border, constructed in one year using the incremental launching method.

Beside the bridge construction, important results were achieved by the "Hidépitők (Bridge Builders)" in the field of foundation's technological development as well, in the introduction and general use of the bored piles with large diameter, of jet grouting and of CFA (Continuous Flight Auger) pile preparation, further also a new method, subject of patent protection, was developed for very quick and economic constructing bridge piers in living water.

The Company was privatised (bought by the French Company GTMI) in year 1993. Following the multiple merger of the foreign interest parent Company, today Hidépitő Rt. belongs to the multinational Company "VINCI".



The 1400 m long viaduct on the Hungarian-Slovenian railway line at Nagyrákos

By working in good quality the Company makes efforts to inspire the confidence of the Clients. For this purpose have been introduced and operated the Quality Assurance and Environment Controlling Systems meeting the requirements of the international Standards ISO 9001:1994 and ISO 14001:1997, justified by international certificates.

The Company is hopefully awaiting the new tasks in order to enhance the reputation of the "Hidépitők (Bridge Builders)".